ADVANCED STRATEGIES FOR COMPOSITION CONTROL IN SEMI-CONTINUOUS EMULSION POLYMERIZATION

Nida Sheibat-Othman

▶ To cite this version:

HAL Id: tel-00366694

https://theses.hal.science/tel-00366694

Submitted on 9 Mar 2009

N° d'ordre 145-2000   Année 2000

THESE

présentée devant

l'UNIVERSITE CLAUDE BERNARD LYON 1

Ecole Doctorale de Chimie

pour l'obtention du

DIPLOME DE DOCTORAT

arrêté du 30 mars 1992

Spécialité: **Génie des Procédés**

par

Nida SH'EIBAT OTHMAN

ADVANCED STRATEGIES FOR COMPOSITION CONTROL IN SEMI-CONTINUOUS EMULSION POLYMERIZATION

Soutenue le 10 Juillet 2000

JURY

Dr. D. Colombié

Prof. G. Févotte

Prof. H. Hammouri

Prof. C. Kiparissides   (Rapporteur)

Prof. J. R. Leiza   (Rapporteur)

Prof. J. Liéto   (Président)

Dr. T. F. McKenna

UMR 140-Laboratoire de Chimie et Procédés de Polymérisation CNRS - CPE

Bâtiment 308 F - BP 2077, 43, Bd du 11 Novembre 1918, 69616 Villeurbanne cedex.

ADVANCED STRATEGIES FOR COMPOSITION CONTROL IN SEMI-CONTINUOUS EMULSION POLYMERIZATION

TABLE OF CONTENTS

RESUME _____

Stratégies Avancées de Contrôle de Composition Lors de Polymérisations Semi-Continues en Emulsion

La nécessité de produire des polymères avec des propriétés spécifiques et reproductibles, de minimiser le temps et les coûts et de contrôler la sécurité de l'expérience nous contraint à utiliser des méthodes avancées de contrôle de procédés de polymérisation.

Les polymères sont aujourd'hui utilisés dans des domaines différents. Une grande partie de ces polymères est produite en émulsion. La formulation de base d'une réaction de polymérisation en émulsion classique, contient de l'eau qui constitue la phase continue, et des monomères qui sont dispersés dans l'eau et stabilisés grâce à un agent émulsifiant. Les particules de polymère ainsi produites sont suspendues dans l'eau, grâce à l'émulsifiant. Le milieu résultant est donc appelé 'latex'.

Les propriétés du latex dépendent de beaucoup de paramètres, tels que la distribution de la masse molaire de polymère, la distribution des tailles de particules, la température de transition vitreuse, la morphologie, et la composition du polymère, si la réaction fait intervenir plusieurs monomères. Ces propriétés sont influencées par plusieurs variables, la nature et la quantité des additifs tels que, l'amorceur, le tensioactif les agents de transfert éventuels, la façon dont ces produits et les monomères sont introduits dans le réacteur, la température de la réaction, l'agitation, et le type de réacteur utilisé. Ces nombreuses variables sont alors nos variables de commande, que nous devons faire varier pour obtenir les propriétés désirées.

En réalité, afin d'obtenir des propriétés spécifiques, tout en assurant la sécurité du procédé, plusieurs paramètres sont fixés a priori, tels que la quantité initiale de réactifs et la température de la réaction. Ceci dit, plusieurs paramètres restent à faire varier en ligne, pendant la réaction, comme la température de la double enveloppe, pour maintenir la réaction à la température prévue, et le débit d'ajout des monomères, qui nous permettront de contrôler les propriétés du latex (la taille des particules et la composition du polymère). Ce genre

d'intervention en ligne pour améliorer la qualité et la sécurité du procédé, le contrôle en ligne du procédé de polymérisation en émulsion, sont l'objet but principal de ce travail.

Du point de vue du contrôle, le procédé est un système dynamique (représenté par des équations différentielles) possédant des entrées, des états (les variables décrivant l'évolution du procédé), et finalement des sorties (qui sont les variables mesurées en ligne, et sont en général, une combinaison des états du système).

Pour contrôler un procédé, un modèle représentatif de ce procédé est nécessaire. Faute de trouver un modèle parfait du procédé, des informations en ligne provenant des sorties du système, s'avèrent nécessaires pour accomplir la stratégie de contrôle. En réalité, les raisons pour lesquelles, les méthodes de contrôle avancées n'ont pas été utilisées lors des procédés de polymérisation en émulsion sont le manque de capteurs en ligne capables de donner des mesures pour la plupart des propriétés des polymères, la rapidité de la réaction, la sensibilité de la réaction à la présence de petites quantités d'additifs, la nonlinéarité du modèle du procédé et le grand nombre de paramètres inconnus dans le modèle et l'interaction entre ces paramètres.

Une des propriétés intéressantes à contrôler lors des procédés de polymérisation en émulsion, est la composition du polymère, pour les procédés faisant intervenir plusieurs monomères à une composition non azéotropique. La composition du polymère intervient au niveau de la détermination de la température de transition vitreuse, des propriétés mécaniques, ainsi que de la morphologie du polymère. Il a été trouvé dans la littérature que l'ajout du monomère le plus réactif à des débits variables est la méthode la plus efficace pour contrôler la composition tout en assurant une vitesse de réaction relativement élevée. En utilisant une méthode avancée de contrôle, nous pouvons alors maintenir la composition à une valeur désirée. Ceci nécessite une connaissance approfondie du procédé ainsi que la mesure en ligne de la composition de polymère.

Les capteurs en ligne utilisés pour suivre les procédés de polymérisation en émulsion peuvent être divisés en deux catégories: des capteurs nécessitant une boucle de circulation externe, ou un système de prise d'échantillons afin d'effectuer l'analyse (Chromatographie en phase gazeuse, densimétrie); et des capteurs *in situ* qui effectuent les analyses dans le réacteur

(Spectroscopie Infrarouge, sondes ultrasons). La chromatographie en phase gazeuse peut être utilisée pour mesurer, en ligne, la composition du mélange de monomère résiduel, si le réacteur est équipé d'un système automatique de prise d'échantillons, de dilution, dans certains cas, et d'injection dans le chromatogramme. La densimétrie a été également utilisée pour la mesure en ligne de la composition du polymère. Une boucle de circulation du latex dans l'appareil est donc indispensable pour effectuer l'analyse. Cependant ces deux méthodes présentent quelques difficultés expérimentales, telles que la floculation du latex dans les appareils et le retard des analyses, qui sont dues, pour partie, au transfert du latex. C'est pourquoi, les expériences sont préférablement suivies avec les capteurs *in situ*, où l'analyse est effectuée dans le réacteur. Cependant, ces capteurs, tels que l'infrarouge, l'ultrason et la spectroscopie Raman sont en phase de développement, et nous ne possédons pas encore de modèles complets liant ces mesures avec les propriétés du latex.

Le manque de capteurs en ligne qui donnent des mesures réelles des procédés est un problème fréquent dans plusieurs domaines. Dans les procédés de polymérisation en émulsion, ce manque est d'abord dû à la nature hétérogène et visqueuse du latex qui rend la mesure directe des propriétés du polymère souvent difficile. Ensuite, l'équipement d'un procédé avec plusieurs capteurs serait économiquement impossible. A cause du manque de capteurs, et du manque de modèles exacts des procédés, des efforts ont été faits dans le domaine de l'estimation logicielle des états, non mesurés expérimentalement, en se basant sur des mesures réelles et le modèle du procédé. Ces observateurs, ou estimateurs, ou encore capteurs logiciels, sont conçus à partir du modèle du procédé en utilisant les sorties réelles du procédé. Si le système est observable, l'observateur nous permettra d'obtenir des informations sur les états non mesurés du procédé. Les observateurs sont souvent utilisés pour le suivi des procédés, mais sont également très utiles pour le filtrage, la détection de panne et le contrôle des procédés.

Les méthodes d'estimation et de contrôle linéaire ont souvent été appliquées dans le domaine de la polymérisation en émulsion, et ce malgré la nonlinéarité des modèles représentant ces procédés. Ceci est dû premièrement à la difficulté de manipuler les outils non linéaires, au temps nécessaire à l'ordinateur pour résoudre ces observateurs et au fait que les observateurs non linéaires proposés dans la littérature étaient souvent limités à un groupe de systèmes non linéaires. Ces sujets ne posent aucune difficulté aujourd'hui, avec le

9

développement de la théorie non linéaire, et l'évolution de la rapidité et de la capacité des ordinateurs.

L'objectif de ce travail est le contrôle de la composition des polymères, tout en assurant une vitesse de réaction élevée, ainsi que la sécurité de l'opération. Puisque les modèles représentant ce procédé sont nonlinéaires, nous allons utiliser des méthodes d'estimation et de contrôle nonlinéaires adaptées au procédé.

La stratégie d'estimation est constituée de trois parties. Dans la première partie, nous allons développer un capteur qui fournit des informations précises et rapides sur le procédé. La deuxième partie est constituée de l'estimation de la composition du polymère lors des procédés de co- et terpolymérisations en émulsion. La dernière étape est la construction de lois de commande adéquates qui nous permettent d'obtenir la composition et la vitesse de réaction désirées.

Dans le premier chapitre, une introduction générale du sujet ainsi que la stratégie de recherche sont proposées. Le deuxième chapitre contient les théories d'estimation et de contrôle nonlinéaires que nous allons utiliser tout au long de ce travail.

Le troisième chapitre traite des capteurs en ligne pour les procédés de polymérisation en émulsion. D'après certains critères , nous choisissons d'utiliser la calorimétrie pour suivre le procédé. Cependant, ce capteur ne nous donne pas directement une mesure de la vitesse de la réaction, car plusieurs paramètres dans le bilan thermique restent inconnus. Pour contourner ce problème, nous allons utiliser une méthode d'optimisation de la conversion globale du monomère, en corrigeant les paramètres inconnus. Pour ce faire, les mesures de la température du réacteur, de la double enveloppe, et quelques mesures expérimentales de la conversion sont nécessaires.

Dans le quatrième chapitre nous utilisons les informations obtenues par calorimétrie, pour estimer la composition du polymère lors des procédé de copolymérisation. Nous traitons le cas d'un observateur nonlinéaire à grand gain qui tient compte de la réaction dans la phase aqueuse et un autre où on néglige l'effet de la phase aqueuse. Il s'avère que, pour les monomères étudiés, la composition du polymère n'est pas sensible à la réaction dans la phase

aqueuse. Ce phénomène est peut être dû au fait que la plupart des radicaux sont dans les particules, surtout pour un taux de solide élevé. La deuxième raison est que les monomères utilisés ici sont seulement partiellement solubles dans l'eau, ce qui fait que la quantité de monomère dans les particules est plus importante que dans la phase aqueuse.

Dans le cinquième chapitre, un observateur nonlinéaire à grand gain est construit pour suivre la composition du polymère lors des procédés de terpolymérisation. Puisque le quatrième chapitre montre clairement que nous n'avons pas besoin de tenir compte de la phase aqueuse pour l'estimation de la composition, un modèle de monomères hydrophobes est choisi pour construire l'observateur.

Le chapitre 6 expose les lois de commande développées pour maintenir la composition de co- et de terpolymères sur une trajectoire prédéfinie. Des lois de commande nonlinéaires avec une linéarisation entrée-sortie sont utilisées. Dans ce chapitre, nous établissons un contrôleur local de la pompe, qui assure l'exécution des débits envoyés par la commande de la composition.

Dans le dernier chapitre nous évoquons le concept de maximisation de productivité. Notre objectif est de maintenir la composition à une valeur prédéfinie, et en même temps maximiser la vitesse de la réaction. Les variables de commande sont les débits d'ajout de monomères. La variable contrôlée est la concentration de monomère dans les particules. Cependant, pendant le contrôle de la concentration de monomère dans les particules il faut faire attention à ce que la chaleur produite par la réaction soit inférieure à la chaleur maximale que la double enveloppe est capable d'évacuer.

CHAPTER I ——————————

INTRODUCTION AND OBJECTIVES

1 INTRODUCTION AND OBJECTIVES

Advanced control is becoming imperative for various processes, and polymerization processes are absolutely no exception. The major objectives of on-line monitoring and control of polymerization processes are maintaining the process safety, manufacturing polymers with well-defined properties, and reducing costs.

Polymers are found in a large variety of products. It is a well accepted fact that a significant quantity of polymers are manufactured in emulsion polymerization, and that the economic importance of these products is beyond question. The reaction medium in emulsion polymerization involves the dispersion of one or more monomers (which are usually partially or totally hydrophobic) in a continuous aqueous phase[*] with a water soluble initiator and an emulsifier. The reaction therefore takes place under heterogeneous conditions, and the final product, called a latex, consists of suspended polymer particles in water, stabilized by the emulsifier.

Industrial emulsion polymerization processes can be classified into two groups according to the final use of the latex. In some emulsion polymerization processes the produced latex is an intermediate product, and it is coagulated after the fact to give the final bulk polymer (e.g. polyvinyl chloride, styrene butadiene rubber). In other processes, the produced polymer is used directly (or perhaps after some intermediate formulation steps) in the form of a latex. Polymers produced in this way are used as water-based paints (acrylics lattices), adhesives (polyvinyl acetate latex), and finishes for textiles, paper or leather (acrylic polymers).

Of course not all emulsions use water as the continuous phase. Water-in-oil, or inverse processes also exist. However, we will limit our discussion to the more common oil-in-water processes.

The final latex properties depend on the polymer molecular weight distribution, particle size distribution, morphology, glass transition temperature, and composition (when several monomers are used). These properties are strongly determined by the amount and type of additives, initiator, emulsifier and chain transfer agent, the monomer addition policy, the reaction temperature and the reactor configuration. Hence, emulsion polymerization processes are characterized by a large number of manipulated variables, which means that, in order to describe the relationships between them, we would need highly complex process model.

In order to ensure the economical production of a polymer with the desired properties under safe conditions, important decisions must usually be made during plant operation, by means of automatic on-line control. In the context of control, the process is a dynamic system (described by a set of differential equations) with well-known inputs (that can usually be used as manipulated variables), process 'states' that are the variables representing the evolution of the process, and finally measured process outputs (which are usually a combination of the process states). Control of the process states is based on a suitable process model. It also requires some on-line state measurements. In spite of the importance of emulsion polymerization, process control is still a particularly difficult task. The difficulties in controlling emulsion polymerization are often associated with the lack of on-line measurements of several properties, the high reaction rate, the sensitivity of the reaction to small amounts of additives, and the highly complex reaction networks that result in a complex nonlinear model combined with a number of unknown variables.

One of the main control objectives in an emulsion polymerization process is to track polymer composition. This is of absolute importance in terms of final properties of the produced polymer-e.g. glass transition temperature, particle morphology, mechanical and chemical resistances. Controlling polymer composition is indispensable if several monomers with different reactivity ratios are involved in the reaction at a nonazeotropic monomer composition, which is the case of most industrial systems. If no control action is taken in this case, the polymer composition will vary during the reaction, and this will lead to a heterogeneity in the polymer properties (unless the polymer is made in a CSTR). Polymer composition can however be controlled by employing appropriate monomer feed flow rates. The most efficient monomer addition policy, in terms of composition control and

simultaneous minimization of process time consists of applying a variable monomer feed flow rate of the more reactive monomer(s), that should be a function of the residual amount of monomer remaining in the reactor and their reactivity ratios. Therefore, controlling polymer composition requires on-line measurement of the polymer composition and the instantaneous quantity of residual monomers, an adequate mathematical model correlating the monomer feed flow rates with the produced polymer composition (inputs-outputs), and finally the use of a robust control technique.

On-line sensors developed for the direct monitoring of emulsion polymerization can be classified into two broad categories: sensors that require a sampling device or a circulating loop to perform the analysis (e.g. gas chromatography and densimetry), and *in situ* sensors (e.g. Spectroscopic and ultrasonic probes). The copolymer composition can be monitored by means of on-line gas chromatography (based on the analysis of the residual monomer), or by densimetry (if combined with an additional sensor). However, the measurements in these sensors present some difficulties related to the latex sampling and treatment, and sometimes, time delays caused by long analysis times. This is not to say that we cannot use these sensors, by rather we must be aware of their limitations. In the second category, the analysis is performed in the reactor, and therefore problems related to time delays and to plugging of the sampling loop are minimized. However, some sensors such as the infrared spectroscopy, while very promising, are still in the stage of development, and we are still faced with the problem of coagulation on the sensor. When these techniques become available, they will provide valuable information on the state of the reactor. Nevertheless, given the complicated nature of emulsion systems, we will still need to apply advanced control strategies such as those outlined in what follows.

Due to the difficulty of performing on-line measurements of all the states of the process, combined with a lack of accurate phenomenological models, estimation techniques have been developed to infer estimates of certain variables that are not available on-line, from auxiliary measurements. State observers, or software sensors, are designed based on the process model and on the process outputs. If the observability conditions are satisfied, the observer reconstructs some of the unmeasurable states of the model from the available measurements. Good state observers can overcome modeling uncertainties and measurement

17

noise, and are therefore useful for process monitoring, control, fault detection, and are also used as filters of random effects associated to the measurements.

Despite the highly nonlinear behavior of the polymerization process, mainly due to the reaction rate, linear estimation (e.g. Kalman filter) techniques have usually been used to infer information about the evolution of several unmeasurable states of the process. Similarly, linear control techniques (PID, adaptive) have usually been applied to track several variables of the linearized nonlinear system. This is due to the difficulty of dealing with nonlinear systems and to the fact that nonlinear estimators are usually restricted to a class of nonlinear systems. However, linear estimation and control techniques are inadequate for highly nonlinear processes. Nowadays, recent developments in nonlinear theory allow us to implement nonlinear estimation (e.g. high gain observer) and control (e.g. geometric control) techniques to several classes of systems without extensive calculations.

The main objective of this research is to apply such nonlinear techniques to estimate and control the polymer composition, and to maximize the process productivity under safe reactor operation. The fundamental on-line information about the evolution of the process is obtained by calorimetry. Calorimetry is often useful in vinyl polymerization reactions, since they tend to be very exothermic. On an industrial level, the main use of calorimetry is currently reactor safety (by reactor temperature control), and the estimation of the rate of heat produced by the polymerization, which is proportional to the overall reaction rate.

In Chapter 2 we will review the theoretical nonlinear estimation and control techniques that will be used throughout this research. Calorimetry will be discussed in Chapter 3. The observer development to estimate the polymer composition in co- and terpolymerization processes is presented in Chapters 4 and 5. In Chapter 6, we develop a control strategy for polymer composition for both co- and terpolymerization processes. Finally, in Chapter 7, we treat the topic "Maximizing productivity under safe conditions", where the polymer composition is controlled and the reaction rate is simultaneously maintained at a predefined maximum limit.

Composition control strategy

CALORIMETRY

Optimization of the conversion ← Gravimetric measurements of X

UA and Qloss

Initial masses

Physical constants: C_P, ΔH_P

Energy balance + Observer of Qr ← Temperature mesurements

← Monomer addition flow rates

X

ESTIMATION

Kp, ri, MW, density →

High gain observer of the polymer composition Copo- and Terpo-

Composition

CONTROL

Composition controller Controller of Qr and Mp

Qi

CHAPTER II ————————————

STATE ESTIMATION AND CONTROL

2 STATE ESTIMATION AND CONTROL

2.1 Introduction

For several years, limitations in computer hardware were the major restriction on the implementation of advanced automatic methods. Nowadays, development in both computer hardware and control theory, allows automatic control methods to be successfully applied to several processes. Online monitoring and control of a process is important for an improved process safety (safety and environmental considerations), the control of product quality (accuracy, reproducibility and uniformity of quality), the optimization of the productivity (saving time, increasing output, process intensification), and reducing manpower.

Effective control of a process requires sufficient information on the state of the process (inputs, outputs and state variables). Firstly, a mathematical representation of the process is required. Secondly, a measurement or an estimation of the properties to be controlled must be available in real time. Finally, an adequate control law that is robust with respect to mismodeling (model inadequacies and inaccuracies) and measurement disturbances, must be implemented to fulfill the control objectives.

First of all, a mathematical description of the evolution of the variables, called the 'states' of the process is required to identify the control variables and to correlate the process inputs and outputs. The advantages of process modeling are not limited on the control purpose. Good mathematical models enhance our knowledge of the process, and can be employed to anticipate the evolution of the states of the process, and are necessary for process simulation, optimization and control. Process models are usually founded on physical laws, statistical rules or empirical or semi-empirical relations. The expression of this information takes the form of differential and/or algebraic equations that describe the state of the model and their relationship to inputs and outputs. Modeling of polymerization processes is now well understood. Nevertheless, references have treated the reaction modeling and the

estimation of kinetic parameters in polymerization processes, including: Penlidis et al. (1985), Makgawinata et al (1984), Hamielec et al. (1987), Dimitratos (1989), Mead and Poehlein (1988), Richard and Congalidis (1989), Lopez de Arbina et al. (1997), Saldivar and Ray (1997), and Saldivar et al. (1998), Storti et al. (1989), Urretabizkaia et al. (1992), Dubé and Penlidis (1996a and b) and Dubé et al. (1997). Most of these models are nonlinear. It is important to chose an adequate model (simple but accurate) for the control purpose, (will be discussed in Chapter 4).

Secondly, it is obvious that a measure of the properties to be controlled would be to synthesize a controller. However, in a large number of processes, for example fermentation or chemical processes, only few variables, such as temperature, pressure, flow rate, PH, etc, are measured on-line. The most important properties, such as composition, molecular weight distribution or particle size distribution in polymerization reactors are difficult, and sometimes impossible, to measure directly, at the current time. These properties cannot be obtained from the open-loop mathematical model of the process because chemical, and particularly polymerization, processes are difficult to model in detail. The models proposed in the literature to describe the polymerization process involve several uncertain and time varying parameters, and the states of the model (reaction rate, molecular weight, particle size and number) are very sensitive to unmeasured disturbances (resulting typically from trace amounts of polymerization inhibitors or other compounds which may be present in the ingredients), and to initial conditions, that are not always known precisely.

Problems related to model mismodeling and unknown initial conditions can be overcome either by using parameter optimization based on iteration techniques, or by using state estimators based on the minimization of a criterion. Both of these techniques combine the available process model with the measured output to infer information about unmeasured parameters or properties, under identifiable or observable conditions. The identification or optimization techniques are based on the minimization of a criterion that compares the model with the measured process output. The difficulty with the optimization algorithm is that it generally takes a lot of time to run on a typical on-line PC platform, plus it might converge to a local optimum rather than to the true value. On the other hand, when the conditions of observability are satisfied, and if the observer is well tuned, it has the advantage of being able to converge rapidly to the 'true' states, and solving the observer equations can usually be

performed quickly. For these reasons, in this work we will use state estimation techniques wherever possible.

Therefore, when the on-line measurement of polymer properties is the major obstacle to feedback control, state estimation theory will be used to reconstruct the states necessary for the control strategy. The control strategy is thus composed of a model representing the process, some online measurements, an observer, and finally a robust control strategy.
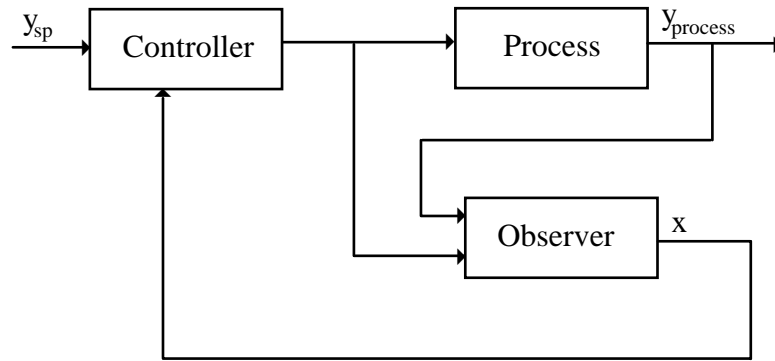
Figure 2.1: Process estimation and control.

In this work, the problem of the control of an emulsion polymerization is addressed. Since the model of a typical emulsion polymerization process is nonlinear, we will be interested in nonlinear estimation and control theories. In the following section we will review some appropriate state estimators for polymerization processes. This will be followed by a review of some control laws that will be used at a later stage.

First of all, we recall some definitions that will be used below. Consider the following nonlinear system:

$$\dot{x}(t) = f\big(x(t), u(t)\big) \qquad (2.1)$$
$$y(t) = h\big(x(t)\big)$$

where $x(t) \in M$, $M \in \Re^n$ is the states space, $y \in \Re^p$ the measured outputs and $u \in U$, $U \in \Re^m$ is the bounded input space. Given f, g C^∞ vector fields on R^n and h, a C^∞ scalar field on R^n:

➢ Define the Lie derivative as:

25

$$L_f h(x) = \sum_{i=1}^{n} f_i(x) \frac{\partial h(x)}{\partial x_i}$$

which is the directional derivative of the function $h(x)$ in the direction of the vector $f(x)$. One may also differentiate $h(x)$ first in the direction of $f(x)$, and then in the direction of $g(x)$

$$L_g L_f h(x) = \sum_{i=1}^{n} g_i(x) \frac{\partial \left(L_f h(x) \right)}{\partial x_i}$$

Also, higher order derivatives can be written as:

$$L_f^k h(x) = L_f \left(L_f^{k-1} h(x) \right),$$

$$\text{with } L_f^0 h(x) = h(x)$$

➢ The Lie derivative of h with respect to f can also be defined as

$$L_f h = < dh, f >$$

where $<.,.>$ denotes the dual product, i.e.,

$$< dh, f > = \frac{\partial h}{\partial x_1} f_1 + \cdots + \frac{\partial h}{\partial x_n} f_n$$

➢ The successive Lie brackets are defined by:

$$ad_f^0(g) = g$$
$$ad_f^1(g) = [f, g]$$
$$\vdots$$
$$ad_f^k(g) = [f, ad_f^{k-1}(g)]$$

with:

$$[f, g] = \frac{\partial g}{\partial x} f - \frac{\partial f}{\partial x} g$$

➢ $\|x\|$ stands for the euclidien norm of x, i.e.

$$\|x\| = \sqrt{x_1^2 + x_2^2 + \ldots + x_n^2}$$

2.2 State observers

2.2.1 Introduction

An observer is a mathematical representation of a given system that consists of a model of the process plus a corrective term that is proportional to the difference between the process output and its estimated value times a gain, where the choice of the gain depends on the structure of the system. In order to develop an observer, one needs measurements of the process inputs and outputs and a mathematical model that correlates the outputs with the states of the process and that ensures the observability of the state.

Unlike the case of linear systems, the **observability** of nonlinear systems depends on the input. A system is observable if and only if the outputs and the inputs can be used to reconstruct the initial states of the system, as given by the following definition:

Definition 2.1: The system 2.1 is observable if, $\exists$ an input u on the interval [0,T], such that the system 2.1 is observable. If for an input u, x(t) and $\overline{x}(t)$ are two trajectories associated with this input with the initial conditions $x(0) \neq \overline{x}(0)$, then there exist $t \in [0,T]$ such that $h\big(x(t)\big) \neq h\big(\overline{x}(t)\big)$.

It should be clear that the condition of observability tells simply whether or not it is possible to estimate a set of states, but tells us nothing about the quality or precision of those estimates, or which observer to use.

For linear systems, the most widely applied observers are the Luenberger, and Kalman observers. The linear Kalman filter, firstly proposed by Kalman and Bucy (1961), is an optimal observer based on the solution of the dynamic Riccati equation. The use of these observers gives generally good results.

At the current time, there is no general theory of estimation for nonlinear systems. The extended Kalman filter (EKF), which is a direct extension of Kalman filter of linear stochastic systems, has been successfully applied to several 'linearized' nonlinear systems (Kiparissides et al. (1981), Dimitratos (1989), Dimitratis et al. (1991), Gagnon and MacGregor (1991), Leiza (1991), Terwiesch and Agarwal (1995), Chang and Chen (1995), Kafjala and Himmelblau (1996), Régnier et al. (1996), Mutha et al.(1997)). However, the EKF has some disadvantages:

- The convergence and stability of the observer are not theoretically proven.
- The possibility of unpredictable bias in estimations is the main reason which has prevented the use of EKFs in many realistic systems monitoring. This is because the KF supposes that the process model is exact. The EKF is therefore not able to overcome problems related to mismodeling.
- Several tuning variables are involved in the covariance matrix and it is even sometimes difficult to distinguish between numerical problems related to solving the differential equations and the sensitivity to measurement and model structure.
- The computation time needed to solve the observer equations may be very long because it integrates the states and the gain matrix at each step.

Kozub and MacGregor (1992) combined the EKF with a recursive prediction error algorithm and proposed the incorporation of adequate nonstationary disturbance in order to handle bias and to track the real problem. This improved the performance of the filter under conditions of model mismatch, but increased the required computational effort relative to the standard EKF. Moreover, an elementary simulation study is required to find a suitable set of covariance matrices which will not even ensure good convergence if the model used for the simulation is not accurate.

The first observers for monovariable nonlinear systems were developed by Krener and Isidori (1983) and Bestle and Zeitz (1983). The extension to multi-input/multi-output systems was done by Krener and Respondek (1985). These observers are not easy to employ since they require a complex change of coordinates that renders the system linear. Recently, a Kalman-like observer was developed by Hammouri and De Leon (1990) for a class of

nonlinear systems, where the state matrix might depend on the inputs, outputs or on time and all the inputs are regularly persistent. For this class of nonlinear systems, the Kalman-like observer is easier to implement than the Kalman observer since the gain matrix relies on a unique tuning parameter. At the same time, the high gain observer was developed for a class of nonlinear single-output systems that are observable for every input and under the condition that a change of coordinates puts the system under a canonical form of observability, (Gauthier et al. 1992). Later, this observer was extended to a multi-input/multi-output case, with a constant state matrix, Bornard and Hammouri (1991). An extension of the high gain observer to a new class of nonlinear systems, MIMO with a time varying state matrix was done by Farza et al. (1997).

The stability of these nonlinear observers is theoretically proven and their robustness has been demonstrated through applications to several kinds of processes. The high gain observer was tested in simulation on a bio-reactor (Gauthier et al. 1992), on a chemical reactor (Gibon-Fargeot et al. 1994) and on polymerization reactors by Févotte et al. (1998).

In the following sections, we briefly review three kinds of nonlinear observers that are going to be used in this work: a Kalman-like observer for systems with a time varying state matrix and a high gain observer for SISO and MIMO systems. The choice of the observer type will obviously be a function of the classification of the process model.

2.2.2 Kalman-like observer

The Kalman-like observer was proposed by Bornard et al. (1988) and Hammouri and De Leon (1990) for a class of nonlinear systems. The observer equations are based on the minimization of a quadratic convex criterion.

Consider the nonlinear system:

$$\begin{cases} \dot{x} = A(u,y)x + G(u) \\ y = Cx \end{cases} \qquad (2.2)$$

29

with a single output, $y \in \Re$ and the state matrix A might depend on the inputs and the outputs.

Let us call $\phi_u(s, t_0)$ the unique solution of

$$\frac{d\phi_u(s, t_0)}{ds} = A\big(u(s)\big).\phi_u(s, t_0)$$

with $\phi_u(t_0, t_0) = I$ the identity matrix and $\phi_u(t_0, s) = \phi_u^{-1}(s, t_0)$. We denote $\phi_u(s, t) = \phi_u(s, t_0).\phi_u(t_0, t)$. We denote by $G(u, t_0, t_0 + t_1)$ the Gramian of observability related to the input u on the interval [t_0,T]:

$$G\big(u, t_0, t_0 + t_1\big) = \int_{t_0}^{t_0+t_1} \phi_u^T(t, t_0) C^T C \phi_u(t, t_0) dt$$

T stands for the transposed matrix or vector.

Definition 2.2:

An input $u \in R^m$ is regularly persistent for the system 2.2 if $\exists\ t_1 > 0,\ \exists\ \alpha_1 > 0,\ \exists\ \alpha_2 > 0$ and $\exists$ $t_0 \geq 0$ such that $\forall\ t \geq t_0$:

$$\lambda_{min}\big(G\big(u, t_0, t_0 + t_1\big)\big) \geq \alpha_1$$
$$\lambda_{max}\big(G\big(u, t_0, t_0 + t_1\big)\big) \leq \alpha_2$$

where λ_{min} and λ_{max} stand for the less and largest eigen values of G, respectively.

Theorem 2.1: (Hammouri et al. 1991)

If u is regularly persistent then

$$\begin{cases} \dot{\hat{x}} = A(u)\hat{x} + G(u) - R^{-1}C^T\big(Cx - y\big) \\ \dot{R} = -\theta R - A^T(u)R - RA(u) + C^T C \end{cases} \tag{2.3}$$

is an observer for equation 2.2 with $\theta > 0$, $\hat{x}(n) \in \Re^n$. Moreover, the norm of the estimation error goes exponentially to zero. The tuning parameter of the Kalman-like observer is θ, which must be superior than zero. The convergence of the observer is guaranteed if the matrix R is a symmetric positive definite matrix.

2.2.3 High gain observer

In this subsection, we consider the nonlinear system 2.1 with $y \in \mathfrak{R}$.

Definition 2.3:

The function f is global Lipschitz if $\exists \, c > 0$ such that $\forall \, x, x' \in R^n$,

$$\left| f(x) - f(x') \right| \le c \| x - x' \|$$

The following assumptions are needed in the sequence:

H1) The system 2.1 is locally uniformly observable, i.e. observable $\forall$ input.

H2) **Theorem 2.2:** (Gauthier et al. (1981 and 1992))

If the system is uniformly observable, the change of coordinates, $\phi(x)$, for the system 2.1 given by:

$$\xi = \phi(x) = \begin{bmatrix} h(x) \\ L_f h(x) \\ \vdots \\ L_f^{n-1} h(x) \end{bmatrix}$$

is a global diffeomorphism with respect to x and leads to the following system:

$$\begin{cases} \dot{\xi}(t) = A\xi(t) + F\big(\xi(t)\big) + \sum_{i=1}^{m} u_i(t) g_i(\xi(t)) \\ y(t) = C\xi(t) \end{cases} \tag{2.4}$$

with

$$A = \begin{pmatrix} 0 & 1 & 0 & \dots & 0 \\ 0 & 0 & 1 & & \vdots \\ \vdots & & & \ddots & 0 \\ 0 & & & & 1 \\ 0 & \dots & & 0 & 0 \end{pmatrix}, \; F(\xi) = \begin{pmatrix} 0 \\ \vdots \\ 0 \\ F_n(\xi) \end{pmatrix}, \; C = \begin{bmatrix} 1 & 0 & \dots & 0 \end{bmatrix} \text{ and}$$

$$\begin{cases} g_j(\xi) = \begin{bmatrix} g_{j1}(\xi) & \cdots & g_{jn}(\xi) \end{bmatrix}^T \\ g_{ji}(\xi) = g_{ji}(\xi_1, \dots, \xi_i) \end{cases} , \; 1 \le i \le n \; \text{and} \; 1 \le j \le m.$$

31

H3) The nonlinear terms F, g_1, ... , g_m are global Lipschitz. This assumption is always reliable if the states are bounded.

Theorem 2.3: (Gauthier et al. 1992)

For $\theta > 0$ large enough, the system:

$$\dot{\hat{\xi}}(t) = A\hat{\xi} + F\big(\hat{\xi}(t)\big) + \sum_{i=1}^{m} u_i(t)g_i\big(\hat{\xi}(t)\big) - S_\theta^{-1}C^T\big(C\hat{\xi}(t) - y(t)\big) \tag{2.5}$$

is an exponential observer of the state ξ of the system 2.4 and S_θ is the unique symmetric positive definite matrix satisfying the algebraic Lyapunov equation:

$$\theta S_\theta + A^T S_\theta + S_\theta A - C^T C = 0$$

The observer for the original state x(t) in system 2.1 is given by:

$$\dot{\hat{x}}(t) = f\big(\hat{x}(t), u\big) - \left(\frac{\partial \phi}{\partial x}\bigg|_{\hat{x}(t)}\right)^{-1} S_\theta^{-1}C^T\big(C\hat{x}(t) - y(t)\big) \tag{2.6}$$

The gain used does not require the resolution of any dynamical system and it is explicitly given. The tuning of the estimator is reduced to the calibration of a single parameter. Moreover, the observer provides estimations of some parameters without assuming a model for these parameters.

2.2.4 Extended high gain observer, for multi-output systems

The high gain observer has been extended for the estimation of multi-output nonlinear systems, Hammouri and Bornard (1991). An extension of this observer to a new class of nonlinear systems, where the state matrix is time varying, was proposed by Farza et al. (1997). The observer presented in their work is valid for multi-output nonlinear system.

We consider the following system:

$$\dot{\xi}(t) = A(u(t),t)\xi + G\big(u(t),t,\xi(t)\big) + \bar{\varepsilon}(t) \qquad (2.7)$$
$$y(t) = C\xi(t)$$

where

$$\xi = \begin{bmatrix} \xi_1 & \cdots & \xi_q \end{bmatrix}^T \in R^n, \ \xi_i = \begin{bmatrix} \xi_{i1} & \cdots & \xi_{ik} \end{bmatrix}^T \in \Re^{k_i}, \ (n=k_1+...+k_q), \ y \in \Re^p, \ C = \begin{bmatrix} I_P & 0 \end{bmatrix},$$

$$\bar{\varepsilon} = \begin{bmatrix} \varepsilon_1 & \cdots & \varepsilon_q \end{bmatrix}^T \text{ represent the model uncertainties, } \varepsilon_i \text{ must be bounded.}$$

$$A(u,t) = \begin{pmatrix} 0 & A_1(u,t) & 0 & \cdots & 0 \\ 0 & 0 & A_2(u,t) & & \vdots \\ & & & \ddots & 0 \\ 0 & & & & A_{q-1}(u,t) \\ 0 & & 0 & 0 & \end{pmatrix} \text{ and } G(u,t,\xi) = \begin{pmatrix} g_1\big(u,t,\xi_1\big) \\ \vdots \\ g_{q-1}\big(u,t,\xi_1,...,\xi_{q-1}\big) \\ g_q\big(u,t,\xi\big) \end{pmatrix}.$$

Assumptions:

A1) The matrices $A_i(u,t)$ are derivable with respect to t and their derivatives are bounded.

A2) $\forall i, \ \exists \alpha_i > 0 \ ; \ \exists \beta_i > 0$ such that:

$$\forall t \geq 0, \ \alpha_i I \leq A_i^T\big(u(t),t\big) A_i\big(u(t),t\big) \leq \beta_i I$$

where I is the identity matrix of $\Re^{k_i}$

Theorem 2.4: (Farza et al. 1997):

If system 2.7 satisfies assumptions A1 and A2 and if g_i of system 2.7 are global Lipschitz, then the following system is an exponential observer for system 2.7:

$$\dot{\hat{\xi}} = A(u,t)\hat{\xi} + G\left(u,t,\hat{\xi}\right) - \Lambda^{-1}S_\theta^{-1}C^T\left(C\hat{\xi} - y\right) \tag{2.8}$$

where

$$\Lambda(t) = \begin{pmatrix} I & 0 & \cdots & & 0 \\ 0 & A_1(u,t) & & & \vdots \\ \vdots & & \ddots & & 0 \\ 0 & \cdots & 0 & A_{q-1}(u,t)\times\ldots\times A_1(u,t) \end{pmatrix}.$$

2.3 Control

2.3.1 Introduction

One of the characteristics of chemical processes that presents a problem for rigorous control is the inherent nonlinearity of the model. In spite of this nonlinearity, such processes have traditionally been controlled with tools based on linear systems analysis and design. The common approach was to neglect nonlinear effects by locally linearizing the 'nonlinear' model around the operating point and then to apply linear theory to design linear controllers.

A major reason for the widespread use of linear systems theory to treat nonlinear systems is the existence of an analytical solution, which means that the Lyapunov stability analysis can be performed almost immediately, plus computational demands for linear systems are usually quite small when compared to a nonlinear simulation. In addition, early work in the nonlinear field did not address the problem of controller synthesis and was essentially pursued to provide valuable understanding of nonlinear stability and dynamic optimization.

The justification for this simplification is the assumption that a nonlinear system with 'regular' nonlinearities possesses a linear slope around an operating point. The system can therefore be described by a linear model around an equilibrium point. However, there exists a large number of nonlinear systems where it is impossible to correctly represent the system with a linear model on a functional domain. In this case, the application of a linear system technique is quite restrictive.

These considerations have motivated a growing activity in the area of nonlinear chemical process control. Instead of designing a linear controller whose function is only assured in the neighborhood of the linearized states, efforts were devoted to design a nonlinear controller valid over a larger, delimited region of the state space. However, this induces a lot of technical difficulties which prevents the development of general nonlinear

design methodologies. An understanding of the structural characteristics of nonlinear systems can be obtained using differential geometric concepts. Differential geometric nonlinear control techniques transform the nonlinear system into a partially or globally linearized dynamic, by acting on the model states, which is completely different from the linearizing approximations (Isidori (1989), Kravaris and Chung (1987), and Kravaris and Soroush (1990)).

It is important to mention that some other nonlinear techniques exist, such as the internal model, robust control design, model predictive and optimal control that are extended from the linear theory. A broad overview of developments in nonlinear systems theory is presented by Wayne Bequette (1991). However, most of these techniques approximate the process dynamic by calculating the linearizing Jacobian matrix.

Nonlinear control theory is an extension of the originally developed linear theory (Wonham 1985). Several notions used in the nonlinear theory are, therefore, similar to those defined for the linear theory. Therefore, in the following section we quickly survey the linear techniques and the notions necessary to compare with the nonlinear theory.

2.3.2 Linear feedback control

We consider the following linear system:

$$\dot{x} = Ax + Bu \tag{2.9}$$
$$y = Cx$$

with $x \in \Re^n$, $u, y \in \Re$, (SISO) and A, B and C are matrices of the dimensions, n×n, n×1 and 1×n, respectively.

Before applying a control technique, it is useful to verify the controllability conditions and to evaluate the relative order of the system. The relative order, also called the characteristic number, of a linear system is the difference between the order of the numerator and the denominator of the transfer function of the linear system. Hirschorn (1979) defined the relative order, r, of linear systems to be the smallest integer such that:

$$CA^{r-1}B \neq 0$$

The relative order can also be obtained by explicitly writing the derivatives of the output y. The relative order is the lowest order of the output that depends explicitly on the input.

Definition 2.4:

The system 2.9 is controllable if and only if $\forall$ initial state x_0, $\forall$ final state x_T and $\forall$ time T>0, there exists an input u on the interval [0,T] such that applying this input on the interval [0,T] gives the final state $x(T)=x_T$ from the initial state $x(0)=x_0$.

Among the well known controllers, the Proportional-Integral-Derivative (PID) controller has been the dominant control strategy for decades, since 1930 when it was commercially available for the first time. The PID algorithm is:

$$u(t) = \kappa_P \left(\varepsilon(t) + \frac{1}{\tau_I} \int_0^{t_f} \varepsilon(t)dt + \tau_D \frac{d\varepsilon(t)}{dt} \right)$$

$$\varepsilon(t) = \left(y_{sp}(t) - y(t) \right)$$

(2.10)

The PID algorithm is intuitive and quite simple. The tuning parameters, κ_p, τ_I and τ_D, are usually obtained by trial and error. They can also be optimized by using an identification technique in order to account for the process model. The primary disadvantage of the PID controller is that it is not based on a process model and process dynamics. For example, dead-time and model nonlinearity are not explicitly used in the control law.

More recent research efforts were focussed on providing control system techniques to handle constraints on manipulated and state variables, unmeasured state variables, unmeasured and frequent disturbances and dead-time on inputs and measurements. For example, robust control system theory (Doyle, 1982) was developed to account for model uncertainty. Internal Model Control (IMC), (Garcia and Morari (1982)) was developed to provide a transparent framework for process control system design. Adaptive control technique is based on the estimation of the unknown parameters, by recursive least square, of the model and then calculate the control parameters. This controller has been applied to

control polymerization reactors by Mendoza-Bustos et al. (1990), to control a solution CSTR of methyl methacrylate by manipulating the initiator feed rate and by Dittmar et al. (1991) for the temperature control of a solution polymerization reactor. However, the control theory of these controllers is well developed only for linear systems and thus, they are not directly applicable to nonlinear systems. Concerning polymerization process control, in most of the cases observed in the literature, optimal control theory was applied (e.g. Kiparissides et al. (1981) and Ponnuswamy et al. (1987)). The optimization algorithm is based on a linear, usually discretized, quadratic feedback control law.

These linear techniques were usually applied to highly nonlinear processes, by assuming a linear, sometimes discrete process. For processes with soft nonlinearities, the error introduced by locally linearizing around the steady state might be small enough that it can be rejected easily by a sufficiently robust linear regulator. For the regulation of severely nonlinear chemical processes a linear controller may have extremely poor performance, and the use of nonlinear elements may be a necessity. In the following section, we review the differential geometric nonlinear control techniques that exactly map the nonlinear system into input/output or global linear systems via state feedback.

2.3.3 Differential geometric nonlinear control

A major development in nonlinear theory was made when Herman and Krener (1977), Hunt et. al. (1983), Isidori (1989) and Vidyasagar (1986) adapted techniques from differential geometry, which are now used as an effective tool for the analysis and design of nonlinear control systems. The results generalize concepts and tools from linear control theory for a class of nonlinear systems, such as the state feedback. A background on the geometric methods for nonlinear process control can be found in Kravaris and Kantor (1990a) and (1990b).

There are two main ways of designing state feedback transformation for process control:
(i) state equation linearization renders the closed-loop state model linear.
(ii)input/output, (I/O), linearization which renders the I/O closed-loop system linear.

Global linearization control (GLC) involves finding global nonlinear transformations of the states and/or the manipulated inputs so that the transformed system possesses certain linear characteristics, (Isidori 1989).

When complete state exact linearization cannot be accomplished, input/output (I/O) linearization can be used (Isidori (1989)). The idea of globally linearizing a nonlinear system in an input/output sense was first introduced by Gilbert and Ha (1984). The GLC framework (Kravaris and Chung (1987), for SISO and Kravaris and Soroush (1990), for MIMO) is the calculation of a static-state feedback, under which the closed-loop I/O system is exactly linear. The state of the model need not be transformed into linear one. Once the inner loop is closed, the controller design reduces to the design of an external linear controller with integral action. Daoutidis and Kumar (1994) synthesized an output feedback controller concerning a general mutivariable nonlinear process, particularly those with singular characteristic matrix. The authors tested the technique by simulating several kinds of reactors.

Applications of the differential geometric approach to simulated control polymerization processes have appeared rather quickly. Alvarez et al. (1990) used the multivariable control technique to control the reactor temperature and the conversion in a free-radical polymerization CSTR of methyl methacrylate by manipulating the initiator feed rate and the heat removal rate. The use of a multivariable controller was indispensable since the analysis of the zero dynamics has shown that manipulating the heat removal rate alone does not ensure reactor temperature stability.

Soroush and Kravaris (1992) experimentally implemented the globally linearizing control method SISO and a PID controller to control the reactor temperature in a batch polymerization reactor of methyl methacrylate. Two manipulating variables were used: an electrical heat and the cooling water flow rate. The experimental results revealed the superiority of the nonlinear controller with respect to the conventional PID controller. A multivariable nonlinear controller (MIMO) was experimentally applied by Soroush and Kravaris (1993) to control a continuous solution polymerization reactor of methyl methacrylate. The manipulated variables were the initiator stream and the heat removal rate, and the controlled variables were the monomer conversion and the reactor temperature. For the same control outputs, conversion and temperature in a polymerization CSTR, Soroush and

Kravaris (1994) used as control inputs the heat input to jacket and the reactor residence time. Due to the interaction between the manipulated and controlled variables, the characteristic matrix became singular. The solution proposed to synthesize a controller for such a system was to use a dynamic input/output linearizing state feedback rather than a static feedback. Alvarez et al. (1994) used a semi-global nonlinear control based on complete input-output linearization to control a continuous polymerization reactor.

The I/O linearization is robust and applies to more general nonlinear systems, under the condition that the uncontrolled states are stable, which can be ensured by studying the so called zero dynamics (see Isidori (1987)). In the following sections, we present the controllability conditions and some definition necessary for the application of I/O linearizing control.

2.3.3.1 Relative order for SISO systems

Consider nonlinear single-input/single-output (SISO) systems of the form:

$$\dot{x} = f(x) + g(x)u \qquad\qquad (2.11)$$
$$y = h(x)$$

where $x = \begin{bmatrix} x_1 & \cdots & x_n \end{bmatrix}^T$ are the states, y is the output, f, g and h are C^∞ vector fields on R^n and $u \in R$, is the manipulated input.

For nonlinear systems, the system cannot be written under a transfer function and therefore the relative order is defined to be the smallest integer, r, such that:

$$L_g L_f^{r-1} h(x) \neq 0$$

Or again, the relative order was defined by Isidori (1989) and Kravaris and Kantor (1990) to be the smallest integer such that:

$$L_{ad_f^{r-1}} h(x) \neq 0$$

Finally, as for linear systems, the relative order of nonlinear systems can be obtained by explicitly writing the derivatives of the output y. The relative order is the lower order derivative of the output that depends explicitly on the input.

2.3.3.2 Input/output linearizing control for SISO systems

Isidori (1989) and Kravaris and Chung (1987) were the first to present a framework for transforming the nonlinear input/output system into a linear input/output system where the nonlinear process control system design problem reduces to the linear control system design problem.

First of all we review the I/O linearization problem for nonlinear single-input/single-output (SISO) systems of the form of 2.11. The objective is to find a function $\upsilon = \Omega(x, u)$ such that the dependence of y on υ is linear.

Definition 2.5: (Kravaris and Chung (1987)):
A system of the form 2.11 is called input/output linearizable if there exists a C^{∞} function from R^{n+1} to R^{n}, $\upsilon = \Omega(x, u)$, with $\partial\Omega / \partial u \neq 0$ and a linear differential operator of the form

$$L_r = \sum_{k=0}^{r} \beta_k \frac{d^k}{dt^k} \qquad (2.12)$$

such that:

$$L_r y = \upsilon \qquad (2.13)$$

Definition 2.6: (Kravaris and Chung (1987))
Assume that 2.11 is input/output linearizable. The smallest integer r for which there exists a transformation $\upsilon = \Omega(x, u)$ and a differential operator L_r of the form of 2.12 so that 2.13 is satisfied, is called the linearizablitiy index of 2.11.

Theorem 2.5: (Kravaris and Chung (1987))

A necessary and sufficient condition for input/output linearizability is the existence of a positive integer r such that

$$< dh, ad_f^{r-1} g > \neq 0 \tag{2.14}$$

The linearizability index is the smallest integer r for which 2.14 is satisfied.

Theorem 2.6: (Kravaris and Chung (1987))

Assume that 2.11 is input/output linearizable with linearizability index r. Then the state feedback transformation

$$\upsilon = \Omega(x, u) = \sum_{k=0}^{r} \beta_k \, L_f^k h + (-1)^{r-1} \beta_r < dh, ad_f^{r-1}(g) > u \tag{2.15}$$

transform the input/output system of 2.11 into

$$\sum_{k=0}^{r} \beta_k \frac{d^k y}{dt^k} = \upsilon \tag{2.16}$$

In the GLC, the external controller consists of a linear controller. Note however that the input/output linearizing control is a model based technique. If the model presents a deviation from the process, a steady-state difference between the set-point and the output will be present. Therefore the external controller must contain an integral action, for example, a PI or PID controller. Therefore, for the PI controller we can write,

$$\upsilon(t) = K_P \left(\varepsilon(t) + \frac{1}{\tau_I} \int_0^t \varepsilon(t) dt \right) \tag{2.17}$$

$$\varepsilon(t) = \left(y_{sp}(t) - y(t) \right)$$

This state feedback transformation gives the following:

$$u = \psi(x, u) = \frac{K_P \left(\varepsilon + \frac{1}{\tau_I} \int_0^t \varepsilon dt \right) - \sum_{k=0}^{r} \beta_k \, L_f^k h}{(-1)^{r-1} \beta_r < dh, ad_f^{r-1}(g) >} \tag{2.18}$$

β_k are chosen such that the poles of 2.16 are as far left in the complex plane as possible. The PI parameters must be tuned in a way that ensures the rapid and smooth convergence of the controller.

2.3.3.3 Relative order for MIMO systems

Consider the following nonlinear MIMO system, where the number of inputs equals the number of outputs:

$$\dot{x} = f(x) + \sum_{j=1}^{m} g_j(x)u_j$$

$$y_i = h_i(x), \quad i = 1...m$$

(2.19)

where $x = \begin{bmatrix} x_1 & \cdots & x_n \end{bmatrix}^T \in \mathfrak{R}^n$, $u = \begin{bmatrix} u_1 & \cdots & u_m \end{bmatrix}^T \in \mathfrak{R}^m$, $y = \begin{bmatrix} y_1 & \cdots & y_m \end{bmatrix} \in \mathfrak{R}^m$.

The relative order of the output y_i with respect to the input variables, is by definition, Kravaris and Soroush (1990), the smallest integer r_i such that

$$\begin{bmatrix} L_{g_1} L_f^{r_i-1} h_i(x) & L_{g_2} L_f^{r_i-1} h_i(x) & \cdots & L_{g_m} L_f^{r_i-1} h_i(x) \end{bmatrix} \neq \begin{bmatrix} 0 & 0 & 0 & 0 \end{bmatrix}$$

The characteristic matrix for MIMO systems, is defined by the following equation:

$$C(x) = \begin{bmatrix} L_{g_1} L_f^{r_1-1} h_1 & \cdots & L_{g_m} L_f^{r_1-1} h_1 \\ \vdots & & \vdots \\ L_{g_1} L_f^{r_m-1} h_m & \cdots & L_{g_m} L_f^{r_m-1} h_m \end{bmatrix}$$

If the characteristic matrix is nonsingular, the analysis and controller synthesis is conceptually similar to the one for SISO nonlinear processes.

2.3.3.4 Input/output linearizing control for MIMO systems

We now consider the nonlinear MIMO system given by equation 2.19.

Definition 2.7: (Kravaris and Soroush (1990))

A multivariable nonlinear system of the form of 2.19 is called input/ouput linearizable if there exists a static state feedback of the form:

$$u = P(x) + Q(x)\upsilon \qquad (2.20)$$

with $Q(x)$ nonsingular and linear vector differential operators of the form

$$L_{\rho i} = \sum_{k=0}^{\rho i} \beta_{ik} \frac{d^k}{dt^k}$$

with constant coefficients $\beta_{ik} = \begin{bmatrix} \beta_{ik}^1 & \beta_{ik}^2 & \cdots & \beta_{ik}^m \end{bmatrix}^T \in R^m$ satisfying $\beta_{ip_i} \neq 0$ and

$$\det\left[\left(\sum_{k=0}^{\rho_1}\beta_{1k}s^k\right)\left(\sum_{k=0}^{\rho_2}\beta_{2k}s^k\right)\cdots\left(\sum_{k=0}^{\rho_m}\beta_{mk}s^k\right)\right] \qquad (2.21)$$

such that

$$\sum_{i=1}^{m} L_{\rho i} y_i = \upsilon \qquad (2.22)$$

where s is the Laplace transform variable.

Theorem 2.7: (Kravaris and Soroush 1990)

A necessary condition for a system of the form of 2.19 to be input/output linearizable is that each output y_i possesses a relative order. Furthermore, if ρ_i are the orders of the linear opeators in the closed-loop response 2.22 and r_i are the relative orders of the outputs of 2.19, then

$$\rho_i \geq r_i, \qquad i = 1,\ldots,m$$

Theorem 2.8: (Kravaris and Soroush 1990)

The following conditions are sufficient for a system of the form of 2.19 to be input/output linearizable:

i) Each output y_i possesses a relative order r_i.

ii) Its characteristic matrix is nonsingular for all x.

Furthermore, if the above conditions hold, then for any arbitrary $\beta_{ik} \in R^n$ (k=0,...,r_i and i=1,...,m) that satisfy equation 2.21 and

$$\det\left[\beta_{1_{r1}} \quad \beta_{2_{r2}} \quad \cdots \quad \beta_{m_{rm}}\right] \neq 0$$

the state feedback

$$u = \left\{\left[\beta_{1_{r1}} \quad \beta_{1_{r1}} \quad \cdots \quad \beta_{1_{r1}}\right] L_g \begin{bmatrix} L_f^{r_1-1}h_1(x) \\ \vdots \\ L_f^{r_m-1}h_m(x) \end{bmatrix}\right\}^{-1} \left\{\upsilon - \sum_{i=1}^{m}\sum_{k=0}^{r_i}\beta_{ik}L_f^k h_i(x)\right\} \qquad (2.23)$$

produces the closed-loop response:

$$\sum_{i=1}^{m}\sum_{k=0}^{r_i}\beta_{ik}\frac{d^k y_i}{dt^k} = \upsilon \qquad (2.24)$$

υ consists of a linear external loop, for example PI or PID controller, as in equation 2.17.

2.4 Conclusion

The nonlinear estimation and control techniques reviewed in this chapter will be used throughout this work for the monitoring and control of emulsion polymerization.

Several factors must be accounted for when applying nonlinear observers, such as the form of the model, the observability of the states of interest, and the sensitivity of the measured outputs to changes in the states. These parameters will be investigated for each model used.

The application of nonlinear linearizing input/output control ensures the stability of the states of the process if the control parameters are well chosen, and if the stability of the uncontrolled states is not influenced by the controlled states.

Since the main difficulty for the application of process control is the lack of on-line measurements of most of polymer properties, in the next chapter, we will develop an on-line sensor of the overall monomer conversion, based on calorimetry. Different estimation techniques will be utilized throughout this chapter, such as on-line optimization procedure, and high gain and Kalman-like observers. Based on this real information, the material balances of co- and terpolymerization are used to construct observers of the polymer composition in real time, using the estimation techniques presented in this chapter. The control issue will be treated in the last part of this thesis (chapters 6 and 7).

2.5 Nomenclature

Notation

A	state matrix of dimension n×n
B	input matrix of dimension n×m
C	output matrix of dimension 1×n
C(x)	characteristic matrix
f	nonlinear state field
F	vector field in the nonlinear state model
G	input matrix of dimension n×m
g_i	i^{th} nonlinear dynamic function between inputs and states
h	nonlinear function between states and outputs
K_P	proportional gain of the PID controller
L_r	linear differential operator
m	number of inputs
n	number of states
p	number of outputs
r	relative order of the output y with respect to the input u
R	*the unique solution of the differential Riccati equation*
$\Re$	set of real numbers
t, t_0, t_1	time
T	transpose
u	manipulated input vector
u_i	i^{th} manipulated input
x	vector of state variables
x_i	i^{th} state variable
y	output vector variables
y_i	i^{th} output variable
y_{sp}	set-point
$\hat{x}$	estimated process state

Greek letters

β_j	tunable parameters of input/output linearized system
ε	error
ε_i	model uncertainties
ϕ	change of co-ordinates
θ	observer tuning parameter
S_θ	the unique solution of the algebraic Lyapunov equation
τ_I	integral time constant of the PID controller
τ_D	derivative time constant of the PID controller
υ	transformed control variable
ξ	transformed state
Ω	input/output linearizing transformation
Ψ	transformation

Acronyms

CSTR	continuous stirred tank reactor
EKF	extended Kalman filter
GLC	globally linearizing control
IMC	internal model control
I/O	input/output
KF	Kalman filter
MIMO	multi-input multi-output
P	proportional
PI	proportional intergral
PID	proportional integral derivtive
SISO	single-input single-output
sp	setpoint

Mathematical symbols

C^1	class of differentiable functions with continuous partial derivatives.
$[f,g]$	Lie brackets
$L_f h(x)$	Lie derivative of the scalar field $h(x)$ with respect to the vector field $f(x)$
$L_f^{r-1} h(x)$	$(r-1)$th-order Lie derivative of the scalar field $h(x)$ with respect to the vector field $f(x)$
$L_g L_f^{r-1} h(x)$	Lie derivative of the scalar field $L_f^{r-1} h(x)$ with respect to the vector field $g(x)$.
$\|x\|$	euclidien norm

List of definitions

Definition 2.1	observability
Definition 2.2	regularly persistent input
Definition 2.3	global Lipschitz
Definition 2.4	controllability
Definition 2.5	I/O linearizability in SISO systems
Definition 2.6	relative order
Definition 2.7	I/O linearizability in MIMO systes

List of theorems

Theorem 2.1	Hammouri et al. (1991)
Theorem 2.2	Gauthier et al. (1981 and 1992)
Theorem 2.3	Gauthier et al. (1992)
Theorem 2.4	Farza et al. (1997)
Theorem 2.5	Kravaris and Chung (1987)
Theorem 2.6	Kravaris and Chung (1987)
Theorem 2.7	Kravaris and Chung (1990)
Theorem 2.8	Kravaris and Chung (1990)

2.6 Bibliography

1.   Alvarez, J., R. Suarez and A. Sanchez, Nonlinear decoupling control of free radical polymerization continuous stirred tank reactors. *AIChE*, **45**, 11, 3341-3357, (1990).

2.   Alvarez, J., R. Suarez and A. Sanchez, Semiglobal nonlinear control based on complete input-output linearization and its application to the start-up of a continuous polymerization reactor. *Chem. Eng. Sci.,* **49**, 21, PP 3617-3630, (1994).

3.   Barudio, I., Développement d'une stratégie globale pour le contrôle d'un procédé de copolymerization en émulsion, Thesis, Université Claude Bernard-Lyon 1, (1997).

4.   Bestle, D. and M. Zeitz, Canonical form design for nonlinear observers with linearizable error dynamics, *Int J Control*, **23**, 419-431, (1983)

5.   Bornard, G., N. Couenne, and F. Celle, Regularly persistent observers for bilinear systems, Proceedings of the 29 international conference on nonlinear system theory, *Springer Verlag,* **122***,* (1988).

6.   Bornard, G., and H. Hammouri, A high gain for a class of nonlinear systems under locally regular inputs, 28th *IEEE CDC*, Brighton, UK, (1991).

7.   Chang, C.T. and J.-W. Chen, Implementation issues concerning the EKF-based fault diagnosis techniques, *Chem. Eng. Sci.* **50**, 18, 2861-2882, (1995).

8.   Daoutidis, P., and A. Kumar, Structural analysis and output feedback control of nonlinear multivariable processes, *AIChE*, April , 40, 4. (1994).

9.   Dimitratos, Y. N., Modeling and control of semi-continuous emulsion copolymerization, Thesis, Lehigh University, (1989).

10. Dimitratos, J., C. Georgakis, M. El-Aasser and A. klein, An experimental study of adaptive Kalman filtering in emulsion copolymerization*, Chem. Eng. Sci*, 46, 12, pp. 3203-3218, (1991).

11. Dittmar, R., Z. Ogonowski, K. Damert, Predictive control of a nonlinear open-loop unstable polymerization reactor, *Chem Eng Sci*, **46**, 10, 2679-2689, (1991).

12. Doyle, J., Analysis of feedback systems with structured uncertainties, *IEEE Proc*, **129**, 242-250, (1982).

13. Dubé, M. A., J. B. P. Soares, A. Penlidis and A. E. Hamielec, Mathematical modeling of multicomponent chain-growth polymerisation in batch, semicontinuous and continuous reactors: A review, *Ind Eng Chem Res* ,36, pp 966-1015, (1997).

14. Dubé, M. A., A. Penlidis, and P. M. Reilly, A systematic approach to the study of multicomponent polymerization kinetics: the butyl acrylate/methyl methacrylate/vinyl acetate example. IV. Optimal bayesian design of emulsion terpolymerisation experiments in a pilot plant reactor*, j of polymer science, part A: Polymer Chemistry*, 34, 811-831, (1996a).

15. Dubé, M. A., A. Penlidis, Emulsion terpolymerisation of butyl acrylate/ methyl methacrylate/vinyl acetate: experimental results*", The canadian journal of chemical engineering*, p 1659, (1996b).

16. Farza, M., H. Hammouri, S. Othman and K. Busawon, Nonlinear observers for parameter estimation in bioprocesses", *Chem. Eng. Sci*, 52, 23, 4251-4267, (1997).

17. Févotte, G., T.F. McKenna, S. Othman and H. Hammouri, Nonlinear tracking of glass transition temperature for free radical emulsion copolymers", *Chem. Eng. Sci*, 53, 4, 773-786, (1998).

18. Gagnon, L. and J. F. MacGregor, State estimation for continuous emulsion polymerization", *The canadian journal of chemical engineering*, 69, 649, (1991).

19. Garcia, C. E. and M. Morari, International model control. 1. A unifying review and some new results, *Ind. Eng. Chem. Proc. Des. Dev.*, **21**, 2, 308-323 (1982)

20. Gauthier, J.P. and G. Bornard, Observability for any u(t) of a class of bilinear systems, *IEEE Trans Automat Control*, 26, 922-926, (1981).

21. Gauthier, J.P., H. Hammouri and S. Othman, A simple observer for nonlinear systems. Application to bioreactors, *IEEE Trans. Automat Control*, 37, 875-880, (1992).

22. Gibon-Fargeot, A. M., H. Hammouri and F. Celle, Nonlinear estimators for chemical reactors, *Chem. Eng. Sci*, **42**, 14, 2287-1300, (1994).

23. Gilbert, E., and I. J. Ha, An approach to nonlinear feedback control with applications to robotics, *IEEE Trans. Syst. Man. Cybern.*, **SMC-14**, 879 (1984)

24. Hamielec, A. E., J. F. MacGregor, and A. Penlidis, Multicomponent free-radical polymerization in batch, semi-batch and continuous reactors, *Makromol. Chem. Macromol. Symp.*, **10**, 11, 521-570, (1987).

25. Hammouri, H., and G. Bornard, High gain observer for a class of uniformly observable systems, *30th IEEE CDC*, Brighton, (1991).

26. Hammouri, H, J. De Leon Morales, Observer synthesis for state-affine systems, *29th IEEE CDC*, Honolulu, Hawaii, (1990).

27. Herman, R., and A. Krener, Nonlinear controllability and observability, *IEEE Trans on automatic control*, **AC-22**, 5, (1977),

28. Hirschorn, R. M. Invertibility of multivariable nonlinear control systems, *IEEE Trans. Aut. Cont.*, **AC-24**, 6, 855-865, (1979).

29. Hunt, R., Su, G. Meyer, Global transformations of nonliner sustems, *IEEE Trans Aut. Cont.,* **AC-28**, 24-31, (1983).

30. Isidori, A., Nonlinear control systems. An introduction (2nd Edition), Springer-Verlag, (1989).

31. Karjala, T. W. and D. M. Himmelblau, Dynamic rectification of data via recurrent neural nets and the extended Kalman filter, *AIChE*, **42**, 8, 2225-2238, (1996),

32. Kalman R. E. and Bucy, New results in linear filtering and prediction theory, *Journal of basic engineering, Transactions of the ASME*, 95-108, (1961).

33. Kiparissides C., J. McGregor , A. Hamielec, Suboptimal sochastic control of a continuous latex reactor, *AIChE*, **27**, 1 , 13-19, (1981).

34. Kizub J.D., J. F. MacGregor, feed back control of polymer quality in semi-batch copolymerization reactors, Chem Eng Sc, **47**, 4, 929-942, (1992).

35. Kozub, D., J., and J. F. MacGregor, State estimation for semi-batch polymerization reactors, *Chem. Eng. Sci.*, **47**, 5, 1047-1062, (1992).

36. Kravaris C., C.B. Chung, Nonlinear state feedback synthesis by global input/output linearization, *AIChE*, **33,** 4, (1987).

37. Kravaris, C., and J. C. Kantor, Geometric methods for nonlinear process control. 1. Background. *Ind. Eng. Chem. Res.*, **29**, 2295-2310, (1990a).

38. Kravaris, C., and J. C. Kantor, Geometric methods for nonlinear process control. 2. Controller synthesis. *Ind. Eng. Chem. Res.*, **29**, 2310-2323, (1990b).

39. Krener, A. J., and A. Isidori, Linearization by output injection and nonlinear observers, *Syst Control Lett*, **3**, 47-52, (1983)

40. Krener, A. J., and W. Respondek, Nonlinear observers with linear error dynamics, *SIAM J. Control Optim*, **23**, 197-216, (1985).

41. Leiza, J. R. R., Desarrollo de un sistema automatico composicion de polymeros obtenidos en emulsion, Thesis, Euskal Herriko Unibertsitatea, (1991).

42. Lopez de Arbina L, M. J. Barandiaran, L. M. Gugliotta and J. M. Asua, Kinetics of the emulsion copolymerization of styrene and butyl acrylate, **38**, 1, 143-148, (1997).

43. Makgawinata T., M. S. El-Aasser, A. Klein and J. W. Vanderhoff, Kinetic studies of semi-batch emulsion copolymerization of 80 :20 vinyl acetate-butyl acrylate, *J. Dispersion Science and Technology*, **5,** (3&4), 301-322, (1984).

44. Mead, R. N., and G. W. Poehlein, Emulsion copolymerization of styrene-methyl acrylate and styrene-acrylonitrile in continuous stirred tank reactors. 1, *Ind. Eng. Chem. Res.*, **27**, 2283-2293, (1988).

45. Mendoza-Bustos S. A., A. Penlidis, and W. R. Cluett, Robust adaptive process control of a polymerization reactor, *Computer chem Eng,* **14**, 3, 251-258, (1990).

46. Mutha, R. K., W. R. Cluett, and A. Penlidis, Nonlinear model-based estimation and control of a polymer reactor: experimental results, *AIChE J.*, **43**, 11, 3042-3070, (1997).

47. Penlidis, A., J. F. MacGregor and A. E. Hamielec, A theoretical and experimental and experimental investigation of the batch emulsion polymerization of vinyl acetate, **3**, 3, 185-218, (1985).

48. Ponnuswamy, S. R., S. L. Shah, C. Kiparissides, Computer optimal control of batch polymerization reactors, *American Chemical Society,* **26,** 11, 2229-2236, (1987).

49. Régnier, N., G. Defaye, L. Caralp and C. Vidal, Software sensor based control of exothermic batch reactors, *Chem. Eng. Sci.*, 51, 23, 5125-5136, (1996).

50. Richard, J., J. P. and Congalidis, Mathematical modeling of emulsion copolymerization reactors, *J. Appl. Polym. Sci.*, **37**, 2727-2756, (1989).

51. Saldivar, E., and W. H. Ray, Control of semicontinuous emulsion copolymerization reactors, *AIChE*, **43**, 8, 2021-2033, (1997).

52. Saldivar, E., P. Dafniotis, and W. H. Ray, Mathematical modeling of emulsion copolymerization reactors I. model formulation and application to reactors operating with micellar nucleation, *Macromol Chem Phys*, **C38**, 2, 207-325, (1998)

53. Soroush, M, C. Kravaris, Nonlinear control of a batch polymerization reactor: an experimental study, *AIChE*, **38**, 9, 1429-1447, (1992).

54. Soroush, M., C. Kravaris, Multivariable nonlinear, control of a continuous polymerization reactor: an experimental study, *AIChE*, **39**, 12, 1920-1937, (1993).

55. Soroush, M, C. Kravaris, Nonlinear control of a polymzrization CSTR with singular characteristic matrix, *AIChE*, **40**, 6, (1994).

56. Storti, G., S. Carra, M. Morbidelli, G. Vita, Kinetics of multimonomer emulsion polymerization. The pseudo-homopolymerization approach, *J. Appl. Polym. Sci.*, **37**, 2443-2467, (1989).

57. Terwiesch, P. and M. Agarwal, A discretized nonlinear state estimator for batch processes, *Comp. Chem. Eng.*, **19**, 2, 155-169, (1995).

58. Urretabizkaia, A., G. Arzamendi and J. M. Asua," Modeling semicontinuous emulsion terpolymerization", *Chem Eng Sci*, **47**, 9-11, 2579-2584, (1992).

59. Wayne Bequette, B., Nonlinear control of chemical processes: A review. *Ind. Eng. Chem. Res.*, **30**, 1391-1413, (1991).

60. Wonham, W. M, Linear multivariable control. A geometric approach. Springer-Verlag, (1985).

CHAPTER III ──────────────

CALORIMETRY

3 CALORIMETRY

3.1 Introduction

The production of polymers with prespecified qualities requires continual monitoring and control of the process, in order to insure that the "real" properties do not deviate from the desired ones. The process must therefore be equipped with accurate on-line sensors to measure these properties in real time (i.e on-line). For each application, specific equipment, that is sensitive to variations in the properties of interest, and that are able to handle the multiphase, viscous nature of a latex system is required. Therefore, research into the development of on-line sensors, estimation and control techniques in polymerization reactors is an important on-going activity.

The on-line measurements that are usually available in a typical polymerization reactor are the temperature, pH, pressure and flow rate(s). Measurements of parameters that significantly influence polymer properties, such as particle size, molecular weight distributions, polymer composition and morphology are more difficult to obtain on-line. Nevertheless, several on-line techniques have been developed to monitor specific properties in emulsion polymerization reactors, such as densimetry (based on the density difference between the monomer and the polymer, giving thus an estimation of the monomer conversion), gas chromatography (GC), which is an extension of the apparatus developed for off-line measurements, refractive index measurements, infrared (IR), dielectric, Raman and ultrasonic spectroscopy. Some of these sensors require a sampling device or an auxiliary circulating loop, in order to perform the analysis. Others are in situ but require an extensive calibration, or are very sensitive to polymer viscosity and coagulation of polymer particles in the device. However, as we will see later, some sensors, such as Raman, IR, and Ultrasonic spectroscopy, seem to be promising.

The most widely used on-line sensor over the past 30 years is probably calorimetry, the science of measuring a quantity of heat. Reaction calorimetry is based on temperature

measurements and an energy balance around a reactor. If the heat capacity of all substances present in the calorimeter, and the heat exchange coefficients with the surroundings are known, then the amount of heat liberated by the chemical reaction can be readily calculated by writing down the heat balance of the reactor.

Calorimetry in safety studies. Since calorimetry is based on the measurement of the rate of heat generated, it has found widespread use in chemical process work, and in particular polymerization reactions as they tend to be very exothermic. As such, calorimetry finds a variety of uses, in safety studies, basic research, and process optimization and scale-up.

A high priority application of calorimetry is temperature control to ensure safe reactor operation, especially for reactions which can change mechanism suddenly causing a runaway reaction. A runaway reaction can lead to the release of environmentally dangerous substances, and can cause serious physical equipment damage (reactor vessel failure if the temperature increase elevates system pressure) or even provoke explosions, etc. The cost of accidents, in material and human terms, can be significant for an industrial reactor, and therefore monitoring and control of reactor temperature is necessary from an economical, human, and environmental point of view. References related to safety via reactor temperature control of exothermic batch and semi-batch polymerizations are manifold-e.g. Schmidt and Reichert (1988), Dittmar et al. (1991), Soroush and Kravaris (1992 and 1993), Landau et al. (1994), Berber (1996), Debelak and Hunkeler (1997), Regenass (1997), and Uchida et al. (1998).

Calorimetry for basic research. In addition to applications related to safety, calorimetry has been used as a tool of basic research in chemical processes. Thermo-analytical microcalorimeters, Differential Thermal Analyzis (DTA) and Differential Scanning Calorimeter (DSC), can be used to provide thermokinetic parameters (e.g. heat capacity and enthalpy measurements), kinetics (the activation energy, the reaction order and the reaction rate constant) and potential hazard of chemical reactions. Estimation of kinetic parameters in free-radical polymerization have also been done in an adiabatic calorimeter by Mosebach and Reichert (1997). Much work on the use of isothermal calorimetry for parameter estimations in emulsion polymerization has also been reported, e.g. Barandiaran et al. (1995), de la Rosa et al. (1996) and (1999[a,b]), Tauer et al. (1999).

Calorimetry for process optimization and scale up. If we have a good understanding of the physical system, calorimetry can be used in the optimization and control of the plant operation. By controlling the reaction rate, the temperature can be maintained inferior to the onset of thermal runaway, allowing us to maintain safe operation, and simultaneously improve productivity and the product quality, which leads to reduced costs and added capacity. Several references dealing with maximizing productivity, estimating properties, and control in free radical polymerizations by calorimetry can be found in the literature (e.g. Tirrell and Gromley (1981), Arzamendi and Asua (1991), Gugliotta et al. (1995), Buruaga et al. (1996), Gloor and Warner (1996), Bururaga et al. (1997[a,b,c]) and Gugliotta et al. (1999)).

In this work, we will focus on the calorimetry as a tool for analyzing and scaling-up polymerization process, and for monitoring and controlling laboratory, pilot scale and industrial reactors, with particular attention placed on composition control under safe conditions. In the following section we present the heat balance of a typical well mixed semi-continuous reactor. In section 3.1.2, we discuss the different types of calorimeters used to realize emulsion polymerizations. Finally, in section 3.1.3, a quick review of the other on-line sensors for polymerization processes is presented.

3.1.1 Energy balance

One of the main objectives of using calorimetry is to estimate the amount of heat produced by the reaction. The energy balance that is solved when we apply calorimetry contains both kinetic and thermodynamic terms that contribute to the temperature change. The heat released by the reaction cannot therefore be directly determined from the total rate of heat accumulation. In this section, we will briefly develop an energy balance for the reactor used for free-radical polymerizations.

Consider a well-mixed, semi-continuous, jacketed reactor. The energy balance involves: the heat due to reaction being carried out, the heat flow through the wall, the accumulation of energy in the reactor, the sensible heat effect of the feed, the latent heat of vaporization, and possibly a heat loss term. The energy balance around the reactor therefore takes the following form:

$$Q_{accu} = Q_R + Q_{feed} + Q_j + Q_{stirrer} - Q_{loss} - Q_{condenser} \tag{3.1}$$

The amount of energy that is accumulated in the reactor, Q_{accu}, is a function of the temperature change and the heat capacities of the reactor components and the reactants. It can be written under the following form:

$$Q_{accu} = \left(m_{ins}C_{Pins} + \sum_i m_i C_{pi} \right) \frac{dT_R}{dt} \tag{3.2}$$

$$m_r C_{Pr} = \sum_i m_i C_{pi}$$

where T_R is the temperature in the reactor, $m_{ins}C_{pins}$ is the heat capacity of the reactor components (wall, stirrer, baffle), $m_r C_{Pr}$ is the total capacity of the chemical components in the reactor, and $m_i C_{Pi}$ is the heat capacity of substance i present in the reactor. It is important to point out that under isothermal conditions the derivation in equation 3.2 is zero, and one can therefore neglect the thermal capacity of the reactor components. However, under non-steady state conditions this term must be introduced in the energy balance, which requires us

to divide the reactor components into two parts: the part wetted by the reactant mass and the part that is maintained dry inside the reactor, and to calculate their heat capacities individually. Since the reactor is usually operated under isothermal condition and because of the difficulty of precisely calculating the heat capacity of the reactor components, they will be neglected in this work.

Q_R refers to the heat produced by the reaction. It is directly related to the reaction rates and their respective enthalpy changes. When the individual rates of polymerization are defined in moles per second, the rate of heat generated is

$$Q_R = \sum_{i=1}^{N_R} \left(-\Delta H_{Pi}\right) R_{Pi} \tag{3.3}$$

where N_R is the number of monomers.

In general, several components can be added in semi-continuous fashion to the reactor, at a temperature lower than the reactor temperature. The contribution of this variable to the energy balances is Q_{feed}, the sensible heat change:

$$Q_{feed} = \dot{m}_f C_{Pfeed} \left(T_{feed} - T_R\right) \tag{3.4}$$

where, T_{feed}, $\dot{m}_f C_{Pfeed}$ are the temperature and the heat capacities of the introduced components respectively.

The conductive heat flux through the jacket varies linearly with the temperature gradient (T_R-T_j). With the exception of adiabatically operated reactors, heat transfer to the jacket is determinant for the reactor behavior. For a well mixed reactor, and if the temperature of the circulating fluid in the jacket is homogeneous (high circulating flow rate in the jacket), the rate of heat transfer through the reactor wall is given by:

$$Q_j = UA\left(T_j - T_R\right) \tag{3.5}$$

where U (W/m²/K) is the overall heat transfer coefficient between the reaction mass and the jacket, and A is the wetted surface area available for heat transfer, that should be calculated as a function of the reaction mixture volume, physical properties, and the effect of stirring. In this work, A will not be calculated separately since we will estimate the global effective heat

transfer coefficient UA. The temperature T_j, in equation 3.5, is the average jacket temperature. In our calorimeter (usually operated under isoperibolic conditions), T_j is almost constant due to a high flow rate in the jacket. If the jacket temperature is not constant, it must be corrected, as a function of the inlet and outlet temperatures.

$Q_{stirrer}$ represents the power input dissipated in the reactor by stirring. However, in most emulsion polymerizations we maintain relatively low agitation rates with moderate viscosity, and therefore $Q_{stirrer}$ can be neglected.

Q_{loss} represents the heat flow loss with the surroundings. Q_{loss} becomes important when the temperature difference between the reactor and the surroundings increases. If a radiation interchange between the jacket and the reactor is considered, Q_{loss} can be written under the following form:

$$Q_{loss} = A_R \alpha_{Ra} T_R^4 - A_a \alpha_{aR} T_{amb}^4 \qquad (3.6)$$

where $A_R \alpha_{Ra}$ is the total heat exchange area between the reactor and the ambient (on the unjacketed part of the reactor), and T_{amb} is the ambient temperature. In general, we assume that $A_R \alpha_{Ra} \cong A_a \alpha_{aR}$.

In a jacketed calorimeter, almost all the reactor surface is surrounded by the jacket. The majority of heat loss is due to the condenser, $Q_{condenser}$ (usually polymerization reactors are equipped with a condenser to prevent monomer evaporation and to help to evacuate Q_R, especially in industrial reactors). $Q_{condenser}$ is therefore the number of watts exchanged with the condensed materials. It therefore depends on the amount of vapor in the condenser (which is proportional to the amount of monomer in the reactor) and on the temperature difference between the vapor and the fluid circulating in the condenser serpentine. For these reasons, $Q_{condenser}$ is not easy to model and we will therefore not try to estimate it separately from Q_{loss}.

In this work, we will assume a global time varying heat loss term Q_{loss} that accounts for the heat loss to the surroundings, the heat loss by the condenser $Q_{condenser}$, and, under non-steady state conditions, the heat absorbed or released by the reactor components, $m_{ins} C_{Pins} \dfrac{dT_R}{dt}$. Landau (1996) noted that the heat capacity of the reactor components increases

with volume and becomes significant under non-steady state conditions. When temperature ramps are executed in the reactor temperature or when an abrupt increase in the heat produced by the reaction takes place, the reactor temperature takes much longer time to reach equilibrium in a large reactor than in a little one, since the reactor itself absorbs or releases heat.

A separate energy balance can be done on the cooling jacket. The heat balance on the jacket is useful for temperature control, and can be used to obtain further information on the process, such as the heat transfer coefficient with the reactor wall, U. Two main terms are determinant for the total heat change in the jacket $Q_{accu,j}$: a convective term, $Q_{conv,j}$, due to circulation loop, and the conduction with the reactor wall, $Q_{cond,j}$ according to the following energy balance:

$$Q_{accu,j} = Q_{conv,j} + Q_{cond,j} + Q_{loss,j} \qquad (3.7)$$

where, (for a high flow rate in the jacket, and a well mixed reactor):

$$Q_{accu,j} = m_j C_{Pj} \frac{dT_j}{dt}$$

$$Q_{conv,j} = \dot{m}_j C_{Pj} \left(T_j^{in} - T_j^{out} \right) \qquad (3.8)$$

$$Q_{cond,j} = UA \left(T_R - T_j \right)$$

T_j^{in} and T_j^{out} are the inlet and outlet temperatures of the jacket respectively, $m_j C_{Pj}$ is the specific heat capacity of the amount of liquid circulating in the jacket and $\dot{m}_j$ is the mass flow rate of the circulating fluid.

The heat loss from the jacket to the surroundings, $Q_{loss,j}$, is a function of the temperature difference between the jacket and the ambient temperature and the surface of contact. This term becomes less important in a large reactor since the surface to volume ratio decreases with volume (if we keep the same height to diameter ratio while expanding the reactor).

In the event that the $(T_j^{in}-T_j^{out})$ can be measured, the energy balance of the jacket can be used to estimate U. This requires that either $Q_{accu,j}$ or $Q_{conv,j}$ be non zero. However, since

we assume a high flow rate in the jacket in order to introduce T_j in $Q_{cond,j}$, then high accuracy of estimation of U is obtained when T_j varies a lot, varying thereby $Q_{accu,j}$.

In conclusion, we restate that our objective is to use calorimetry to estimate the heat produced by the reaction which will allow us to obtain direct information about the reaction rates and the final polymer properties. Q_R can be determined from the energy balance if the different temperatures involved in the energy balance, and the feed stream flow rates are measured, and if the heat transfer coefficient, U, is known.

In the following section a brief review of calorimeters used for polymerization processes is presented. The objective of this review is to reveal the importance and wide spread use of the calorimetry, and to justify our choice of calorimeter design. We cannot avoid naming the other sensors that can be applied for the on-line monitoring of emulsion polymerizations. In section 3.1.3, a quick review of these on-line sensors is presented. The estimation of initial values of U and Q_{loss}, will be treated in section 3.3, and section 3.4 treats the on-line estimation of UA and Q_{loss} during the polymerization.

3.1.2 A review of polymerization calorimeters

A great variety of calorimeters, with various experimental operating conditions, have been designed for chemical reactions. They can be classified according to their design or method of heat flow control and operation mode: isothermal and nonisothermal (isoperibolic, adiabatic or oscillatory) calorimeters. Note that we are interested by calorimeters of simple design for which the data can be treated in a straightforward and rapid manner, and in particular in a method of data interpretation that can be directly implemented in industrial plants.

With these restrictions we intentionally leave out all microcalorimeter designs (volume~20μl) including DTA and DSC. The operating conditions in the microcalorimeters are not comparable with those of large scale reactors (in terms of heat transfer, temperature control, and stirring effects). The microcalorimeters find their main use in the measurement of the integral heat evolution giving thus an estimate of kinetics or thermokinetic parameters of the polymerization. They are used to detect endo- or exothermic effects on the sample. The principle of detecting these effects is based on cooling or heating the sample that causes its solidification and melting.

Likewise, we will not consider adiabatic calorimeters. The design of an adiabatic reactor is rather simple. No heat transfer to the surroundings is permitted. This can be done by thermally isolating the reactor, or by maintaining the temperature of the surroundings as high as the reactor temperature, and there are cases where the reaction is so fast that during the reaction time no heat can be carried off or supplied into the system. The energy balance for an adiabatic polymerization reactor takes the following form:

$$\underbrace{\frac{dT_R}{dt}\sum_i m_i C_{Pi}}_{Q_{accumulation}} = \underbrace{V_R C_{M,0} \frac{dX}{dt}}_{Q_R} \tag{3.9}$$

where $C_{M,0}$ is the initial monomer concentration, V_R is the reactor volume, T_R the reactor temperature, m_iC_{Pi} the heat capacity of the substance i, and X is the conversion.

The advantage of this design, as given by equation 3.9, is that the change in the reactor temperature is proportional to the conversion. Therefore, it can be used for the determination of kinetic parameters (the overall reaction rate constant, the reaction order), and thermodynamic data (reaction enthalpy). Adiabatic calorimetry is also an important tool in studying the risk of thermal runaway in exothermic reactive systems. Process design parameters, such as the adiabatic temperature rise or maximum attainable pressure, can directly be determined. An additional advantage of adiabatic calorimeters with respect to the other isothermal and non-isothermal calorimeters, is that one does not need to calculate the heat exchange with the surroundings or the jacket. References on adiabatic calorimetry for heat capacity, enthalpy or kinetic studies, on the micro- and medium scale instruments, are numerous, e.g. Tufano (1993), Helt and Anderson (1996) and Maschio et al. (1999). A recent example of adiabatic reaction calorimeter for the determination of kinetic and thermodynamic data of free-radical polymerization was developed by Mosebach and Reichert (1997).

However, adiabatic conditions cannot usually be extended to large scale reactors since there is no control of the reactor temperature. On the other hand, the head plate temperature must be well controlled to prevent heat exchange. Finally, even if problems related to thermal runaway can be avoided a high temperature increase will strongly affect the rate of reaction and final properties of the polymer mixture.

The simplest design in terms of interpreting data from a calorimeter and the most efficient means of maintaining safe conditions is to perform experimental and kinetic studies under isothermal conditions. In isothermal reactors, the reactor temperature is controlled at a fixed pre-determined set-point. The common and most efficient design of isothermal reactors requires a control loop including a cooling system in addition to the thermostat. Other techniques for maintaining isothermal conditions are reviewed by Karlsen and Villadsen (1987). An example of commercially jacketed isothermal calorimeters is the RC1 (Reaction Calorimeter 1), developed by Mettler Instruments (able to carry out isothermal adiabatic, and temperature programmed experiments). Isothermal calorimeters hold certain advantages over nonisothermal calorimeters (isoperibolic and adiabatic). They have a very substantial

potential for use in the process industry. From the point of view of process operating conditions and kinetic studies, the interpretation is more straightforward if the reaction temperature remains constant.

In some reactors the control objective is to maintain the jacket temperature at a fixed set-point, and in this case the reactor is isoperibolic. From the point of view of its construction and operation, an isoperibolic reactor is the simplest type of calorimeter, since one only needs to maintain a constant jacket temperature and it therefore only requires a thermostat. Moreover, if the flow rate of cooling fluid is high enough, and the reaction rate remains reasonable, this design is sufficient in some cases to directly eliminate the heat released by the reaction through the jacket.

The main difficulty of using non-adiabatic (isothermal or isoperibolic) calorimetry is the estimation of the lumped jacket heat exchange coefficient, UA. One approach to solve this problem is to independently estimate the heat flux of the reaction and the heat transfer coefficient by combining the heat balance of the reactor and the jacket, ex. Schmidt and Reichert (1988) where the derivatives of the reactor and jacket temperatures were introduced. MacGregor (1986) proposed a Kalman filter, to estimate Q_R and Q_j, to avoid problems related to the calculation of the temperature derivative (that might give an increase in the measurement noise), and to take into account model uncertainties. MacGregor also proposed a recursive least square to estimate Q_j, using the energy balance on the jacket, and only Q_R is estimated by Kalman filter. It should be noted however, that studying the heat balance on the jacket requires that the jacket be insulated to prevent heat loss to the surroundings, and some constraints on the jacket flow rate must be considered.

Another way to estimate UA and Q_R independently is by combining the temperature measurements with some off-line measurements of the monomer conversion. For instance, Févotte et al. (1996), described a strategy, that the authors refer to as "adaptive calorimetry", for the determination of conversion during batch polymerizations. In this method, calorimetric data were combined with occasional discrete gravimetric measurements to up-date the estimation of the heat transfer coefficient, U, and the heat loss. The unknown parameters were corrected as a function of the conversion introducing some parameters to be optimized by minimizing the sum of least square error between the off-line gravimetric measurements and

the estimated conversion. The use of off-line gravimetric measurements to update estimations of UA and Q_R will be clarified in section 3.5.

Buruaga et al.(1997[a,c]) used calorimetry for the composition and heat flux control in semi-batch emulsion polymerization. Experiments were carried out in an RC1 heat-flow reactor to find the initial and final values of the heat exchange coefficient with the jacket, by calibration. During the reaction, the heat exchange with the jacket was supposed to vary mainly as a function of the viscosity and solid contents. In addition to the RC1 computer, a supplementary PC was used to run the heat and mass balances with a variable heat exchange with the jacket. This is fine just so longer no unforeseen coagulation takes place, but not a strategy that can be directly applied in an industrial reactor.

Finally, in order to estimate UA and Q_R during the reaction, a new apparatus, that employs a non-stationary calorimetric technique, was used on the laboratory scale to monitor polymerization processes. The reactor is equipped with an electrically oscillating resistance that periodically induces sinusoidal temperature oscillations either in the reaction mass or in the jacket. The corresponding temperature, on the opposite site from the resistance heater, is used to decouple the term related to Q_R from the variable heat transfer through the jacket during the reaction. The concept of evaluation is based on the assumption that the overall conductive heat flow may be subdivided into a slowly changing part.

Carloff et al. (1994) applied temperature oscillation calorimetry to the free radical polymerization of methyl methacrylate (MMA) in ethyl acetate (EAc). A characteristic of this reaction is the strong increase of viscosity in the reaction mass and therefore the decrease in heat transfer coefficient. Nevertheless, this technique allowed the authors to obtain good estimations of the varying UA and Q_R. In a more recent work, Tietze et al. (1996), presented an application of temperature oscillation calorimetry to free radical semi-continuous polymerization of acrylic monomers in solution to determine U and Q_R. First of all, the continuous estimation of U during the reaction shows that the initial estimate of U, obtained before the reaction, is correct, which means that calibration heater is no longer necessary. Secondly, an increase of UA was found noticed during the semi-batch stage, due to the increasing heat transfer area. In the subsequent batch period, UA decreases because of the increasing viscosity, which is a characteristic of acrylic monomers.

This type of calorimeter is interesting at the laboratory scale, but is not applicable in large scale reactors, since the reactor is not well mixed and we might have temperature gradients inside the reactor. In this case, temperature oscillations cannot be measured on the opposite side from the resistance heater generating the oscillations.

In conclusion, isothermal, or isoperibolic calorimeters seem to be the best adapted to kinetic and experimental studies, and the same techniques used to interpret the data at the laboratory scale can be used on large scale reactors. Isoperibolic calorimeters can be used if the temperature variations in the reactor do not provoke runaway conditions. We have therefore constructed a new calorimeter in the laboratory, where we can use both operating modes, isoperibolic or isothermal. In both of these designs, the heat transfer coefficient, U, must be determined by an additional sensor. This problem is studied in more detail in sections 3.3 and 3.4.

In the following section we briefly review different on-line sensors used to monitor polymerization processes. The objective of this review is to point out some of the difficulties of on-line measurement in emulsion polymerization, and to briefly describe how they can be developed to monitor specific properties, such as the overall conversion and/or composition. After this review, the discussion will be consecrated to the use of calorimetry in polymerization reactor control.

3.1.3 On-line sensors for emulsion polymerization

This section is intended to provide the reader with some tendencies in the area of developing other types of on-line sensors. It is not meant to be exhaustive. For more detailed discussions, the reader is referred to reviews by Chien and Penlidis(1990), Kammona et al. (1999), and Guinot et. al. (2000).

Initial efforts in the development of on-line sensors were focused on the extrapolation of existing off-line techniques, such as GC, dynamic light scattering or nuclear magnetic resonance (NMR), by analyzing either the monomer or the polymer content. However, these techniques usually require a number of operations on the sample before it is analyzed-e.g. dilution, drying or phase separation. Therefore, in order to realize these operations on-line, the process must be equipped with a sampling device, such as in the on-line GC, or a supplementary circulation loop, as in on-line densimetry, which can be costly in terms of time and installation, and can be problematic in an industrial environment. Afterwards, efforts were devoted to develop in situ sensors that are better for on-line process monitoring.

Densimetry can be used to monitor conversion based on the density difference between the polymer (typically between 1 and 1.2 g/cm^3) and the unreacted monomer (between 0.8 and 1 g/cm^3). A highly accurate measurement of the density of the reaction mixture must be realized to obtain an accurate estimate of the conversion. This technique is straightforward for homopolymerization reactions. For example, Ponnuswamy et al. (1986) were able to predict monomer conversion in solution polymerization of MMA precisely. In absence of temperature gradients or polymer scale, the method seems to be useful for on-line monitoring of monomer conversion for homopolymerization. In the case of copolymerization or terpolymerization, another on-line copolymer composition sensor, or a mathematical model that relates polymer composition to copolymer density, is required to predict the individual conversions from the density of the reaction mixture. Several works in the literature treat the monitoring of emulsion copolymerization by densimetry, e.g. Abbey (1981), who was the first to use an oscillating tube density meter, Shork and Ray (1988), Canegallo et al. (1993), and Barudio (1997).

The advantage of this technique is that it does not require the destruction of the latex , the device is independent of the reactor size and design, and it does not require frequent recalibration. Moreover, data collection can be realized rapidity.

However, in emulsion polymerization, sampling problems, such as pump failure due to monomer attack, flocculation of the latex particles in the circulation loop at high conversions, polymer scale formation, phase separation in the density cell, and the lag time for rapid polymerization, were reported by Barudio (1997). Moreover, the measurement can be significantly disturbed by nitrogen bubbles and monomer droplet coalescence within the sampling circuit. It was also found that the addition of an external circulating loop inhibits the reaction rate. In addition, this technique requires a complex, often empirical, model to link the densimetry of a copolymer to individual monomer conversion.

Another real-time technique that necessitates the installation of a sampling loop, is the on-line gas chromatography (GC). GC is a standard method for analyzing the residual monomer to estimate the copolymer composition, the individual conversions and therefore the reaction rates. Leiza (1991) used GC for the composition control in the emulsion copolymerization of ethyl acrylate (EA) and MMA, where the latex was directly analyzed to give the number of moles of free monomer. Only discrete and delayed measurements could be obtained. However, on-line GC usually involves a dilution system before the sample analysis. Guyot et al. (1984) used on-line GC, provided by a dilution cell to control the composition in the emulsion copolymerization of butyl acrylate (BuA) and vinyl acetate (VAc).

To avoid problems involved in analyzing a latex sample or latex flocculation in the pump, the reactor head space vapor can also be analyzed to estimate the monomer composition in the reaction mixture. This technique was used by Alonos (1987) for the composition estimation during batch emulsion copolymerisation. Measurements could be obtained more frequently than while using a latex analyzing GC. The main disadvantage of this approach with respect to the latex analyzing GC is that it requires an adequate thermodynamic equilibrium model of the liquid-vapor, and solid phases in the reactor, and the knowledge of the monomer partition coefficients between the different phases.

In summary, it is clear that the latex transfer, by sampling or pumping, might induce shear coagulation and damage the pump or sampling device and presents time delays. Moreover, these auxiliary devices must be frequently cleaned of polymer deposits with solvent. This necessitates also the use of advanced control laws tolerating time delays and dealing with a sampling loop or circulation pumps, and an effective cleaning system. Consequently, a significant effort has recently been made in the development of in situ on-line polymerization sensors such as spectroscopic (IR, MIR, Raman) and ultrasonic probes. The development of such on-line sensors requires an improved study of the process and the reactor design and accurate mathematical correlations that relate the measured signals to the physical properties of the product, or to the reaction rate.

A promising on-line robust technique for emulsion polymerization is infrared (IR) spectroscopy. The spectroscopic information, obtained by the interpretation of vibration data, is based on the combined Beer-Lambert law. Near-infrared spectroscopy, NIR, is suitable for structural and kinetic data analysis, and requires (in principle) only a fiber-optic probe in the reactor (eg. Gossen et al. (1993), Aldridge et al. (1993), Santos et al. (1998), Johnson et al.(1998)). Calibration of the device must be done using solutions of polymers with known composition. However, it is necessary that the monomers have specific absorbances in the NIR region in order that they can be characterized. A major drawback of this technique is that, throughout the NIR region, absorption peaks are very broad and can overlap. On the other hand, by using the midrange infrared spectroscopy (MIR), the individual conversions can be estimated by characterizing the monomer and polymer vibrations over a wide range of concentrations (eg. Chatzi et al. (1997)). The main obstacle for the application of the MIR measurements is the lack of materials that can adequately transmit radiation in this region.

Ultrasonic propagation velocity (UPV) measurements have traditionally been used to evaluate some properties of the latex, such as monomer solubility in polymer particles and the critical micellar concentration of surfactants in water. Recently, measurements of ultrasound propagation have been employed for the monomer conversion estimation. The technique is based on the measurement of velocity and attenuation of high frequency sound wave passing through a sample. In a homogeneous system, the UPV depends on the inverse of the square root of the product of density and compressibility, which both change as a function of conversion.

$$UPV(m/s) = \frac{1}{\sqrt{\rho\beta}}$$

where: ρ, density of the homogeneous medium (kg/m^3).

β, a compressibility factor ($s^2.m/kg$).

Ultrasonic sensors combined with a good mathematical model have successfully been used to estimate on-line conversion and polymer composition, ex. Siani et al. (1998). The advantage of this technique is the absence of sampling devices since the measurement is realized in situ. However, this sensor requires extensive calibration for each copolymer composition. Siani et al. (1999) treated the calibration problem and proposed a procedure for on-line conversion and polymer composition estimation.

This section clearly shows that in situ sensors have many advantages for process on-line monitoring, since they do not present a time delay in the measurement, they are nondestructive and do not need supplementary sampling devices. Some of these sensors, such as NIR and MIR, seem to be encouraging. But, much work remains to be done in order to apply them for on-line control of emulsion polymerization. Thus, at the current time, calorimetry seems to be an excellent method (simple, rapid, noninvasive, less expensive and requires less calibration than the other on-line sensors) for on-line monitoring of emulsion polymerization.

In this work we will use calorimetry for process development and control. Our main objective is to monitor and control polymer composition under safe conditions. We will thus use isothermal or isoperibolic calorimeters, especially that we are interested by extrapolating the technique to large reactors.

3.2 Experimental set-up

Two laboratory scale reaction calorimeters are used in the current work. The first, described by Barudio (1997), was a 7-liter, jacketed glass reactor, equipped with a feed pump and a computer platform for data acquisition and state estimation. A second, 3-liter reaction calorimeter was built to perform control studies. A schema of this new calorimeter is shown in Figure 3.1. Some experiments were also carried out in a 250 liter pilot scale reactor.

The configuration of the 3-liter calorimeter was chosen in such a way that it behaves as much like an industrial reactor as possible. In this way, we will be able to directly transpose the estimation and control techniques developed in the laboratory to larger reactors. The reactor jacket contains serpentine coils to improve the hydrodynamics and the heat transfer capacity. A constant jacket inlet temperature is maintained by using a thermostat batch equipped with a resistance heater. The reactor lid is also jacketed (at the same temperature as the reactor jacket) in order to reduce heat loss.

A plastic tube of Nitrogen passes through an opening in the lid, and is immersed in the reaction mixture to evacuate the oxygen from the reactor, which is a well-known free radical inhibitor. A condenser also passes through the lid of the reactor to prevent monomer evaporation. Cold tap water is circulated through the serpentine in the condenser in order to refrigerate the vapors leaving the reactor. No attempt is made to control the temperature of the condenser cooling water. The reactor is also equipped with an anchor-type stirrer. The agitation speed is fixed at 200 rpm for solids contents up to 30% and 150 rpm for solids content in the range of 30-50%. The reactor system is equipped with two feed pumps and two balances for semi-batch operations.

The reactor, the pumps and the balances are housed in a plexiglass casing to eliminate emissions and to help maintain the reactor surroundings at a constant temperature.

A platinium resistance, PT100 (precision=0.1°C), is placed in the reactor to measure the reaction temperature. To protect the sensor against aggressive products, it was placed in a

metal tube, serving also as a baffle. Two other Platinium resistances are used to measure temperatures of the inlet and the outlet of the circulating liquid. Ambient and feed temperatures are measured by thermometers.

The electric signals of the sensors and of the balances are sent to a PC through equipped a specifically designed numerical system of control, HP 34970A, that is connected to an RS-232 serial port of the PC. The temperatures are acquired via the HP acquisition unit. The masses of the two balances are also sent to the computer by a serial communication port RS-232. The HP acquisition unit sends the command, received from the computer, to the two pumps as voltage, in the range 0-10V or 0-1.5 V.

The data acquisition software is written in Visual Basic and runs under Windows$^{®}$ on the micro computer connected to the balances and the HP acquisition. The control schemes were implemented using Matlab$^{®}$ and the toolbox Simulink$^{®}$ on the same micro computer.

Samples can be withdrawn from the bottom of the reactor. The reaction in the samples is stopped by adding hydroquinone to the sampling vials. They were analyzed to determine overall and individual conversions, polymer composition and particle size. The mass conversion is gravimetrically obtained using a thermobalance at 140°C. This ensures the availability of measurements for use in the state estimator with a delay as five to ten minutes. When compared with the traditional gravimetric method (4 hours under 120°C), the thermobalance was found to be accurate enough.

The polymer composition can be obtained off-line by either using a gas chromatograph, (based on the analysis of the residual monomer) or by Nuclear Magnetic Resonance, NMR (based on the analysis of the polymer). In fact, the NMR is used when the GC cannot be used to separate the monomers. Unless otherwise mentioned, the particle size is measured by means of dynamic light scattering. Finally, a DSC, Differential Scanning Calorimeter, is used to measure the glass transition temperature of the final polymer.
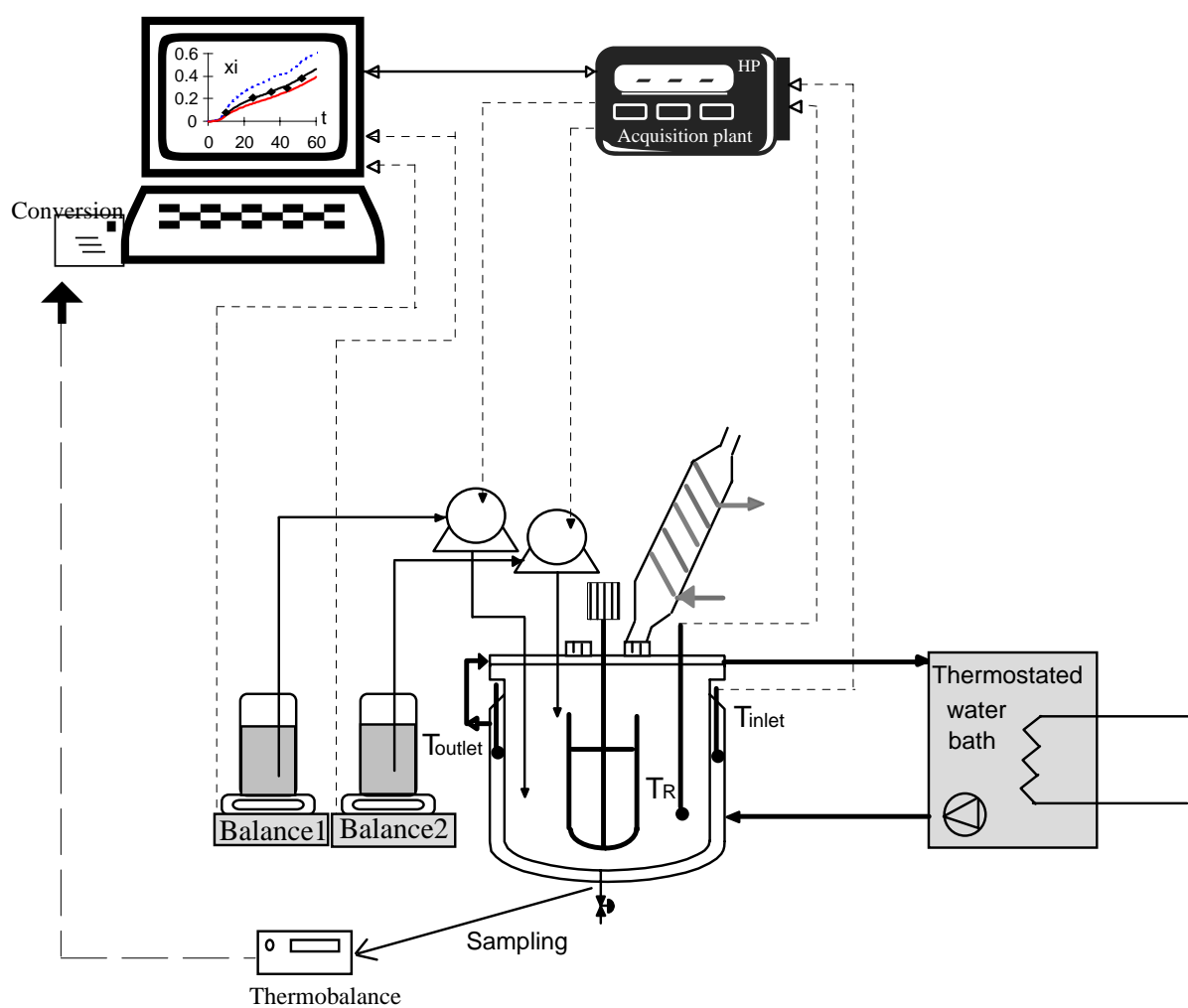
Figure 3.1: A schematic representation of the reactor.

In order to estimate Q_R on the laboratory scale reaction calorimeters, we will make the following assumptions:

- It is assumed that there are no temperature gradients in the laboratory-scale reaction calorimeter. It is common to observe temperature differences in industrial scale reactors. In this case, the use of an average value of those measured in different parts of the reactor can be satisfactory to estimate the heat released by the reaction, as we will see later.
- The effect of the stirrer is neglected. The viscosity of the reaction mass is, in any case, relatively low.
- Components introduced in small amounts (e.g. initiator, surfactant) are not included in the calculation of the specific heat capacity of the reaction mixture. The heat capacities of the reactor wall, stirrer and baffle were also neglected.
- Q_{loss} will implicitly account for the heat loss by the condenser and the heat loss to the surroundings.

As we invoke these assumptions, the energy balance model used in the state estimators that we will discuss below is:

$$Q_{accu} = Q_R + Q_{feed} + Q_j - Q_{loss} \tag{3.10}$$

The heat change in the reactor, Q_{accu} of equation 3.2, is reduced to:

$$Q_{accu} = m_r C_{Pr} \frac{dT_R}{dt}$$
$$m_r C_{Pr} = \sum_i m_i C_{pi} \tag{3.11}$$

Equations 3.3-3.5 are conserved.

3.3 Estimation of UA_0 and $Q_{loss,0}$

3.3.1 A review

The estimation of the initial values of UA and Q_{loss} is of great importance in the design of safe reactors, and to complete the energy balance in order to estimate the heat released by the reaction, Q_R. On-line estimation of U is a real problem since it depends on the medium viscosity and the deposits on the reactor wall, both of which are difficult to measure during the reaction. In stirred vessels, A is also difficult to measure precisely. Therefore, we will try to estimate the product of the overall heat transfer coefficient by the transfer area in a global unknown term UA.

For systems with constant UA and Q_{loss}, these terms can be determined by calibration before the reaction, then introduced in the energy balance to estimate Q_R. If U varies only slightly during the reaction, a linear interpolation of UA between its calibrated value at the start and at the end of the reaction might be acceptable. However in the case of a distinct change of U, this method fails and cannot be used for on-line estimation of the heat of the reaction, since final U is not known. In this case more sophisticated methods for determining UA are needed, such as the application of Kalman filtering using the equation of heat conservation in the jacket, or by using initial values of UA and Q_{loss} during the reaction, and applying corrections to them from time to time by a supplementary measurement. In all these cases, initial values of UA and Q_{loss} are required to solve the energy balance.

Several works treated the estimation of UA and Q_{loss} when no reaction is taking place. Experimental and empirical approaches were proposed, e.g. Arzamendi and Asua (1991), Soroush and Kravaris (1994), Kumpinsky (1996), Hariri et al. (1996), Nomen et al. (1996), Molga (1997) and Zaldivar et al. (1997). The most widely used approach is by direct calorimetric calibration. It consists of introducing a known thermal power in the reaction mass by means of an electrical resistance. By comparing the area under the curve plot of (T_R-T_j) versus time, the effective heat transfer coefficient can be estimated. For instance, Févotte

et al. (1996) and Buruaga et al. (1997) placed an electrical resistance in the reactor. Several ramps in the resistance power were realized and afterwards an optimization technique was used to estimate initial values of UA and Q_{loss}. This approach gives good estimates of these parametrs, but the main difficulty with this technique is that it takes a lot of time, since thermal equilibrium must be attained for a given temperature before executing another ramp. It takes a minimum of about one hour to complete the calibration in laboratory scale reactors, and in large scale reactors, this approach is not really practical and cannot be used to estimate UA and Q_{loss}.

Another method was proposed by Soroush and Kravaris (1994) to estimate the initial values of UA and Q_{loss}. They introduced two new factors:

$$\alpha_1 = \frac{UA}{m_r C_{Pr}} \quad \text{and} \quad \alpha_2 = \frac{Q_{loss}}{m_r C_{pr}(T_{amb} - T_R)}$$

The estimation of these two parameters is done in two steps. First of all, the reactor is charged with a non-reactive substance. At steady state conditions (T_R and T_j constant), the slope of fitted regression line of (T_R-T_{amb}) vs. (T_j-T_R) gives the least squares estimate of α_1/α_2. In the second step, a step change in the jacket temperature is realized. The solution of the differential equation representing the heat balance in the reactor, yields a value for the term $\alpha_1 + \alpha_2$. Initial values of UA and Q_{loss} can be determined by the two solutions.

A method similar to that proposed by Soroush and Kravaris (1994) was developed by Maschio et al. (1999), for a commercial reactor APOLREAC. The heat loss was calibrated by an internal heater and the initial value of UA is estimated by solving the heat balance equation when T_j is constant and no reaction takes place during the calibration. In some commercial calorimeters, such as the RC1, the calibration of UA is done at the beginning and at the end of the reaction, and the experimenter can choose a profile of some predetermined shape to estimate it off-line a posteriori.

Finally, oscillatory calorimeters can be used to estimate UA before the reaction begins, when all the reactants are at the desired temperature. The analysis of temperature oscillations is done in the same manner as during the reaction. The disadvantage of this method is that it is not applicable on a large scale reactor.

Our objective is to develop a technique for the estimation of UA and Q_{loss}, that is efficient and that does not require a calibration period. We will be interested in both laboratory scale and industrial appilcations. In the following sections, we will present two methods of estimating the initial conditions: UA_0, and $Q_{loss,0}$. The first method consists of estimating the initial value of the heat transfer coefficient by neglecting the heat loss. This method is satisfactory in laboratory and industrial scale reactors. In the second method, an alternative estimator for the heat transfer coefficient and the heat loss is proposed. This method is applicable uniquely to laboratory scale reactors. Both techniques do not require any holding period at the reaction temperature and can be realized during the heat-up phase of the reactor.

3.3.2 Estimation of UA_0 using a high gain observer

Normal reactor preparation requires that a pump circulates hot fluid in the reactor jacket during the 'heat-up' phase (i.e. during the time where we bring the reactor contents from the ambient to the reaction temperature). In the absence of chemical reaction, the heat balance of the reactor and its contents during the heat-up phase takes the following form:

$$Q_{accu} = Q_j - Q_{loss}$$

$$\Rightarrow m_r C_{Pr} \frac{dT_R}{dt} = UA\left(T_j - T_R\right) - Q_{loss} \tag{3.12}$$

The unknown variables in this model are UA and Q_{loss}, if T_R and T_j are measured. We do not consider equation 3.6 to represent the dynamics of Q_{loss}. The heat loss is supposed to be time-varying and unknown. If we consider UA and Q_{loss} as variable states, we can represent the nonlinear system 3.12 by the following augmented system:

$$\begin{bmatrix} \dot{T}_R \\ \dot{UA} \\ \dot{Q}_{loss} \end{bmatrix} = \begin{bmatrix} 0 & \left(T_j - T_R\right)/m_r C_{Pr} & -1/m_r C_{Pr} \\ 0 & 0 & 0 \\ 0 & 0 & 0 \end{bmatrix} \begin{bmatrix} T_R \\ UA \\ Q_{loss} \end{bmatrix} + \begin{bmatrix} 0 \\ \varepsilon_{UA} \\ \varepsilon_{Q_{loss}} \end{bmatrix} \tag{3.13}$$

where ε_{UA} and $\varepsilon_{Q_{loss}}$ represent the unknown dynamics of UA and Q_{loss} respectively. The system 3.13 is linear up to output injection. The states UA(T) and Q_{loss} are observable from the output measurement T_R if the following conditions are satisfied:

$$\frac{d\left(T_j(t) - T_R(t)\right)}{dt} \neq 0, \quad \dot{Q}_{loss}(t) \cong 0 \text{ and } \dot{UA}(t) \cong 0 \tag{3.14}$$

In reality, the second and third conditions, that assume that the heat transfer coefficient and the heat loss to the surroundings are constant, can be supposed to be true on a small period of time. However, the first condition is not valid during the normal reactor heat-up, where the reactor/jacket temperature difference decreases linearly with time (as shown by

Figure 3.2 at right), and it is therefore not possible to distinguish heat transfer through the jacket from the heat loss.

In order to get around this problem, we can neglect Q_{loss} during the preparation stage. This is probably a reasonable assumption for both large and small reactors during the initial part of the heating phase since the difference between the reactor/jacket temperature and the ambient temperature, during the heating, is small (for reasonably low temperatures). In this case, the heat balance becomes:

$$\Rightarrow\ m_r C_{Pr} \frac{dT_R}{dt} = UA\left(T_j - T_R\right) \tag{3.15}$$

The observability condition of UA from this model is reduced to:

$$\frac{T_R - T_j}{m_r C_{Pr}} \neq 0$$

Since $\infty > m_r C_{Pr} > 0$, then the condition indicates that UA can be estimated before thermal equilibrium, ($T_j = T_R$) is attained.

Neglecting the heat loss, the system 3.13 reduces to the following system:

$$\begin{bmatrix} \dot{T}_R(t) \\ \dot{UA}(t) \end{bmatrix} = \begin{bmatrix} 0 & \left(T_j(t) - T_R(t)\right)/m_r C_{Pr} \\ 0 & 0 \end{bmatrix} \begin{bmatrix} T_R \\ UA \end{bmatrix} + \begin{bmatrix} 0 \\ \varepsilon_{UA}(t) \end{bmatrix} \tag{3.16}$$
$$y(t) = T_R(t)$$

where the variation of the heat transfer, UA, is represented by the function $\varepsilon_{UA}(t)$ and y(t) is the available measurement ($T_R(t)$). In order to estimate UA we can use a Kalman-like or a high gain observer, presented in chapter 2. Since the system is already under a canonical form of observability, a high gain observer can be used directly (without a change of co-ordinates). Moreover, the high gain observer is tuned by a constant gain, while the Kalman-like observer requires that we solve the Riccati differential equation simultaneously with the observer equations.

A nonlinear estimator of UA is given by the following system:

$$
\begin{bmatrix} \dot{\hat{T}}_R(t) \\ U\dot{\hat{A}}(t) \end{bmatrix} = \begin{bmatrix} 0 & \dfrac{\left(T_j(t) - T_R(t)\right)}{m_r C_{Pr}} \\ 0 & 0 \end{bmatrix} \begin{bmatrix} T_R(t) \\ U\hat{A}(t) \end{bmatrix} - \Lambda^{-1} S_\theta^{-1} C^T \left(\hat{T}_R(t) - y(t)\right)
\tag{3.17}
$$

with $\Lambda = \begin{bmatrix} 1 & 0 \\ 0 & \dfrac{\left(T_j(t) - \hat{T}_R(t)\right)}{m_r C_{pr}} \end{bmatrix}$, C=[1 0].

The symbol ^ is used to characterize the estimated states. S_θ is the unique solution of the algebraic Lyapunov equation. For a 2×2 matrix, it is given by:

$$
S_\theta = \begin{bmatrix} \dfrac{1}{\theta} & -\dfrac{1}{\theta^2} \\ -\dfrac{1}{\theta^2} & \dfrac{2}{\theta^3} \end{bmatrix}
$$

θ is the tuning variable of the observer. In fact, there is not a theoretical method to adjust θ. It must be chosen sufficiently large to converge quickly. However very large values of θ are to be avoided in practice since the estimator may become noise sensitive. Thus the choice of θ is a compromise between fast convergence and sensitivity to noise. Experience has shown that θ can be regulated by simulation and the best value obtained in this way can be applied under experimental conditions. The best way would be to regulate the parameter θ off-line for one experiment, which will allow us to account for modeling errors and measurement noise. This value can thereafter be used during any other heating up phase.

The advantage of the method proposed here is that we can use the heat-up phase of a given experiment in order to obtain our initial estimate of UA, rather than being obliged to run a series of calibrations. Of course, a small estimation error is induced in UA_0 because we neglect the term Q_{loss}. Nevertheless, it was found that the results of this new method are similar to those found by employing a calibration resistance. A second advantage of this observer is its applicability to laboratory reactors as well as to large scale reactors. It was initially applied on a 7 liter jacketed reactor, in figure 3.2. The observer estimates the product of U and the surface area A. In order to deduce U, A was calculated as a function of the volume of substances in the reactor, ignoring the vortex effect.
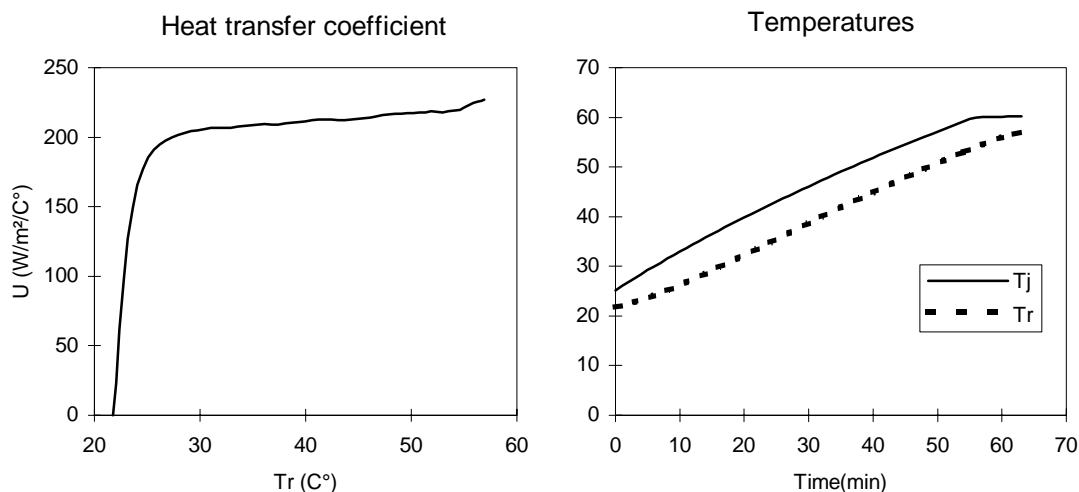
Figure 3.2: At left, heat transfer coefficient, U, in a 7 liter jacketed reactor. At right, the reactor and jacket temperatures.
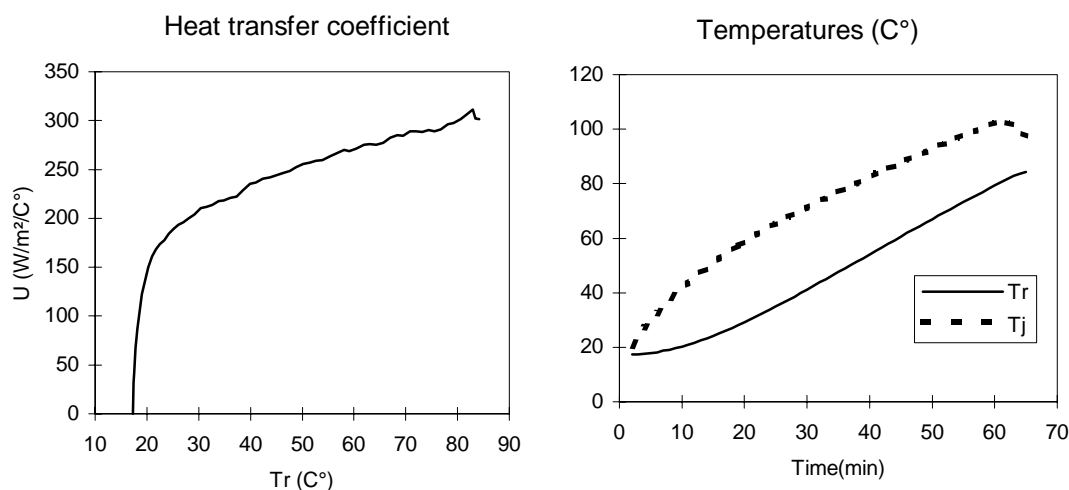
Figure 3.3: The heat transfer coefficient (U) as a function of temperature in the 250-liter pilot reactor, at left. Jacket and reactor temperatures, at right.

The 250 pilot reactor was charged with 100 kg of water and 500g of surfactant. A normal reactor heat-up was done. The reactor temperature was measurements at three different places in the reactor. In order to use the observer, an average value was considered to represent the reactor temperature.

A first glance at the Figures representing U (Figure 3.2 and 3.3) shows that the time of convergence that the observer requires before attaining the correct estimation of UA is about

10 minutes. The first part of the curves, in Figures 3.2 and 3.3 at left, where U changes sharply, correspond to the convergence of the observer, since it was initialized far from the real value ($U_{init}=0$). Thereafter, the value of U remains almost constant as a function of temperature.

In the 7 liter reactor, the estimated value of U, Figure 3.2, was found to remain constant as the temperature varies, whereas in the 250 liter reactor (Figure 3.3) U seems to increase with temperature. Several factors must be taken into consideration while interpreting these curves. Firstly, several phenomena are neglected in the heat balance, the heat loss to the surroundings (which is assumed to be less important in a large reactor than in a small reactor), and the heat capacity of the reactor components and inserts (this term is more important in large reactors, and decreases as we get closer to steady state conditions). Since the heat loss due to the reactor components becomes negligible when we get closer to the isothermal conditions, then we can assume that the estimated value of U is more realistic at the end of the estimation, especially in Figure 3.3 at left. The increase of U as a function of the reactor temperature can also be due to neglecting Q_{ins}. Effectively, neglecting Q_{ins} during the heat up phase will give an estimate of U that is less than the real value during the non stationary phase. When we get closer to the stationary state, Q_{ins} can be neglected and therefore U is well estimated.

As we mentioned earlier, in the observer we also neglect the heat loss to the surroundings. In order to more precisely estimate U and to study the sensibility of the estimations to the heat loss to the surroundings, we will take into account the heat losses in the estimator of U. In the next section, another, more precise method of estimating simultaneously UA and Q_{loss} is presented.

3.3.3 Estimation of UA$_0$ and Q$_{loss,0}$ using a Kalman filter

As mentioned earlier, the observability conditions 3.14, can be satisfied by varying the jacket and reactor temperature independently. For instance, this can be done by placing a resistance in the reactor and adding incrementally increasing amount of heat to the reactor. Another variation of this term would be to send sinusoidal signals either in the reactor or in the jacket, (see Tietze et al. (1996)). This can also be done simply by heating the jacket by steps, thereby causing a variation of the term $T_j(t) - T_R(t)$ as a function of time, which will allow us to differentiate UA and Q$_{loss}$. It should be noted that it is difficult to apply this way of heating in a large reactor, because temperature gradients in the reactor make it difficult to distinguish the oscillations from the measurement noise or mixing problems.

The two conditions, $\dot{Q}_{loss}(t) \cong 0$ and $\dot{UA}(t) \cong 0$, can be supposed to be valid for short periods of time, UA and Q$_{loss}$ do not vary abruptly. It should be pointed out however, that the observability in this case is not theoretically proved, (since the model of Q$_{loss}$ is unknown) but is founded on some hypothesis, such as $\dot{Q}_{loss}(t) \cong 0$, and assuming that the model of Q$_{loss}$ is different than Q$_j$. Otherwise, U and Q$_{loss}$ are not observable.

Once the observability conditions are satisfied, the augmented system including Q$_{loss}$, given by 3.13, can be written under the form:

$$\dot{x}(t) = A(u,y)x(t) + \bar{\varepsilon}(t) \tag{3.18}$$
$$y(t) = Cx(t)$$

where x=[T$_R$, UA, Q$_{loss}$]', C=[1 0 0], $\bar{\varepsilon} = [0 \quad \varepsilon_{UA} \quad \varepsilon_{Q_{loss}}]'$,

$$A = \begin{bmatrix} 0 & f_1 & f_2 \\ 0 & 0 & 0 \\ 0 & 0 & 0 \end{bmatrix}, \; f_1 = \frac{(T_R - T_j)}{m_r C_{Pr}} \text{ and } f_2 = \frac{-1}{m_r C_{Pr}}. \tag{3.19}$$

This system does not take the triangular calform of observability. Therefore, we cannot directly use a high gain nonlinear observer to estimate UA and Q$_{loss}$. The use of a high gain

observer, in this case, necessitates a change of co-ordinates. However, the system is linear up to output injection and therefore, a Kalman-like observer can be used to estimate the different states. The Kalman-like observer takes the following form:

$$\begin{cases} \dot{\hat{x}} = A(u,y)\hat{x} - S_\theta^{-1}C^T(C\hat{x} - y) \\ \dot{S}_\theta = -\theta S_\theta - A^T S - S_\theta A + C^T C \end{cases} \tag{3.20}$$

The second differential equation is the Riccati equation that must be solved simultaneously with the estimated state differential equations, $\hat{x}$. In order to avoid the inversion of S_θ in the corrective term, we denote $R = S_\theta^{-1}$, therefore, R is also a symmetric positive defined matrix.

$\Rightarrow \dot{S}_\theta = -R^{-1}\dot{R}R^{-1}$, and this gives the following differential equation:

$$\dot{R} = R\theta + RA^T + AR - RC^T CR$$

The observer system can be written in the form:

$$\begin{cases} \dot{\hat{x}} = A(u,y)\hat{x} - RC^T(C\hat{x} - y) \\ \dot{R} = R\theta + RA^T + AR - RC^T CR \end{cases} \tag{3.21}$$

Since R is symmetric, there are 6 equations to integrate along with the states equations. We pose:

$$R = \begin{bmatrix} a & d & e \\ d & b & f \\ e & f & c \end{bmatrix}$$

The second equation in system 3.21 gives rise to the following six differential equations:

$$\begin{cases} \dot{a} = \theta a + 2df_1 + 2ef_2 - a^2 \\ \dot{b} = \theta b - d^2 \\ \dot{c} = \theta c - e^2 \\ \dot{d} = \theta d + bf_1 + ff_2 - ad \\ \dot{e} = \theta e + ff_1 + cf_2 - ae \\ \dot{f} = \theta f - de \end{cases} \tag{3.22}$$

The final observer of T_R, UA and Q_{loss} is:

$$\begin{cases} \dot{\hat{T}}_R = \left(\dfrac{T_j - T_R}{m_r C_{Pr}} \right) U\hat{A} - \dfrac{1}{m_r C_{Pr}} \hat{Q}_{loss} - a\left(\hat{T}_R - T_R \right) \\[4mm] U\dot{\hat{A}} = -d\left(\hat{T}_R - T_R \right) \\[4mm] \dot{\hat{Q}}_{loss} = -e\left(\dot{T}_R - T_R \right) \end{cases} \qquad (3.23)$$

In order to estimate UA and Q_{loss}, the nine differential equations must be solved simultaneously. R is usually initialized at the identity matrix. Experimentally, in order to validate the observability conditions 3.14, temperature ramps are done on the jacket temperature in the 3 liter reactor, as shown in Figure 3.4a.
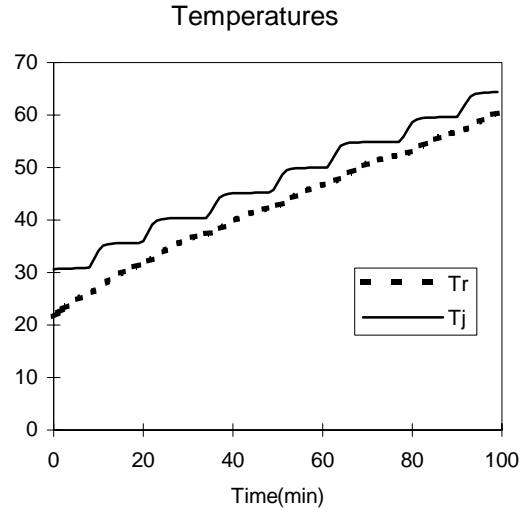
Figure 3.4a: Temperature ramps on the jacket and the corresponding reactor temperature (3L).
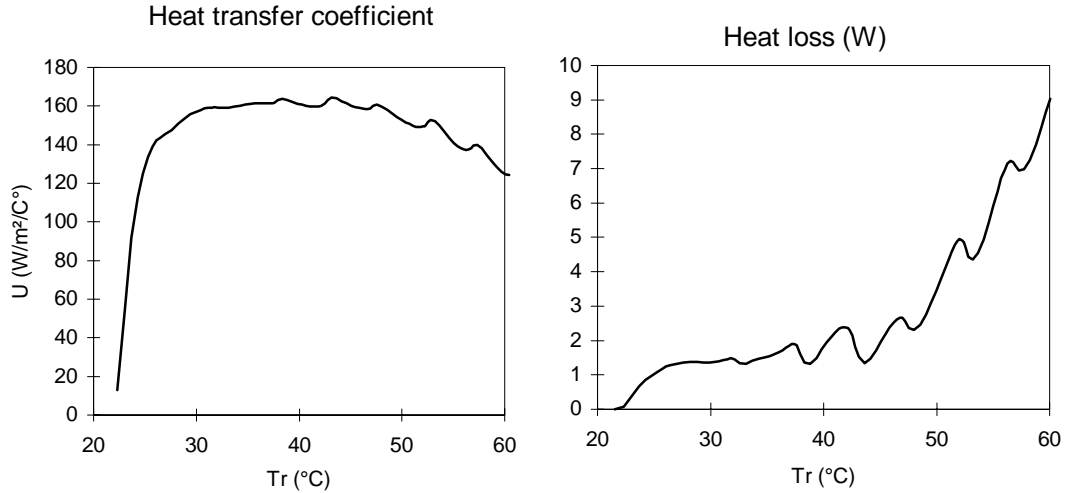
Figure 3.4b: Heat transfer, at left, and heat loss, at right, versus reactor temperature in a 3L jacketed glass reactor.

It can be seen on Figure (3.4b) that the heat transfer coefficient does not vary with temperature, whereas, the heat loss increases exponentially with the temperature difference between the reactor and the ambient. The oscillations in the estimated values of U and Q_{loss} might be due to the observer tuning parameter θ, which was voluntarily chosen big in order to ensure rapid convergence to the real process.

It should be pointed out, that the observer cannot be experimentally validated. We cannot therefore affirm that Figure 3.4 gives the real Q_{loss}, since the system might not be observable, and we might therefore have several solutions that satisfy the observer. However, we try to obtain the real curves of U and Q_{loss} by making some realistic hypotheses.

In Figure 3.5a, Kalman-like observer that takes into account the heat losses to the surroundings, is compared to the high gain observer that neglects the heat losses. It can be seen that neglecting Q_{loss} reduces the estimated value of U. Both observers give however the same estimate of U, when we get close to steady state conditions.

Heat transfer coefficient
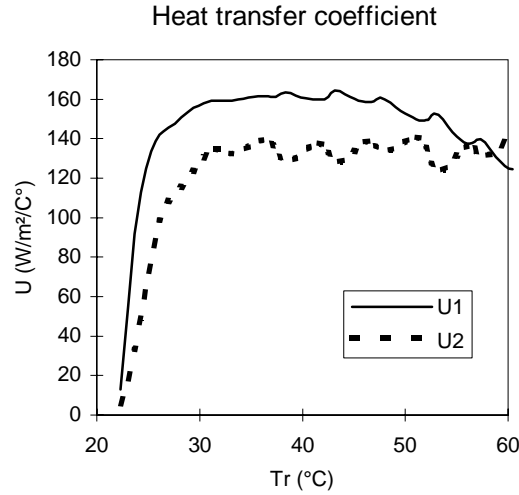
Figure 3.5a: Estimation of U, by employing temperatures ramps in the 3 liter reactor.

(--) U_2 obtained by the high gain observer and (__) U_1 by Kalman-like observer.

Therefore, in conclusion, we recommend the Kalman-like observer (that takes into consideration the heat loss to the surroundings) be used wherever possible. When it is not possible to impose temperature ramps on the jacket, the high gain observer (neglecting Q_{loss}) can be used to accurately estimate an initial value of U, since the experiments have shown that the percentage of heat loss with respect to the total accumulated heat not significant, as shown in Figure 3.5b.
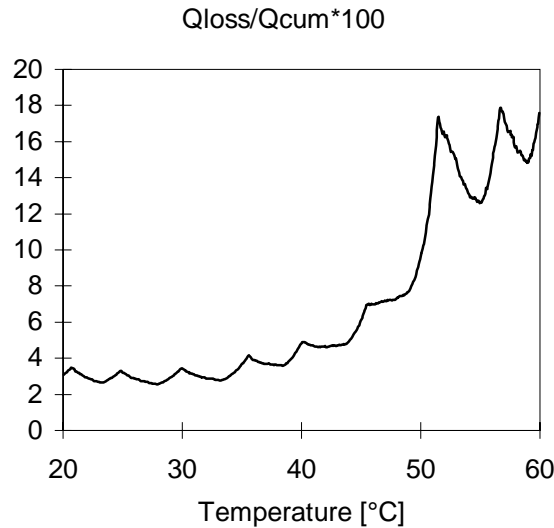
Figure 3.5b: The percentage of Q_{loss} to the total cumulated heat, based on the estimation of Q_{loss} by the Kalman like observer.

The estimation of U, or UA, and Q_{loss} is done when no chemical reaction is taking place. In some processes, where the viscosity does not change, these values can be used throughout the reaction. In emulsion polymerization, these values can be used only at the beginning of the reaction to complete the energy balance in order to estimate Q_R. But the change of viscosity during the reaction as well as the dependence of Q_{loss} on the difference between the reactor and the ambient temperatures, makes the estimated UA and thus Q_R deviate from its "real" value. In the following section, we consider the energy balance, during the reaction.

3.4 Determination of the conversion

Estimation Q_R is of primary importance in the monitoring and control of a chemical process. Since Q_R depends directly on the global reaction rate, it can infer a large number of the polymer properties, as we will see later. Therefore, Q_R can be used to control some of these properties, and especially the rate of heat released by the reaction, in order to work under safe conditions.

In order to estimate Q_R from the heat balance, all the terms involved in the energy balance must be known. In fact, the unknown variables in the energy balance are UA and Q_{loss}. In the last section, we proposed an estimator to identify the initial values of UA and Q_{loss}. We must assume that there is an increase in the reaction temperature and a change in the latex viscosity during the reaction. Since, Q_{loss} depends on the difference between the reactor and the ambient temperatures and U depends on the solids content, (or on the latex viscosity, and therefore on the monomer conversion, solids content or the degree of reaction), then U and Q_{loss} must vary during the reaction. Therefore, the initial estimates of these parameters cannot be used for a long while of time after the beginning of the reaction, and they must thus be estimated by another way.

It is clear that the observer 3.23, cannot be used during the reaction to estimate UA and Q_{loss} because the heat balance includes now the term representing the heat generated by the reaction. Subsequently, the observability conditions of the new states, UA, Q_{loss} and Q_R are different. However, if we neglect Q_{loss}, then we can use this observer to estimate UA and Q_R during the reaction. This technique is not easy to employ during the reaction since this necessitates employing temperature ramps, which is practical only in the case of small reactors. Since we are also interested in laboratory scale analysis, we will however test the observer experimentally.

Before using the observer, one must be aware of the observability of the system. The heat balance of the reactor, including the heat of the reaction term, is:

$$\Rightarrow \frac{dT_R}{dt} = \frac{UA}{m_r C_{Pr}}\left(T_j - T_R\right) - \frac{Q_{loss}}{m_r C_{Pr}} + \frac{Q_R}{m_r C_{Pr}} + \frac{Q_{feed}}{m_r C_{Pr}} \qquad (3.24)$$

One new condition of observability is assuming that the dynamics of Q_R are not very rapid, which means that Q_R can be assumed to be constant on a small period of time, which is not usually true. Q_R might be considered constant during the semi-continuous period, but during the nucleation or a self accelerating due to a gel effect, the heat produced by the reaction cannot be assumed constant even over a short period of time.

In order to validate this hypothesis, we will treat the observer experimentally. As we will see later, under the conditions of this experiment, the system does not seem to be observable. Therefore, this observer is not going to be used in the subsequent parts of this work.

By neglecting Q_{loss}, the system has now the same form as that used to estimate UA and Q_R. It can be represented by the system 3.18, with x=[T_R,UA,Q_R]' and $f_2 = 1/m_r C_{Pr}$. If the condition $\dot{Q}_R \cong 0$ is satisfied, and temperature ramps are executed on the jacket temperature, then the system is observable and a Kalman-like observer can be used to estimate UA(t) and Q_R(t).

An experiment of polystyrene was done in a 7L reactor, during which temperature ramps were imposed on the jacket, as shown in Figure (3.6a). The reaction recipe is given by Table 3.1. The matrix R was initialized at the identity matrix and several values of θ were examined. No attempt was made to calculate how the temperature ramps must be done. The objective was to vary the derivative of T_j-T_R during the reaction, as shown in Figure (3.6b) at right. It can be seen, that T_j-T_R varies significantly during the reaction.

Table 3.1: Experiment of homopolymerization of poly styrene.

\ Experiment	Poly styrene
	amount(g)

Component \	
Styrene	600
H_2O	2415
Dodecyl sulfate, sodium salt	4.5
Potassium persulfat	4.41
Final solid contents	20%
Final particle size	84 nm
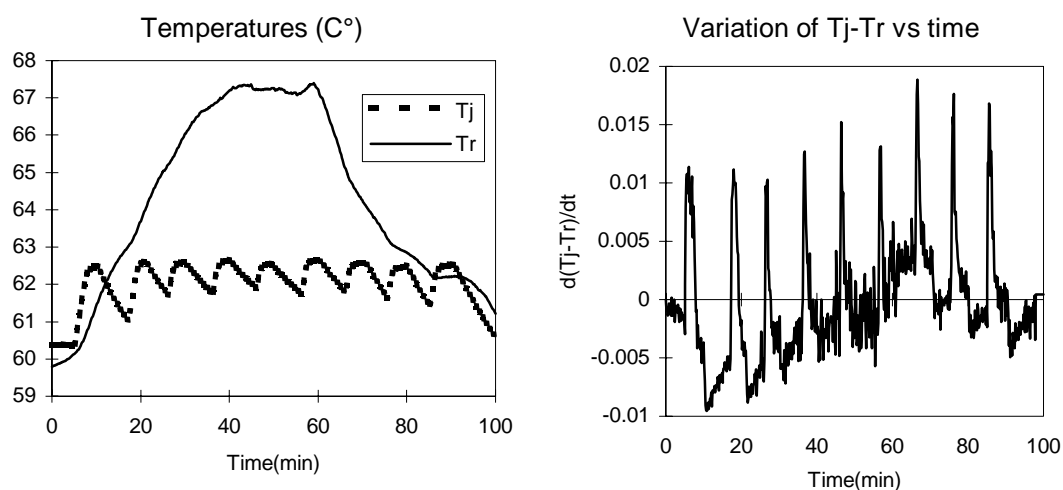
Figure 3.6a: Homopolymerization of styrene. Temperature ramps on the jacket temperature: Tj(--), at left. The corresponding value of $d(T_j - R_R)/dt$ as a function of time, at right.

Figure 3.6a shows the temperature ramps done during the reaction. It can be seen that the difference between T_j and T_R, which is one of the observability conditions, is not constant with time.

In Figure (3.6b), at left, Q_R was estimated by two ways: ① using the observer, and ② the 'real' heat released by the reaction was calculated, off-line, by using some gravimetric measurements, that are shown in Figure 3.6c. It can be seen that Q_R is not in agreement with the "real" value, especially, when Q_R varies rapidly. At right, of Figure 3.6b, we can see the estimated U as a function of time.
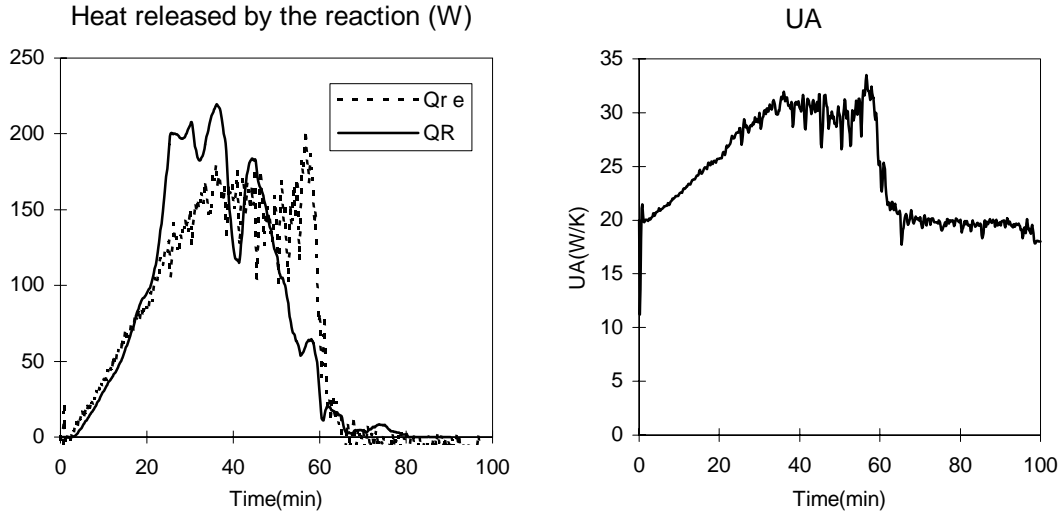
Figure 3.6b: Homopolymerization of styrene. The heat released by the reaction obtained by Kalman-like observer $Q_{r\,e}$, at left, compared to the real value Q_R calculated from the conversion. At right, the estimated UA.
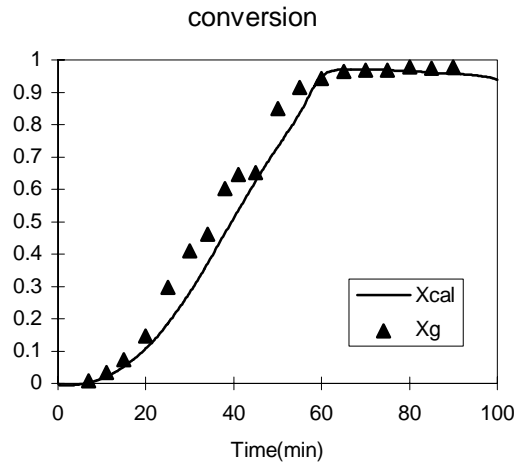
Figure 3.6c: Homopolymerization of styrene. The calorimetric conversion, X_{cal} calculated from the estimated heat of the reaction, compared to the mass conversion, X_g.

It can also be seen that the slow convergence of Q_R is compensated by an increase in the estimation of UA. In a batch reaction, UA usually decreases due to an increase in the viscosity and eventual deposition of latex on the reactor wall. We can therefore say that these variables are not really observable, either because the behavior of Q_R is very fast or because the size of the temperature ramps in the jacket was not significant. In order to better understand this phenomena, one must go further into the analyses of the temperature ramps

(amplitude and frequency). We will not do so here, because even though estimating Q_R in this way might be interesting on laboratory scale rectors, it seems that in large reactors it might be difficult to use rapid temperature ramps on the jacket. Moreover, an important parameter that might influence the estimation is the heat losses that are neglected in the estimator. If we refer back to (Figure (3.6a)), we can observe a significant increase in the reactor temperature, which implies an increase in Q_{loss}.

As a result, we need another technique to obtain the evolution of U, Q_{loss} and Q_R simultaneously. The estimation method of UA from the energy balance of the jacket suffers from problems of accuracy. First of all, the heat loss from the jacket to the surroundings, $Q_{loss,j}$ is important when compared to the heat loss in the reactor. Applying the jacket side energy balance means that it must be insulated, especially if the inlet temperature varies and that $Q_{loss,j}$ cannot be assumed to be constant. Also, the heat balance of the jacket involves two terms, the conductive heat exchange with the wall of the reactor and the convective change due to the circulation of the liquid. High accuracy of estimations is obtained when steady-state conditions are attained and a high difference between the inlet and the outlet is supplied. Ordinary operating conditions, demands to maximize the capacity of heat evacuated by the jacket and therefore high flow rates (i.e. $T_j^{in} = T_j^{out}$) are preferable. With these restrictions, we can say that the ordinary operating conditions of chemical reactors (high circulation rates in the jacket and no ramps on the jacket temperature) do not allow us to estimate Q_R, UA and Q_{loss} simultaneously from the unique temperature measurements of the reactor and the jacket, even if we combine both the energy balance of the reactor and the jacket. A supplementary sensor must therefore be used to measure one of these variables independently.

In the literature, the usual application consists of introducing occasional measurements of the mass conversion X, or individual mass conversion obtained by GC, in an optimization technique that gives the unknown variables Q_R, Q_{loss} and UA. Févotte et al. (1996) proposed an adaptive calorimetric technique that relies on occasional measurements of the mass conversion X ①. In order to do so, they proposed the following hypothesis to represent the variation of Q_{loss} and UA with conversion:

$$Q_{loss}(t) = b_3 + b_4 X_{cal}(t) \tag{3.25}$$

$$UA(t) = UA_{init} + b_1 X_{cal}(t) + b_2 X_{cal}^2(t) \tag{3.26}$$

The heat loss (Q_{loss}) can also be written as a function of the difference between the reactor temperature and the ambient, as given by the following equation:

$$Q_{loss}(t) = Q_{loss,0} + b_3(T_R(t) - T_{amb}) \tag{3.27}$$

Equations 3.25 and 3.27 are equivalent if the difference between the reaction and the ambient temperatures varies only as a function of the conversion. However, as we mentioned earlier, Q_{loss} accounts also for the heat loss by the condenser, which depends on the amount of monomer in the reactor (which depends on X) and on the reactor temperature. Therefore, in batch reactors, equation 3.25 is perhaps more representative than equation 3.27. On the other hand, an increase in T_R is not always proportional to the conversion (especially in semi-continuous operations or in batch operations if a gel effect arises). At this time, equation 3.27 is more representative (if X is constant and T_R varies, Q_{loss} is a function of T_R-T_{amb}).

In this work we will adopt these hypotheses (3.25, 3.26 or 3.27) to represent the variations of UA and Q_{loss}. Of course, we could use other hypotheses, such as writing U as a function of the medium viscosity of solids content, and Q_{loss} as a function of the amount of volatile substances in the reactor. However, as we will see later, equations 3.26 and 3.27 give the same estimates of the monomer conversion, which is our objective. However, if we want to estimate real values of U and Q_{loss} then we have to be precise in modeling them.

The different parameters b_i are obtained by optimization of the overall conversion values that can be obtained by on-line gravimetric measurements (done manually in the experiments presented in this work), or using one of the techniques discussed in section 3.1.3.

The objective function used for this purpose, $J(b_i)$, is the sum of the squares of the conversions difference between predicted and measured conversions, equation 3.28. It should be pointed out that, the parameters b_i will be well estimated if and only if they are identifiable. However, since the models 3.25 and 3.26 are not physical, then the optimization might give a local solution of the objective function.

$$J(b_i) = \sum_{z=1}^{k}\left(X_{g,z} - k_{cal,z}X_{cal,z}\right)^2 \tag{3.28}$$

where $X_{g,z}$ denotes the experimentally measured mass conversion value at the "z^{th}" measurement interval, and $X_{cal,z}$ is the corresponding model predicted calorimetric conversions evaluated at a given time. The correction factor, $k_{cal,z}$, is in fact the ratio of the mass to the calorimetric conversion at the "z^{th}" measurement.

$$k_{cal,z} = \frac{X_{g,z}}{X_{cal,z}} \tag{3.29}$$

These conversions are identical for homopolymerization. However, if we have two or more monomers these values are not equal and depend on the molecular weight and the heat enthalpy of each monomer, as given by the following equations:

$$X_g(t) = \frac{\sum_j MW_j\left(N_j^T - N_j(t)\right)}{\sum_k MW_k N_k^T} \tag{3.30}$$

$$X_{cal} = \frac{\sum_j \left(-\Delta H_{Pj}\right)\left(N_j^T - N_j\right)}{\sum_k \left(-\Delta H_{Pk}\right)N_k^T} \tag{3.31}$$

If $\left(MW_1 / MW_2\right) \cong \left(-\Delta H_{P1} / -\Delta H_{P2}\right)$, then the value of $k_{cal,z}$ can be taken to be close to one. For certain monomers such as styrene and butyl acrylate ($MW_1/MW_2=104/128=0.809$ and $\Delta H_{P1}/\Delta H_{P2}=71060/78000=0.911$, where MW(g/mol) and ΔH_P(J/mol)) we can suppose that this condition is valid. However, for other monomers pairs such as vinyl acetate (VAc) and MMA, the value of $k_{cal,z}$ is far from one ($MW_1/MW_2=86/100=0.859$ and $\Delta H_{P1}/\Delta H_{P2}=88000/55500=1.5855$). In this case, $k_{cal,z}$ must be estimated. In this work, we will assume that $k_{cal,z}$ is equal to one, which means that the conversion obtained by the optimization is the mass conversion and not calorimetric one. This means that an error will be incorporated in the estimation of Q_R, since by definition, Q_R is related to the calorimetric conversion 3.31 and not directly to the mass conversion 3.30, according to the following equation:

$$X_{cal}(t) = \frac{\int_0^t Q_R(t)dt}{Q_{max}} \quad (3.32)$$

where Q_{max} is total potential heat that would be generated if we obtained 100% conversion. It is a linear product of the total number of moles of each monomer introduced multiplied by the heat of reaction of each substance ΔH_{pi}, $Q_{max} = \sum_i N_i^T \left(- \Delta H_{p_i} \right)$.

The hypothesis (3.25 and 3.26), allows us to have a continuous estimation of UA and Q_{loss}. All the terms in the energy balance are known directly except the heat released by the reaction which involves the derivative of the reactor temperature. In order to avoid problems related to noise propagation, it is recommended to construct an observer for Q_R. We take therefore the following augmented system, with Q_R as a new state with an unknown dynamic ε_{Q_R}:

$$\begin{bmatrix} \dot{T}_R(t) \\ \dot{Q}_R(t) \end{bmatrix} = \underbrace{\begin{bmatrix} 0 & \frac{1}{m_r C_{Pr}} \\ 0 & 0 \end{bmatrix}}_{A} \begin{bmatrix} T_R \\ Q_R \end{bmatrix} + \begin{bmatrix} \frac{Q_f(t) + Q_j(t) - Q_{loss}(t)}{m_r C_{Pr}} \\ \varepsilon_{Q_R} \end{bmatrix} \quad (3.33)$$

$$y = C \times \begin{bmatrix} T_R \\ Q_R \end{bmatrix} = \begin{bmatrix} 1 & 0 \end{bmatrix} \times \begin{bmatrix} T_R \\ Q_R \end{bmatrix}$$

The system given by the equations 3.33 is linear. We can therefore apply the Kalman criterion of observability to test the observability of the system, that is the matrix governed by:

$$\begin{bmatrix} C \\ CA \end{bmatrix}$$

be of order 2. In our case:

$$\begin{bmatrix} C \\ CA \end{bmatrix} = \begin{bmatrix} 1 & 0 \\ 0 & \frac{1}{m_r C_{Pr}} \end{bmatrix}$$

Therefore, the system is observable if and only if $m_r C_{Pr} \neq 0$, which is always the case. The observability of Q_R requires also knowledge of the sum of Q_j-Q_{loss}, i.e. the total amount of heat removed from the reactor. If we assume that the method cited above allows us to

obtain continuous "measurements" of (Q_j - Q_{loss}), we can define an observer of Q_R. If we refer back to chapter 2, the system is already under a canonical form of observability, and one can apply a high gain observer to estimate $Q_R(t)$ without a change of co-ordinates. Note however, that in this case, the original Kalman, or Luenberger observers can be used. The advantage of the high gain observer with respect to the Kalman observer is its unique tuning parameter. A high gain observer of Q_R is given by the following system, with $\theta = 0.02$:

$$\begin{cases} \dot{\hat{T}}_R(t) = \dfrac{Q_j(t) + Q_f(t) - Q_{loss}(t)}{m_r C_{Pr}} + \dfrac{\hat{Q}_R(t)}{m_r C_{Pr}} - 2\theta\left(\hat{T}_R(t) - y(t)\right) \\ \dot{\hat{Q}}_R(t) = -\theta^2 m_r C_{pr}\left(\hat{T}_R(t) - y(t)\right) \end{cases} \tag{3.34}$$

A summary the concept of optimization is:

↓ Initial values of UA and Q_{loss} are obtained from the calibration procedure during the heat-up phase, where X=0.

↓ The different parameters b_i are initialized at zero, which means that (UA;Q_{loss})=(UA_0;$Q_{loss,0}$) until first optimization iterations are done.

↓ The heat released by the reaction is estimated by the high gain observer, equation 3.34.

↓ Continuous estimation of the conversion is obtained by the equation 3.32 by integrating the heat of the reaction.

↓ An experimental measurement of conversion becomes available.

↓ Optimization of the criterion 3.28, which gives b_i.

↓ Calculation of the continuous values of UA and Q_{loss} as a function of X_{cal}.

3.5 Experimental

In the adaptive calorimetric approach, gravimetric measurements of appropriate intervals (15-30 minutes) are used to fit the convergence of the mathematical model by correcting the parameters b_i. A new optimal trajectory can be recomputed every time new measurements are obtained, and current values of the states re-estimated. Use of the measurements allows us to recompute a trajectory of X_{cal} as the reaction progresses, and to obtain $Q_R(t)$, which provides a great deal of information about what is occurring in the reactor. The combined use of on-line and off-line measurements can therefore be employed to infer values for immeasurable quantities such as Q_{loss} and UA.

Initially, the required amounts of distilled and deionised water is charged with the emulsifier. Nitrogen is then introduced to get rid of the oxygen present in the reactor. During this time the reactor is heated by fixing the bath at the reaction temperature (if we neglect Q_{loss}) or at a temperature ramp program (to estimate UA and Q_{loss}). The reactor temperature is set at 60°C, unless otherwise mentioned. The initial values of UA and Q_{loss} are estimated on-line. This procedure takes about 45 minutes. We will be interested by the last estimate obtained at or near the reaction temperature. Then the monomers (usually used without purification) are added to the reactor. Nitrogen flow maintained for during about 15 more minutes. When thermodynamic equilibrium is attained, the initiator (usually, potassium persulfate, KPS), is added.

The obtained initial values of UA and Q_{loss} are supplied to the program where the optimization procedure is written. The data acquisition routine turned on. The optimization procedure gives us an estimate of the heat of the reaction and monomer conversion almost immediately, assuming that UA and Q_{loss} are constant during the initial interval.

Samples are withdrawn from the reactor at a frequency of one every twenty minutes at the beginning of the reaction, and one every thirty or even sixty minutes once the reaction is well underway. The overall conversion is determined by a thermobalance which usually gives the gravimetric results in 5 minutes. Once available, these values are fed to the Matlab®

program which corrects the estimation of X by varying b_i defined in equations (3.25 and 3.26). The required optimization time increases with the number of samples withdrawn if the optimization takes into account all the samples. In order to accelerate this procedure, we have programmed a moving horizon optimizing technique that uses only the last three experimental points. This produced a discontinuity in the estimation of UA and Q_{loss}, but the estimation of X and Q_R were reasonable and rapidly obtained. This minimization of the run time becomes important when on-line control is required.

The recipes of two batch homopolymerizations of styrene and vinyl acetate, both done in the 7-liter reactor, are given in Table 3.2. The estimated conversion and heat produced by the reaction are shown in Figures (3.7a) and (3.8), for styrene and vinyl acetate, respectively.

Table 3.2: Experiments of homopolymerization for the validation of the adaptive calorimetric observer.

\ experiment Component \	STY (STY-15-3-a)	VAc initial charge (g)
Styrene	600	-
Vinyl acetate	-	600
Water	2403	2400
SDS	4.56	-
DSS	-	3
KPS	4.42	1.84
Final solid contents	20 %	19%
Final particle size	107 nm	120 nm
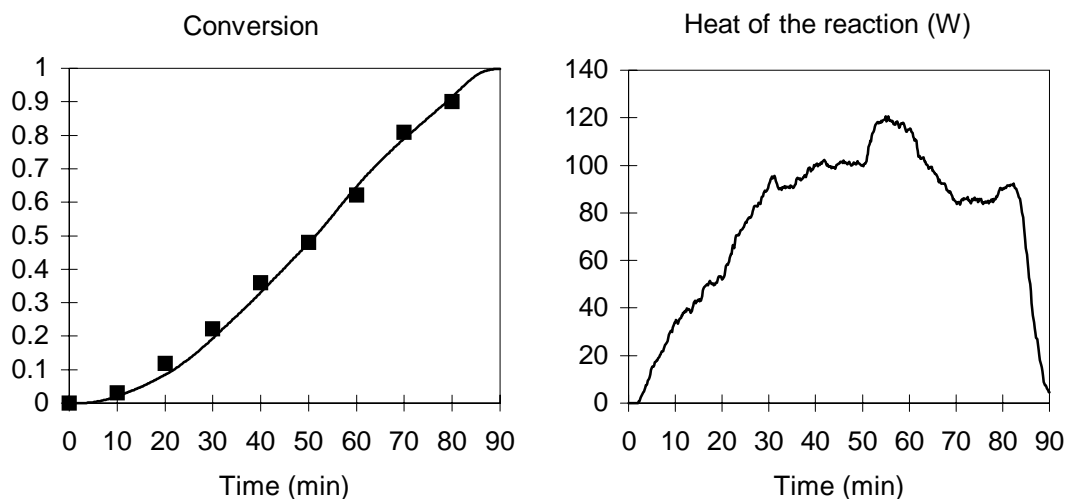
Figure 3.7a: Experiment STY-15-3-a: Mass conversion, at left, and heat of the reaction, at right.
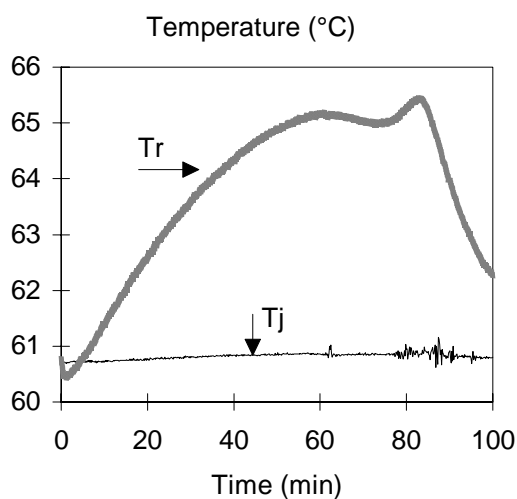
Figure 3.7b: Experiment STY-15-3-a: Reactor and jacket temperatures.

For the homopolymerization of polystyrene , since the reaction is not very rapid, it was possible to estimate the conversion in real time. A gel effect caused an increase in the reaction rate at about 70% of the overall conversion. This effect can be seen on the reaction temperature, Figure 3.7b, and on the heat produced by the reaction, Figure 3.7a at right.
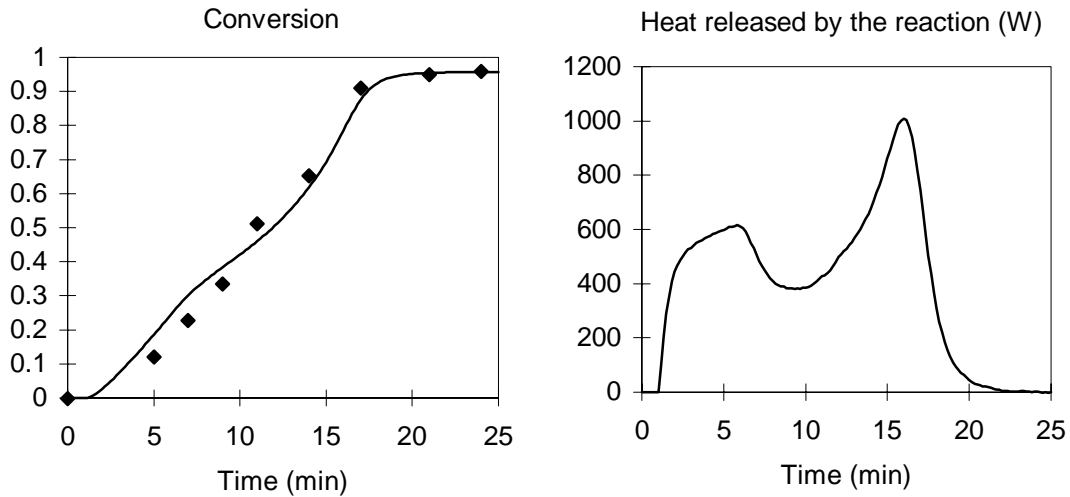
Figure 3.8a: Vinyl acetate homopolymerization. Overall mass conversion fitted to the experimental gravimetric conversion, at left. At right, the heat released by the reaction.

The rate of polymerization of vinyl acetate was higher than during the polymerization of styrene, as shown in Figure 3.8a. Therefore the optimization procedure was done off-line. A gel effect seems to take place at high conversion during this experiment, which allow us to have almost 100% of conversion at the end of the reaction.
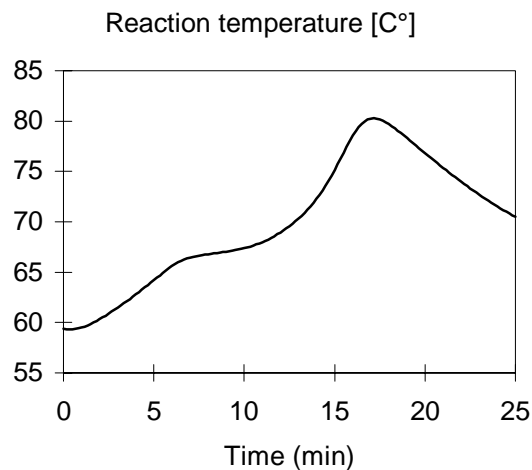
Figure 3.8b: Reactor temperature during the polymerization of vinyl acetate.

Table 3.3 gives the recipes of two seeded copolymerization experiments done in the 7-liter reactor as well. The seed used is a latex of previously prepared polystyrene. The latex was diluted to 4% solids contents, washed with cationic and anionic resins to get rid of all ionic substances due to the dissolution and decomposition of KPS and free surfactant in the aqueous phase. This procedure is repeated until the conductivity of the latex is stable. The latex is then concentrated to 6-8% solids contents. The latex washing procedure allows us to be sure seed contains no initiator. The required amount of seed is then charged to the reactor, with water, surfactant and monomers. The mixture is left for 14 hours under mixing at ambient temperature to allow the polymer particles to be swollen with monomer. Afterwards, the mixture is heated to the reaction temperature, usually 60°C. During the heating period an estimation of the initial value of the heat transfer coefficient U is obtained by the observer developed in section 3.3.2 (without Q_{loss}). A constant value of about 200 W/m²/°C is obtained during the calibration, and is shown in Figure (3.9).

Table 3.3: Experiments of copolymerization for the validation of the calorimetric observer.

\ Experiment Component \	STY-BuA-1c		STY-BuA-7		
	Seed (g)	Initial charge (g)	Seed (g)	Initial charge (g)	preemulsion (g)
STY	1200	116	600	116.4	232
BuA	-	143.3	-	286	286
Seed (PSTY)	-	86.6	-	124	-
Water	4800	1711	2400	-	300
Water in the seed	-	1009	-	1875	-
SDS	16	5	6.5	5.5	5
NaHCO3	4.5	-	2.25	-	-
KPS	4.5	1.7	2.65	4	-
Final particle diameter	86 nm	126 nm	76.5	148	
Final solids contents	-	20 %	-	20.3 %	
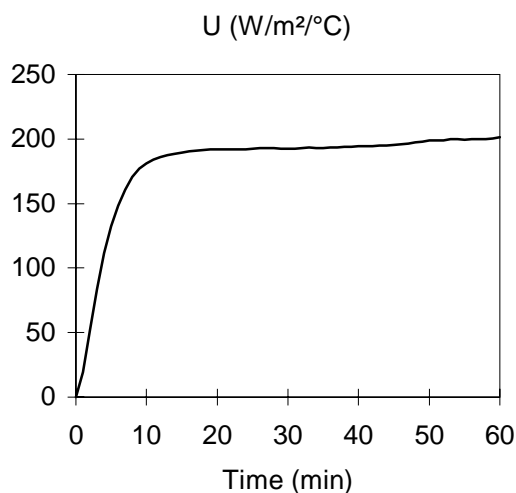
Figure 3.9: Experiment STY-BuA-1c: Calibration of U.

The reaction starts when the initiator is introduced to the reactor. Estimation of the overall conversion and the heat of the reaction is done using the initial value of U until samples are withdrawn and values of X are fed to the heat balance software program. The corrected value of U is shown on Figure (3.11). It can be seen that U decreases with time as expected, since the medium viscosity increases. In order to calculate U from UA, an approximate value of A was calculated from the reactor geometry and the reaction mixture volume, taking into account the mass in the withdrawn samples. The obtained conversion and heat released by the reaction are shown in Figure (3.10) below.

Heat produced by the reaction (W)   Conversion
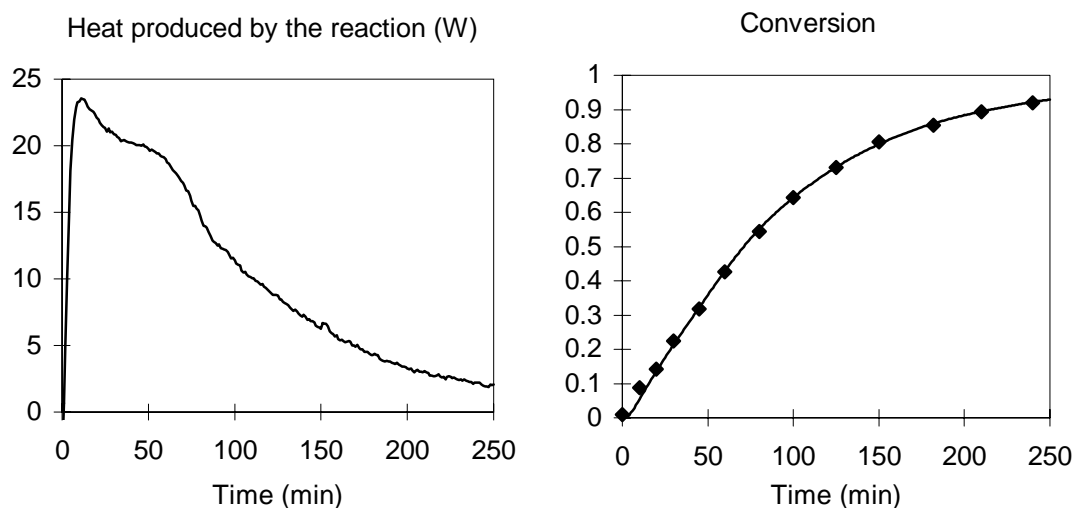
Figure 3.10: Experiment STY-BuA-1C: On-line optimization of the monomer conversion and heat released by the reaction.

Heat transfer coefficient
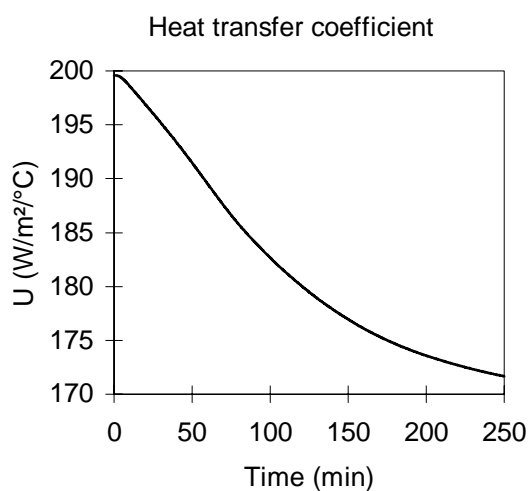
Figure 3.11: Experiment STY-BuA-1c: Evolution of the heat transfer coefficient with time.

The calorimetric technique has also been tested for a semi-batch experiment, STY-BuA-7. The seed was swollen as in experiment STY-BuA-1c. The preemulsion, detailed in Table 3.3, is prepared and stabilized for about one hour before the reaction. Feeding the preemulsion starts at 60 minutes of the reaction at a flow rate of about 3.2 g/min. The mass of preemulsion added to the reactor is fed to the computer along with the measured temperatures to perform the optimization of the overall conversion, the results of which are shown in Figure (3.12). The conversion is maintained almost constant during the semi-continuous

107

operation. Therefore, we can decrease the number of samples withdrawn during a period where no significant change in the viscosity or reactor temperature are supposed. The corresponding rate of heat production is shown in Figure (3.12) at right. It can be seen also that a constant heat flow is produced during the semi-continuous period, which correspond to the relatively constant conversion, also measured during this period.
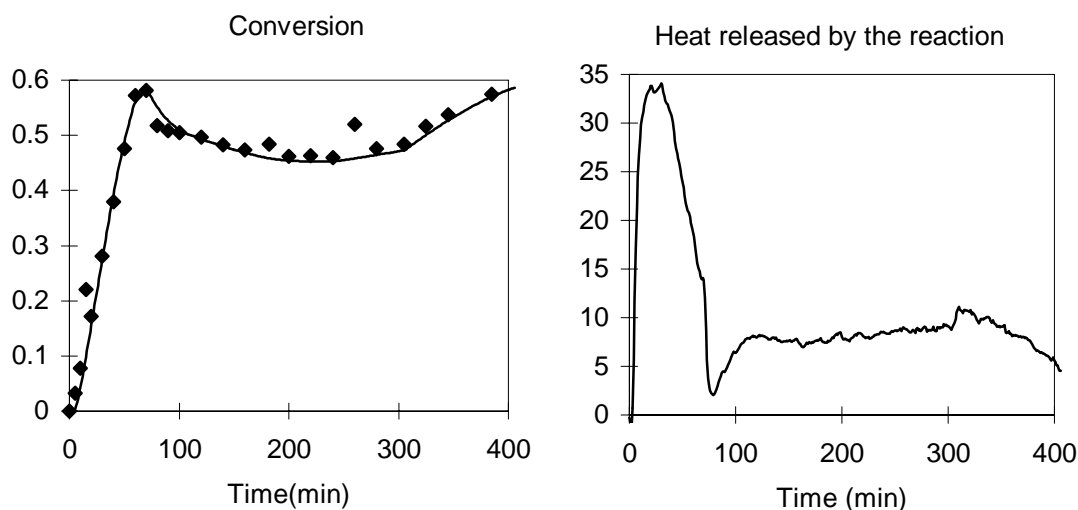
Figure 3.12: Experiment STY-BuA-7: The overall mass conversion at left, and the corresponding rate of heat production by the reaction, at right.

The calorimetric technique can therefore be used for the on-line monitoring of the overall conversion and the heat produced by the reaction. The technique seems to be transparent to the reactor, since it was applied to both the 3 and 7 liter reactors. However, it is important to test the technique to large scale reactors, where the problems of mixing, and temperature gradients are more marked. We have therefore tested the technique on a 250 liter pilot scale reactor. Table 3.4 presents the recipe used for this application. A terpolymerization of butyl acrylate, VAc and ethyl hexyl acrylate was carried out, under isothermal conditions.

Table 3.4: Experiments of terpolymerization in the 250 liter pilot reactor. Validation of the calorimetric observer.

\ Experiment	Experiment 18/6/99		
Final composition (mass)	**60 - 23.7 - 12.02 - 3.4 % BuA-VAc-EHA-AA**		
Temperature	80 °C		
Component \	Initial charge (g)	preemulsion (g)	Initiator solution(g)
H_2O	41000	23000	4000
AA	124	3950	-
EHA	437	13960	-
VAc	860	27480	-
BuA	2212	70660	-
Surfactant	700	7660	-
Ammonium persulfat	118+2kg water	-	390
Final solids contents	**50%**		
Final particle size	92 nm		

Two probes were placed in the reactor for the measurement of the reaction temperature. One of the probes is placed in the baffle and the second one at the bottom of the reactor. In order to apply our technique, the baffle temperature was used to represent the reactor temperature, since the experience has shown that this probe gives more realistic measurements. The probe that is place in the bottom of the reactor was very sensitive to the change in the jacket temperature. The jacket temperature was replaced by the average between the inlet and the outlet temperatures. In this relatively large reactor, and under the chosen jacket flow rate, the difference between the inlet and outlet temperatures varies between 2 and 3 degrees (see Figure 3.13a).
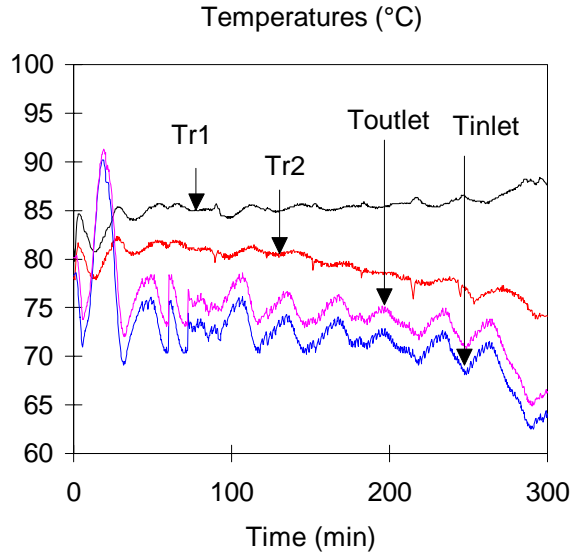
Temperatures (°C)

Figure 3.13a: (Experiment 18/6/99) Temperature measurements in the 250 liter pilot reactor. Tr_1, the measurement of the reactor temperature obtained from a probe placed in the baffle, and Tr_2 the measurement obtained by a probe placed at the bottom of the reactor.
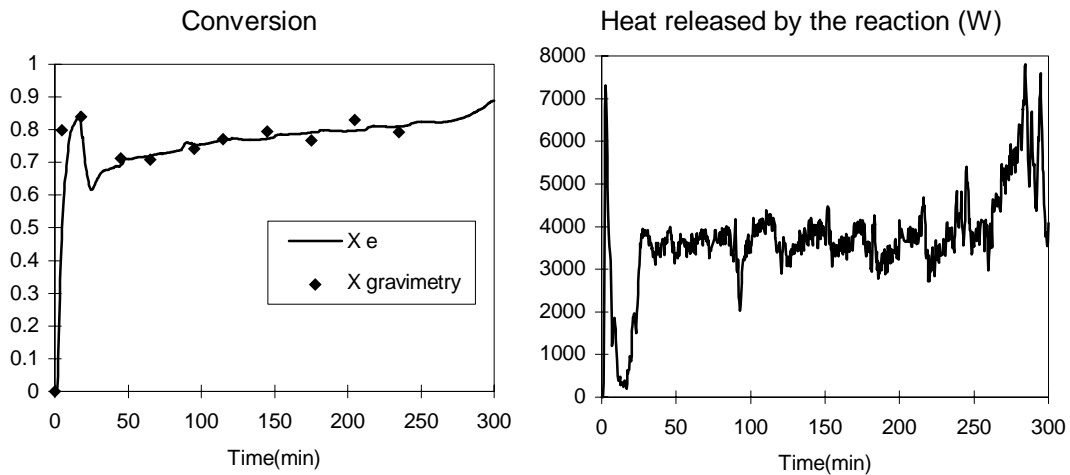
Figure 3.13b: The conversion (at left) and the heat of the reaction (at right) obtained using the adaptive calorimetric observer. (experiment 18/6/99)

Figure (3.13b) shows that the conversion fitting was possible in spite of the temperature simplifications mentioned above. It can be seen that the conversion and the heat produced by the reaction increase importantly during the nucleation part, that was done in batch. During the semi-continuous part of the experiment, the monomer conversion and Q_R remain relatively constant.
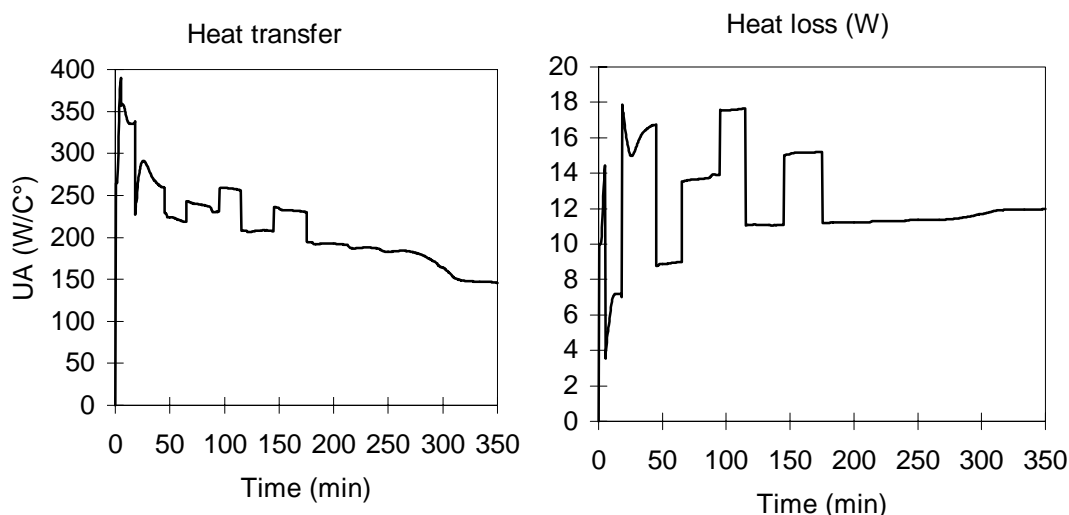
Figure 3.13c: Estimation of UA and Q_{loss}, for the experiment 18/6/99.

Figure (3.14c) shows that the estimated heat transfer coefficient varies between UA=300W/°C at the beginning and 150W/°C at the end of the reaction, but can be considered constant during the semi-continuous period. The discontinuities in the estimation of UA and Q_{loss} are due to the sliding horizon used for the conversion fitting. As we mentioned earlier, this option was added in the software program containing the optimization procedure and the energy balance, in order to accelerate the optimization procedure. The estimated values of UA and Q_{loss} in this case are not ensured to converge to the real values, which is due to the fact that the models used to represent their dynamics are not very realistic. However, since our interest is focused on estimating the monomer conversion and Q_R, we can estimate the values of UA and Q_{loss} in this way.

3.6 Conclusion

In this chapter, we demonstrated that the joint use of calorimetry, some occasional off-line measurements of the monomer conversion, and methods of estimation, can be used to monitor batch and semi-continuous emulsion homo-, co- and terpolymerizations in real time. The technique is robust to modeling errors, and measurement noise. The technique is also transparent to the reactor size, since it is applicable to laboratory scale as well as industrial scale reactors.

Concerning laboratory scale reactors, the Kalman-like observer is recommended to estimate the initial values of UA and Q_{loss}. For large scale reactors, the high gain observer can be used to estimate the initial value of UA without Q_{loss} which is negligible on large reactors. During the reaction, introducing real measurements of the monomer conversion seem to be necessary to update the estimation. Of course it would be better to use a more developed on-line in situ technique to obtain real measurements of the monomer conversion than taking samples and measuring the conversion gravimetrically.

The information obtained by calorimetry seem therefore to be useful for process control: reaction temperature control by means of feed-forward and feed-back control, the heat released by the reaction and the reaction rate control, and controlling specific polymer properties. However, the estimation of the overall conversion does not give direct information about these properties. Monitoring of these properties requires the development of a mathematical model relating the properties of interest with the overall conversion.

In the following two chapters, we will develop a procedure for the on-line estimation of the polymer composition in emulsion co- and terpolymerization processes based on the estimated overall conversion. The development of such estimators requires the use of an adaptive mathematical representation of the processes. Two models of copolymerization process will be studied in Chapter 4, and in chapter 5 we study the estimation of terpolymerization processes. These estimators are necessary for the composition control and maximizing productivity that will be discussed in chapters 6 and 7.

3.7 Nomenclature

Notation

A	state matrix of dimension n×n
b_i	corrective parameters defined by equation 3.25 and 3.26
C_{pi}	heat capacity of the substance i (J/kg/°C)
C_{Pr}	total heat capacity of the substances in the reactor (J/kg/°C)
C_{pins}	heat capacity of the reactor inserts (J/kg/°C)
C_{pfeed}	heat capacity of the feed (J/kg/°C)
C_{Pj}	heat capacity of the cooling fluid in the jacket (J/kg/°C)
h_R,	reactor side heat transfer coefficient (W/m²/K),
h_j,	jacket side heat transfer coefficient (W/m²/K),
m_i	mass of substance i in the reactor (kg)
m_r	total mass of substances in the reactor (kg)
$\dot{m}_f$	mass flow rate of the feed (kg)
$\dot{m}_j$	mass flow rate of fluid in the jacket (kg)
m_j	mass flow rate of the cooling fluid in the jacket (kg)
MW_i	molecular weight of monomer i (g/mol)
N_i	number of moles of residual monomer i (mol)
N_i^T	total number of moles of monomer i (mol)
Q_{accu}	heat accumulated in the reaction (W)
$Q_{accu,j}$	heat accumulated in the jacket (W)
$Q_{condenser}$	heat loss due to the condenser (W)
$Q_{cond,j}$	conductive heat change between the reactor and the jacket (W)
$Q_{conv,j}$	convective heat change in the jacket (W)
Q_{feed}	sensible heat change due to the feed (W)
Q_j	heat change in the reactor due to the jacket (W)
$Q_{j,loss}$	heat loss from the jacket to the surroundings (W)
Q_{loss}	heat loss from the reactor to the surroundings (W)
Q_R	heat produced by the reaction (W)

$Q_{stirrer}$	power produced by the stirrer (W)
R_{pi}	rate of reaction of monomer i (mol/s)
t	time
T_{amb}	ambient temperature (°C)
T_R	reactor temperature (°C)
T_j	jacket temperature (°C)
T_{feed}	temperature of the feed (°C)
T_j^{in}	jacket inlet temperature (°C)
T_j^{out}	jacket outlet temperature (°C)
U	heat transfer coefficient between the reactor and the jacket (W/m²/°C)
UA	lumped heat transfer coefficient with the jacket (W/°C)
UA_{init}	initial value of UA (W/°C)
V_R	reactor volume (cm^3)
x	state
X_g	gravimetric mass conversion
X_{cal}	calorimetric conversion
y	output

Greek letters

β_j	tunable parameters of input/output linearized system
ε	error
ε_i	a bounded function representing the dynamic of i
ΔH_{Pi}	molar heat of polymerization (J/mol)
θ	observer tuning parameter
S_θ	the unique solution of the algebraic Lyapunov equation
λ_W	reactor wall heat conductivity (W/m²/K).

Acronyms

AA	Acrylic acid
BuA	Butyl acrylate
CSTR	Continuous stirred tank reactor
DTA	Differential Thermal Analysis
DSC	Differential Scanning Calorimeter
EA	Ethyl acrylate
EAc	Ethyl acetate
EHA	Ethyl hexyl acrylate
FTIR	Fourier Transformation, Infrared
GC	Gas chromatography
HP	Hewlett-Packard
MBC	Model Based Control
MMA	Methyl methacrylate
MPC	Model Predictive Control
IR	Infrared
NIR	Near-infrared
NMR	Nuclear Magnetic Resonance
MIR	Midrange-infrared
RC1	Reaction Calorimeter 1
RLS	Recursive least square
STY	Styrene
UPV	Ultrasonic Propagation Velocity
VAc	Vinyl acetate

3.8 Bibliography

1.   Abbey, K. J., Polymerization kinetics by precision densimetry, *American Chem. Soc.*, **21**, 345-356, (1981).

2.   Alonos, M., M. Oliveres, L. Puigjaner, and F. Recasens, *IND. Eng. Chem. Res.*, **26**, 65, (1987).

3.   Aldridge, P. K., J. J. Kelly, J. B. Callis, and D. H. Burns, Noninvasive monitoring of bulk polymerization using short-wavelenght near-infrared spectroscopy, *Anal. Chem.*, **65**, 3581-3585, (1993).

4.   Arzamendi, G., and J. Asua, Copolymer composition control of emulsion copolymers in reactors with limited capacity for heat removal, *Ind. Eng. Chem.*, **30**, 1342-1350, (1991).

5.   Barandiaran, M. J., L. L. de Arbinal, J. C. de la Cal, L. M. Gugliotta, and J. M. Asua, Parameter estimation in emulsion copolymeriztion using reaction calorimeter data, *J. Appl. Polym. Sci.*, **55**, 12311239, (1995).

6.   Barudio, I., Développement d'une stratégie globale pour le contrôle d'un procédé de copolymerization en émulsion, Thesis, Université Claude Bernard-Lyon 1, (1997).

7.   Berber, R., Control of batch reactors- A review (reprinted from methods of model based process control, 1995), *Chem. Eng. Res. Des.*, **74(A1)**, 3-20, (1996).

8.   Buruaga, I. S., M. Arotçarena, P.D. Armitage, L.M. Gugliotta, J.R. Leiza and J.M. Asua, On-line calorimetric control of emulsion polymerization reactors, *Chem. Eng. Sci.*, **51**, 11, 2781-2786, (1996).

9.   Buruaga, I. S., A. Echevarria, P. D. Armitage, J. C. de la Cal, J. R. Leiza, and J. M. Asua, On-line control of a semibatch emulsion polymerization reactor based on calorimetry, *AICHE*, **43**, 4, (1997)[a].

10.   Buruaga, I. S., P. D. Armitage , J. R. Leiza, and J. M. Asua, On-line Control for maximum production rat of emulsion polymers of well defined polymer composition, *ECCE1*, **4,7**, 117-120, (1997)[b].

11.   Buruaga, I. S., P. D. Armitage , J. R. Leiza, and J. M. Asua, Nonlinea control for maximum production rate of latexes of well-defined composition, *Ind. Eng. Res.*, **36**, 4243-4254, (1997)[c].

12.   Canegallo, S., G. Storti, M. Morbidelli, and S. Carra, Densimetry for on-line conversion monitoring in emulsion homo- and copolymerization, *J. Appl. Polym. Sci.*, **47**, 961-979, (1993).

13.   Carloff, R., A. Prof, and K. -H. Reichert, Temperature oscillation calorimetry in stirred tank reactors with variable heat transfer, *Chem. Eng. Technol.*, **17**, 406-413, (1994).

14.   Chatzi, E. G., O. Kammona and C. Kiparissides, Use of midrange infrared optical-fiber probe for the on-line monitoring of 2-ethylhexyl acrylate/styrene emulsion copolymerization, *J. Appl. Polym. Sci.*, **63**, 6, 799-809, (1997).

15.   Chein, D. C. H., and A. Penlidis, On-line sensors for polymerization reactors, *JMS-REV. Macromol. Chem. Phys.*, **30**, 1, 1-42, (1990).

16.   Debelak, H. NI, K., D. Hunkeler, Temperature control of highly exothermic batch polymerization reactors, *J., Appl. Polym. Sci.*, **63**, 761-772, (1997).

17.   de la Rosa, V. E. D. Sudol, M. El-Asser, and A. Klein, Details of the emulsion polymerization of styrene using a reaction calorimeter, *J. Polym. Sci.: Part A: PolymerChem.*, **34**, 461-473, (1996).

18.   de la Rosa, L. V., E. D. Sudol, M. S. El-Aasser, A. Klei, Emulsion polymerization of styrene using reaction calorimeter. III. EFFECT of initial monomer/water ratio, *J. Polym. Sci.* **37**, 4073-4089, (1999)[a].

19.   de la Rosa, L. V. E. D. Sudol, M. S. El-Aasser, and A. Klein, Emulsion polymerization of styrene using reaction calorimeter. II. Importance of maximum in rate of polymerization, *J. Appl. Polym. Sci.: Part A: Polymer Chem.*, **37**, 4066-4072, (1999)[b].

20.   Dittmar, R., Z. Ogonowski, K. Damert, Predictive control of a nonlinear open-loop unstable polymerization reactor, *Chem. Eng. Sci.*, **46**, 10, 2679-2689, (1991).

21.   Févotte, G., I. Barudio, J. Guillot, An adaptive inferential measurement strategy for on-line monitoring of conversion in conversion in polymerization processes, *Thermochimica acta*, **289**, 223-242, (1996).

22.   Gloor, P. E., R. J. Warner, Developing feed policies to maximize productivity in polymerization process ", *Thermochimica Acta*, **289**, 2, 243-265, (1996).

23.   Gossen, P. D., J. F. MacGregor, and R. H. Pelton, Composition and particle diameter for styrene/methyl methacrylate copolymer latex using UV and NIR spectroscopy, *J. Appl. Polym. Sci.*, **70**, 1737-1745, (1993).

24.	Gugliotta, L. M. J. R. Leiza, M. Arotcarena, P. D. Armitage, and J. M. Asua, Copolymer composition control in unseeded emulsion polymerization using calorimetric data, *Ind. Eng. Chem. Res.*, **34**, 3899-3906, (1995).

25.	Gugliotta, L.M., J.R. Vega, C.E. Entonione, and G.R. Meira, Emulsion copolymerization of acrylonitrile and butadiene in an industrial batch reactor, Estimation of conversion and polymer quality from on-line energy measurements, *Polymer Reac. Eng.*, **7**, 4, 531-552, (1999).

26.	Guinot, Ph., Othman N., Févotte G., McKenna T. F., On-line monitoring of emulsion copolymerizations using hardware sensors and calorimetry, *Polymer Reaction Engineering*, **8**(2), 115-134, (2000).

27.	Guyot, A., J. Guillot, C. Graillat, and M. F. Llauro, Controlled composition in emulsion copolymerization application to butadiene-acrylonitrile copolymers, *J. Macromol. Sci. Chem.*, **A21(6&7)**, 683-699, (1984).

28.	Hariri, M. H., R. A. Lewis, T. R. Lonis, The effect of operating conditions on a reaction calorimeter, *Thermochimica acta*, **289**, 343-349, (1996).

29.	Heldt, K., and HL. Anderson, Possibility of adiabatic precision calorimetry for kinetic evaluations, *J. Thermal Analysis*, **47**, 2, 559-567, (1996).

30.	Johnson, F. J., M. E. Connell, E. F. Dike, W. M. Cross, and J. J. Kellar, New fiber sensor for in situ near-infrared monitoring of polymer matrix composites, *Applied Spectroscpoy*, **52**, 8, 1126-1129, (1998).

31.	Kammona, O., E. G. Chatzi and C. Kiparissides, Recent developments on hardware sensors for the on-line monitoring of polymerization reactors, Journal of molecular science, *JMS-REV. Macromol; Chem. Phys.*, **C39**, 1, 57-134, (1999).

32.	Kumpinsky, E., A method to determine heat-transfer coefficient in a heat-flow reaction calorimeter, *Thermochimica Acta*, **289**, 2, 351-366, (1996).

33.	Karlsen, L. G. and J. Villadsen, Isothermal reaction calorimeters-I. A literature review, *Chem. Eng. Sci.*, **42**, 5, 1153-1164, (1987).

34.	Landau, R. N., Calorimetric investigation of an exothermic reaction -Kinetic and flow modeling, *Ind. Eng. Chem. Res.*, **33**, 4, 814-820, (1994).

35.	Landau, R. N., Expanding the role of reaction calorimetry, *Thermochimica Acta*, **289**, 101-126, (1996).

36. Leiza, J. R., Dearrollo de un sistema automatico para el control en linea de la composicion de polymeros obtenidos en emulsion, Thesis, Euskal Herriko Unibertsitatea, (1991).

37. MacGregor, J. F., On-line reactor energy balances via Kalman filtering, *IFAC-PRP-6 conf. Akron*, USA, (1986).

38. McKenna, T., G. Févotte, C. Graillat, J. Guillot, Joint use of calorimetry densimetry and mathematical modeling for multiple component polymerizations, *Inst. Chem. Eng.*, **74**, 340-348, (1996).

39. Maschio, G., I. Ferrara, C. Bassani, H. Nieman, An integrated calorimetric approach for the scale-up of polymerization reactors, *Chem. Eng. Sci.*, **54**, 3273-3282, (1999).

40. Mosebach, M. K.-H. Reichert, Adiabatic reaction calorimetry for data acquisition of free-radical polymerisations, *J. Appl. Polym. Sci.*, **66**, 673-681, (1997).

41. Nomen, R., J. Sempere, R.L. Cunha, Dynamic evaluation of heat flow reaction calorimeters under reflux conditions, *Thermochimica acta*, **289**, (1996).

42. Ponnuswamy, S., S. L. Shah, and Kiparissides, On-line monitoring of polymer quality in a batch polymerization reactor, *J. App. Polym Sci.*, **32**, 3239-3253, (1986).

43. Regenass, W., The development of stirred-tank heat flow calorimetry as a tool for process optimization and process safety, *Chimia*, **51**, 189-200, (1997).

44. Santos A.M., Févotte G., Othman N., Othman S., McKenna T. F., The on-line monitoring of methyl methacrylate-vinyl acetate emulsion copolymerisation, *J. Appl. Polym. Sci.*, **75**, 1667-1683, (2000).

45. Shork, F. J., and W. H. Ray, On-line measurement of surface tension and density with application to emulsion polymerization, *J. Appl. Polym. Sci.*, **28**, 407-430, (1988).

46. Schuler, H., and C.-H. Schmidt, Calorimetric-state estimators for chemical reactor diagnosis and control: Review of methods and applications, *Chem. Eng. Sci.,* **47**, 4, 899-915, (1992).

47. Schmidt, C.-U., K.-H. Reichert, Reaction calorimeter a contribution to safe operation of exothermic polymerizations, C*hem. Eng. Sci.*, **43**, 8, 2133-2137, (1988).

48. Siani, A., G. Storti, M. Morbidelli, Procedure for calibrating an ultrasonic sensor for online monitoring of conversion in latex reactors, *J App. Polym. Sci.*, **72**, 1451-1477 (1999).

49. Soroush, M, C. Kravaris, Nonlinear control of a batch polymerization reactor: an experimental study, *AICHE*, **38**, 9, 1429-1447, (1992).

50. Soroush, M., C. Kravaris, Multivariable nonlinear, control of a continuous polymerization reactor: an experimental study, *AICHE*, **39**, 12, 1920-1937, (1993).

51. Soroush, M, C. Kravaris, Nonlinear control of a pol7ymzrization CSTR with singular characteristic matrix, *AICHE*, **40**, 6, (1994).

52. Tauer, K., H. Muller, C. Schellenberg, L. Rosengarten, Evaluation of heterophase polymerizations by means of reaction calorimetry, *Colloid and Surface A,* **153**, 143-151, (1999).

53. Tietze, A., I. Ludke,,K.-H. Reichert, Temperature oscillation calorimetry in stirred tank reactors, *Chem. Eng. Sci.*, **51**, 11, 3131-3137, (1996).

54. Tirrell, M., and K. Gromley, Composition control of batch copolymerization reactors, *Chem. Eng. Sci.*, 36, 367 (1981).

55. Tufano, V., Adiabatic calorimetry- A contribution to an advanced method of data analysis, *J. Thermal Analysis*, **39**, 7, 803-815, (1993).

56. Uchida, T., M; Surianaraymanan, M. Wakakura, and H. Tokioka, Hazards of radicals polymerizations: Thermokinetic investigation of styrne polymerization methods, *J. Chem. Eng. Japon*, **31**, 6, 960-968, (1998).

57. Urretabizkaia, A., E. D. Sudol, M. S. El-Aasser, and J. M. Asua, Calorimetric monitoring of emulsion copolymerization reactions, *J. Polym. Sci.*, **31**, 2907-2913, (1993).

58. Zaldivar, J.M., H. Hernadez, and C. Barcons, Development of a mathematical model and a simulator for the analysis and optimization of batch reactors: experimental model characterization using a reaction calorimeter, *Thermochimica Acta*, **289**, 267-302, (1996).

CHAPTER IV ———————————

STATE ESTIMATION, APPLICATION TO COPOLYMERIZATION PROCESS

4 STATE ESTIMATION, APPLICATION TO COPOLYMERIZATION PROCESS

4.1 Introduction

In chapter 2 we showed that state estimation techniques are highly powerful means of obtaining safe and effective monitoring and/or control in chemical processes, especially in cases where on-line measurement of all process states and/or where perfect modeling of these processes is not possible. Emulsion polymerization is of course no exception, since the most important properties of polymer, such as MWD, PSD, composition, are not usually measurable on-line. As we discussed earlier, certain on-line measurements, such as GC or densimetry are inconvenient because of frequent coagulation in the sampling device, and other techniques, such as spectroscopy, are still largely undeveloped and it is still difficult to use them to obtain direct information about the polymer quality. On the other hand, decisions for process control cannot be taken based only on the process model, since emulsion polymerizations usually contain time-varying and poorly known variables. However, when specific observability conditions are satisfied, state estimators can be used to circumvent model uncertainties, errors in the initial values and measurements containing random noise, and to infer reliable information on the state of the process.

For these reasons, state estimation has been widely applied in emulsion polymerization. Several estimation methods have been proposed with the most widely used estimation technique for parameter estimation being the Kalman filter. For instance, Kiparissides et al. (1981) developed an optimal control of a continuous reactor that is based on the use of an EKF. Gagnon and MacGregor (1991) showed that KF allows to account for impurity flow rates in the model by means of stochastic states. Dimitratos et al. (1991) showed that the use of KF allows to account for model uncertainties (in their model, uncertainties were in the model representing monomer distribution between the aqueous and polymer phases). The use of KF allowed the authors to successfully estimate the copolymer

composition of a seeded emulsion copolymerization of vinyl acetate/butyl acrylate, and the average number of radicals per particle, based on GC measurements, performed by employing a sampling device. Kozub and MacGregor (1992) applied a nonlinear optimization procedure and EKF for state estimation of a semi-continuous polymerization reactor of styrene/butadiene rubber. They reported that the major problems with the optimization procedure were the significant computational efforts required, that it does not account for possible model disturbances, and the assumption that the parameters to be optimized were time-invariant over the optimization horizon.

Data fitting with experimental measurements was also used for parameter estimation. For instance, Févotte et al. (1996[b]) employed an optimization technique for the estimation of the conversion in emulsion and solution polymerization based on calorimetry. Asua et al. (1990) used technique for the estimation of kinetic parameters related to the number of moles of radicals in the aqueous phase (R_w) in homopolymerization processes and de la Cal et al. (1990) applied the same procedure for the estimation of R_w in copolymerization processes. Barandiaran et al. (1995) used the Levenberg-Marquardt method for the estimation of kinetic parameters in batch seeded emulsion copolymerization systems.

Estimations were also frequently obtained by means of an open-loop observer (e.g. Urretabizkaia et al. (1993), for the estimation of the conversion (X) and composition (F_i) based on calorimetry, Gugliotta et al. (1999), for the estimation of X, F_i and MW in an industrial batch reactor of acrylonitrile and butadiene).

On the other hand, recent developments in nonlinear theory and observers have been reported in the literature and in some cases, applied to parameter estimation in polymerization reactors. For example, a high gain nonlinear observer was successfully applied by Févotte et al. (1998[a] and 1998[b]) to estimate the residual number of moles of monomers and the number of moles of radicals in the polymer particles, based on calorimetry. Nonlinear observers were used also for state estimation in solution polymerization reactors, e.g. Dootingh et al. (1992), Soroush (1997), Tatiraju et al. (1999), and Alvarez et al. (1999).

As we mentioned in chapter 2, the application of KF to nonlinear emulsion polymerization models requires that the model be linearized around an operating point. Even

if this technique has successfully been applied in several cases, as indicated in the literature review, in others it does not precisely represent the process, and for several processes, a nonlinear estimation technique must be used. On the other hand, the use of conventional nonlinear optimization techniques requires a significant computational effort and cannot therefore be effective in a control procedure. Finally, it is well known that open-loop observers do not ensure accurate results. They are sensitive to initial conditions, measurement random noise and model disturbances and mismatch. As a result, we will use nonlinear observers for state estimation where ever possible in this work.

State estimation techniques are based on a measurement that is sensitive to the state to be estimated, and a mathematical model that relates the state and the output and ensures the observability of the state of interest. Mathematical models of emulsion copolymerization reactors are now reasonably well-understood, and have been widely reported in the literature in recent years, e.g. Hamielec et al. (1987), Richard and Congalidis (1989), Scott et al (1995), Dubé and Penlidis (1995[a]), Lopez de Arbina et al. (1997) and Saldivar et al. (1998). Penlidis et al. (1985) reported a study on the modeling and experimental investigation of the batch emulsion polymerization of vinyl acetate. The dynamics of the continuous seeded emulsion homopolymerization were published by Chen-Cong and Wen-Yen Chiu (1982), and Schork and Ray (1987) studied the polymerization of methyl methacrylate. Gilmore et al. (1993) modeled the homopolymerization of vinyl acetate involving the nucleation and growth mechanisms of polymer particles.

The objective of this chapter is to estimate the rate of reaction and therefore polymer composition, in emulsion copolymerization systems. Theses estimates are required for the composition control strategy that we will discuss in chapter 6. In the previous chapter, we developed an on-line estimation technique that provided the overall conversion, based on calorimetry. However, in emulsion co- or terpolymerization, the overall conversion does not provide unambiguous information about the polymer properties. This is due to the fact that the monomers do not usually react at the same rate (excepting under azeotropic composition), and therefore the overall conversion is not equal to individual conversions. They must therefore be estimated by another technique.

In order to estimate the polymer composition, we need a mathematical model that represents the composition and relates it to the overall conversion. The material balance of monomers involves the reactivity ratios, and can therefore be used to infer information about the individual reaction rates of the different monomers if the overall conversion is known. In this chapter, we will first develop the material balance of a semi-batch copolymerization reaction. Since the material balance includes always some unknown and/or difficultly modeled variables (e.g. average number of radicals per particle), it cannot be used to directly simulate the reaction and to determine the polymer composition. To overcome this problem, we propose an observer for the individual monomer conversions, and thus of the copolymer composition, based on the calorimetric estimation of the overall conversion.

4.2 Mathematical model

The choice of an adequate mathematical model for each application is of primary importance. A compromise must be found between model simplicity and accuracy. On one other hand, we want the model to allow us to monitor polymer properties and to optimize the process (improve polymer quality and decrease time under safe conditions). But, on the other hand, a highly complex model that involves many parameters is to be avoided if it does not offer a significant advantage for the application of interest with respect to a simpler model. What we mean by this should become clear as we move through the rest of the chapter.

One of the most important features in latex synthesis that cannot be overlooked when developing an adequate model of emulsion polymerization (and in particular when our objective is the composition control) is that these polymerization systems frequently involve more than one monomer. These monomers do not usually have the same reactivities, which means that they will react at different rates, and that if we do not control these rates, this will have a negative impact on the resulting polymer composition, which is in turn of the utmost importance in terms of the product properties.

The polymer composition is determined by the rate of reaction of each monomer, which in turn depends on the amount of monomer and radicals at the reaction site, and on the kinetic parameters (which we assume to be known in the work done here). In fact, the heterogeneous nature of emulsion polymerization implies that the monomers and radicals are partitioned in a complex way between the different phases in the reactor (aqueous phase, monomer droplets and polymer particles) depending on the water solubility of the different species and their interactions with the resulting polymer. The reaction can therefore take place in the polymer particles and in the aqueous phase (if the concentration of radicals and monomer dissolved in the water is sufficient). It is therefore of interest to know under what circumstances must the reaction in the aqueous phase be considered and accurately modeled in order to adequately design and control a reaction system. Therefore, for the moment, we make our model of the process as general as possible.

In general terms, the time variation of the number of moles of each monomer in a perfectly mixed semi-continuous reactor takes the following form:

$$\frac{dN_i}{dt} = Q_i - R^p_{pi} - R^w_{pi}$$

(4.1)

According to the mechanism of emulsion polymerization (appendix I), the reaction rate that appears in the material balance is a function of various parameters related to monomer concentration in the different phases, $[M_i{}^j]$, and the number of radicals in each phase (the number of moles of radicals in the polymer particles (μ) and the number of moles of radicals in the aqueous phase (R_w)), as follows:

$$R^p_{pi} = \mu[M^p_i]\left(Kp_{1i}P^p_1 + Kp_{2i}\left(1 - P^p_1\right)\right)$$

(4.2)

$$R^w_{pi} = R_w[M^w_i]\left(Kp_{1i}P^w_1 + Kp_{2i}\left(1 - P^w_1\right)\right)$$

(4.3)

where $P_i{}^j$ is the time averaged probability that the ultimate unit of an active chain in the phase j is of type i. These probabilities are defined by the following equations:

$$P^j_1 = \frac{1}{1 + \dfrac{Kp_{12}}{Kp_{21}}\dfrac{[M^j_2]}{[M^j_1]}}, \quad P^j_2 = 1 - P^j_1, \quad j = w, p$$

(4.4)

and

$$\mu = \frac{\overline{n}N^T_P}{N_A}$$

(4.5)

where $\overline{n}$ is the average number of radicals per particle, $N_P{}^T$ the total number of particles in the reactor, and N_A is the Avogadro's number.

Since the monomers involved in emulsion polymerization are usually partially hydrophilic and have thus different solubilities in the aqueous phase, they are unequally partitioned between the different phases. This partitioning of monomer between the different phases must be determined in order to estimate the reaction rate of the different monomers in the different phases. Models for the monomer and radical concentrations measurement in the different phases are presented below.

4.3 Monomer concentration in the different phases, $[M_i^j]$

In emulsion polymerization, the conversion from monomer to polymer occurs principally in the monomer-swollen polymer particles. Monomer is transferred from the monomer droplets to the reaction site by diffusion through the aqueous phase. The polymer particles absorb a certain amount of monomer that is limited by thermodynamic equilibrium. On the other hand, free radicals are formed in the water-phase and diffuse to the polymer particles. The solubility of monomer in the water phase influences: radical transport out of the monomer-swollen-polymer particle, the rate of polymerization in the aqueous phase, the monomer ratio in each phase, and hence the overall rate of the reaction and the product formed (Poehlein (1995)). The monomer solubility and reaction in the aqueous phase can also provoke homogeneous nucleation of new particles which also influences the rate of reaction, as well as final latex properties. Therefore, determining the monomer concentration in the aqueous phase is of interest.

Let us introduce the following definitions:

$$\phi_p^p = V_p^p / V^p$$

$$\phi_i^p = V_i^p / V^p \tag{4.6}$$

$$\phi_i^d = V_i^d / V^d , \ i=1, 2$$

where ϕ_i^j is the volumetric fraction of monomer i in phase j, 1 and 2 are monomers 1 and 2 respectively, p and d are the polymer and droplet phases, V_i^j is the volume of monomer i in phase j, V_i is the total volume of monomer i and V^j is the total volume of phase j.

Assuming that the volume change on mixing is zero and that water does not dissolve in the latex particles or in the pure monomer, the overall material balances are presented by the following equations and are valid whatever is the model of partitioning used:

$$V_1 = V_1^d + V_1^{aq} + V_1^p$$

$$V_2 = V_2^d + V_2^{aq} + V_2^p \tag{4.7}$$

$$V^{aq} = V_w^{aq} + V_1^{aq} + V_2^{aq}$$

$$V^p = V_1^p + V_2^p + V_p^p$$

$$V^d = V_1^d + V_2^d$$

where aq is the aqueous phase and w is water.

The polymer particles are under saturation conditions if the following condition holds:

$$V_1 + V_2 > V^p\left(\phi_1^p + \phi_2^p\right) + V^{aq}\left(\phi_1^{aq} + \phi_2^{aq}\right) \tag{4.8}$$

The end of interval II is characterized by the disappearance of monomer droplets in the reactor (i.e. $V^d = V_1{}^d = V_2{}^d = 0$) and the total residual volume of monomer exactly saturates the polymer particles and the aqueous phase. During phase III, the concentration of monomer is partitioned between the polymer particles and the aqueous phase.

Several models have been developed in the literature to predict the concentration of monomer in the different phases, based on theoretical considerations (thermodynamics, swelling capability of the latex particles by monomer, interactions), or 4on empirical or semi-empirical relationships.

Morton et al. (1954) developed an equation to determine the swelling of latex particles in phase II, based on the original thermodynamic model of Flory-Huggins (Flory 1953). Vanzo et al. (1965) used the theory developed by Morton (1954) and added a contribution to the phase III partitioning. A second model was proposed by Maxwell et al. (1992[a,b] and 1993[a,b]) who developed a semi-empirical relationship based on the simplification of the equations of Morton (1954) and Vanzo et al. (1965). A review on the theoretical considerations concerning the determining of the concentration of monomer in latex particles, was done by Gardon (1968). Ugelstad et al. (1983) studied the thermodynamics of swelling of polymer, oligomer and polymer-oligomer particles. Schoonbrood et al. (1994), derived equations similar to that developed by Maxwell, from Morton's equation for partial and saturation swelling with n monomers, depending only on the saturation concentrations of each monomer in the polymer particles and in the aqueous phase. A third, simpler model to

determine the concentration of monomers in the different phases is based on the use of constant partition coefficients, was used by Omi et al. (1985) for monodisperse systems. Armitage et al. (1994) improved the algorithm for the calculation of the monomer partitioning in polydisperse emulsion copolymerization systems.

These three kinds of models have been used in several systems for several applications. For instance, Mead and Poelein (1988) developed a model to predict the rate of reaction in a seed-fed CSTR of styrene/methyl acrylate and styrene/acrylonitrile, where the monomer partitioning was calculated by Morton and Vanzo models. Guillot (1981 and 1985), used the Morton relationship (Morton (1954)) to study the thermodynamic aspects of acrylonitrile/styrene emulsion copolymerization. Urquiola et al. (1991) used the Morton relationship in the semi-continuous seeded emulsion copolymerization of vinyl acetate and methyl acrylate, to construct a predictive model of the evolution of the polymer composition, the average number of radicals per particle and the number of polymer particles. Recently, a dynamic swelling method was used by Okubo et al. (1999) to synthesize large monodisperse polymer particles, based on Morton's equation and the variations given by Uglestad et al. (1983). The partition coefficients necessary for these models have been determined in the literature for several monomers and under different conditions (pH, temperature), e.g. Santos et al.(1998) and Arzamendi and Asua (1989). A recent review of the three main algorithms used to determine the monomer concentration in the different phases was done by Gugliotta et al. (1995). In their work, the authors considered that the model developed by Morton represents well the monomer partitioning. They reported that constant partition coefficient algorithm was the simplest in terms of number of involved parameters and the time required to solve the corresponding partitioning equations on the PC. Based on these assumptions, they developed a criterion that helps to chose a model for a specific application. The constant partition coefficient algorithm, gives the same results as Morton's model when used to determine the monomer partitioning in seeded and unseeded systems with high solids content, if the monomers are partially soluble in water. Whereas, for unseeded low and medium solids content polymerizations involving completely water soluble monomers the authors recommended Morton's equation.

Since the monomers used in most of the recipes are usually partially water soluble, then, as we will see in the next section, the constant partition coefficient model can be used to

calculate the monomer partitioning in the different phases. In the following sections, we briefly review the three kinds of models proposed to determine the monomer partitioning between the different phases. The aim of this comparison is to chose the simplest partitioning model that gives us accurate and rapid results. Algorithms that necessitate long calculation times are to be avoided when the objective of the application is the on-line control of polymer properties. Therefore, the algorithm based on the constant partition coefficients will be used in the material balance to determine $[M_i^p]$ and $[M_i^{aq}]$.

4.3.1 A model based on theoretical thermodynamic considerations

Morton et al. (1954) derived a theoretical relation for the saturation swelling of latex particles by one monomer, based on the classical Flory-Huggins (Flory (1953)) lattice theory for monomer-polymer mixtures. At equilibrium, the interfacial free energy between the latex particles and the aqueous phase counterbalances the swelling force. The concentration of monomers in the polymer particles is determined by the balance between the gain in interfacial free energy caused by the increase in surface area on swelling and the loss in free energy caused by mixing monomer with polymer. This relation shows that the equilibrium volume fraction of monomer absorbed by the latex particles $(1-\phi_p^p)$ increases by increasing the particle radius (r) and the temperature and decreases by increasing the interfacial tension (γ) at the surface of the particles, as following:

$$\frac{2v_1\gamma}{rRT} = -\left(\ln\left(1 - \phi_p^p\right) + \phi_p^p + \chi\left(\phi_p^p\right)^2\right) \qquad (4.9)$$

where χ is the polymer-monomer interaction parameter, R is the universal gas constant, T, temperature (K), and v_1 the molar volume of monomer. A variation of the Morton equation to deal with partial swelling of latex particles was derived by Vanzo et al. (1965). The balance between the partial monomer free energies ($\Delta G/RT$) of monomers in the different phases during a copolymerization process can be represented by the following equations:

$$\left(\frac{\Delta G}{RT}\right)_i^p = \left(\frac{\Delta G}{RT}\right)_i^{aq} \tag{4.10}$$

$$\left(\frac{\Delta G}{RT}\right)_i^d = \left(\frac{\Delta G}{RT}\right)_i^{aq}, \quad i=1,2$$

where p, d, aq, are the polymer, droplet and aqueous phases. The partial molar free energies are calculated by the following equation:

$$\left(\frac{\Delta G}{RT}\right)_i^j = \ln\phi_i^j + \sum_{k=1}^{n}\left(1-m_{ik}\right)\phi_k^j + \sum_{k=1\neq i}^{n}\chi_{ik}\left(\phi_k^j\right)^2 \tag{4.11}$$

$$+ \sum_{k=1\neq i}^{n-1}\sum_{l=k+1\neq i}^{n}\phi_k^j\phi_l^j\left(\chi_{ik}+\chi_{il}-\chi_{ik}m_{ik}\right)+\frac{2\gamma\nu_i}{r_iRT}$$

$$i=1,2 \quad \text{and} \quad j=d, p, aq$$

where ϕ_i^j is the volume fraction of monomer i in phase j, χ_{ik} interaction parameter between species i and k, and m_{ik} the ratio of the equivalent number of segments of the components i and k.

Equations based on this thermodynamic principle predict with good accuracy the saturation of latex particles and the partitioning of monomer between the aqueous phase and latex particles at partial saturation and at saturation swelling. However, several unknown or difficult to measure parameters are involved, such as the monomer-polymer interaction parameters and the interfacial energy. Moreover, the model needs a significant computational effort, and is therefore difficult to implement on-line.

4.3.2 The semi-empirical equations of Maxwell

Maxwell et al. (1992[a,b] and 1993[a,b]) found that partitioning was insensitive to temperature, latex particle radius, polymer composition, and polymer molecular weight. The concentration of monomer in the different phases was mainly a function of the swelling ability of monomer in polymer particles, and the saturation solubility of monomer in water. They thus derived a semi-empirical relation from Morton's equation, to determine the partitioning of two monomers between the latex particles, monomer droplets and aqueous phase of an emulsion polymer latex which requires only the saturation monomer concentrations in the particle and aqueous phases. First of all, when there are droplets in the system (i.e. during interval I and II), the following equations were proposed:

$$V_i^{aq} = \frac{V^{aq}}{V^d} V_i^d \phi_{i,sat}^{aq} \quad i = 1,2 \tag{4.13}$$

$$V_1^p = V_1^d \frac{V^p}{V^d} \left\{ \left(\phi_{1,sat}^p - \phi_{2,sat}^p \right) \frac{V_1^d}{V^d} + \phi_{2,sat}^p \right\}$$

$$V_2^p = V_2^d \frac{V^p}{V^d} \left\{ \left(\phi_{2,sat}^p - \phi_{1,sat}^p \right) \frac{V_2^d}{V^d} + \phi_{1,sat}^p \right\}$$

where p, d, aq, are the polymer, droplet and aqueous phases, V_i^j is the volume of monomer i in phase j, $\phi_{i,sat}^j$ the volumetric fraction of monomer i in phase j under homosaturation conditions. In the absence of monomer droplets, interval III, the equations proposed by Maxwell are the following:

$$V_1^{aq} = V^{aq} \phi'_{1,sat}^{aq} \left\{ \frac{V_1^p}{V^p \phi'_{1,sat}^p} \exp\left(\frac{V_p^p}{V^p} - \phi'_{p,sat}^p \right) \right\} \tag{4.14}$$

$$V_2^{aq} = V^{aq} \phi'_{2,sat}^{aq} \left\{ \frac{V_2^p}{V^p \phi'_{2,sat}^p} \exp\left(\frac{V_p^p}{V^p} - \phi'_{p,sat}^p \right) \right\}$$

where $\phi'_{i,sat}^j$ is the volumetric fraction of monomer i in phase j under saturation conditions, and depends on the monomer ratio in this phase.

4.3.3 Partition Coefficient Model

In the constant partition coefficient model, the equilibrium distributions among the droplets, particles and water is described though empirical partition coefficients that are considered constant thought the reaction. There are several possible definitions for partition coefficients, (e.g. Guillot (1986), Leiza (1991)). They are defined by Gugliotta et al (1995) as:

$$k_i^j = \frac{\phi_i^j}{\phi_i^{aq}}, \quad i=1,2 \quad \text{and} \quad j= p, d \tag{4.15}$$

where k_i^j is the partition coefficient of monomer i between phase j and aqueous phase.

In order to use the coefficient partition model, equations 4.15 must be solved with the material equations 4.7. In emulsion copolymerization this gives 9 equations with 9 unknowns. This set of equations can then be solved by means of an optimization algorithm such as Newton algorithm that ensures a global rapid convergence to the solution. Omi (1986) proposed an algorithm that guarantees a quick convergence to the real solution, for monodisperse systems, and Armitage et al.(1994) for polydispersed emulsion copolymers. The algorithm proposed by Armitage et al. (1994) is developed here for 2 monomers.

The iteration algorithm used to calculate $[M_i^j]$ during interval II is resumed in these steps:

1. Chose initial values for V^p, V^d, V^{aq}.

2. Calculate V_i^p from the following equation:

$$V_i^p = \frac{V_i}{1+\dfrac{k_i^d}{k_i^p}\dfrac{V^d}{V^p}+\dfrac{V^{aq}}{V^p k_i^p}} \tag{4.16}$$

3. Calculate V_i^d and V_i^{aq} with the following equation:

$$V_i^d = \frac{k_i^d}{k_i^p}\frac{V_i^p}{V^p}V^d \tag{4.17}$$

$$V_i^{aq} = \frac{V_i^p}{k_i^p}\frac{V^{aq}}{V^p}$$

4. Calculate V^d, V^p and V^{aq}:

$$V^d = V_1^d + V_2^d$$

$$V^p = V_1^p + V_2^p + V_p^p$$

$$V^{aq} = V_w^{aq} + V_1^{aq} + V_2^{aq}$$

(4.18)

5. Iteration until convergence in V^{aq}, V^p, and V^d is reached.

The principle of the iteration algorithm does not change in interval III. It is no longer a function of the monomer droplets volume. The iteration algorithm is therefore reduced to the following steps:

1. Guess initial values for V^p and V^{aq}.

2. Calculate V_i^p with the following equation:

$$V_i^p = \frac{V_i}{1 + \dfrac{V^{aq}}{V^p k_i^p}}$$

(4.19)

3. Calculate V_i^{aq} using the following equation:

$$V_i^{aq} = \frac{V_i^p}{k_i^p} \frac{V^{aq}}{V^p}$$

(4.20)

4. Calculate V^p and V^{aq}:

$$V^p = V_1^p + V_2^p + V_p^p$$

$$V^{aq} = V_w^{aq} + V_1^{aq} + V_2^{aq}$$

(4.21)

5. Iteration until convergence in V^p and V^{aq}.

In this work, this iterative algorithm with the coefficient partition model will be used to determine $[M_i^j]$. It is important to note that the same iteration algorithm can also be used with the Morton or maxwell models to estimate of $[M_i^j]$.

The evolution of monomer concentration in the different phases is calculated from the different volumes, obtained from the partition coefficient model, as follows:

$$\begin{cases} [M_i^p] = \dfrac{N_i^p}{V^p} = \dfrac{V_i^p \times \rho_i / MW_i}{V^p} \\[4mm] [M_i^w] = \dfrac{N_i^w}{V^{aq}} = \dfrac{V_i^w \times \rho_i / MW_i}{V^{aq}} \end{cases} \qquad (4.22)$$

$$[M_i^p] = \dfrac{N_i^p}{V^p} = \dfrac{V_i^p \times \rho_i / MW_i}{V^p}$$

$$[M_i^w] = \dfrac{N_i^w}{V^{aq}} = \dfrac{V_i^w \times \rho_i / MW_i}{V^{aq}}$$

4.4 Radical Concentration in the different phases

Using the well-known hypotheses of equal reactivity for all radical species, and ignoring the reaction of chain transfer to polymer, the radical balance in the aqueous phase can be represented by the following equation:

$$\frac{dR_w}{dt} = 2fk_I I - \frac{k_a R_w N_p^T}{V^{aq} N_A} - \frac{R_w^2}{V^{aq}}\left(k_{t_{11}} P_1^{aq^2} + 2k_{t_{12}} P_1^{aq} P_2^{aq} + k_{t_{22}} P_2^{aq^2}\right)$$
$$+ \frac{k_d \bar{n} N_p^T}{N_A} - R_{i\,crit}\left([M_1^{aq}]\left(K_{P11} P_1^{aq} + K_{P21} P_2^{aq}\right) + [M_2^{aq}]\left(K_{P12} P_1^{aq} + K_{P22} P_2^{aq}\right)\right) \qquad (4.23)$$

where R_w is the total number of moles of free radicals in the aqueous phase (mol), f efficiency factor for initiator decomposition, k_I the rate constant for initiator decomposition (s^{-1}), k_a the entry rate coefficient for absorption of radicals of type i (s^{-1}), k_{tij} the termination rate constant (cm^3/mol/s), k_d overall desorption rate coefficient (s^{-1}), and the index icrit, in $R_{i\,crit}$, is the critical degree of polymerization for particle formation by homogeneous nucleation.

If the pseudo-steady-state assumption for the radical concentration in the aqueous phase is applied then:

$$\dot{R}_w = 0 \qquad (4.24)$$

Asua et al. (1990) compared the integration of the radical balance under pseudo-steady-state and non-steady-state conditions, and showed that the difference between these two cases is not significant, and that invoking the quasi-steady state assumption considerably reduces computer time.

On the other hand, in order to accurately model the number of radicals in the polymer particles (μ), two separate models are needed: for the average number of radicals per particle $\bar{n}$, and anther for the number of particles. There is obviously a relationship between $\bar{n}$ and R_w as $\bar{n}$ depends on the rate of radical generation and termination in the aqueous phase, the rate of radical absorption into the particle and desorption from the particle, and on the rate of

termination within the particle. It is difficult to estimate $\bar{n}$ from the proposed methods in the literature since it depends on the absorption and desorption parameters, and termination within the particle that are usually not well determined and are very sensitive to small amounts of inhibitors. Phenomena like the gel effect are also difficult to model a priori and significantly influence the termination constant within the particle. On the other hand, the number of particles depends on the concentration of surfactant and initiator, the rate of homogeneous nucleation, and eventually on the concentration of impurities in the reactor. Determining N_p^T form the population balance necessitates modeling the different types of nucleation (homogeneous and micellar) and account for possible particles flocculation, which depends on a large number parameters. Therefore, in this work, we try to estimate a global kinetic term (μ) that corresponds to the total number of moles of radicals in the polymer particles, without using a model for either $\bar{n}$ or N_P^T.

4.5 A nonlinear observer for water soluble monomers

The objective of this section is to estimate the copolymer composition using the mathematical model developed for copolymerization of partially water soluble monomers and to evaluate the importance of the contribution of water phase polymerization to the overall polymer composition. The output of the model is the overall conversion, obtained by calorimetry. The material balance of monomers is given by equations 4.1 and the equilibrium distribution of the two monomers between the latex particles, the aqueous phase and the monomer droplets is described using the partition coefficients model, 4.15.

In order to estimate the polymer composition, the rate of the reaction of each monomer in each phase must be determined. The instantaneous copolymer composition can be defined by the following equation:

$$F_1 = \frac{R_{P1}^{p} + R_{P1}^{w}}{\left(R_{P1}^{p} + R_{P1}^{w} + R_{P2}^{p} + R_{P2}^{w} \right)}, \quad F_2 = 1 - F_1 \tag{4.27}$$

The main unknown variables in the model 4.1 are the number of moles of each monomer N_1, N_2, the number of moles of radicals in the polymer particles (μ) and in the aqueous phase (R_w). As we mentioned above, the parameter μ can also be detailed as a function of the number of particles, particle diameter and a lot of kinetic constants. However, this necessitates the on-line measurement of the particle diameter and a considerable knowledge of the kinetics, and μ must therefore be estimated by another way. On the other hand, R_w can be determined from equations 4.23 and 4.24. If the desorption term is neglected, and the radical consumption, propagation and termination, in the aqueous phase is supposed negligible, the total number of moles of radicals in the aqueous phase can be represented by the following equation:

$$R_w = \frac{2fk_I I V^{aq} N_A}{k_a N_p^T} \tag{4.28}$$

The calculation of R_w in this way allows us to approximate the number of moles of radicals in the aqueous phase and to decrease the number of parameter to be estimated in the model. A study of the sensitivity of the estimation of the copolymer composition to the value of R_w will be carried out later, in order to justify this simplification.

In summary, the overall model is divided in two parts: (i) integration of the differential equations constituting the material balances, and (ii) the calculation of the distribution of monomers in the corresponding phases by iteration of the thermodynamic equilibrium equations combined with the algebraic material balances. The equilibrium equations are solved numerically at each integration step. This means that the concentration of monomer in the different phases cannot be represented analytically as a function of N_1, N_2, and μ. R_w is supposed to be a known parameter in the model, from eq. 4.28. If we suppose that μ varies with an unknown dynamic ε_μ , we can write the following augmented system with three unknown states to be estimated, N_1, N_2, and μ:

$$\begin{cases} \dot{N}_1 = Q_1 - R_{P1}^w - R_{P1}^p \\ \dot{N}_2 = Q_2 - R_{P2}^w - R_{P2}^p \\ \dot{\mu} = \varepsilon_\mu \end{cases} \qquad (4.29)$$

The real output of the process is the overall conversion, X. Q_1 and Q_2 are two known variable inputs. In fact, the system is not observable from the measurement of the overall conversion, since it does not allow us to reconstruct the initial conditions of N_1 and N_2. However, in an unseeded system, initial conditions are usually approximately known for N_1 and N_2, but not for μ. We therefore propose another output that is based on X, the initial values of N_1 and N_2, and the monomers flow rates (Q_1, and Q_2) that are usually known as well. In fact, the model output (y) can be the residual amount of monomer that is related to the overall conversion (obtained by calorimetry in this work) by the following equation:

$$\begin{aligned} y &= (1 - X)\left(MW_1 N_1^T + MW_2 N_2^T\right) \\ &= MW_1 N_1 + MW_2 N_2 \end{aligned} \qquad (4.30)$$

It is important to point out that the observer can be implemented using the output y, that can be obtained by any on-line sensor.

The states model, N_1, N_2, and μ are observable if there exists a change of variables that puts the system under the following canonic observability form:

$$\dot{x} = \underbrace{\begin{bmatrix} g_1(x_1) \\ g_1(x_1, x_2) \\ g_3(x_1, x_2, x_3) \end{bmatrix}}_{G(u,y)} u + \begin{bmatrix} 0 \\ 0 \\ \varphi(x) \end{bmatrix} + \begin{bmatrix} 0 & 1 & 0 \\ 0 & 0 & 1 \\ 0 & 0 & 0 \end{bmatrix} x \qquad (4.31)$$

$$y = Cx$$

where x is the vector of the state variables and y is the output vector.

The change of co-ordinates based on the Lie derivative of the augmented system of three unknown states, gives a matrix G that does not have a triangular canonical form of observability (see subsection 2.2.3, Theorem 2.3). We therefore propose an observer that is composed of two cascade observers, where in the first part N_1 and N_2 are estimated supposing that μ is known and in the next step the observer of μ is applied using the estimated values of N_1 and N_2. The observer construction is in this case similar to the observer for hydrophobic monomers published by Févotte et al. (1998[a]). It is important to point out that the observability conditions of the system do not change if we passe from a global observer to two cascade observers of the unknown states. However, the cascade observers become easier to be calculated. Moreover, this allows us to give different tuning variables to each observer to ensure their stabilities and rapidity of convergence. On the other hand, the closed loop cascade observers are not equivalent to an open loop observer. In the cascade observers we have an estimate of the parameter μ without using a model to represent it or initializing it exactly, something that could not be obtained from an open loop observer. Moreover, if the system is observable from the output y, then even if the states N_1 and N_2 are not correctly initialized or modeled the observer would be able to correct these errors. Therefore, we prefer to construct closed loop cascade observers for our system.

In the first observer in the cascade, the part used to estimate N_1 and N_2, the following change of variables puts the system under the canonical form of observability:

$$T = \begin{bmatrix} T_1 \\ T_2 \end{bmatrix} = \begin{bmatrix} y \\ L_f y \end{bmatrix} \qquad (4.32)$$

where $L_f y$ is the Lie derivative of the function f with respect to y.

This gives:

$$T = \begin{bmatrix} T_1 \\ T_2 \end{bmatrix} = \begin{bmatrix} MW_1 N_1 + MW_2 N_2 \\ -MW_1\left(R_{P1}^p + R_{P1}^w\right) - MW_2\left(R_{P2}^p + R_{P2}^w\right) \end{bmatrix} \tag{4.33}$$

The new system (in differential equations) can be written:

$$\dot{T} = \underbrace{\begin{bmatrix} MW_1 Q_1 + MW_2 Q_2 \\ 0 \end{bmatrix}}_{G(u)} + \begin{bmatrix} -MW_1\left(R_{P1}^p + R_{P1}^w\right) - MW_2\left(R_{P2}^p + R_{P2}^w\right) \\ -MW_1\left(\dot{R}_{P1}^p + \dot{R}_{P1}^w\right) - MW_2\left(\dot{R}_{P2}^p + \dot{R}_{P2}^w\right) \end{bmatrix} \tag{4.34}$$

$$y = \underbrace{\begin{bmatrix} 1 & 0 \end{bmatrix}}_{C} T$$

$$= MW_1 N_1 + Mw_2 N_2$$

Therefore,

$$\dot{T} = G(u) + \underbrace{\begin{bmatrix} 0 & 1 \\ 0 & 0 \end{bmatrix}}_{A} T + \underbrace{\begin{bmatrix} 0 \\ \varphi(T) \end{bmatrix}}_{F(T)} \tag{4.35}$$

$$y = CT$$

If we refer back to chapter 2, Theorem 2.3, it can be seen that the form of the new system (A, F, and C) allows us to construct a high gain observer of the states y and $L_f y$. The high gain estimator of the system T, takes the following form:

$$\dot{\hat{T}} = G(u) + \begin{bmatrix} T_2 \\ \varphi(T) \end{bmatrix} - S_\theta^{-1} C^T\left(\hat{T}_1 - T_1\right) \tag{4.36}$$

where S_θ is the unique symmetric positive definite matrix satisfying the algebraic Lyapunov equation:

$$\theta S_\theta + A^T S_\theta + S_\theta A - C^T C = 0 \tag{4.37}$$

The solution of this system, with A and C given by equations 4.35 and 4.34 respectively, is:

$$S_\theta = \begin{bmatrix} \dfrac{1}{\theta} & -\dfrac{1}{\theta^2} \\ -\dfrac{1}{\theta^2} & \dfrac{2}{\theta^3} \end{bmatrix}$$

where $\theta > 0$ is a parameter (see Gauthier et al., 1991).

In order to obtain the observer of the original system with the state N_1, N_2 and μ, we need to inverse the Jacobian matrix $(\partial T / \partial N_i)$, and the new observer becomes:

$$\begin{bmatrix} \dot{\hat{N}}_1 \\ \dot{\hat{N}}_2 \end{bmatrix} = \begin{bmatrix} Q_1 \\ Q_2 \end{bmatrix} + \begin{bmatrix} -R_{P1}^p - R_{P1}^w \\ -R_{P2}^p - R_{P2}^w \end{bmatrix} - \left(\frac{\partial T}{\partial \hat{N}_i} \right)^{-1} S_\theta^{-1} C^T (\hat{y} - y) \tag{4.38}$$

Note that in the corrective term of the observer, the inverse of the derivative of T w.r.t. N_1 and N_2 is involved. This requires us to solve the following set of equations:

$$\frac{\partial T_1}{\partial N_1} = MW_1$$

$$\frac{\partial T1}{\partial N_2} = MW_2 \tag{4.39}$$

$$\frac{\partial T_2}{\partial N_1} = -MW_1 \left(\frac{\partial R_{P1}^p}{\partial N_1} + \frac{\partial R_{P1}^w}{\partial N_1} \right) - MW_2 \left(\frac{\partial R_{P2}^p}{\partial N_1} + \frac{\partial R_{P2}^w}{\partial N_1} \right)$$

$$\frac{\partial T_2}{\partial N_2} = -MW_1 \left(\frac{\partial R_{P1}^p}{\partial N_2} + \frac{\partial R_{P1}^w}{\partial N_2} \right) - MW_2 \left(\frac{\partial R_{P2}^p}{\partial N_2} + \frac{\partial R_{P2}^w}{\partial N_2} \right)$$

In fact, these equations cannot be solved since calculating the derivatives of $R_{pi}{}^j$ with respect to N_i requires an analytical representation of these terms w.r.t. N_i, which is not available, since the monomer partitioning is solved numerically by the iteration procedure.

One way to get around this problem is to simplify these nine equations in order to be able to obtain an analytical representation of $R_{pi}{}^j$ w.r.t. N_i. The simplification of these equations consists of assuming that all the monomer is in the polymer particles. Based on this assumption, the equations 4.22 reduce to the following:

$$[M_i^j] = \frac{N_i^j}{V^j} \cong \frac{N_i}{V^j}, \quad i=1,2 \text{ and } j=p,w \tag{4.40}$$

This simplification will only be taken into account in the corrective term of the observer 4.38, since the first part of the observer contains the model which can be calculated numerically from the original 9 equations.

The second part in the cascade observer includes the estimation of μ from the output y defined in equation 4.30. The following augmented system is therefore considered:

$$\begin{cases} \dot{y} = MW_1\dot{N}_1 + MW_2\dot{N}_2 \\ \quad = \left(MW_1Q_1 + Mw_2Q_2\right) + \mu\lambda - R_{P1}^w - R_{P2}^w \\ \dot{\mu} = \varepsilon_\mu(t) \end{cases} \qquad (4.41)$$

where

$$\lambda = -[M_1^p]\left(\frac{K_{P11}K_{P21}[M_1^p]}{K_{P21}[M_1^p] + K_{P12}[M_2^P]} + \frac{K_{P21}K_{P12}[M_2^p]}{K_{P21}[M_1^p] + K_{P12}[M_2^P]}\right)\dots \qquad (4.42)$$

$$\dots -[M_2^p]\left(\frac{K_{P12}K_{P21}[M_1^p]}{K_{P21}[M_1^p] + K_{P12}[M_2^P]} + \frac{K_{P22}K_{P12}[M_2^p]}{K_{P21}[M_1^p] + K_{P12}[M_2^P]}\right)$$

A change of co-ordinates as defined by Theorem 2.3, in chapter 2, allows us to put the system under a canonical form of observability. The high gain observer proposed in chapter 2, by Theorem 2.3 can then be applied, without a change of co-ordinates. The high gain observer takes the following form:

$$\begin{cases} \dot{\hat{y}} = \left(MW_1Q_1 + MW_2Q_2\right) + \hat{\mu}\hat{\lambda} - R_{P1}^w - R_{P2}^w - 2\theta_2\left(\hat{y} - y\right) \\ \dot{\hat{\mu}} = -\frac{\theta_2^2}{\hat{\lambda}}\left(\hat{y} - y\right) \end{cases} \qquad (4.43)$$

where θ_2 is the observer tuning parameter.

As we mentioned above, the observers work in cascade. They estimate N_1, N_2, and μ simultaneously. In the first step of the first observer N_1 and N_2 are estimated using an initial value of μ. Thereafter, μ is estimated in the second observer that uses the estimated values of N_1 and N_2. The new estimated value of μ is used again in the first observer to estimate N_1 and N_2. The observers are based on the measurement of y, Q_1, Q_2 at every moment. The simulations have shown that the observer of μ is robust to errors in the initial value (that is usually unknown). Therefore, μ can be initialized arbitrarily without influencing the convergence of the observer.

The obtained results by the simulation are shown in Figures 4.1-4.2. The methyl methacrylate (MMA) (water solubility under saturation conditions, $[M^{aq}]^{sat}=0.16$ mol/L) vinyl acetate (VAc) ($[M^{aq}]^{sat}=0.5$ mol/L) system was studied. For reasonable values of the number

of particles, $N_p^T=1\times10^{18}$, I=0.01 mole, and the decomposition rate constant of KPS, we can calculate $R_w=1e^{-7}$. These parameters will be studied in detail later. In the simulation the initial polymer volume was taken to be $50cm^3$, that is necessary to solve the distribution of monomer in the different phases, and the initial charge of monomer contains 50% MMA and 50% VAc. The observer tuning parameters were adjusted $\theta = 1e^{-2}$ and $\theta_2 = 2e^{-2}$.
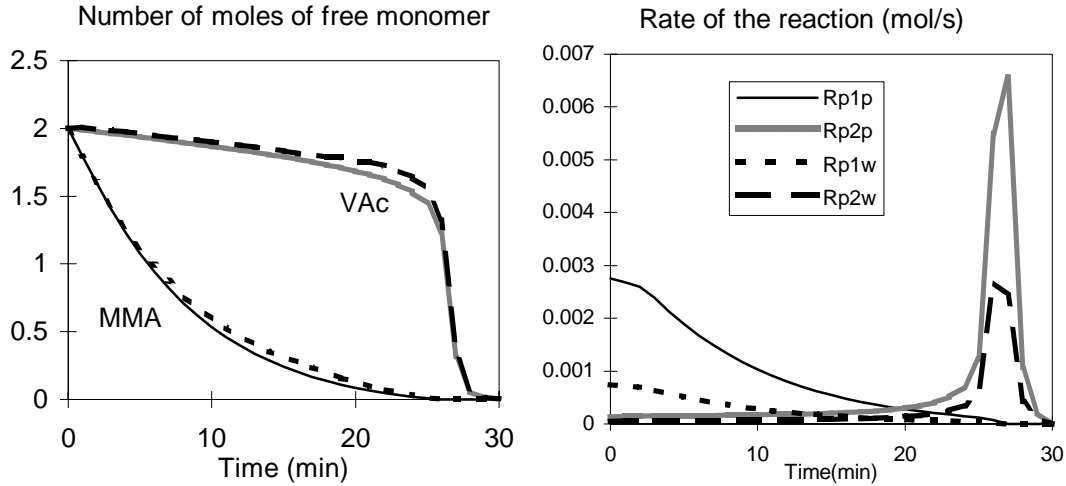
Figure 4.1: Simulation of the polymerization of MMA/VAc. At left, the residual monomer, (—) model, (--) estimator. At right, the estimated rate of the reaction in polymer particles (continuous line) and in the aqueous phase (dashed line).

First of all, the estimated values of N_1 and N_2 are in good agreement with the model, even though they were initialized far from the true initial values of the model. It can be seen that for equivalent values of μ and R_w ($R_w=1\times10^{-7}$ mol), the rate of reaction in the polymer particles is much more important than in the aqueous phase, since there is more monomer in the polymer particles than in water. In the simulation a constant μ was considered in the model. The observer of μ converged almost immediately to the real value, even though a big error in the initial value was implemented to the observer.
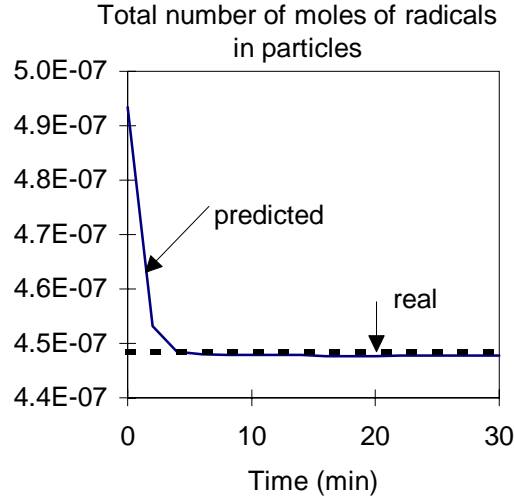
Figure 4.2: Simulation of the observer. Real and predicted μ.

In order to experimentally study the observer and its sensitivity to different parameters such as R_w, K_P and ϕ_P^p, different copolymerization experiments were carried out (recipe shown in Table 4.1 using two monomers with different reactivities and high water solubility: vinyl acetate (VAc), and methyl acrylate (MA), ($[M^{aq}]^{sat}=0.5$ mol/L and $[M^{aq}]^{sat}=0.61$ mol/L respectively, according to Gilbert (1995)). The reactivities and some useful physical properties of monomers are summarized in Annex II.

Table 4.1: Experiments of copolymerization for the validation of the observer for hydrophilic monomers.

\ **experiment** **Component **	VAc-MA-1 amount (g)	VAc-MA-2 amount (g)	VAc-MA-3 amount (g)
Vinyl acetate	301	207	406
Methyl acrylate	305	408	201
Sodium dioctyl sulfosuccinate	3.089	3	3.07
Potassium persulfat	3.02	3.04	3
Sodium hydrocarbonate	3	3.03	3.04
H_2O	2420.6	2430.9	2385.2
Final solids content	18 %	18 %	19 %
Final particle size	102 nm	118 nm	131 nm
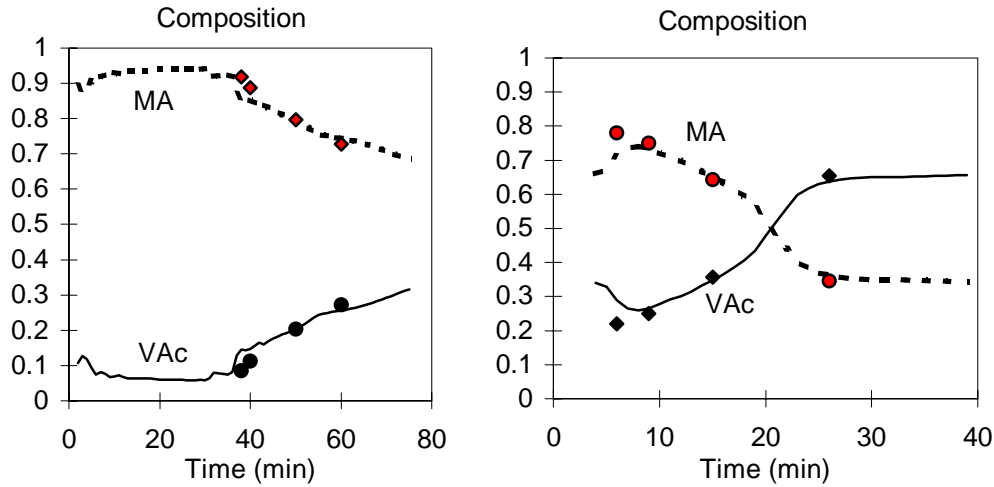
Figure 4.3: At left VAc-MA-2, at right VAc-MA-3. The points represent the experimental composition obtained by NMR.

The on-line estimated composition for VAc-Ma-2 and VAc-Ma-3 is shown in Figure 4.3. The estimations were validated experimentally by off-line NMR, Nuclear Magnetic Resonance. It can be seen that the estimations are in good agreement with the experimental NMR values. The value of R_w was calculated from the amount of initiator added to the reactor and its efficiency factor, rate of descomposition, and using a reasonable number of particles equal to 1×10^{18} particle per liter, which gave $R_w = 1 \times 10^{-7}$ mol. Radical termination, and homogeneous nucleation were neglected in the calculation of R_w. N_P was then measured off-line to calculate the real R_w. However, as we will see late, the error in R_w does not significantly affect the composition estimation. In order to study the sensitivity of the estimated composition to the used value of R_w, we have compared the composition obtained for two different values of R_w, (the one calculated here $R_w = 1 \times 10^{-7}$ mol, and an arbitrarily chosen value $R_w = 1 \times 10^{-5}$ mol). The results are shown on Figure 4.4, for the experiment VAc-MA-1. The figure shows that the composition is not sensitive to the value of R_w, which is due to the fact that the rate of reaction in the polymer particles is more important than in the aqueous phase and that the monomer ratios in the polymer particles and in the aqueous phase are similar. Since the involved monomers have different solubility in the aqueous phase, it seems reasonable to conclude that the contribution of reaction in the aqueous phase on the overall rate of reaction, and therefore on the polymer composition seems to be negligible.

148
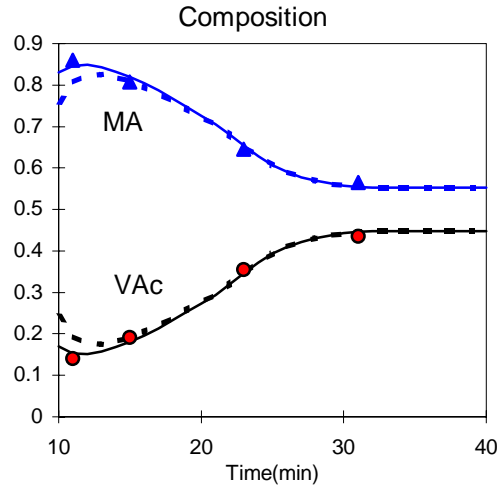
Figure 4.4: VAc-MA-1, sensibility of the estimated composition to the value R_w. (--) $R_w=1e^{-7}$, (—) $R_w=1e^{-5}$ and the points are the experimental NMR results.

Therefore, for the composition estimation and control, the contribution of the aqueous phase can be neglected. The model can therefore be simplified. Simplification of the model means that the model is reduced to differential equations and there is no longer need to develop the iteration steps to calculate the concentration of monomer in the different phases. This simplification significantly reduces the time needed for the computer to solve the equations which is of capital importance in regard to the control application. It also reduces the number of kinetic and physical parameters that we need to know and eliminates the need to know N_P à priori. Note that if we want to study the secondary nucleation in the aqueous phase, we must account for this term, and add the contribution of radical propagation and nucleation to the evolution of the reaction.

The sensitivity of the estimated average number of radicals per particle to the value of R_w is shown in Figure 4.5 for the case of VAc-MMA for very different values of R_w, $R_w=1e^{-7}$ and $R_w=1e^{-5}$. The value of $\overline{n}$ was obtained from the estimated value μ by introducing the total number of particles. Measurements of the particle diameter are obtained by QELS (quasi-elastic light scattering). Clearly, a better estimate of μ will be found if the number of radicals in the aqueous phase is calculated more rigorously, taking into account desorption phenomena, radicals termination and propagation in the aqueous phase. However given the precision of the QELS measurements, R_w seems to have little impact on $\overline{n}$.
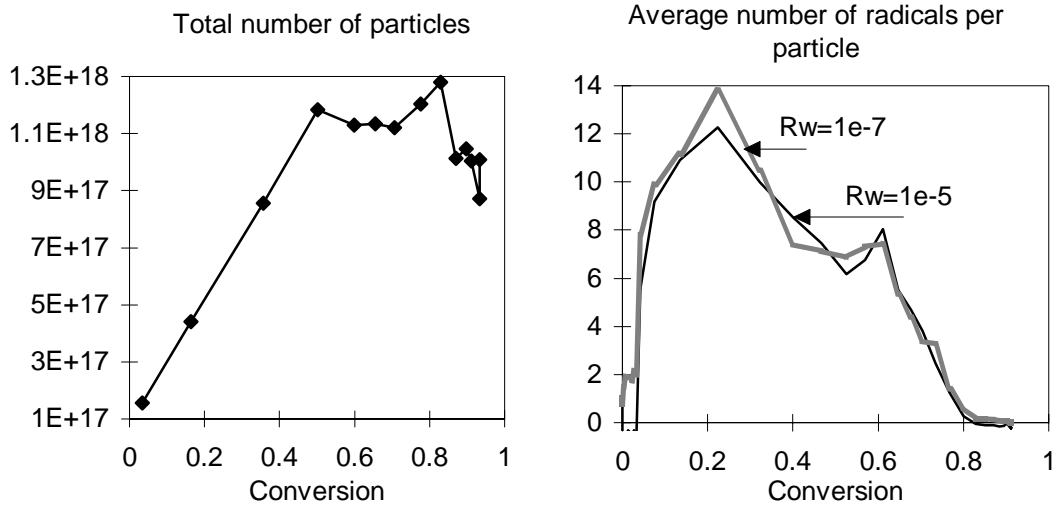
Figure 4.5: VAc-MA-1, N_P^T and $\bar{n}$. Sensitivity of $\bar{n}$ to the value of R_w.

Since the contribution of the aqueous phase can be negligible for the composition estimation and control, we will estimate the composition considering that the reaction takes place just in the polymer particles. An observer was developed by Févotte et al. (1998[a]) concerning the estimation of composition and the glass transition temperature for hydrophobic monomers. In the next section, we briefly review this observer.

4.6 A nonlinear observer for hydrophobic monomers

The main assumption of this observer is that the polymer particles are the only reaction loci. The material balance is simplified to the following differential equations, i =1,2:

$$\dot{N}_i = Q_i - R_{Pi}^p \tag{4.44}$$

$$= Q_i - \mu\left([M_i^p]\left(K_{P1i}P_1^p + K_{P2i}\left(1 - P_1^p\right)\right)\right)$$

The concentration of monomers in the polymer particles is calculated assuming that the monomers are not soluble in the aqueous phase, and therefore they are partitioned only between the monomer droplets and the polymer particles. The composition of monomers in the organic phase, i.e. monomer droplets and polymer particles, are regarded as equal. This simplification was shown to be valid for reasonable particle sizes by Nomura et al. (1985). The simple equipartition hypothesis was also adopted, that is the two monomers are supposed to have the same solubility in the polymer particles. Therefore the concentration of monomers in the polymer particles can be written as a function of the solubility of monomer in the polymer particles.

$$[M_i^p] = \begin{cases} \dfrac{\left(1 - \phi_p^p\right)N_i}{\displaystyle\sum_{j=1}^{2} MW_j N_j / \rho_j} & , \ \text{Interval II} \\[4ex] \dfrac{N_i}{\displaystyle\sum_{j=1}^{2}\left(\dfrac{\left(N_j^T - N_j\right)MW_j}{\rho_{j,h}}\right) + \sum_{k=1}^{2}\left(\dfrac{N_k MW_k}{\rho_k}\right)} & , \ \text{Interval III} \end{cases} \tag{4.45}$$

The condition for the existence of droplets (interval II) is governed by the equation:

$$N_1\delta_1 + N_2\delta_2 - \frac{\left(1 - \phi_p^p\right)}{\phi_p^p}\sigma > 0 \tag{4.46}$$

where

$$\delta_i = MW_i \left(\frac{1}{\rho_i} + \frac{\left(1 - \phi_p^p\right)}{\rho_{1,h} \, \phi_p^p} \right) \tag{4.47}$$

$$\sigma = \sum_{j=1}^{2} \frac{MW_i N_i^T}{\rho_{1,h}} \tag{}$$

We consider again an augmented system with the unknown states N_1, N_2 and μ with the output y, the amount of residual monomer:

$$\begin{cases} \dot{N}_1 = Q_1 - \mu\Big([M_1^p](K_{P11}P_1 + K_{P21}(1 - P_1))\Big) \\ \dot{N}_2 = Q_2 - \mu\Big([M_2^p](K_{P12}P_1 + K_{P22}(1 - P_1))\Big) \\ \dot{\mu} = \varepsilon_\mu(t) \end{cases} \tag{4.48}$$

$$y = MW_1 N_1 + MW_2 N_2$$

A cascade observer can be constructed by the same way as done for the hydrophilic monomers. The first observer in the cascade consists about estimating the residual number of moles of each monomer in the reactor. It is given by the following system:

$$\begin{bmatrix} \dot{\hat{N}}_1 \\ \dot{\hat{N}}_2 \end{bmatrix} = \begin{bmatrix} Q_1 \\ Q_2 \end{bmatrix} - \mu \begin{bmatrix} [\hat{M}_1^p](K_{P11}\hat{P}_1 + K_{P21}(1 - \hat{P}_1)) \\ [\hat{M}_2^p](K_{P12}\hat{P}_1 + K_{P22}(1 - \hat{P}_1)) \end{bmatrix} - \left(\frac{\partial \overline{T}}{\partial \hat{N}_i} \right)^{-1} \Gamma^{-1} S_\theta^{-1} C^T dy \tag{4.49}$$

where S_θ is obtained by the algebraic Lyapunov equation 4.37.

$$\Gamma = \begin{bmatrix} 1 & 0 \\ 0 & \mu \end{bmatrix} \tag{4.50}$$

and,

$$\overline{T} = \begin{bmatrix} MW_1 N_1 + MW_2 N_2 \\ -\Big(MW_1[M_1^p](K_{P11}P_1 + K_{P21}P_2) + MW_2[M_2^p](K_{P12}P_1 + K_{P22}P_2)\Big) \end{bmatrix} \tag{4.51}$$

If the change of co-ordinates is done as in equation 4.33, i.e.:

$$T = \begin{bmatrix} MW_1 N_1 + MW_2 N_2 \\ -R_{P1}MW_2 - R_{P2}MW_2 \end{bmatrix} \tag{4.52}$$

then the corrective term would not contain Γ, since:

$$\left(\frac{\partial \overline{T}}{\partial N_i}\right)^{-1} \Gamma^{-1} = \left(\frac{\partial T}{\partial N_i}\right)^{-1} \tag{4.53}$$

Both change of co-ordinates are possible.

And finally, the second part of the estimator in the cascade consists of estimating μ by the following differential equation:

$$\dot{\mu} = \frac{-\theta_2^2}{[M_1^p]\overline{F}_1 + [M_2^p]\overline{F}_2}(\hat{y} - y) \tag{4.54}$$

where

$$\overline{F}_i = -\left(K_{P1i}P_1 + K_{P2i}(1 - P_1)\right) \tag{4.55}$$

and θ_2 is the adjusting parameter of the observer.

Several experiments were carried out to validate the observer. The observer tuning parameters were adjusted θ = .05 and θ_2 =0.05. Figure 4.6 shows the individual conversions obtained in a batch seeded copolymerization of styrene and butyl acrylate. The recipe used for this experiment is shown in Table 3.3 in chapter 3. The overall conversion is estimated by calorimetry. The estimations were validated by off-line gas chromatographic analysis of the residual monomer. The figure shows that the estimations of the individual conversions agree with the independent off-line gas chromatographic measurements.
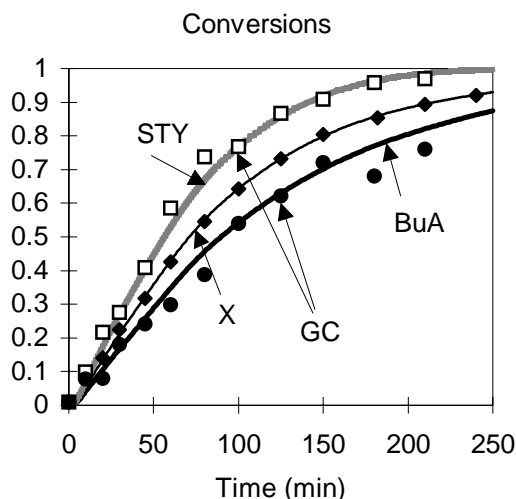
Conversions

Figure 4.6: Experiment STY-BuA-1c: Overall and individual conversions of STY and BuA during a batch seeded copolymerization. The overall conversion is fitted with the gravimetric measurements, and the individual conversions are obtained by GC, given by the points.

In addition to the estimation of the individual conversions, the observer provides an estimate of the total number of moles of radicals in the polymer particles (μ). The average number of radicals per particle, $\bar{n}$, could, in theory, be determined on-line for this seeded experiment, since the number of particles was supposed not to vary during the reaction. The number of particles was measured off-line to verify that no renucleation had occurred.
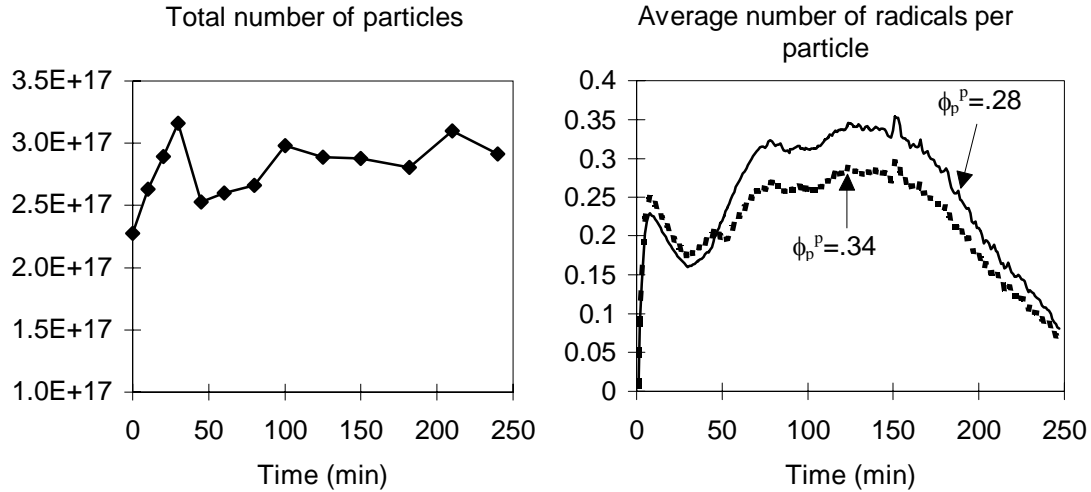
Figure 4.7: Experiment STY-BuA-1c: Number of polymer particles, at left, and average number of radicals per particle, tested for two values of ϕ_p^P.

Figure 4.7 at left shows that the number of particles was almost constant during the reaction. The estimated $\bar{n}$ is shown in Figure 4.7 at right. In order to test the estimation sensitivity to the value of the volumetric fraction of polymer in the particles under saturation conditions, two values of ϕ_p^P were tested (ϕ_p^P =0.28, found in the literature for BuA and ϕ_p^P =0.34 calculated as a function of the volumetric fraction of the final homopolymers in the polymer, see appendix II for references). The figure shows that $\bar{n}$ is slightly sensitive to the value of ϕ_p^P, whereas the same estimates of N_1 and N_2 were obtained for both values of ϕ_p^P.

It should be pointed out that the estimation of $\bar{n}$ is based on the measurement of the particle size, which is not precisely measured in general. Therefore, we must neglect the small disturbances in $\bar{n}$, such as at the beginning of the reaction in Figure 4.7. The value of $\bar{n}$ decreases at the end of the reaction, probably due to the fact that the copolymer is becoming more rich in BuA, which might favor the desorption of radicals.

The observer was also used to estimate the individual conversions and $\bar{n}$ during the semi-continuous seeded copolymerization STY-BuA-7, for which the recipe is shown in Table 3.3, in chapter 3. The reactor was initially charged with the seed (a latex of polystyrene) plus a small amount of monomer to allow the polymer particles to be swollen with monomer, during 14 hours under mixing. Afterwards, the mixture is heated to the reaction temperature, 60°C, and the initiator was introduced to start the reaction. The addition

of the preemulsion, at ambient temperature, started at 60 minutes of the reaction, where the monomer conversion was about 56%. Figure 4.8 shows the on-line estimated individual conversions during this experiment, that are validated by GC.
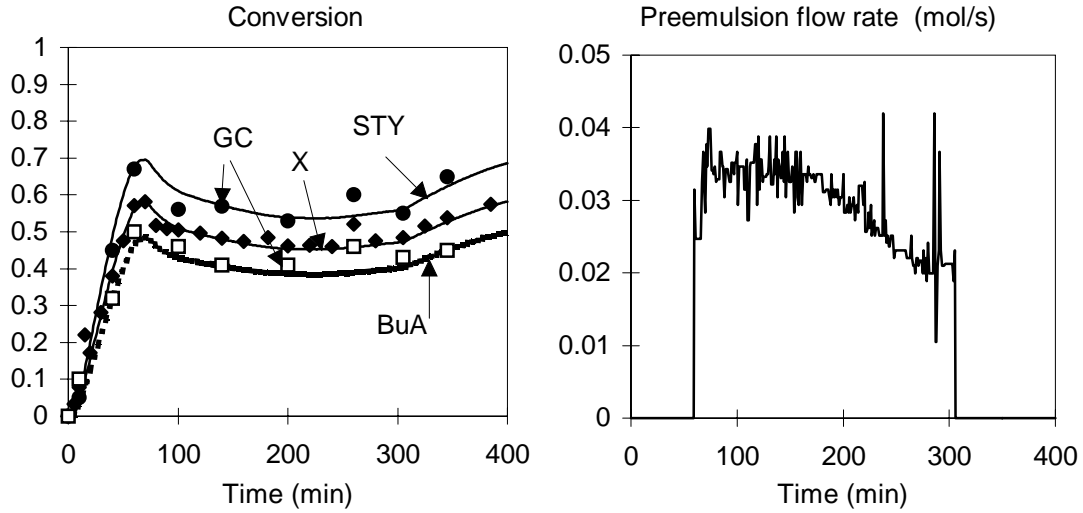
Figure 4.8 : Experiment STY-BuA-7: Seeded semicontinuous copolymerization.
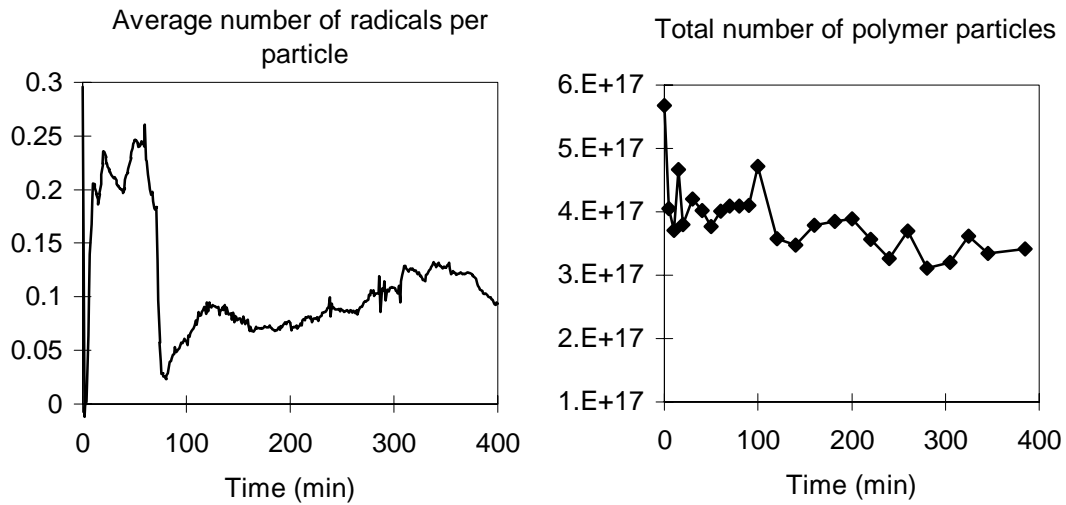
Figure 4.9: Experiment STY-BuA-7: On-line estimation of $\bar{n}$ during a semicontinuous seeded copolymerization.

Since the number of particles is assumed to be constant during this seeded experiment, an on-line estimation of $\bar{n}$ could be performed. The number of particles was measured off-line to ensure that no renucleation or flocculation occurred. Figure 4.9 shows both the measured N_P^T and the estimated $\bar{n}$. It can be seen that N_P^T remains constant during the

reaction, therefore estimating $\bar{n}$ during the reaction based on a constant value $N_P{}^T$ was accurate. During the first part of the experiment, $\bar{n}$ was constant until we start the addition of monomer, where $\bar{n}$ drops down. This must be due to a sensibility in the estimation to changes in the process. During the semi-continuous part of the reaction, the estimated value of $\bar{n}$ is almost constant, but inferior to the initial value. It increases again at 300 minutes when the preemulsion addition is finished. This is perhaps due to the fact that the concentration of monomer in the polymer particles decreases, which might favor the gel effect.

Table 4.2 shows the recipes used to do two batch unseeded copolymerizations of BuA and STY. The monomer composition in the first experiment was 30-70 BuA/STY by mole and 50-50 % in the second experiment.

Table 4.2: Experiments of copolymerization for the validation of the observer for hydrophobic monomers.

\experiment	BuA-STY	BuA-STY
Final composition (by mol)	30 - 70 %	50 - 50 %
Component\	Initial charge (g)	Initial charge (g)
Styrene	526.9	343.7
Butyl acrylate	225.8	422.9
Dodecyl sulfate, sodium salt	4.54	4.54
Potassium persulfat	4.34	4.42
water	3000	3000
Final solids content	19 %	19 %
Final particle size	82 nm	70 nm
Glass transition temperature	~ 70 °C	~ 27 °C
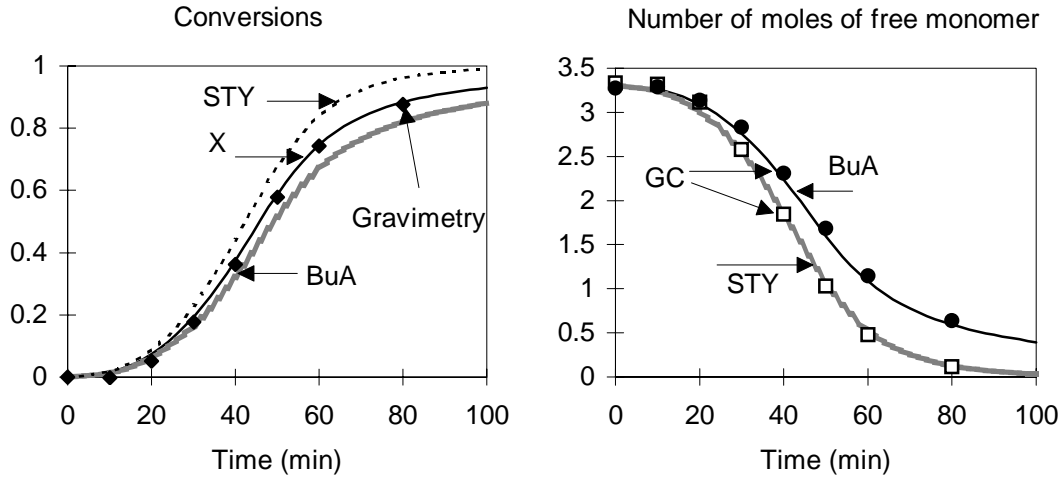
Figure 4.10a: Experiment BuA/STY 50-50 by mol: overall and individual conversions, at left, and the residual number of moles of each monomer, at right. Validation of the observer by GC given by the points.

Figure 4.10a shows the overall and individual conversions, at left, and the estimated and measured (by GC) residual number of moles of each monomer during the experiment of composition 50-50% by mole. Figure 4.11 shows the estimation results obtained during the experiment of composition 30-70% by mole. In both experiments, a good agreement between the observer and the experimental GC measurements was observed.
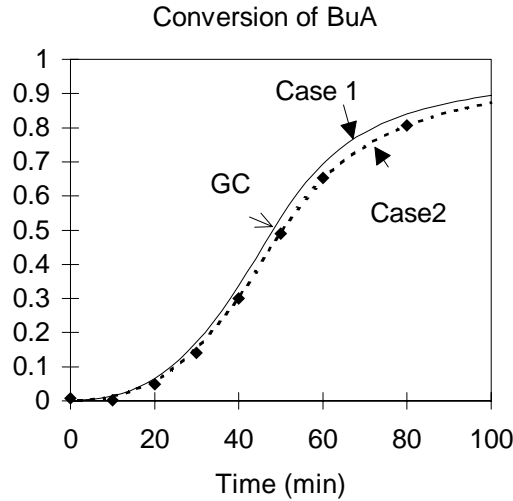
Figure 4.10b: Experiment BuA/STY 50-50. Case 1: $K_{P11}=3.37\times10^7$, $K_{P22}=2.97\times10^5 cm^3/mol/s$ $r_1=.18$, $r_2=.95$, and in cases 2 : $K_{P11}=2.47\times10^5$, $K_{P22}=3.53\times10^5 cm^3/mol/s$ $r_1=.3$, $r_2=.7$, for BuA and STY respectively.

In figure 4.10b, we compared two reaction rate constants of styrene and butyl acrylate. In the first case: $K_P(BuA)=3.37\times10^7 cm^3/mol/s$, $K_P(STY)=2.97\times10^5 cm^3/mol/s$, $r_1=.18$, $r_2=.95$, (van Herk 1997), and in the second case: $K_P(BuA)=2.47\times10^5 cm^3/mol/s$ (Urretabizkaia et al. (1994[a])), $K_P(STY)=3.53\times10^5 cm^3/mol/s$ (van Herk 1997), and the reactivity ratios: $r_1=.3$, $r_2=.7$, (Polymer Handbook). The figure shows that the estimations are slightly sensitive to variations in K_{pij} and r_i. The choice of these kinetics is therefore important in order to obtain accurate estimation.
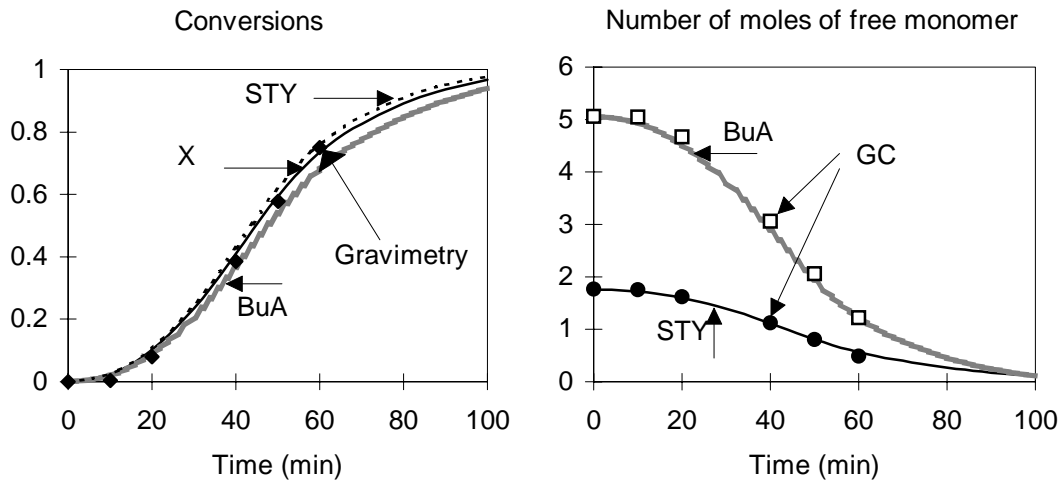
Figure 4.11: Experiment BuA/STY 30-70 by mol: Overall and individual conversions, at left. At right, the estimated number of moles of free monomer is given by the continuous lines and the experimental validation by GC, given by the points.

The observer provides also an estimate of the number of moles of radicals in the polymer particles (μ). An estimate of $\bar{n}$ cannot be obtained on-line during these experiments since the number of particles is not known a priori as in the case of seeded polymerization. However, $\bar{n}$ can be estimated off-line from μ once the particle size is measured. The obtained $\bar{n}$ are shown in figure 4.12.
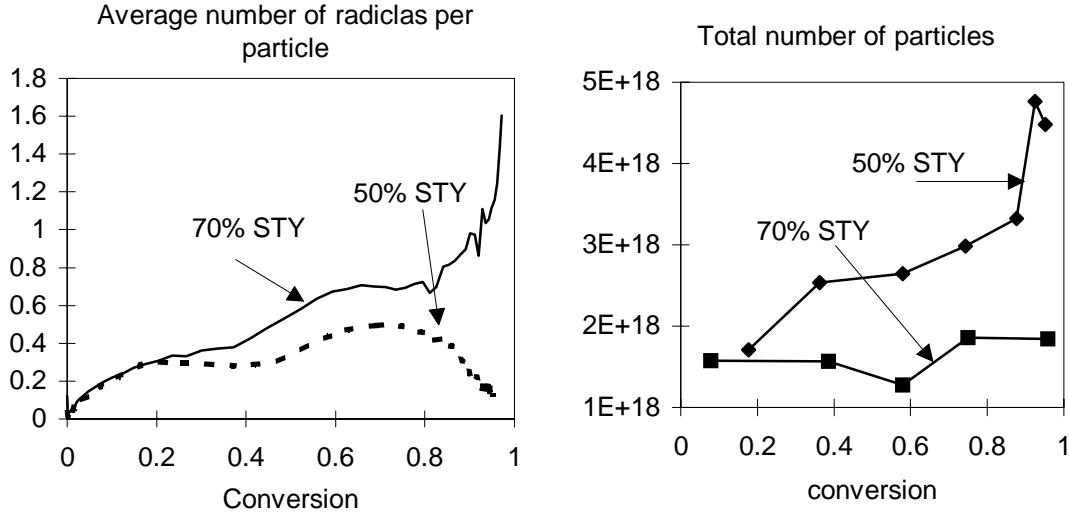
Figure 4.12: Experiments BuA/STY 50-50 and 30-70 by mole: $\overline{n}$, at left, and N_P^T at right.

Figure 4.12 shows that an the value of $\overline{n}$ increased at the end of experiment BuA/STY 30-70, and it decreased during the experiment of composition BuA/STY 50-50. An explanation of this phenomena would be that when styrene constitutes 70% of the polymer a gel effect occurs (Tg=70°C) which induces an increase in $\overline{n}$. Whereas, when the polymer contains 50% of styrene, the glass transition temperature (Tg=27°C) remains inferior to the reaction temperature and no gel effect takes place. The gel effect, or the Trommsdorff-Norrish effect, or autoacceleration, causes a decrease in the mobility of polymer chains, and therefore a decrease in the termination rate. This in turn leads to an increase in $\overline{n}$. On the other hand, it is known that butyl acrylate enhances the radical desorption, which in turn leads to a decrease of $\overline{n}$. Several parameters participate in the variation of $\overline{n}$, and determining their values would enhance our understanding of the process, evolution of the particle number and size, and molecular weight distribution. However, the interpretation of kinetics requires deeper studies of these processes, and since the work presented in this thesis focuses on the monitoring and control of the polymer composition, the estimated value of μ is not used for the on-line control of other kinetics.

These experiments allowed us to validate the observer on the laboratory scale experiments. The observer was then tested on the 250 liter pilot reactor. Several systems were studied in semi-continuous operations. The recipes used for these experiments are shown in Table 4.3 and 4.4.

Table 4.3: Experiment (14/11/97) of terpolymerization in the 250 liter pilot reactor for the validation of the composition observer.

Experiment	Experiment 14/11/97		
Final composition (mass)	48.7 - 47.6 - 3.7 % BuA-MMA-MAA		
Temperature	Temperature = 80°C		
**Component **	Initial charge (g)	preemulsion (g)	Initiator solution(g)
H_2O	49025	10000	3000
BuA	2478	16220	-
MMA	1645	10765	-
MAA	127	835	-
Surfactant	306+3000 water	334+3000 water	-
Sodium persulfat	25.5+2000 water	-	150
Final solids content	33 %		

The first part of these experiments consists of reacting a relatively small amount of monomer (8% solids content) under batch conditions in order to prepare the seed. Thereafter, monomer is added semi-continuously (see Figure 4.15f for experiment 28/4/99). All these experiments contain two main monomers that constitute the majority of the components fed to the reactor and a trace amount of additional monomers. In order to apply the observer to these copolymerizations the monomers present in small amounts are neglected, since the evolution of these monomers should not significantly influence the composition. It should be mentioned that the presence of these additional monomers influences other properties, e.g. stability of the latex particles, and some properties related to the final applications, film formation or degree of adhering. Therefore, if one is interested in understanding these phenomena, all substances must be accounted for in the model.

In Experiment 14/11/97 a monomer mass composition of 48:47 Butyl acrylate/ methyl methacrylate (BuA-MMA) and a trace amount (3.7%) of methacrylic acid (MAA) is carried out. The small amount of MAA was not accounted for in the model. During this experiment, an ultrasonic sensor was used for the monitoring of the overall conversion and the polymer composition. Therefore, the overall conversion was used in the observer to realize the estimation of the polymer composition. In this case, the on-line calorimetric optimization technique is not required. The estimation results of this experiment are given by Figure 4.13.
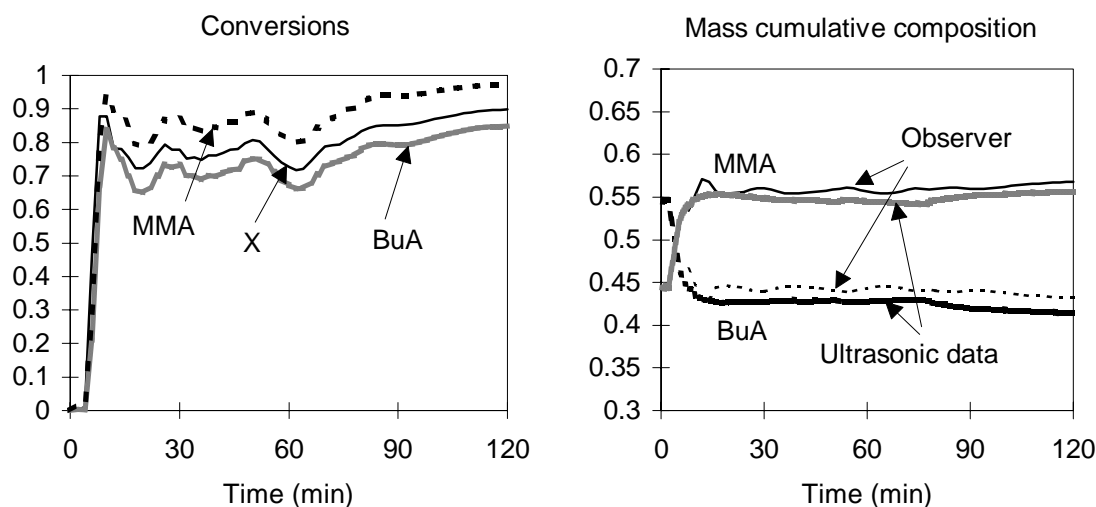
Figure 4.13: Experiment 14/11/97: Copolymerization of BuA and MMA. The overall conversion obtained by an ultrasonic probe and the individual conversions of MMA and BuA estimated by the observer, at left. At right, the estimated composition and its validation obtained by the ultrasonic sensor.

Figure 4.13 at left shows the overall conversion, obtained by the ultrasonic probe, and the individual conversions of MMA and BuA, predicted by the high gain observer. The right hand side of the same figure shows the estimated mass composition compared to the measured composition (given by the ultrasonic sensor). It can be seen that the values obtained by the observer agree with the experimental ultrasonic data. This means that neglecting the amount of MAA in the polymer composition does not significantly influence the composition estimation. Moreover, it is known that the MAA is water soluble and might react in the aqueous phase. This means that with these reasonable amounts of monomer in the aqueous phase, neglecting the reaction in this phase does not influence the estimation of the polymer composition. However, the estimation of the number of radicals per particle, in this case, would not be exact. The first error in estimating $\bar{n}$ can be related to the technique of measuring the particle size. The aqueous rate reaction can cause a nucleation of polymer particles. If these new particles have a smaller size than the latex particles present in majority, they cannot be determined by usual, nonseparative, techniques of measuring particle size. In this case, the estimated value of μ is more representative than $\bar{n}$.

Table 4.4: Terpolymerization experiments (27/4/99 and 28/4/99) in the 250 liter pilot.

experiment	Experiment 27/4/99			Experiment 28/4/99		
Final composition (mass)	58.8 - 38.7 - 3 % BuA:MMA:MAA			48 - 47 - 2.5 - 2.5% BuA-STY-AA-Acr		
Température	80°C			80°C		
**Component **	Initial charge (g)	preemulsion (g)	Initiator solution(g)	Initial charge (g)	preemulsion (g)	Initiator solution(g)
H$_2$O	46000	22000	3000	49600	14420	3000
BuA	2677	42937	-	1930	36615	-
MMA	1777	28502	-	-	-	-
MAA	137	2209	-	-	-	-
STY	-	-	-	1882	35765	-
Acr	-	-	-	100	1893	-
AA	-	-	-	98	1856	-
Surfactant	306+2000 water	736+2000 water	-	3093	1050	-
Sodium persulfat	25.5+1000 water	-	194	29.6	-	272
Final solids content	47 %			44 %		

Experiments 27/4/99 and 28/4/99 were carried out in the 250 liter pilot reactor for the production of lattices with higher solids content. The recipes used for these experiments are given by Table 4.4. In experiment 27/4/99 the same monomers, as in the lastly mentioned experiment 14/11/97, were used with the mass composition: 58.8 : 38.7 : 3 % BuA-MMA-MAA. The final solids content of this experiment is 47%. In this experiment the calorimetric optimization technique was used in order to estimate the overall conversion.
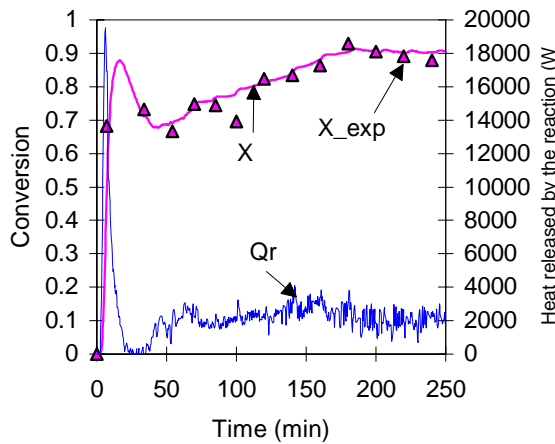
Figure 4.14a: Experiment 27/4/99, 250 liter pilot reactor.
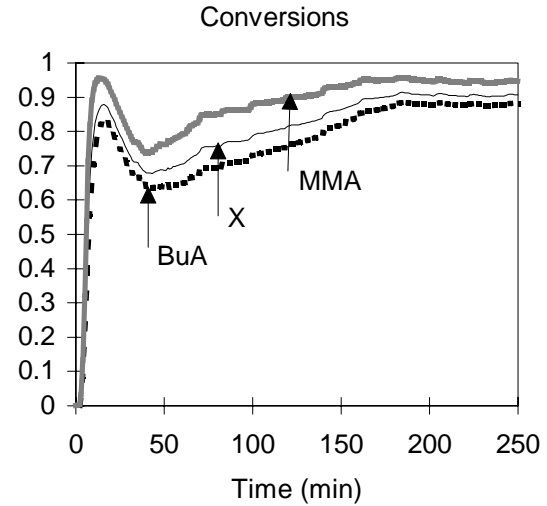
Figure 4.14b: Experiment 27/4/99, 250 liter pilot reactor.

Figure 4.14a shows the estimated overall monomer conversion and the heat produced by the reaction. The material observer was applied using the conversion obtained by calorimetry, and neglecting the small amount (3%) of MAA in the reactor. Figure 4.14b shows the on-line predicted individual conversions. Once the particle size was determined off-line, the number of particles was calculated assuming a monodispersed latex (Figure 4.14c). The evolution of $\bar{n}$ can then be estimated from μ and $\bar{n}$, Figure 4.14d. It should be pointed out that the estimator gives accurate results in the first moment of the reaction if and only if the initial conditions are well known. However, it was found that the observer converges rapidly to the real process even if the initial value of μ is not known. This remark must be kept in mind while interpreting the curves of μ and $\bar{n}$, especially at the beginning of the estimations.

164
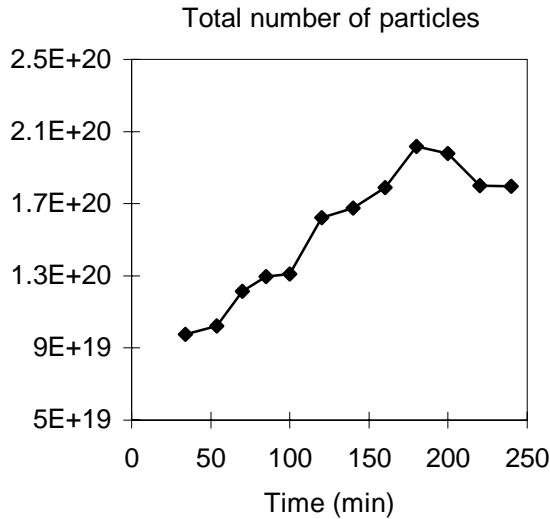
Figure 4.14c: Experiment 27/4/99. Off-line determination of N_P^T from the measurement of the particle size.
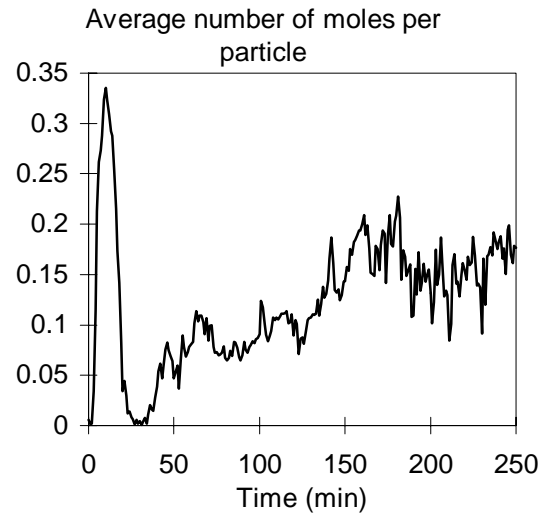
Figure 4.14d: Experiment 27/4/99. Off-line estimation of $\bar{n}$.

The peak in Figure 4.14d correspond to the estimated value of $\bar{n}$ during the particle nucleation. The value of $\bar{n}$ then drops to zero since all the monomer was consumed. When the semi-continuous addition of monomer starts, the reaction again takes place and the value of $\bar{n}$ is estimated. It should be recalled here that a solution of initiator is add to the reactor in a continuous way, and the exact added mass was not registered. Therefore, the variation of the value of $\bar{n}$ as a function of time can be due to the addition mode, and to the other kinetic phenomena such as the radical desorption, the gel effect, and the radical termination. Regarding the tendency of the curve of $\bar{n}$ during the semi-continuous part of the experiment, it can be seen that we obtain a constant value that increases towards the end of the reaction due to the gel effect.

In Experiment 28/4/99 the system: butyl acrylate/styrene/acrylic acid/ acrylamide was studied (48:46:2.5:2.5% by mass BuA-STY-AA-Acr). Monomers AA and Acr were present only in a small amount. The first step consists of estimating the overall conversion and the heat produced by the reaction based on calorimetry, the results of which are shown in Figure 4.15a.
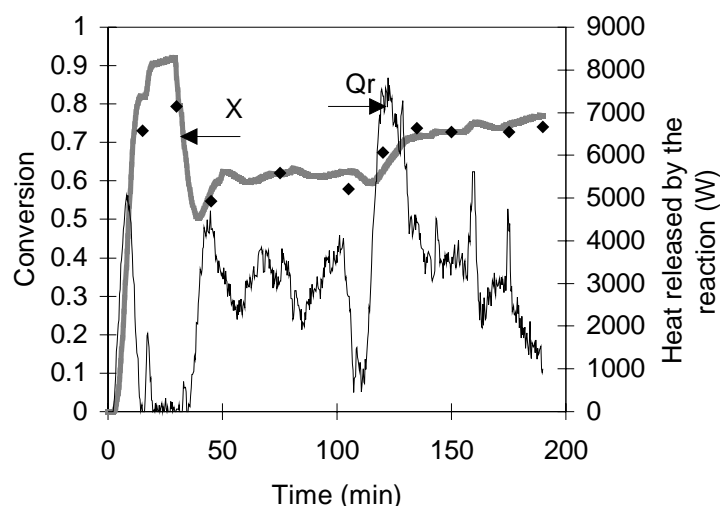
Figure 4.15a: Experiment 28/4/99. On-line estimation of the heat produced by the reaction and the overall mass conversion, in a 250 liter pilot reactor.

During this experiment, we noticed a big increase in the reaction rate at 120 minutes of the reaction, that we later found it was due to a fault in the pump used for the initiator addition. Feeding of the initiator solution stopped at 75 minutes and when it restarted, at 120 minutes, a huge amount of initiator was introduced. This "fault" could be detected on several curves: the overall conversion changes slope, which also produces a peak in the curve of Q_R (Figure 4.15a), the reaction rate of each monomer increases (Figure 4.15c) and finally an increase in the value of μ, the number of moles of radicals in polymer particles, is observed (Figure 4.15h). This might be due to an increase in $\bar{n}$ or to a renucleation, and therefore to an increase in N_P^T. A renucleation in our case is possible especially since during the fault of the pump the reaction rate decreased which caused an accumulation in the amount of monomer in the reactor. The reintroduction of a large quantity of initiator coupled with high monomer concentration could lead to the renucleation of particles, and therefore the increase in N_P^T. However, we could not detect the production of new particles by measuring the particle size by QELS .Note that these QELS measurements were performed on a limited number of samples, thee weeks after the reaction. Figure 4.15i shows that there was not a distinct increase in the number of particles at 120 minutes. It should be mentioned that if very small particles were renucleated, they will not be detectable by the QELS. Based on this measurement, the estimated value of $\bar{n}$ increases at 120 minutes (Figure 4.15j). In this case, the number of radicals in the polymer particles increases, but we cannot confirm whether it is

due to a renucleation (if a significant amount of particles was renucleated) or to an increase in the decomposition rate of radicals. In other systems, where $\bar{n}$ is well-defined during the experiment (e.g. styrene $\bar{n} \leq 0.5$), we can confirm that an increase in the value of μ is due to an increase in the number of particles.
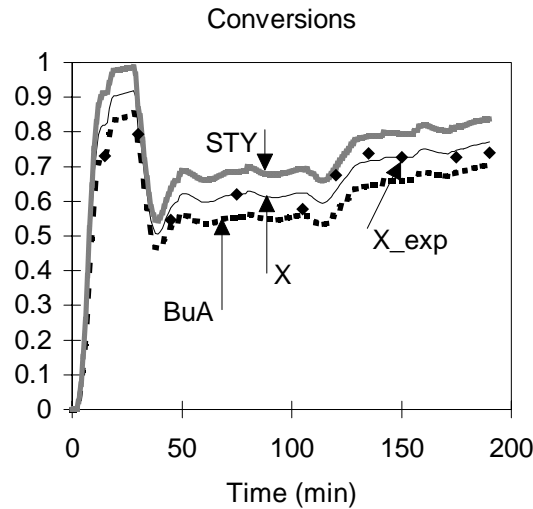
Figure 4.15b: Experiment 28/4/99. The estimator of the individual conversions.
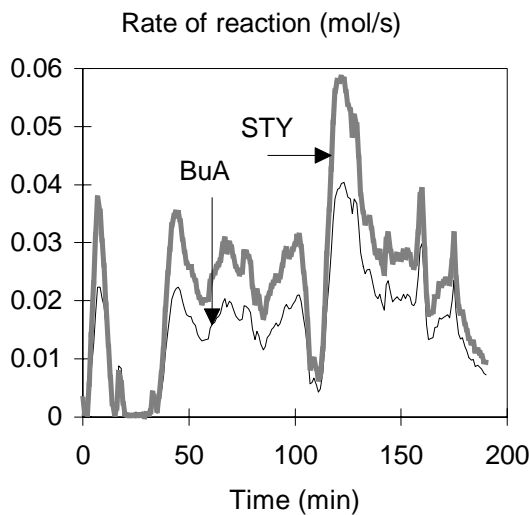
Figure 4.15c: Experiment 28/4/99. Estimated rate of the reaction of each monomer.
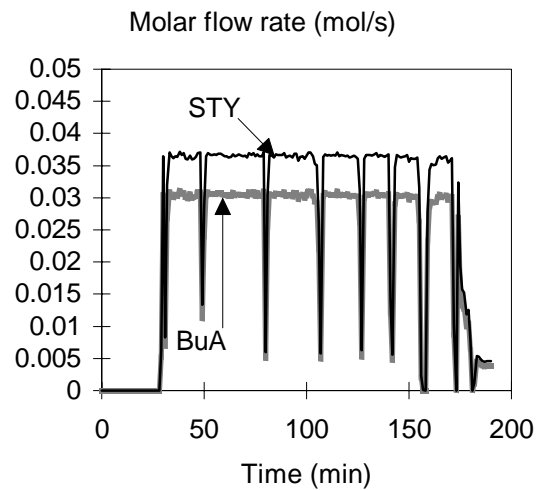
Figure 4.15d: Experiment 28/4/99. Monomer addition.

Figure 4.15c shows the evolution of the reaction rates of styrene and butyl acrylate during this experiment. Between 50 and 100 minutes, the addition flow rate of STY and BuA was higher than the reaction rates. This means that a significant amount of monomer was

accumulated in the reactor, which can be seen from the concentration of monomer in the polymer particles, in Figure 4.15f. At 120 minutes, a big amount of initiator is added which leads to an increase in the reaction rates.

Instantaneous molar composition

Molar cumulative composition
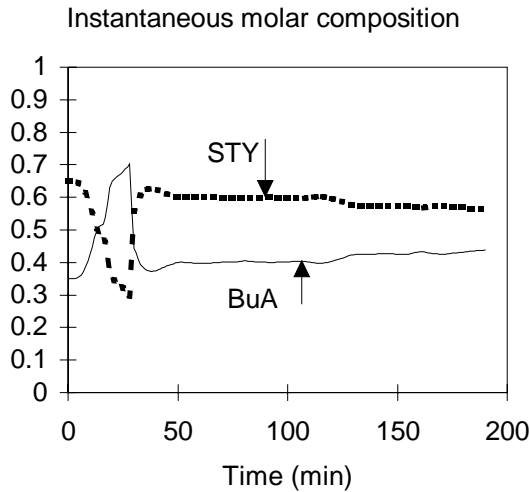
Figure 4.15e: Experiment 28/4/99. Results of the estimator.
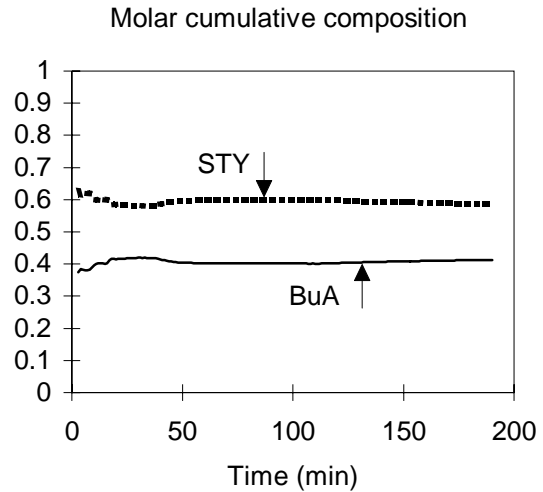
Figure 4.15f: Experiment 28/4/99.

Figure 4.15e shows that while preparing the polymer seed in batch, a composition drift arises. The polymer produced at the beginning of the reaction is more rich in styrene and then more rich in butyl acrylate. However, only 5% of the monomer was used to form the seed. Therefore, if the composition of the polymer produced after the nucleation part is well controlled then the cumulative composition would not be affected by the small amount used to prepare the seed.

It is important to recall that if we correctly control the preemulsion composition equal to the desired polymer composition, we can control the polymer composition if the flow rate of monomer is inferior to its reaction rate. Therefore, in Figure 4.15e, the instantaneous composition was influenced by the accumulation of monomer between 50 and 120 minutes (the preemulsion is 48% BuA and 47% STY and the obtained composition is 60% STY and 40% BuA). This leads to an accumulation of the less reactive monomer, BuA that will react once there is no longer styrene.

Concentration of monomer in polymer particles (mol/cm3)

STY

BuA
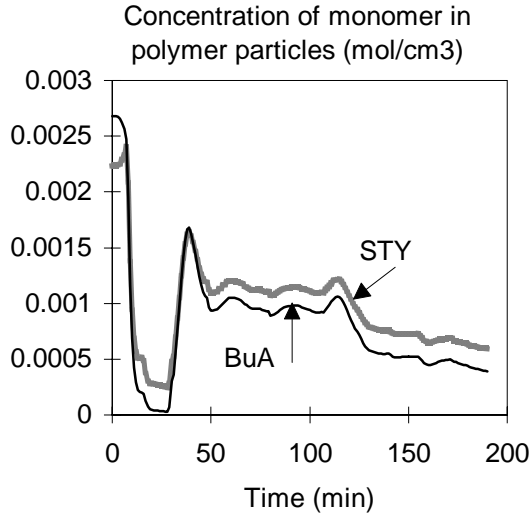
Figure 4.15g: Experiment 28/4/99. On-line estimation of μ.

Total number of moles of radicals in polymer particles
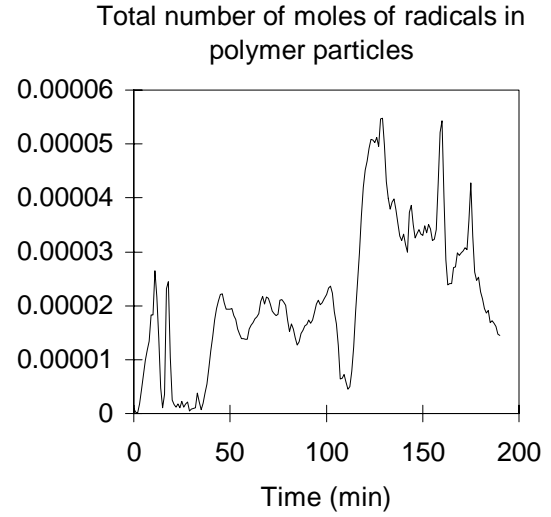
Figure 4.15h: Experiment 28/4/99. On-line estimation of μ.

Total number of particles
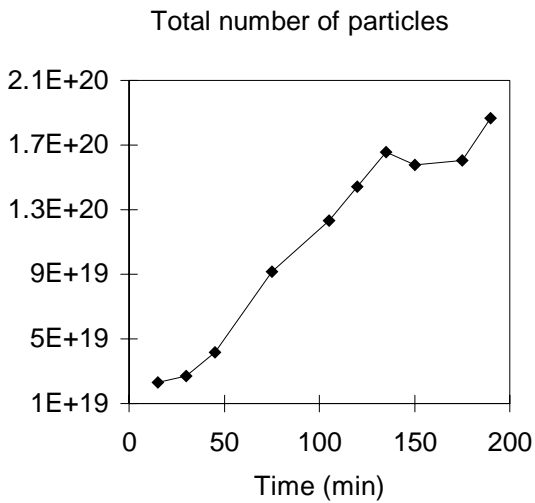
Figure 4.15i : Experiment 28/4/99. Off-line determination of N_P^T.

Average number of radicals per particle
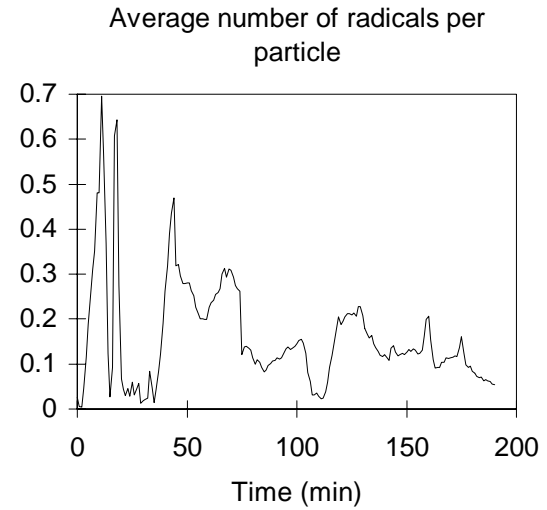
Figure 4.15j:Experiment 28/4/99. Off-line determination of $\bar{n}$.

4.7 Conclusion

In the first part of this chapter we developed an observer that accounts the water solubility and reaction in the aqueous phase. It was found that for the polymer composition monitoring, the monomer solubility in water can be neglected. The observer constructed for hydrophobic monomers gives good estimations of the copolymer composition even when partially water soluble monomers are involved. Finally, it was found that neglecting the monomers present in small amounts does not influence the estimation of the composition. It should be pointed out however that for other applications, such as the estimation of the evolution of the population balance or kinetic studies, the monomer reaction and solubility in the aqueous phase should be accounted for.

The observer requires the measurement of the overall conversion. It was validated on a large reactor for several semi-continuous systems, where the overall conversion was obtained using the calorimetric strategy and/or an ultrasonic probe. In both cases, an accurate on-line estimate of the composition was obtained. Moreover, important information on the evolution of the total number of moles of radicals in the polymer particles can be obtained on-line, which is important for fault detection, and studying the kinetics.

The observer have been experimentally tested on-line and was found to run rapidly on a typical PC. It can therefore be used for the polymer composition control. This topic will be treated in chapter 6. In the following chapter we propose an estimator of the polymer composition in emulsion terpolymerisation systems.

4.8 Nomenclature.

Notation

F_i	molar fraction of homopolymer i in the polymer
F	efficiency factor for initiator decomposition
k_a	entry rate coefficient for absorption of radicals of type i (s^{-1})
k_d	overall desorption rate coefficient (s^{-1})
K_{Pij}	reaction rate constant of radical i and monomer j
k_i^j	the partition coefficient of monomer i between phase j and aqueous phase
k_I	rate constant for initiator decomposition (s^{-1})
k_{tij}	termination rate constant ($cm^3/mol/s$)
I	number of moles of initiator (mol)
$\bar{n}$	average number of radicals per particle
N_A	Avogadro's number
N_i	number of moles of residual monomer i
N_i^j	number of moles of free monomer in phase j
N_p^T	total number of polymer particles
P_i^j	time averaged probability that the ultimate unit of an active chain in the phase j is of type i
Q_i	molar flow rate of monomer i
R_{Pi}^j	reaction rate of monomer i in phase j (mol/s)
R_w	number of moles of radicals in the aqueous phase
V_i	volume of monomer i
V_i^j	volume of monomer i in phase j
V^j	volume of phase j
X	mass conversion
x	state vector
y	output

Greek letters

ε_k	bounded function representing the unknown dynamic of k
θ, θ_2	observer tuning parameters
ρ_i	density of monomer i
$\rho_{i,h}$	density of polymer i
μ	number of moles of radicals in the polymer particles
ϕ_p^p	volumetric fraction of polymer in the polymer particles

Acronyms

AA	Acrylic acid
BuA	butyl acrylate
CSTR	Continuous stirred tank reactor
EKF	Extended Kalman filter
GC	gas chromatography
KF	Kalman filter
MA	methyl acrylate
MAA	methacrylic acid
MW	molecular weigh
MWD	molecular weight distribution
NMR	nuclear magnetic resonance
PSD	particle size distribution
STY	styrene
VAc	vinyl acetate

4.9 Bibliography

1.   Alvarez, and T. Lopez, Robust dynamic state estimation of nonlinear plants, *AIChE J.*, **45**, 1, 107-123, (1999).

2.   Armitage, P. D., J. C. De la Cal, and J. Asua, Improved Methods for solving monomer partitioning in emulsion copolymer systems, *J. Appl. Polym. Sci*, **51**, 1985-1990, (1994).

3.   Arzamendi, G. and J. M. Asua, Monomer addition policies for copolymer composition control in semi-continuous emulsion copolymerization, *J. Appl. Polym. Sci.*, **38**, 2019-2036, (1989).

4.   Asua, J. M., M. E. Adams, E. D. Sudol, An approach for the estimation of kinetics parameters in emulsion polymerization systems. I. Homopolymerization under zero-one conditions, *J. Appl. Polym. Sci.*, **39**, 1183-1213, (1990).

5.   Barandiaran, M. J., L. Lopez de Arbina, J. C. De la Cal, L. M. Gugliotta and J. M. Asua, Parameter estimation in emulsion copolymerization using reaction calorimeter data, *J. Appl. Polym. Sci.*, **55**, 1231-1239, (1995).

6.   Chen-Chong, L., and W.-Y. Chiu, Simulation and optimal design of seeded continuous emulsion polymerization process, *J. Appl. Polym. Sci.*, **27**, 1977-1993, (1982).

7.   De la Cal, J. C., M. E. Adams, and J. M. Asua, Parameter estimation in emulsion copolymerization, *Makromol. Chem., Macromol. Symp.*, **35/36**, 23-40, (1990).

8.   Dimitratos, J., C. Georgakis, M. El-Aasser, and A. Klein, An experimental study of adaptive Kalman filtering in emulsion copolymerization, *Chem. Eng. Sci.*, **46**, 12, 3203-3218, (1991).

9.   Dootingh, M. V., D. Rakatopara, J.P. Gauthier, and P. Hobbes, Nonlinear deterministic observer for state estimation: Application to a free radical polymerization reactor, *Comp. Chem. Eng.*, **16**, 8, 777-791, (1992).

10.   Dubé, M. A., and A. Penlidis, A systematic approach to the study of multicomponent polymerization kinetics-the butyl acrylate/methyl methacrylate/vinyl acetate example: 1. Bulk copolymerization", *Polymer*, **36**, 3, 587, (1995)[a].

11. Févotte, G., I. Barudio, T. F. McKenna, Computer-aided parameter estimation and on-line monitoring of emulsion and solution polymerization reactors, *Comp. Chem. Eng Suppl.*, **20**, S581-S585, (1996)[b].

12. Févotte, G., T. F. McKenna, S. Othman, and H. Hammouri, Nonlinear tracking of glass transition temperature for free radical emulsion copolymers, *Chem. Eng. Sci.*, **53**, 4, 773-786, (1998)[a].

13. Févotte, G., T. F. McKenna, S. Othman, and A. M. Santos, A combined hardware/software sensing approach for on-line control of emulsion polymerization processes, *Comp. Chem. Eng. Suppl.*, **22**, S443-S449, (1998)[b].

14. Flory, P. J., Principles of polymer science, *Cornell University Press*, New York, (1953).

15. Gardon, J. L., Emulsion polymerization. VI. Concentration of monomers in latex particles, *J. of Polym. Sci.: Part A-1*, **6**, 2859-2879, (1968).

16. Gagnon, L., and J. F. MacGregor, State estimation for continuous emulsion polymerization, *The Canadian J. of Chem. Eng.*, **69**, 648-656, (1991).

17. Gauthier J.P., H. Hammouri and S. Othman, A simple observer for nonlinear systems. Application to bioreactors, *IEEE Trans. Automat Control*, **37**, 875-880, (1992).

18. Gilbert, R. G., a mechanistic approach, Colloid Science, R. H. Ottewill, and R. L. Rowell eds, (1995).

19. Gilmore, C. M. G. W. Poehlein, and F. J. Schork, Modeling poly(vinyl alcohol)-stabilized vinyl acetate emulsion polymerization. I. Theory, *J. Appl. Polym. Sci.*, **48**, 1449-1460, (1993).

20. Gugliotta, L. M., G. Arzamendi, and J. Asua, Choice of monomer partition model in mathematical modeling of emulsion copolymerization systems, *J. Appl. Polym. Sci*, **55**, 1017-1039, (1995).

21. Gugliotta, L. M., J. R. Vega, C. E. Antonione, and G. R. Meira, Emulsion copolymerization of acrylonitrile and butadiene in an industrial batch reactor. Estimation of conversion and polymer quality from on-line energy measurements, *Polymer React. Eng.*, **7**, **4**, 531-552, (1999).

22. Guillot, J., Kinetics and thermodynamic aspects of emulsion copolymerization. Acrylonitrile-styrene copolymerization, *Acta Polymer.*, **32**, 593-600, (1981).

23. Guillot, J., Some thermodynamic aspects in emulsion copolymerization, *Makroml. Chem. Suppl.*, **10/11**, 235-264, (1985).

24. Hamielec, A. E., J. F. MacGregor, and A. Penlidis, Multicomponent free-radical polymerization in batch, semi-batch and continuous reactors, *Makromol. Chem. Macromol. Symp.*, **10**, 11, 521-570, (1987).

25. Kiparissides, C., J. MacGregor, and A. Hamielec, Suboptimal stochastic control of a continuous latex reactor, *AIChE J.*, **27**,13-19, (1981).

26. Kozub, D. J., and J. F. MacGregor, State estimation for semi-batch polymerization reactors, *Chem. Eng. Sci.*, **47**, 5, 1047-1062, (1992).

27. Lopez de Arbina, L., M. J. Barandiaran, L. M. Gugliotta and J. M. Asua, Kinetics of the emulsion copolymerization of styrene and butyl acrylate, *Polymer*, **38**, 1, 143-148, (1997).

28. Maxwell, I. A., L. F. J. Noël, H. A. S. Schoonbrood, and A. L. German, Thermodynamics of swelling of latex particles with two monomers: a sensitivity analysis, *Makromol. Chem., Theory Simul.*, **2**, 269-274, (1993).

29. Maxwell, I. A., J. Kurja, G. H. J. Van Doremaele, A. L. German, and B. R. Morrison, Thermodynamics of swelling of latex particles with two monomers, *Makromol. Chem.*, **193**, 2065-2080, (1992).

30. Maxwell, I. A., J. Kurja, G. H. J. Van Doremaele, A. L. German, and B. R. Morrison Partial swelling of latex particles with monomers, *Makromol. Chem.*, **193**, 2049-2063, (1992).

31. Mead, R. N., and G. W. Poehlein, Emulsion copolymerization of styrene-methyl acrylate and styrene-acrylonitrile in continuous stirred tank reactors, *Ind. Eng. Chem. Res.*, **27**, 2283-2293, (1988).

32. Morton, M., S. Kaizerman and M.W. Altier, Swelling of latex particles, *J. Colloid. Sci.*, **9**, 300-312, (1954).

33. Noël, L. F. J., I. A. Maxwell, and A. L. German, Partial swelling of latex particles by two monomers, *Macromolecules*, **26**, 2911-2918, (1993).

34. Nomura M., and K. Fujita, On the prediction of the rate of emulsion copolymerization and copolymer composition, *Makromol. Chem. Suppl.*, **10**, 11, 25-42, (1985).

35. Okubo, M., E. Ise, and T. Ymashita, Synthesis of greater than 10-m-sized, monodispersed polymer particles by one-step seeded polymerization for highly monomer-swollen polymer particles prepared utilizing the dynamic swelling method, *J. Appl. Polym. Sci.*, **74**, 278-285, (1999).

36. Omi, S., K. Kushibiki, M. Negishi, and M. Iso, A generalized computer modeling of semi batch, n-component emulsion copolymerization system and its applications, *Dep. Chem. Eng., Faculty of Tech. Univ agriculture and tech., Tokyo 184*, **3**, **9**, 34-49, (1985).

37. Penlidis, A., J. F. MacGregor and A. E. Hamielec, A theoretical and experimental investigation of the batch emulsion polymerization of vinyl acetate, *Polym. Process. Eng.*, **3**, 3, 185-218, (1985).

38. Poehlein, G. W., Emulsion polymerization with water soluble comonomers in batch and continuous reactors, *Macromol. Symp.*, **92**, 179-194, (1995).

39. John, R. R., and J. P. Congalidis, Mathematical modeling of emulsion copolymerization reactors", *J. Appl. Polym. Sci.*, **37**, 2727-2756, (1989).

40. Saldivar, E., P. Daeniotis, and W. H. Ray, Mathematical modeling of emulsion copolymerization reactors I. model formulation and application to reactors operating with micellar nucleation", *Macromolecules*, **C38**, 2, 207-325, (1998).

41. Santos, A. M., J. Guillot, and T. F. McKenna, Partitioning of styrene, butyl acrylate and methyl mathacrylic acid in emulsion systems, *Chem. Eng. Sci.*, **53**, 00-00 ,(1998).

42. Schoonbrood, H. A. S., M. A. T. Van Den Boom, A. L. German, and J. Hutovic, Multimonomer partitioning in latex systems with moderately water-soluble monomers, *J. Appl. Polym. Sci*, **32**, 2311-2325, (1994).

43. Schork, F. J., and W. H. RAY, The dynamic of the continuous emulsion polymerization of methyl methacrylate", *J. Appl. Polym. Sci.* **34**, 1259-1276, (1987).

44. Scott, P. J., A. Penlidis, and G. L. Rempel, Ethylene-vinyl acetate emulsion copolymerization: monomer partitioning and preliminary modeling, *Polym. React. Eng.*, **3**, 2, 93-130, (1995).

45. Soroush, M., Nonlinear state-observer design with application to reactors, *Chem. Eng. Sci.*, **52**, 3, 387404, (1997).

46. Tatigaju, S., M. Soroush, B. A. Ogunnaike, Multirate nonlinear state estimation with applocation to a polymeriation reactor, *AIChE J.*, **45**, 4, 679-780 (1999).

47. Ugelstas, J., P. C. Mork, H. R. Mfutakamba, E. Soleimany, I. Nordhuus, R. Schmid, A. Berge, T. Ellingsen, O. Aune, and K. Nustad, Thermodynamics of swelling of polymer, oligomer and polymer-oligomer particles. Preparation and application of monodisperse polymer particles, *Sci. And Technology of Polymer Collooids, G. W. Poehlein, R. H. Ottewil, and J. W. Goodwinn, Eds, NATO ASI Series*, 1, 50-99, (1983).

48.   Urquiola, B, G. Arzamendi, J. R. Leiza, A. Zamora, J. M. Asua, J. Delgado, M. El-Aasser, and J. W. Vanderhoff, Semicontinuous seeded emulsion copolymerization of vinyl acetate and methyl acrylate, *J. Appl. Polym. Sci: Part A: Polym. Chem.*, **29**, 169-186, (1991).

49.   Urretabizkaia, A., E. D. Sudol, M. S. El-Aasser, and J. M. Asua, Calorimetric monitoring of emulsion copolymerization reactions, *J. Appl. Polym. Sci.*, **31**, 2907-2913, (1993).

50.   Urretabizkaia, A., and J. M. Asua, High solids content emulsion terpolymerization of vinyl acetate, methyl methacrylate, and butyle acrylate. I. Kinetics, , *J. of Polymer Sci.*: *Part A: Polymer Chem.*, **32**, 1761-1778, (1994)[a].

51.   van Herk, A. M., Pulsed initiation polymerization as a means of obtaining propagation rate coefficients in free-radical polymerizations, *J.M.S.-Rec. Macromol. Chem. Phys.*, **C37**, 4, 633, 648, (1997).

52.   Vanzo, E., R. H., Marchessault, and V. Stannett, *J. Colloid. Sci.*, **20**, 62, (1965).

CHAPTER V ———————————

STATE ESTIMATION FOR TERPOLYMERIZATION PROCESSES

5. STATE ESTIMATION FOR TERPOLYMERIZATION PROCESSES

5.1 Introduction

The economic pressure to produce polymeric materials with suitable final properties has encouraged the use of multimonomer systems. Terpolymerization systems are therefore widely used for creating high performance materials. Since the monomers involved usually have different reactivities, it is extremely difficult to obtain the desired polymer composition without taking some kind of actions on the system at hand. In this chapter we study the on-line monitoring of the polymer composition in emulsion terpolymerization systems, the crucial step towards the implementation of the control strategies outlined in Chapter 6.

Despite the industrial and academic importance of emulsion terpolymerization, most of the studies found in the literature concerning such three monomer systems focused on the experimental and kinetic aspects. For instance, Rios et al. (1980), studied the evolution of the terpolymer composition versus conversion in the terpolymerization of acrylonitile/ styrene/ methyl acrylate terpolymerization by gas chromatography (GC). The authors showed that the monomer solubility in water does not effect the rate of reaction. Storti et al. (1989), studied the modeling of the kinetics of multimonomer emulsion polymerization by using classical homopolymerization equations with averaged kinetics. A prediction of the overall conversion and terpolymer composition was successfully obtained during the batch acrylonitrile/ styrene/ methyl acrylate, under a limited range of experimental conditions. Urretabizkaia and Asua (1994) studied the effects of feed flow rates, amount of emulsifier and initiator on the evolution of a seeded vinyl acetate/ methyl methacrylate/ butyl acrylate (VAc/MMA/BuA) terpolymerization. The authors mentioned that the polymer composition drift was reduced by increasing the amount of initiator and by decreasing the feed rates; and that increasing the amount of initiator and emulsifier increased the secondary nucleation of polymer particles. Dubé and Penlidis (1997) studied the effects of monomer feed composition, initiator and

emulsifier concentration and temperature on the evolution of the VAc/MMA/BuA terpolymerization, using the optimal Baysian design. They reported that the terpolymer composition depends on the monomer feed ratio, as one would expect. The kinetics VAc/MMA/BuA system was also experimentally studied by Dubé and Penlidis (1996) and Dubé et al. (1997). Schoonbrood et al. (1996[a,b]) studied the modeling of the kinetics of a styrene/ methyl methacrylate/ methacrylate terpolymerization. The authors found that composition drift in this system is mainly determined by the reactivity of the monomers and to a lesser extend by monomer partitioning (except in systems where there is a large difference in the water solubility).

Only very few studies have been devoted to the modeling aspects of emulsion terpolymerization. For example, Urretabizkaia et al. (1992) developed a mathematical model for seeded semi-continuous emulsion terpolymerization using the VAc/MMA/BuA system. A direct search algorithm was used by fitting experimental data obtained by GC: mass conversion, polymer composition and particle size, to estimate several unknown parameters in the model, (the radical entry rate, the desorption rate coefficient and a factor related to the gel effect). In their model, the concentration of monomers in the different phases were assumed to be under thermodynamic equilibrium. Dubé et al. (1997[b]) developed a model for multicomponent systems, that accounts for the nucleation, population balance and molecular weight evolutions. The experimental results were compared with the model to validate the use of some reactivity and partition parameters. Urretabizkaia et al. (1994[b]) constructed an open loop composition control of terpolymerization systems based on the mathematical material balance. Urretabizkaia et al. (1994[a]) used the terpolymerization model to perform a closed loop composition control of the VAc/MMA/BuA system. A nonlinear optimization algorithm was used to determine the concentration of monomers in the polymer particles based on the experimental gas chromatographic measurements. A nonlinear adaptive proportional integral (NLA-PI) controller was used to perform the addition in a minimum time. Good results were obtained by the NLA controller and it was found that the PI controller does not improve the controller robustness.

The literature review shows that in almost all cases the terpolymer composition was monitored by GC measurements or obtained from an open-loop model. However, as the

model is not exact, open-loop estimation will deviate from the real values relatively quickly. On the other hand, we do not have available a direct on-line measurement of the composition that allows us to do closed loop control. Therefore, in order to perform composition control, it must be estimated on-line.

The instantaneous terpolymer composition is determined by the ratio of the reaction rate of each monomer to the overall reaction rate, as given by the following equation for monomer 1:

$$F_1 = \frac{R_{P1}}{R_{P1} + R_{P2} + R_{P3}} \qquad (5.1)$$

In chapter 4, it was demonstrated that the overall rate of reaction obtained by calorimetry is not directly proportional to the rate of reaction of each monomer since this latter depends on the reactivities of each monomer. However, when combined with the material balance, it was shown that we could estimate the copolymer composition from the value of the overall conversion. The material balance is more complex in terpolymerization processes, but still involves the reactivity ratio of monomers. Therefore, the polymer composition seems to be observable from this model.

In the first part of this chapter, we define the material balance that will be used to construct the composition observer. Thereafter, we study the observability of the composition based on the developed model, where the overall conversion is an output of said model. At the end of this chapter, an experimental study is performed to test the robustness of the estimation.

5.2 Mathematical model

Based on the literature review and on the results of Chapter 4, the reaction in the aqueous phase can be neglected in the modeling and estimation of the polymer composition. The material balance can therefore be written assuming that the polymer particles are the only reaction loci.

$$\dot{N}_i = Q_i - R_{Pi}, \qquad i = 1, 2, 3 \tag{5.2}$$

According to the mechanism of emulsion polymerization (Appendix I), the reaction rate in the polymer particles, R_{pi}, that appears in the material balance is a function of kinetic parameters, and the concentration of monomer ($[M_P]$) and radical (μ) in the polymer phase:

$$R_{Pi} = \mu [M_i^p]\left(K_{P1i}P_1^p + K_{P2i}P_2^p + K_{P3i}P_3^p\right) \tag{5.3}$$

The time averaged probabilities, $P_i{}^p$, that an active chain be of ultimate unit of type i in the polymer particles are defined by the following equations:

$$P_1^p = \frac{\alpha}{\alpha + \beta + \gamma}, \quad P_2^p = \frac{\beta}{\alpha + \beta + \gamma}, \quad P_3^p = 1 - P_1^p - P_2^p \tag{5.4}$$

where

$$\alpha = [M_1^p]\left(K_{P21}K_{P31}[M_1^p] + K_{P21}K_{P32}[M_2^p] + K_{P31}K_{P23}[M_3^p]\right)$$

$$\beta = [M_2^p]\left(K_{P12}K_{P31}[M_1^p] + K_{P32}K_{P12}[M_2^p] + K_{P32}K_{P13}[M_3^p]\right) \tag{5.5}$$

$$\gamma = [M_3^p]\left(K_{P13}K_{P21}[M_1^p] + K_{P23}K_{P12}[M_2^p] + K_{P13}K_{P23}[M_3^p]\right)$$

It was found from Chapter 4 that the ratio of monomers in the polymer particles was not particularly sensitive to the monomer solubility in the aqueous phase for the tested monomers. Therefore, for the sake of calculation of the composition, the monomers are supposed to be water insoluble and to be partitioned only between the polymer particles and the monomer droplets. While this is, strictly speaking, not true, we will see below that this

assumption turns out to be quite reasonable. Under the assumptions that the ratio of monomer concentrations are the same in the two parts of the organic phase, (i.e. the polymer particles and the monomer droplets, Poehlein (1995)) the concentration of monomer in the polymer particles is only a function of the saturation of polymer particles and the residual number of moles of each monomer:

$$[M_i^p] = \begin{cases} \dfrac{\left(1 - \phi_p^p\right)N_i}{\sum\limits_j \dfrac{N_j MW_j}{\rho_j}} & \text{, Intervals I, II} \\[3em] \dfrac{N_i}{\sum\limits_j MW_j \left(\dfrac{N_j^T - N_j}{\rho_{j,h}} + \dfrac{N_j}{\rho_j}\right)} & \text{, Interval III} \end{cases} \tag{5.6}$$

The condition for the existence of droplets is governed by the following equation:

$$N_1\delta_1 + N_2\delta_2 + N_3\delta_3 - \frac{\left(1 - \phi_p^p\right)}{\phi_p^p}\sigma > 0 \tag{5.7}$$

where:

$$\delta_i = MW_i \left(\frac{1}{\rho_i} + \frac{\left(1 - \phi_p^p\right)}{\rho_{i,h}\,\phi_p^p}\right) \text{, i=1, 2, 3} \tag{5.8}$$

and

$$\sigma = \sum_{j=1}^{3} \frac{MW_j N_j^T}{\rho_{2,h}} \tag{5.9}$$

Under the assumption mentioned earlier that the monomers are not soluble in the aqueous phase, and that the relative composition of monomers is the same in both parts in organic phase (Poehlein (1995)), the following equation can be written:

$$\frac{[M_1^p]}{[M_1^p] + [M_2^p] + [M_3^p]} = \frac{N_1}{N_1 + N_2 + N_3} \tag{5.10}$$

This leads to a simplification in the model, mainly in the definition of the average probabilities of radicals:

$$P_1^p = \frac{\alpha'}{\alpha'+\beta'+\gamma'} \quad , \quad P_2^p = \frac{\beta'}{\alpha'+\beta'+\gamma'} \tag{5.11}$$

were:

$$\alpha' = N_1\left(K_{P21}K_{P31}N_1 + K_{P21}K_{P32}N_2 + K_{P31}K_{P23}N_3\right)$$

$$\beta' = N_2\left(K_{P12}K_{P31}N_1 + K_{P32}K_{P12}N_2 + K_{P32}K_{P13}N_3\right) \tag{5.12}$$

$$\gamma' = N_3\left(K_{P13}K_{P21}N_1 + K_{P23}K_{P12}N_2 + K_{P13}K_{P23}N_3\right)$$

The measured output of the model is the amount of residual monomer that can be calculated from the overall mass conversion, obtained by calorimetry, and the total amount of monomers added to the reactor (initial amounts plus feed flow rates):

$$y = (1-X)\sum_{i=1}^{3} N_i^T MW_i$$
$$= \sum_{i=1}^{3} N_i MW_i \tag{5.13}$$

since the mass conversion is given by,

$$X = \frac{\sum_{i=1}^{3} MW_i\left(N_i^T - N_i\right)}{\sum_{j=1}^{3} MW_j N_j^T} \tag{5.14}$$

In order to estimate the polymer composition, the rates of reaction of each monomer must be determined. In the following section, we will present the development of a closed loop strategy, similar in nature to that presented in chapter 4, for the estimation of the number of moles of residual monomers N_i and μ, based on the material balance of monomers and assuming the dynamic of μ is unknown.

5.3 Nonlinear estimation of the individual conversions and the concentration of radicals in the polymer particles

The terpolymerization material balance can be represented by the following system, considering that μ varies with a certain dynamic ε_μ:

$$\begin{cases} \dot{N} = \overline{Q} - f \\ \dot{\mu} = \varepsilon_\mu \end{cases}$$

$$y = \sum_{i=1}^{3} MW_i N_i$$

(5.15)

where N is the vector representing the residual number of moles of each monomer: $N = [N_1 \ N_2 \ N_3]^T$, $\overline{Q}$ the flow rates of monomers: $\overline{Q} = [Q_1 \ Q_2 \ Q_3]^T$ and f the rates of reaction $f = [R_{P1} \ R_{P2} \ R_{P3}]^T$.

The system 5.15 is not under a canonical form that allows us to apply a high gain observer to estimate N_i and μ. Moreover, the change of co-ordinates proposed by Theorem 2.3, in chapter 2, does not put the system under the desired form. Here again, we propose to use a cascade observer composed of a first observer of N_1, N_2, and N_3 and a second observer for the estimation of the value of μ. In this case, a first change of co-ordinates can be performed assuming that μ is not time varying:

$$T = \begin{bmatrix} T_1 \\ T_2 \\ T_3 \end{bmatrix} = \begin{bmatrix} y \\ L_f y \\ L_f^2 y \end{bmatrix} = \begin{bmatrix} y \\ \dfrac{\partial y}{\partial N_i}.f \\ \dfrac{\partial (L_f y)}{\partial N_i}.f \end{bmatrix}$$

then,

$$T = \begin{bmatrix} MW_1N_1 + MW_2N_2 + MW_3N_3 \\ MW_1R_{P1} + MW_2R_{P2} + MW_3R_{P3} \\ \dfrac{\partial T_2}{\partial N_1}R_{P1} + \dfrac{\partial T_2}{\partial N_2}R_{P2} + \dfrac{\partial T_2}{\partial N_3}R_{P3} \end{bmatrix} \qquad (5.16)$$

The derivation of the new states yields a dynamic system that depends on all the states N_1, N_2, and N_3, considering μ to be a known input in this case:

$$\dot{T} = \underbrace{\begin{bmatrix} 0 & 1 & 0 \\ 0 & 0 & 1 \\ 0 & 0 & 0 \end{bmatrix}}_{A}T + \underbrace{\begin{bmatrix} g_1 \\ g_2(T) \\ g_3(T) \end{bmatrix}}_{G(T)}u + \underbrace{\begin{bmatrix} 0 \\ 0 \\ \varphi(T) \end{bmatrix}}_{\overline{\varphi}(T)} \qquad (5.17)$$

It can be seen that the matrix G is not triangular in T. This means that the system is not uniformly observable (there might be some entries that render the system inobservable). However, we can circumvent this problem by performing a change of co-ordinates that takes into account Q_i, for example we can replace f by $(\overline{Q} - f)$ defined above. The unique supplementary condition in order to be able to realize the estimations from this change of co-ordinates is that $\overline{Q}$ be derivable. We will however avoid using the derivative of $\overline{Q}$ in the observer, since this might amplify the oscillations in the measurements. Moreover, we can assume that, on the bounded interval of flow rates used over the experiments, there is not an input that renders the system inobservable. Therefore, we construct a high gain observer to estimate T:

$$\dot{\hat{T}} = A\hat{T} + G(\hat{T})u + \overline{\varphi}(\hat{T}) - S_\theta^{-1}C^T(\hat{y} - y) \qquad (5.18)$$

where

$$\hat{y} = MW_1\hat{N}_1 + MW_2\hat{N}_2 + MW_3\hat{N}_3$$
$$C = [1 \ \ 0 \ \ 0]^T \qquad (5.19)$$

$$S_\theta^{-1} = \begin{bmatrix} 3\theta & 3\theta^2 & \theta^3 \\ 3\theta^2 & 5\theta^3 & 2\theta^4 \\ \theta^3 & 2\theta^4 & \theta^5 \end{bmatrix}$$

The observer of the original co-ordinates (N_i) takes the following form:

$$\dot{\hat{N}} = \overline{Q} - \mu\,\overline{F}(\hat{N}_1,\hat{N}_2,\hat{N}_3) + \left(\frac{\partial T}{\partial \hat{N}_i}\right)^{-1} S_\theta^{-1} C^T(y - \hat{y}) \tag{5.20}$$

However, the Jacobian matrix $\left(\partial T / \partial N_i\right)$ in the corrective term of the observer 5.20 involves a large number of terms, and it is almost impossible to inverse it on-line in a program of on-line monitoring and control. Therefore, we propose to write the model differently in order to simplify the calculation of the Jacobian matrix.

By introducing equations 5.3, 5.6 and 5.11 in equation 5.2, we obtain the following systems for the intervals II and III, (i=1,2,3):

$$\dot{N}_i = \begin{cases} Q_i - \dfrac{\mu N_i\left(1-\phi_p^p\right)\left(K_{P1i}\alpha'+K_{P2i}\beta'+K_{P3i}\gamma'\right)}{\left(\alpha'+\beta'+\gamma'\right)\displaystyle\sum_{j=1}^{3}\dfrac{MW_jN_j}{\rho_j}} & , \text{ Interval II} \\[4em] Q_i - \dfrac{\mu N_i\left(K_{P1i}\alpha'+K_{P2i}\beta'+K_{P3i}\gamma'\right)}{\left(\alpha'+\beta'+\gamma'\right)\displaystyle\sum_{j=1}^{3}MW_j\left(\dfrac{N_j^T-N_j}{\rho_{j,h}}+\dfrac{N_j}{\rho_j}\right)} & , \text{ Interval III} \end{cases} \tag{5.21}$$

The change of co-ordinates that we want to perform must be chosen in such a way that the Jacobian matrix becomes inversible. One way to do so is to define a new unknown variable μ_2 that contains μ and the complex part in the model. The following equation shows a new possible definition of μ_2:

$$\mu_2 = \begin{cases} \dfrac{\overline{n}N_p^T\left(1-\phi_p^p\right)}{\left(\alpha'+\beta'+\gamma'\right)\displaystyle\sum_{j=1}^{3}\dfrac{MW_jN_j}{\rho_j}} & , \text{ Interval II} \\[4em] \dfrac{\overline{n}N_p^T N_A}{\left(\alpha'+\beta'+\gamma'\right)\displaystyle\sum_{j=1}^{3}MW_j\left(\dfrac{N_j^T-N_j}{\rho_{j,h}}+\dfrac{N_j}{\rho_j}\right)} & , \text{ Interval III} \end{cases} \tag{5.22}$$

By doing this, the material balance can take the following form:

$$\dot{N}_i = Q_i - \underbrace{\mu_2 N_i \left(K_{P1i}\alpha' + K_{P2i}\beta' + K_{P3i}\gamma' \right)}_{f_i} \tag{5.23}$$

The material balance is now represented by equation 5.23 during interval II and III. The corrective term is calculated assuming μ_2 unknown, and we avoid therefore the enormous calculations that would be necessary if the change of variables was not considered. The observer takes now the following form:

$$\dot{\hat{N}} = \overline{Q} - \mu_2 \overline{F}(\hat{N}_1, \hat{N}_2, \hat{N}_3) - \left(\frac{\partial T}{\partial \hat{N}_i} \right)^{-1} S_\theta^{-1} C^T (\overline{y} - \hat{y}) \tag{5.24}$$

where $\mu_2\overline{F} = f$ defined in equation 5.15.

The second observer in the cascade consists of estimating μ_2, and is given by the following equation:

$$\dot{\hat{\mu}}_2 = \frac{-\theta_2^2}{\lambda}(\hat{y} - y) \tag{2.25}$$

with

$$\lambda = \frac{-1}{N_A} \begin{pmatrix} MW_1 N_1 \left(K_{P11}\alpha' + K_{P21}\beta' + K_{P31}\gamma' \right) \\ + MW_2 N_2 \left(K_{P12}\alpha' + K_{P22}\beta' + K_{P32}\gamma' \right) \\ + MW_3 N_3 \left(K_{P13}\alpha' + K_{P23}\beta' + K_{P33}\gamma' \right) \end{pmatrix} \tag{5.26}$$

5.4 Experimental

In order to validate the observer, an initial experiment involving very slightly water soluble monomers, styrene/ butyl acrylate/ ethyl hexyl acrylate (STY-BuA-EHA), was carried out. Then, the observer was tested during the terpolymerization of MMA-BuA-VAc. This system has widely been studied in the literature (e.g. Urretabizkaia and Asua (1994), Dubé and Penlidis (1997), and Beauchemin and Dubé (1999)), and therefore its kinetics (reaction rate constants, reactivity ratios) are well understood. These monomers are known to have different solubilities in the aqueous phase and different reactivities, and therefore a composition drift usually occurs if batch operations are performed.

Table 5.1: Batch experiment for the validation of the observer of terpolymerization.

\Experiment Component \	STY-BuA-EHA amount (g)
Styrene	480
Butyl acrylate	200
Ethyl hexyl acrylate	120
Dodecyl sulfate, sodium salt	4.85
Potassium persulfate	4.6
H_2O	2000
Final particle diameter	71 nm
Final solids content	28 %
Final glass transition temperature	44 °C

The observer was tuned by the parameters $\theta = 1e^{-10}$ and $\theta_2 = 0.1$. The recipe used for the STY-BuA-EHA experiment is given by Table 5.1. The experimental mode is similar to that described during the earlier experiments mentioned in this work. The temperature measurements are fed to the computer, where the energy balance is solved to give an estimate

of the heat produced by the reaction and the overall conversion by the optimization procedure developed in chapter 3. The conversion is then used in the observers 5.24 and 5.25 based on the material balance of the monomers to estimate N_i and μ_2. The total number of radicals in the polymer particles (μ) can then be estimated from μ_2 by using equation 5.22. The average number of radicals per particle can be calculated from μ once the particle size is obtained by off-line measurement.

The estimated conversion and Q_R for this experiment are shown in Figure 5.1. In the right hand part of this figure, Q_R is calculated using the following relation:

$$X_{cal}(t) = \frac{\int_0^t Q_R(t)dt}{Q_{max}}$$

The real heat produced by the reaction is also calculated by the following relation, based on the estimated R_{pi} obtained from the estimator, to evaluate the estimation error due to the approximation done in the calculation of X_{cal}:

$$Q_{R\_real} = \sum_{i=1}^{3} \left(\Delta H_{Pi}\right) R_{Pi}$$
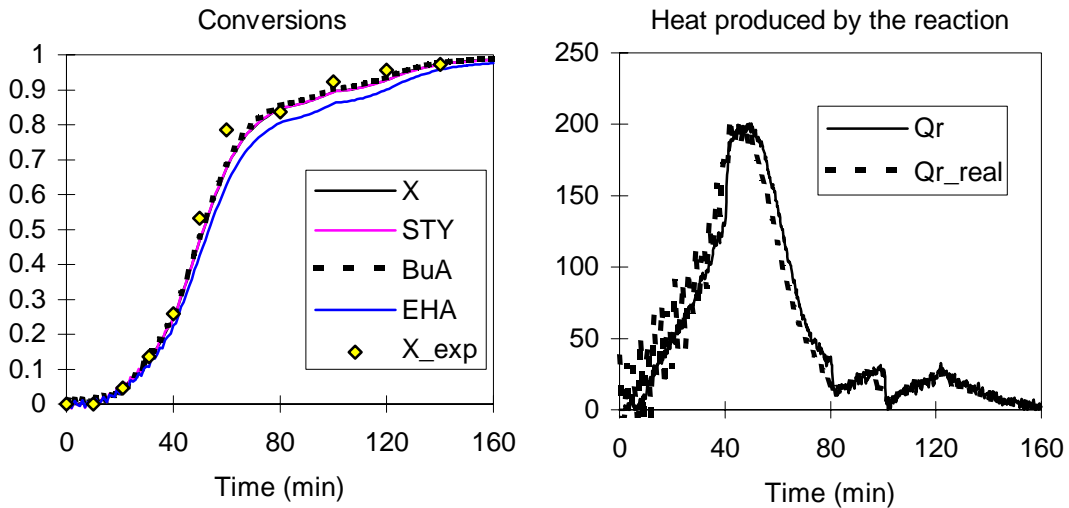
Figure 5.1: STY-BuA-EHA-1 Terpolymerization: Overall and individual conversions at left, and the heat produced by the reaction, at right.

The results of the right hand part of Figure 5.1 show that Q_R and Q_{R_real} are equivalent, which means that assuming that the calorimetric and mass conversions are equal does not noticeably effect the results. Figure 5.2 shows the obtained cumulative composition,

compared to off-line NMR measurements. It can be seen that the composition was correctly estimated by the observer. It is interesting to note that almost no composition drift is observed for this system when we use the initial composition shown in Table 5.1.
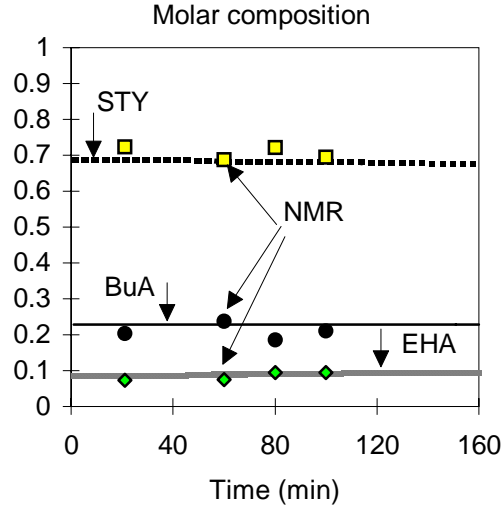
Figure 5.2: STY-BuA-EHA-1 Terpolymerization: Cumulative molar polymer composition, validated by off-line NMR measurements.
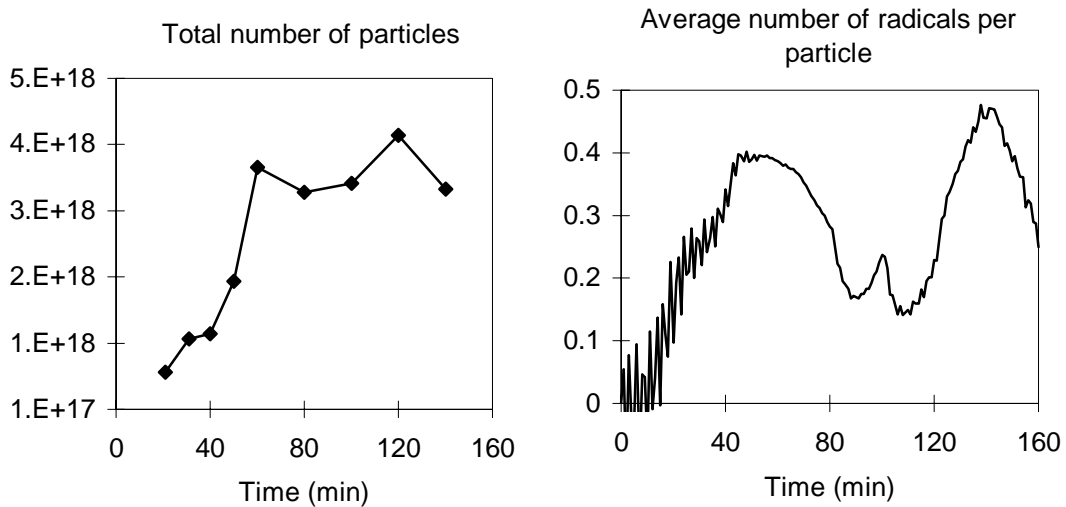
Figure 5.3: STY-BuA-EHA-1 terpolymerization: Total number of particles, at left, and $\bar{n}$ at right.

The estimated value of μ_2 allowed us to estimate $\bar{n}$ off-line, based on the measured number of particles. Figure 5.3 presents the total number of particles in the reactor and the obtained $\bar{n}$. A small variation in $\bar{n}$ was observed during this relatively azeotropic experiment (where the composition remained constant, because of the choice of starting conditions, during the reaction). However, after about 4 minutes, $\bar{n}$ remained relativley constant, and the

peaks seen at the right of Figure 5.3 are likely due to noisy experimental error in the measurement of N_P.

The recipes used for the MMA-BuA-VAc experiments are given by Table 5.2. Two experiments (MMA-BuA-VAc-1 and 2) are carried out in batch and one experiment (MMa-BuA-VAc-3) is carried out in semi-continuous mode.

Table 5.2: Experiments for the validation of the observer of terpolymerization.

\ Experiment Component \	MMA-BuA-VAc-1 charge (g)	MMA-BuA-VAc-2 charge (g)	MMA-BuA-VAc-3	
			initial charge (g)	preemulsion (g)
Vinyl acetate	60	110	110	110
Methyl acrylate	300	290	297	290
Butyl acrylate	300	515	533	533
Sodium dioctyl sulfosuccinate	3	3.07	3.08	3.093
Potassium persulfate	2	2.04	3.2	-
H_2O	2380	1900	2178	500
Final particle size	89 nm	140 nm	120 nm	
Final solids content	21 %	31 %	30 %	
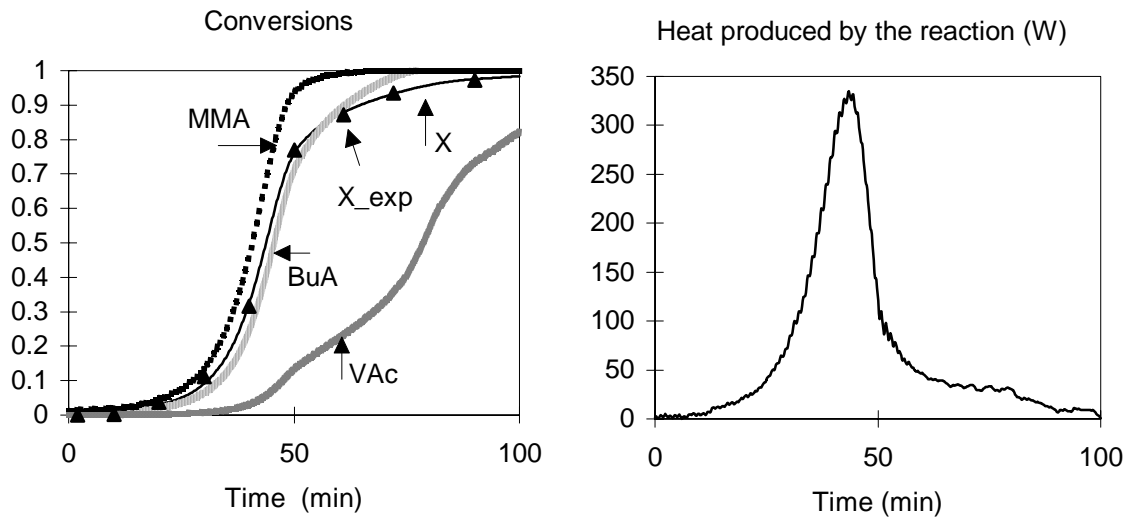
Figure 5.4: MMA-BuA-VAc-1. Overall conversion (X) obtained by calorimetry fitted to the experimental (X_exp) conversion and the estimated individual conversions obtained by the observer, at left. At right, the heat produced by the reaction.

Figure 5.4 shows the overall conversion obtained by calorimetry and the heat produced during the terpolymerization MMA-BuA-VAc-1. The observer was then applied to estimate the individual conversions, the rate of reaction of different monomers and μ_2.
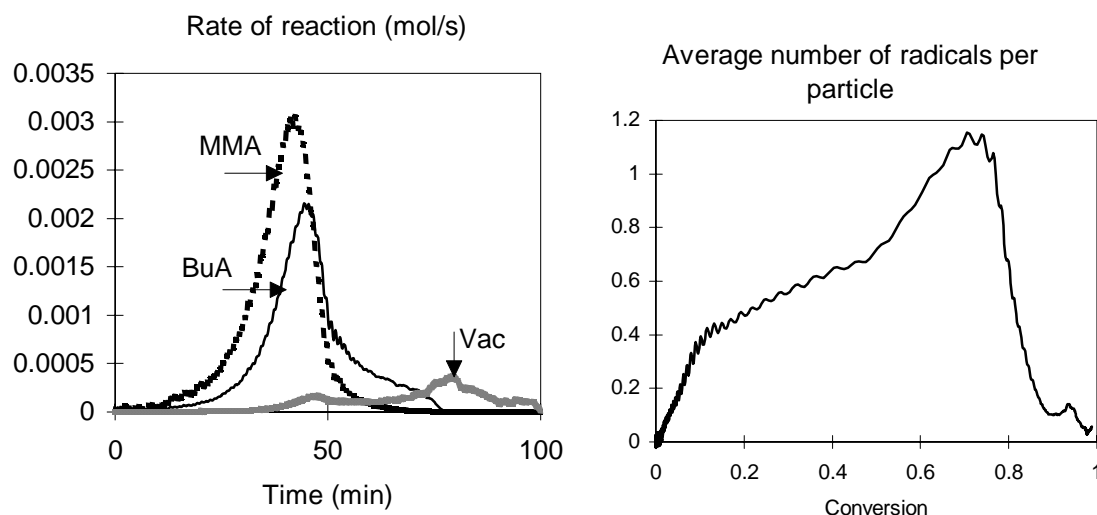
Figure 5.5: MMA-BuA-VAc-1: At left, rate of reaction of each monomer (mol/s). At right, the estimated value of the average number of radicals per particle.

The reaction rates and the average number of radicals per particle are shown in Figure 5.5. IT can be seen that the reaction rate of VAc increases when the amount of BuA and MMA is consumed. This causes an increase in the overall reaction rate and in the average number of radicals per particle.

The instantaneous and cumulative molar compositions are presented in Figure 5.6. The figures clearly show that a composition drift occurred during the experiment. The estimations were validated by NMR measurements, which presented a good agreement with the estimations.
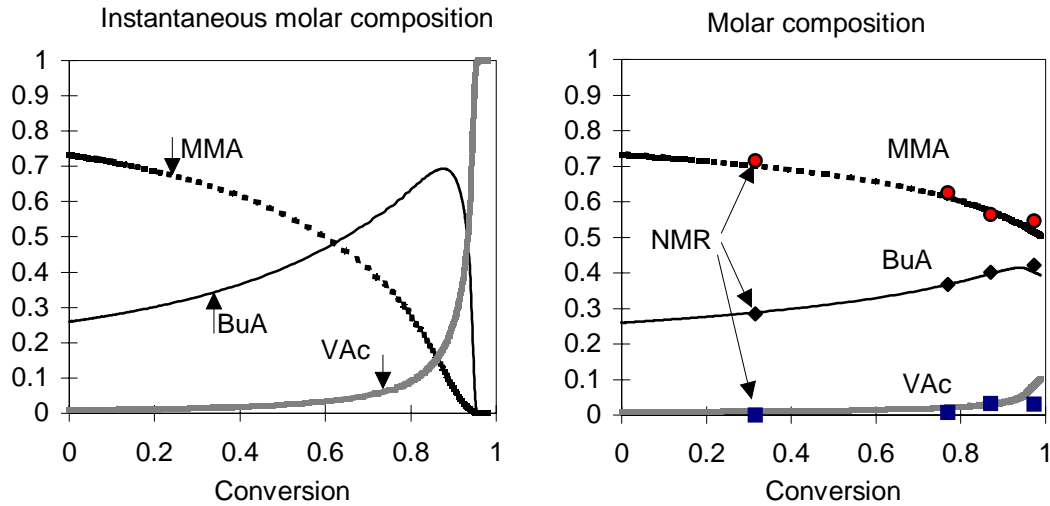
Figure 5.6: MMA-BuA-VAc-1. The cumulative terpolymer composition validated by experimental NMR measurements, at right.

Figure 5.7 shows the results obtained during the experiment MMA-BuA-VAc-2. A clear composition drift was observed during this experiment. The composition was also validated by NMR.
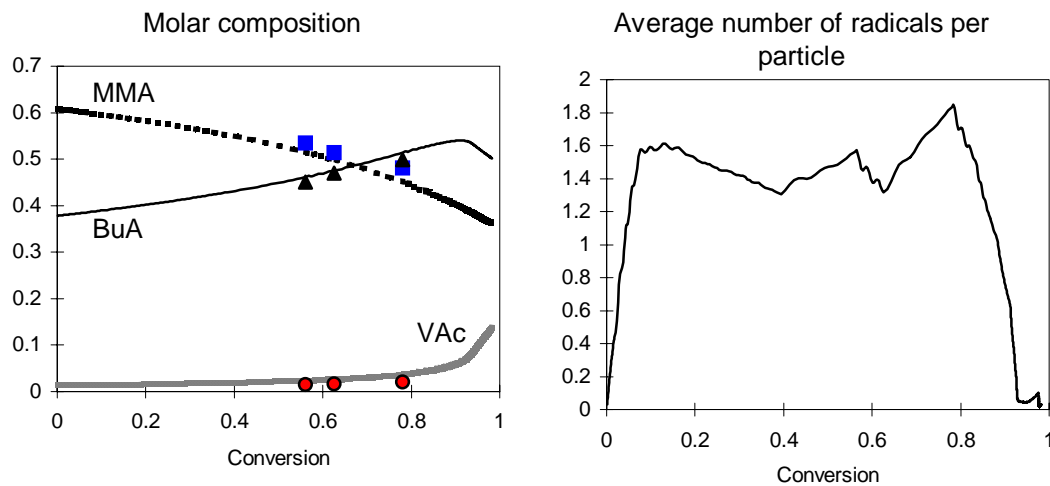
Figure 5.7: MMA-BuA-VAc-2. The cumulative terpolymer composition validated by experimental NMR measurements, at left. At right, the estimated value of the average number of radicals per particle.

The observer was also tested during a semi-continuous terpolymerization (MMA-BuA-VAc-3). The overall conversion obtained by calorimetry is presented on Figure 5.8 at left. To the right of the same figure, the cumulative polymer composition is presented. It can be seen that converting to semi-continuous operation did not eliminate the composition drift. This is because although a high feed flow rate was implemented (4g/min), no attempt was made in this set of experiments to choose the optimal flow rate needed to control the evolution of the composition and to perform the addition in the minimum time.
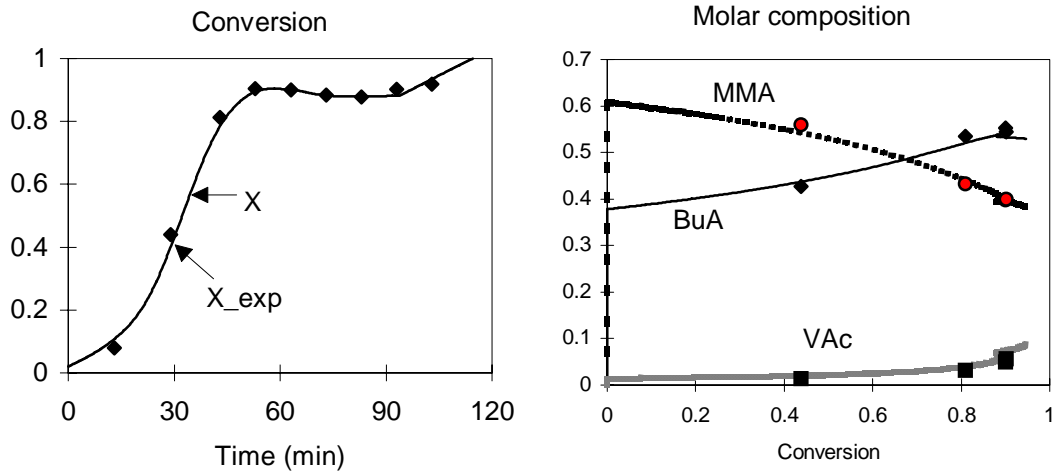
Figure 5.8: Semi-continuous MMA-BuA-VAc-3. The cumulative terpolymer composition validated by experimental NMR measurements.

Finally, the observer was tested in the 250 liter reactor. The recipe used for this application is shown in Table 3.4, in Chapter 3. The monomers used in this experiment are the Butyl acrylate, ethyl hexyl acrylate and vinyl acetate (BuA-EHA-VAc), where EHA is the more reactive monomer. Figure 5.9a shows the overall and individual conversions.
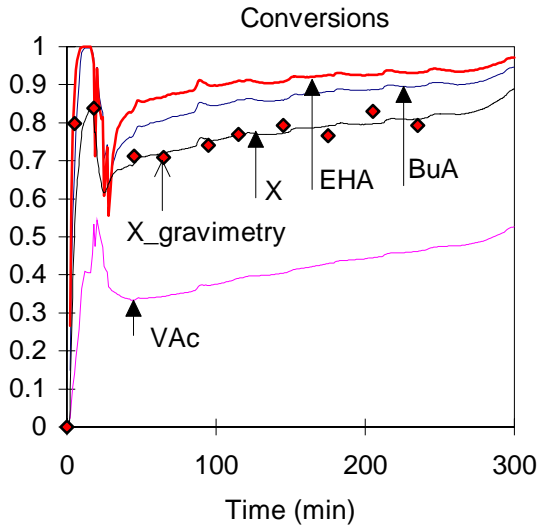
Figure 5.9a: Experiment 18/6/99 in the 250 liter pilot reactor.
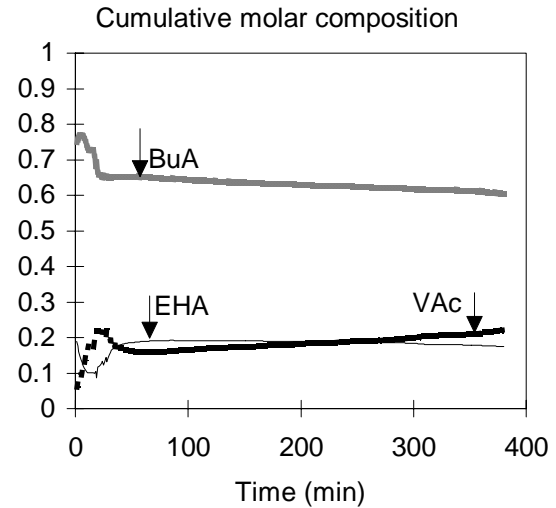
Figure 5.9b: Experiment 18/6/99 in the 250 liter pilot reactor.

Figure 5.9b shows that the cumulative polymer composition changes during the batch preparation of the seed, at the beginning of the reaction. This composition drift is more apparent in Figure 5.9c, representing the instantaneous composition. Unfortunately, no validation of the cumulative composition could be performed. Nevertheless, the estimator returs values coherent with the recipe shown in table 3.4, and the composition was that expected by the people who defined the recipe. It is also important to note that feeding monomers with the composition given in Table 3.4 gives a homogeneous composition during the semi-continuous part of the experiment. However, a large amount of VAc was accumulated in the reactor (see Figure 5.9d for the number of moles of free monomer), which leads to the production of a polymer more rich in VAc at the end of the reaction, as shown in Figure 5.9c. This is due to the fact that the addition flow rate of VAc is higher than the reaction rate of this monomer.

Instantaneous molar composition
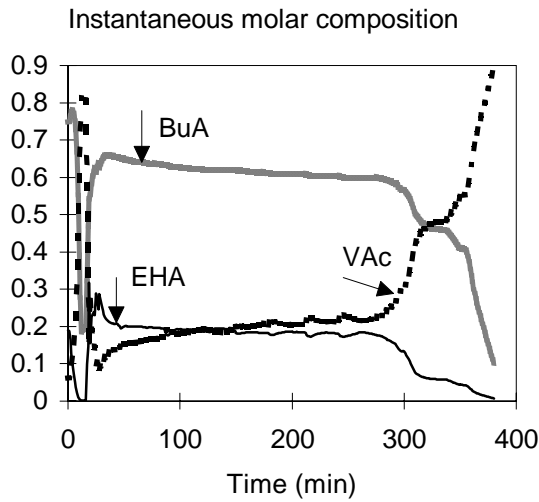
Figure 5.9c: Experiment 18/6/99.

Number of moles of residual monomer
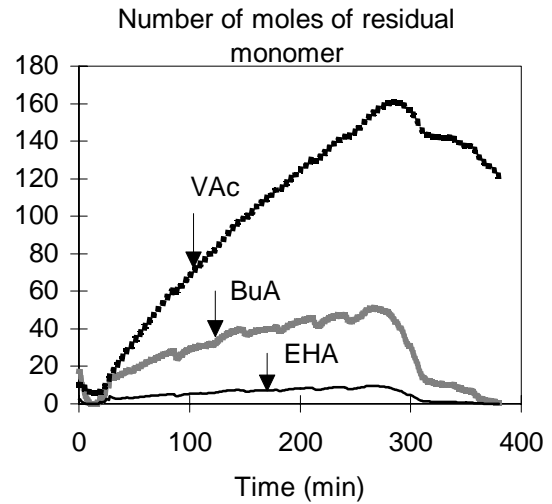
Figure 5.9d: Experiment 18/6/99.

Total number of particles
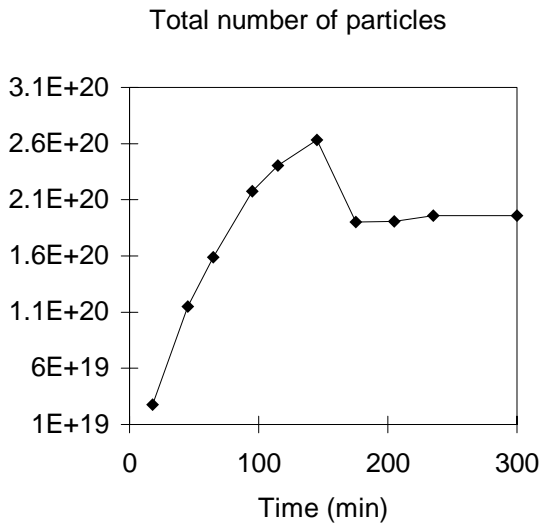
Figure 5.9e: Experiment 18/6/99 in the 250 liter pilot reactor. Off-line measure of N_P^T.

Average number of radicals per particle
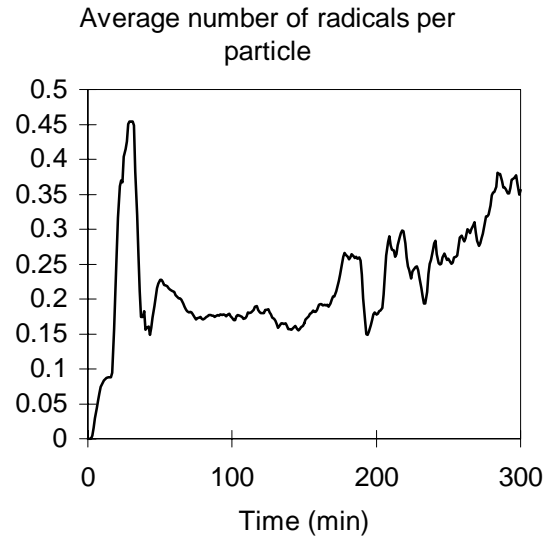
Figure 5.9f: Experiment 18/6/99 in the 250 liter pilot reactor. Off-line estimate of $\bar{n}$.

Finally, the particle size and number were determined off-line. The estimated value of $\bar{n}$ based on the on-line estimated μ and the off-line measured number of particles is given in Figure 5.9f. It can be seen that during the nucleation period, the estimation of $\bar{n}$ oscillates, which is once again probably due to the difficulty in accurately estimating the highly varying overall conversion during this period.

Table 5.3 presents the recipe used for a second experiment in the 250 liter pilot reactor. The monomer composition is 55% BuA, 36% Styrene, 18% MMA, and 2% acrylic acid, by mass.

199

Table 5.3: Experiments of terpolymerization in the 250 liter pilot reactor. Validation of the observer.

\ Experiment	Experiment 263 (April/2000)		
Composition (mass)	55 - 36.2 - 18 - 2 % BuA-STY-MMA-AA		
Temperature	80 °C		
Component \	Initial charge (g)	preemulsion (g)	Initiator solution(g)
H_2O	54549	27860	4860
BuA	2113	39800	-
STY	1761	33170	-
MMA	880	16580	-
AA	105	1990	-
Surfactant	710	5480	-
Initiator	30+660g water	-	260
Final solids contents	46 %		
Final particle size	102 nm		
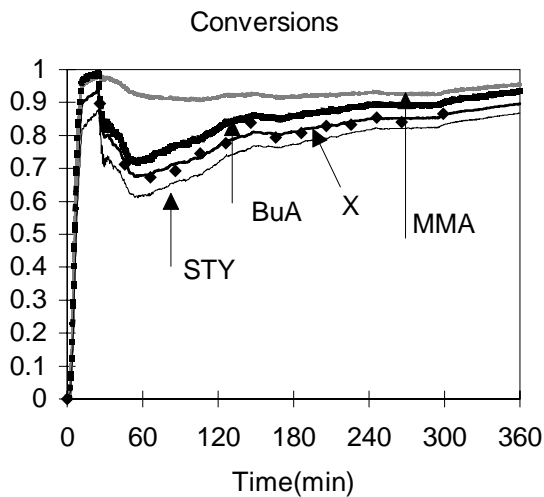
Figure 5.10a: Overall and individual conversions. Experiment 263.
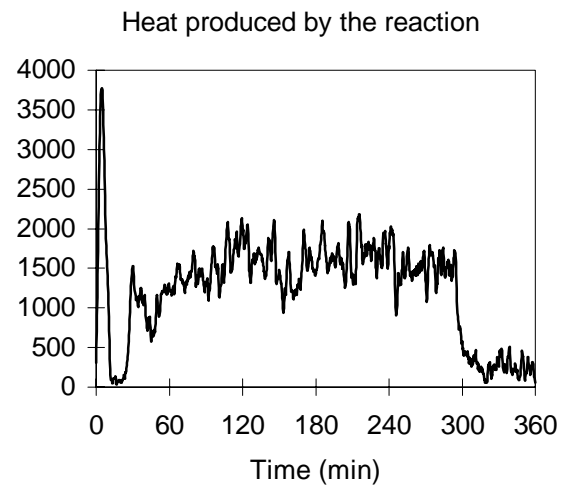
Figure 5.10b: $Q_R(W)$. Experiment 263.

200
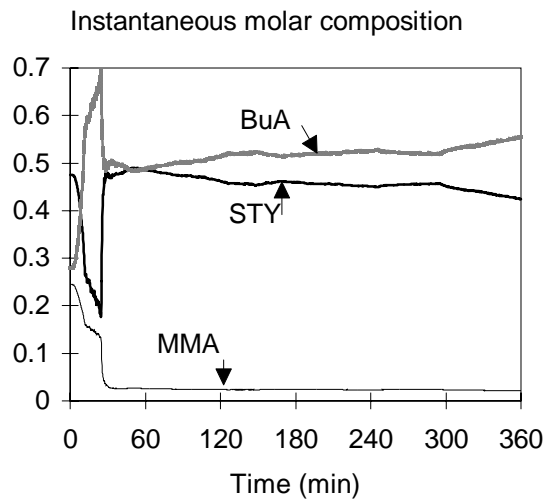
Figure 5.10c: Instantaneous composition. Experiment 263.
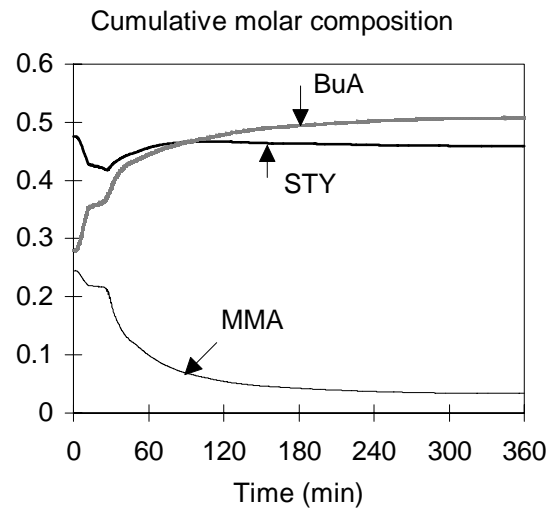
Figure 5.10d: Cumulative composition. Experiment 263.
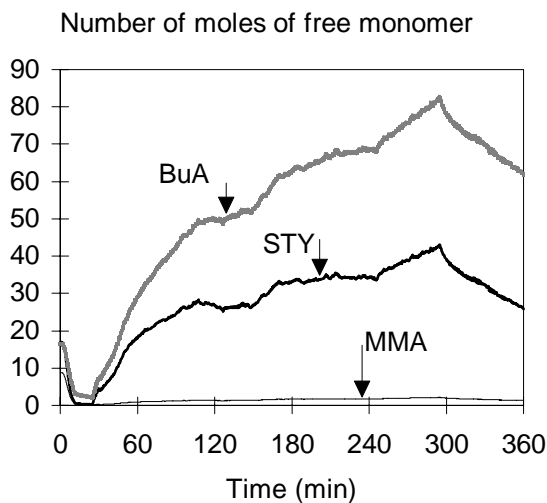
Figure 5.10e: Experiment 263 in the 250 liter pilot reactor.
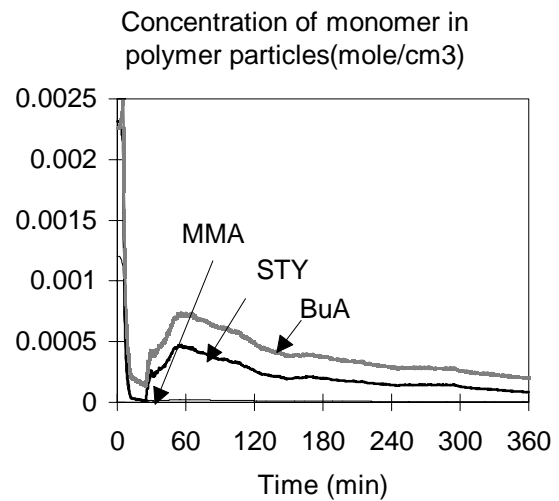
Figure 5.10f: Experiment 263

Figures 5.10b shows the heat produced during the reaction. It can be seen that a peak of heat was produced during the rapid nucleation part of the experiment. During the semi-continuous part, Q_R was almost constant. Therefore, the overall conversion, Figure 5.10a, was almost constant during the semi-continuous part. The addition flow rate was predefine à priori in order to ensure the production of a homogeneous polymer during the semi-continuous part. Figure 5.10c shows that the instantaneous composition is almost constant during the semi-continuous part. However, the composition drift produced at the beginning of the reaction affects the cumulative composition until the end of the reaction. Moreover, it can be seen the

201

ratio of BuA in the reactor is increasing as the reaction progresses. This accumulation of monomer will introduce another composition drift at the beginning of the reaction, when all the amounts of STY and MMA are consumed. Unfortunately, this cannot be seen on the composition curve, since the reaction was stopped before the end.
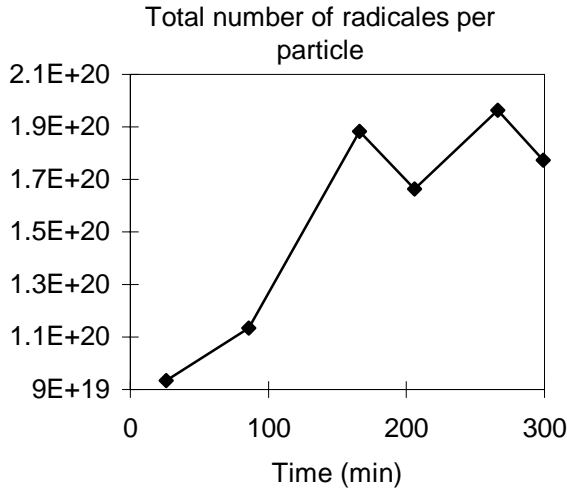
Figure 5.10g: N_P^T. Experiment 263.
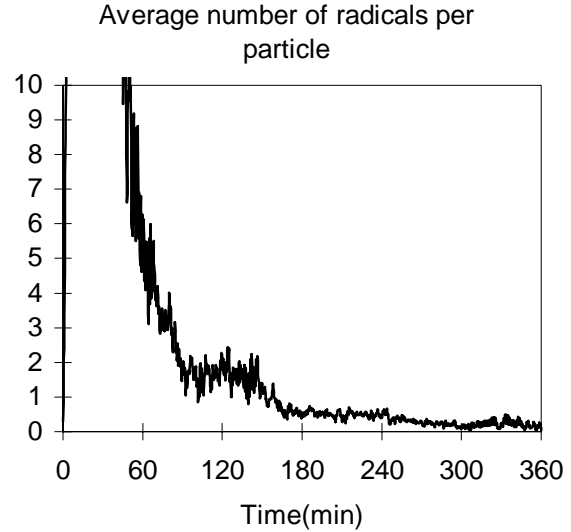
Figure 5.10h: $\bar{n}$.

The particle size was measured off-line to calculate the total number of particles, Figure 5.10g. It can be seen that N_P^T increases with time, which means that the particles nucleation continued during the reaction. The estimated value of μ was then used to estimate $\bar{n}$, Figure 5.10h. A high value was obtained at the beginning of the reaction. During the semi-continuous part, the value of $\bar{n}$ was inferior to 1. No increase of $\bar{n}$ was noticed at the end of the reaction, which is probably due to the accumulated amount of BuA, and that the oligomers of BuA enhances the radical desorption. Moreover, no gel effect is supposed to take place during the reaction since the glass transition temperature of the polymer produced is superior to the reaction temperature.

5.5 Conclusion

The estimation strategy developed in this chapter is based on the calorimetric adaptive observer constructed in Chapter 3, and on the material balance of terpolymers. The implementation of the observer requires temperature measurements in the reactor and in the jacket, some off-line gravimetric measurements of the monomer conversion and the knowledge of the monomers reactivities.

The observer estimates accurately the evolution of the terpolymer composition and the number of radicals in the polymer particles. The estimator is adapted for water insoluble, or moderately water soluble monomers. Good estimates were obtained on a laboratory scale and pilot scale reactors.

The combined use of calorimetry and mathematical modeling is therefore an efficient technique for the on-line monitoring of several parameters in the polymerization process. The polymer composition control can now directly be applied based on these estimates.

In the next chapter, we develop a control strategy that maintains the composition at a predefined value, in co- and terpolymerization systems. The control strategy will be based on the different observers developed in the first part of this thesis: the adaptive calorimetric observer that gives an on-line estimation of the conversion (chapter 3), the observer of the individual conversions in copolymerization systems (in chapter 2), and the observer developed in this chapter for the composition monitoring in terpolymerization processes.

5.6 Nomenclature

Notation

F_i	instantaneous molar fraction of homopolymer i in the polymer.
MW_i	molecular weight of monomer i (g/mol)
$L_f h$	Lie derivative (see chapter 2)
N_i	number of moles of residual monomer (mol)
P_i^j	time averaged probability that the ultimate unit of an active chain in the phase j is of type i
Q_i	molar flow rate of monomer is (mol/s)
R_{pi}	rate of reaction of monomer i (mol/s)
T	transformation of co-ordinates
y	output

Greek letters

μ	number of moles of radicals in the polymer particles.
ρ_i	density of monomer i (g/cm^3)
$\rho_{i,h}$	density of polymer i (g/cm^3)
θ, θ_2	observer tuning parameters

5.7 Bibliography

1.   Beauchemin, R.-C., and M. A. Dubé, bulk terpolymer composition prediction from copolymer reactivity ratios, *polym. react. Eng.*, **7**, 4, 485-499, (1999).

2.   Dubé, M. A., and A.Penlidis, Hierarchical data analysis of a replicate experiment in emulsion terpolymerization, *AIChE J.*, **42**, 7, 1985-1994, (1996)

3.   Dubé, M. A., and A. Penlidis, Emulsion terpolymerization of butyl acrylate/methyl methacrylate/vinyl acetate: experimental results, *J. Polym. Sci A: Polym. Chem.*, **35**, 1659-1672, (1997).

4.   Dubé, M. A., A. Penlidis, and P. M. Reilly, A systematic approach to the study of multicomponent polymerization kinetics: the butyl acrylate/methyl methacrylate/vinyl acetate example. IV Optimal Bayesian design of emulsion terpolymerization experiments in a pilot plant reactor, *J. of Polym. Sci.: Part A: Polymer Chem.*, **34**, 811-831,(1996).

5.   Dubé, M. A., J. B. P. Soares, A. Penlidis, and A. E. Hamielec, Mathematical modeling of multicomponent chain-growth polymerization in batch, semibatch, and continuous reactors: A review, *Ind. Eng. Chem. Res.*, **36**, 4, 966-1015, (1997).

6.   Rios, L., C. Pichot, and J. Guillot, terpolymèrisation acrylonitrile-styrène-acrylate de méthyle, 1 Etude cinétique de la terpolymérisation en émulsion en réacteur fermé, *Makromol. Chem.*, **181**, 677-700, (1980).

7.   Schoonbrood, H. A.S., R. C; P. M. van Eijnatten, B. Van den Reijen, A. M. Van Herk, and A. L. German, Emulsion co- and terpolymerization of styrene, methyl methacrylate, and methyl acrylate. I. Experimental determination and model prediction of composition drift and microstructure in batch reactions, *J. of Polym. Sci.: Part A: Polymer Chem.*, **34**, 935-947,(1996)[a].

8.   Schoonbrood, H. A. S., R. C; P. M. van Eijnatten, and A. L. German, Emulsion co- and terpolymerization of styrene, methyl methacrylate, and methyl acrylate. II. Control of emulsion terpolymer microstructure with optimal addition profiles, *J. of Polym. Sci.: Part A: Polymer Chem.*, **34**, 949-955,(1996)[b].

9.   Storti, G., S. Carra, M. Morbidelli, and G. Vita, Kinetics of multimonomer emulsion polymerization. The pseudo-homopolymerization approach, *J. of Appl. Polymer Sci.*, **37**, 2443-2467, (1989).

10.   Urretabizkaia, A., G. Arzamendi, and J. M. Asua, Modeling semicontinuous emulsion terpolymerization, *Chem. Eng. Sci.*, **47**, 9, 2579-2584, (1992).

11.   Urretabizkaia, A., and J. M. Asua, High solids content emulsion terpolymerization of vinyl acetate, methyl methacrylate, and butyl acrylate. I. Kinetics, , *J. of Polymer Sci.: Part A: Polymer Chem.*, **32**, 1761-1778, (1994)[a].

12.   Urretabizkaia, A., G. Arzamendi, M. J. Unzué, and J. M. Asua, High solids content emulsion terpolymerization of vinyl acetate, methyl methacrylate, and butyl acrylate. II. Open loop composition control, *J. of Polymer Sci.: Part A: Polymer Chem.*, **32**, 1779-1788, (1994)[b].

13.   Urretabizkaia, A., J. Leiza, and J. M. Asua, On-line terpolymer composition control in semicontinuous emulsion polymerization, *AIChE J.*, **40**, 11, 1850-1864, (1994)[a].

CHAPTER VI ———————————

COMPOSITION CONTROL

6. COMPOSITION CONTROL

6.1 Introduction

In several applications of polymeric materials made of more than one monomer, the ideal objective would be to employ polymers with a well-defined composition. However, the preparation of these polymers usually involves monomers that do not have the same reactivities. This results in a composition drift during the polymerization, and therefore a heterogeneous polymer if no action is made to control the reaction rate of monomers.

The instantaneous polymer composition, or the molar fraction of monomer i being added to the polymer (F_i), is related to the reaction rates by the following equation, where n is the total number of monomers involved in the reaction:

$$F_i = \frac{R_{Pi}}{\sum_{j=1}^{n} R_{Pj}} \tag{6.1}$$

The ideal objective to control the composition would therefore be to maintain the instantaneous composition, defined in equation 6.1, at a predefined trajectory during the reaction. Typically, this would be at a constant set-point, but one could also envisage a profile of composition that evolves during the reaction. In the rest of this chapter we will only treat the constant composition.

The control variables. In the case of copolymerization processes, equation (6.1) yields:

$$F_1 = \frac{r_1 f_1^2 + f_1 f_2}{r_1 f_1^2 + 2 f_1 f_2 + r_2 f_2^2} \tag{6.2}$$

where f_i is the mole fraction of monomer i in the unreacted monomer mixture and the reactivity ratios are defined in terms of the propagation rate constants as follows:

$$r_i = \frac{K_{Pii}}{K_{Pij}} \tag{6.3}$$

where K_{pij} (L/mol/s) is the rate constant for the reaction of a growing polymer chain (i.e. a radical) of type i with a monomer with type j. K_{Pij} is temperature dependent according to the Arrhenius equation:

$$K_{Pij} = A_{ij}e^{\left(\frac{-Ea_{ij}}{RT}\right)} \tag{6.4}$$

where the temperature T is expressed in K, Ea_{ij} the activation energy in kJ/mol, A_{ij} a frequency factor (L/mol/s), and R is the universal gas constant (kJ/mol/K).

Equation 6.2 clearly shows that the composition is determined by the monomer reactivities (r_1 and r_2) and the ratio of monomers in the reactor (f_1). If the monomers have different reactivities, the polymer composition will firstly be dominated by the most reactive monomer, in a closed reactor, and then will change as the different components are depleted, thus causing f_1 to vary as the reaction progresses. It is important to mention that certain pairs of monomers possess an azeotropic monomer composition that yields the production of a constant composition throughout a batch reaction (if r_1 and r_2 are both inferior or superior than one). This composition can be calculated from the following relationship, depending on the reactivity ratios of the monomers:

$$f_1 = \frac{1 - r_2}{2 - r_1 - r_2} \tag{6.5}$$

Since the two determining variables in the evolution of the copolymer composition, as shown by equation 6.2, are the monomer composition (f_1) and the monomer reactivities (r_i), we can take advantage of these variables to control the copolymer composition. The first parameter f_i can be manipulated during the reaction by converting to a semi-continuous operation. One can also try to modify the monomer reactivities by manipulating the reaction temperature since they are temperature dependent, equation 6.4. As a result, the control variables are the monomer flow rates and the reaction temperature.

How to control the composition by manipulating the reaction temperature? The first method consists of imposing a constant reaction temperature that gives values of r_1 and r_2 that yields the desired composition through the reaction (for systems with azeotrop). However, this approach is not very flexible since only small changes in the azeotropic composition are produced over a large temperature range, as reported by Tirrell and Gromley (1980). Moreover, this technique is restricted to pairs of monomers that possess an azeotropic composition at a given temperature. Figure 6.1, shows the azeotropic composition obtained from the temperature variation for the styrene/acrylonitrile system. It can be seen from this figure that a large variation in the reaction temperature gives only a small change in the polymer composition. Furthermore, a such important change in the reaction temperature significantly alters the reaction rate and molecular weight, which might seriously affect the final polymer properties.
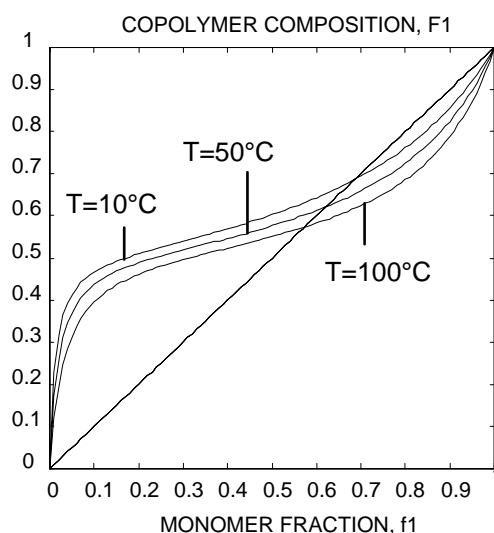
Figure 6.1: The azeotropic composition dependence on the temperature. F_1 =0.572, 0.616 , 0.686 for T=10°C, 50°C and 100°C respectively.

A second approach to controlling the polymer composition, by manipulating the temperature, consists of employing a temperature trajectory. The technique is based on the dependence of the reactivity ratios on the temperature and that for certain monomers (with specific activation energies, reactivity ratios) there exists a temperature trajectory for the composition control. Tirrell and Gromley (1980) explored this possibility for real copolymerization reactors with free radical initiation. They performed an open-loop control of the composition of the styrene-acrylonitrile system. The authors mentioned that even if this

technique may yield good results in terms of composition control, the temperature change during the reaction must have an influence on the molecular weight and the sequence distribution. This technique was also used by Kravaris et al. (1989) in the simulation of composition control of a free-radical copolymerization system. In this case, a nonlinear feedforward-feedback control was applied, based on the energy balance.

Temperature control to track the composition can be applied to the production of small amounts of polymer in small batch reactors, where agitation is not an issue. It might be useful in viscous systems where converting to semi-continuous operations is difficult. The disadvantages of this approach are that it is limited to pairs of monomers with very different activation energies and on a limited range of composition. Moreover, implementing the sensitive temperature control on industrial reactors is more complex. Finally, the increase in the reaction temperature might cause the evaporation of the solvent used, and an increase in the conversion per unit volume which influences the molecular weight distribution.

Monomer addition policies. Manipulating the instantaneous monomer concentration can directly be obtained by controlling the feed flow rates of monomers. Therefore, the monomer flow rates have a direct influence on the evolution of the polymer composition and seem to be an efficient control method. Moreover, converting to semi-continuous operation, if done correctly, does not in general have a negative impact on the reaction rate. Semi-continuous emulsion polymerization processes are frequently used for the preparation of high performance polymer lattices. In theory, semi-continuous operations offer flexible means of controlling particle morphology and the chemical composition of the polymer.

Several addition techniques have been reported in the literature (Hamielec et al. (1987), Arzamendi and Asua (1989), and Canu et al. (1994)). Two addition policies can be distinguished in terms of their influence on the evolution of the polymer composition:

❶ the first policy consists of slowly adding a mixture of monomers at the desired composition,

❷ the second policy consists of adding the monomers separately, at certain flow rates.

The first policy, that consists of adding a **mixture of monomers** at the desired composition, is the most widely used one. Two situations can be distinguished regarding the flow rate of the added mixture: first, the addition under starved conditions (polymer particles are not saturated with monomer), and second addition under flooded conditions (excess of monomer). In the first case, the addition of a mixture of monomers guarantees the production of a constant composition during the reaction if the flow rate (usually constant) is chosen in a way to maintain extremely starved conditions. However, this may lead to long process times if not properly optimized. In the second situation, adding a mixture of monomers under flooded conditions allows us to maximize the reaction rate, but might yield to an accumulation of the less reactive monomer, and therefore to a composition drift, not to mention creating conditions that favor secondary nucleation.

The second addition policy consists of adding the monomers **separately**. In this way, monomer accumulation in the reactor can be avoided and we have a greater flexibility in manipulating the individual reaction rates. As we have mentioned above, the objective of the monomer feed is to maintain the monomer ratios in the reactor at a predefined value. In emulsion copolymerization, if monomer 1 is the more reactive, the feed rate of the this monomer must be used to control the monomer ratio during the reaction. Monomer 2 can be completely charged at the beginning of the reaction or can be added at a known flow rate. The feed rate of monomer 1 is added in a manner to maintain f_1/f_2 at the desired value. This means that a variable feed rate of monomer 1 must be determined as a function of the residual amounts of monomers, which means that these quantities must be measured, or estimated, on-line.

Several authors studied the different addition policies in simulation, in order to chose the optimal addition that gives the desired composition in a reasonable process time. For instance, Arzamendi and Asua (1989) simulated the seeded copolymerization process, where the models of Morton and Vanzo were used to determine the monomer partitioning between the different phases. The authors showed that the variable addition rate policy of the more reactive monomer was the favorite policy that ensures the production of a copolymer of constant composition. Starved conditions give also a constant composition but prolong the process time. These results were experimentally validated by Arzamendi and Asua (1990),

and therefore in the more recent works the variable addition policy was usually used to control the polymer composition.

In our work we will be interested in the second technique, which consists of adding the monomers separately since the addition of a mixture under highly starved conditions increases the process time.

How to calculate a variable flow rate of monomer? The calculation of the flow rate of monomer 1 depends on the ratio of the residual monomers, which must therefore be measured or estimated on-line. In the literature, the flow rate of monomers was calculated either by an open-loop strategy (based on the model, no on-line measurements are implemented), or in a closed loop fashion based on the direct on-line measurement of the polymer composition or on the measurement of the conversion (and in this case the conversion is combined with the material balance of monomers that involves the reactivities of monomers).

As we mentioned earlier, the control strategy cannot be based only on the simulation of the **open-loop** polymerization model, since this model contains a lot of unknown and time varying parameters, and under real industrial conditions it will not take a long time before the model predictions deviate from the real process. Saldivar and Ray (1997) developed open-loop strategies for the subsequent control of copolymer composition and the molecular weight distribution in semi-continuous unseeded emulsion polymerizations. Choi (1989) presented an open-loop analytical solutions for the feed rate profiles required to obtain homogeneous copolymers in bulk and solution copolymerizations. Buruaga et al. (1997[a,b,c]) used calorimetric measurements of the heat of the reaction to calculate the feed flow rate of the more reactive monomer to be fed to the reactor to control the copolymer composition.

On the other hand, **closed loop** techniques provide a continuous on-line correction of the model, and therefore offer the possibility of accurately estimating and controlling the process. If the polymer composition is directly measured on-line (e.g. by mass spectroscopy NMR, or GC), the use of this information in the control strategy will allow us to correct possible errors in the model, and especially in the monomer reactivity ratios. Canu et al. (1994) proposed to calculate a priori the desired flow rate of the most reactive monomer as a

function of the conversion, which necessitates the on-line measurement of the overall conversion. This approach was experimentally applied by Canegallo et al. (1994). The conversion, in this case, was obtained on-line using a densimeter. Monomer addition was carried out at relatively large flow rates, discretized into very short addition time intervals with constant amplitudes (bang-bang control). The closed loop correction is in this case model dependent, since the flow rates are calculated based on the reactivity ratios of monomers. These ratios have however been frequently reported in the literature and are precisely known for several monomers (Hand book, Gilbert (1995), van Herk (1997)).

Guyot et al. (1984) developed a closed-loop composition control strategy for the emulsion copolymerization of butadiene-acrylonitrile based on the on-line gas chromatography (GC) measurements where a dilution system was added. The GC gives a measure of the residual monomer concentrations. The separate monomer flow rates were then calculated in order to keep the monomer concentrations at a constant level. A gas chromatographic technique was also used by Doremaele et al. (1992) and Schoonbrood et al. (1996[b]) for the monitoring of the overall monomer ratio. The optimal addition profile was calculated by iterative procedure involving reactivity ratios, monomer partitioning and a series of strategic experiments without a need to estimate $\bar{n}$ on-line. Leiza et al (1992) developed a nonlinear adaptive proportional integral (NLAPI) composition controller based on the gas chromatography measurements. A Kalman filter was used to give state estimation of the monomer concentrations in the polymer particles and the total number of radicals in polymer particles.

Arzamendi and Asua (1990) applied the technique that they developed in Arzamendi and Asua (1989) to the vinyl acetate-methacrylate system. They developed a semi-empirical relation that correlates $\bar{n}$ with the volume fraction of polymer in the latex particles, which involves doing a series of semi-continuous emulsion copolymerizations. The monomer flow rate was then calculated from the model by fitting the unknown parameters related to $\bar{n}$.

As a result from the literature review presented above, and in previous chapters, we can draw the following conclusions:

- The key parameter for composition control is the monomer feed rates, while the temperature is much less useful as a manipulated variable.
- The addition of the more reactive monomer allows us to work under semi-flooded conditions while the addition of a mixture of two monomers require that we work under extremely starved conditions to produce a homogeneous polymer, which requires a long reaction time.
- Control strategies that involve the material balance depend on the reactivity ratios and on the reaction rate constants, are considered to be closed loop strategies. These parameters are well known in the literature for a certain number of monomers. On the other hand, open-loop control strategies that depend on unknown parameters, such as those related to the evolution of $\bar{n}$ might be irreproducible.
- In most of the cases of closed-loop composition control cited in the literature, the control strategies, ex. PID, do not take into account the nonlinearity of the mathematical model of the process.

In this chapter, we will use the observers developed in the previous chapters using calorimetry, in order to control the composition in co- and terpolymerization processes.

In the first section of this chapter, we study the composition control in emulsion copolymerization process. In order to experimentally apply the controller, a second local controller of the pump was required to ensure that desired mass (calculated by the composition controller) is really fed to the reactor. A linear controller will be used to achieve this objective since the relation between the voltage of the pump and the flow rate is usually linear. In the second part of this chapter, we will study the control of terpolymerization systems. This requires us to add a second pump to the installation and therefore to add another local controller of the second pump. Both controllers are experimentally validated.

6.2 Copolymer composition control

6.2.1 Control law

The strategy we present below is based on the on-line calorimetric measurements of the overall mass conversion. The instantaneous copolymer composition is estimated by the nonlinear observer developed in chapter 4. Since we found that for several monomers the reaction in the aqueous phase does not significantly contribute to the evolution of the polymer composition, we will use the observer developed for hydrophobic monomers.

The overall polymer composition is determined by the instantaneous polymer composition produced per unity of time. The ideal way to control the copolymer composition is to control the instantaneous composition, i.e. to maintain F_i at some desired value F_i^d. In a copolymerization process, the molar fraction of homopolymer i in the copolymer is given by the following equation:

$$F_i = \frac{R_{Pi}}{R_{P1} + R_{P2}}$$

(6.6)

The composition is well controlled if the ratio F_1/F_2 remains at the desired value during the reaction. This ratio is given by:

$$\frac{F_1}{F_2} = \frac{R_{P1}}{R_{P2}}$$

(6.7)

In this work, we will be interested in the production of a constant composition during the reaction. Therefore, the objective of our control strategy will be to maintain the molar ratio of polymers at a desired constant value. Considering the model of hydrophobic monomers, (the reaction in the aqueous phase does not influence the evolution of the composition):

$$\dot{N}_i = Q_i - R_{Pi}$$

(6.8)

$$= Q_i - \mu\left([M_i^p]\left(K_{P1i}P_1^p + K_{P2i}\left(1 - P_1^p\right)\right)\right)$$

and assuming that the monomers are not water soluble (the solubility of monomers does not significantly influence the monomer ratio in the organic phase), and that they have the same solubility in both portions of the organic phase, droplets and particles, (Poehlein (1995)), the composition ratio becomes:

$$\frac{F_1}{F_2} = \frac{N_1\left(K_{P11}\dfrac{N_1}{N_2} + K_{P12}\right)}{N_2\left(K_{P12}\dfrac{N_1}{N_2} + K_{P12}\dfrac{K_{P22}}{K_{P21}}\right)} \tag{6.9}$$

This equation shows clearly that it is sufficient to control the ratio of monomers N_1/N_2 in order to maintain the instantaneous composition at a constant set-point (if K_{pij} are well known). If we assume that monomer 1 is more reactive than monomer 2, the ratio N_1/N_2 decreases as a function of time. Hence, the number of moles of monomer 1 must be manipulated to control the ratio N_1/N_2. The ratio N_1/N_2 can be calculated from the following equation:

$$\frac{N_1}{N_2} = \frac{K_{P12}}{2K_{P11}}\left(\frac{F_1}{F_2} - 1\right) + \frac{1}{2K_{P11}}\sqrt{K_{P12}^2\left(1 - \frac{F_1}{F_2}\right)^2 + 4K_{P11}K_{P12}\frac{K_{P22}}{K_{P21}}\frac{F_1}{F_2}} \tag{6.10}$$

If we fix the desired composition and therefore $(F_1/F_2)^d$, we can directly calculate the desired monomer ratio $(N_1/N_2)^d$ from equation 6.10. The controller objective now becomes to control the monomer ratio in the reactor. As we mentioned above, Q_2 can be set to be constant, but its value must be known at every moment in order to be able to calculate N_1/N_2. If we suppose that N_1, N_2 and μ are obtained from the observer, we can write the mass balance of copolymerization assuming the output $y = N_1$ that will be used in the controller:

$$\dot{x} = \begin{bmatrix} \dot{N}_1 \\ \dot{N}_2 \end{bmatrix} = \underbrace{\begin{bmatrix} -R_{P1} \\ Q_2 - R_{P2} \end{bmatrix}}_{f(x)} + \underbrace{\begin{bmatrix} 1 \\ 0 \end{bmatrix}}_{g(x)}\underbrace{Q_1}_{u} \tag{6.11}$$

$$y = \underbrace{N_1}_{h(x)}$$

The system given by 6.11 is a nonlinear single input single output system with the states x, u is the manipulated input and y the model output. Q_2 is not considered as a manipulated

variable, but assumed to be a known input. In order to test the controllability of the system and whether or not u can be used to control N_1, we first calculate the relative order. For r=1, we calculate $< dh, ad_f^{r-1}(g) >$ as defined in chapter 2:

$$L_f h = \frac{\partial h}{\partial x} f \qquad (6.12)$$

$$= \begin{bmatrix} 1 & 0 \end{bmatrix} \begin{bmatrix} -R_{P1} \\ Q_2 - R_{P2} \end{bmatrix}$$

$$= -R_{P1} \neq 0$$

The relative order of the system r is equal to one and we can therefore calculate a nonlinear input/output linearizing controller. In order to do so, we define the following state feedback transformation (Kravaris et al. (1989)):

$$\upsilon = \Omega(x,u) = \sum_{k=0}^{1} \beta_k L_f^k h + (-1)^0 \beta_1 < dh, ad_f^0(g) > u \qquad (6.13)$$

$$= \beta_0 h + \beta_1 \frac{\partial h}{\partial x} f + \beta_1 \frac{\partial h}{\partial x} g$$

$$= \beta_0 N_1 + \beta_1 (-R_{P1}) + \beta_1 u$$

and we can therefore calculate the input u:

$$u = \frac{\upsilon - \beta_0 N_1 + \beta_1 R_{P1}}{\beta_1} \qquad (6.14)$$

$$= \frac{\upsilon}{\beta_1} - \frac{\beta_0}{\beta_1} N_1 + R_{P1}$$

where u is in mol/s. The external input υ can be used to add a linear PI loop, as follows:

$$\upsilon - \beta_0 N_1 = \kappa_P \underbrace{(y^d - y)}_{\varepsilon} + \frac{1}{\tau_I} \int_0^{t_f} (y^d - y) dt \qquad (6.15)$$

which means that if $\beta_0 = \kappa_P$, then υ can directly be replaced by the set-point.

Hence, the complete control variable becomes:

$$u = Q_1 = \frac{1}{\beta_1} \left(\kappa_P \varepsilon + \frac{1}{\tau_I} \int_0^{t_f} \varepsilon \, dt \right) + R_{P1} \qquad (6.16)$$

The parameters β_0 and β_1, must be chosen in a way that ensures the stability of the states of the model.

In equation 6.16, we can take $\beta_1=1$ without any loss of generality. In the case where υ is taken to be a PI linear controller, the stability of the system is governed by κ_P and τ_I. Note that the other states of the model (N_2) are stable for all values of Q_1. N_2 decreases if all of monomer 2 is added to the reactor at t=0, or it can depend on Q_2, where Q_2 must be set at some reasonable rate (see next chapter). The PI gains must be chosen in a way that guarantees stable and rapid convergence to the desired composition. We will study the influence of the values of these gains experimentally. Equation 6.16 is therefore reduced to:

$$Q_1 = \underbrace{\kappa_P\left(N_2\left(N_1 / N_2\right)^d - N_1\right)}_{P} + \underbrace{\frac{1}{\tau_I}\int_0^t\left(N_2\left(N_1 / N_2\right)^d - N_1\right)}_{I} + R_{P1} \qquad (6.17)$$

Equation 6.17 shows that the nonlinear controller accounts for the model nonlinearity. This means that while the reaction is proceeding, if the value of N_1 is at the desired point (therefore $\varepsilon=0$), then the flow rate of monomer 1 is not zero, but equal to the reaction rate of this monomer. This avoids oscillations around the set-point, which occurs if only a PID is applied. However, the proportional (P) action is indispensable in order to account for the set-point. The use of the integrator (I) part allows us to eliminate possible steady-state offsets, due to modeling uncertainties. However, the integrator gain must be chosen wisely. The integrator augments the order of the linear model and the integral gain might add an imaginary pole of the linear system, which causes oscillations in the response.

The controller was initially tested in simulation. To study the controller robustness, the system methyl methacrylate (MMA) and butyl acrylate (BuA) is chosen since it is known to introduce a large composition drift in batch operations and it does not have an azeotropic composition. During the copolymerization of these monomers, MMA is the more reactive monomer. The control manipulated variable is therefore the flow rate of MMA and is therefore calculated by equation 6.17. The different gains of the controller are adjusted, $\kappa_P=0.1$, and since no modeling error is assumed in the simulation test, we can take $\tau_I=\infty$. The flow rate of BuA, in Figure 6.2, is supposed to be zero. The initial number of moles of BuA is fixed at 3.1209 mol. The composition set-point is 30% MMA and 70% BuA, by mole. The initial number of moles of MMA is therefore calculated by equation 6.10, and was found to be 0.5250 mol. An error of 10% of the initial value of MMA was voluntary introduced in order

to test the rapidity of the convergence of the controller to the set-point. The value of μ was supposed to be constant during the simulation (the models of $\bar{n}$ and N_P^T are not used).
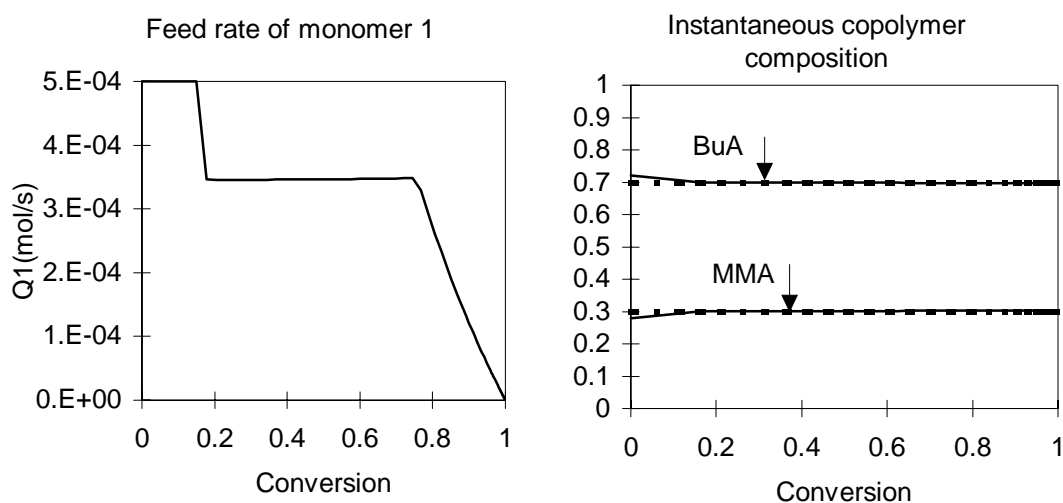
Figure 6.2: Simulation of the copolymerization of MMA and BuA. At left, the flow rate of MMA calculated by the controller. At right, the instantaneous composition, with an intentional error in the initial mass to test the robustness of the controller.

Figure 6.2 shows that the flow rate of MMA is, as expected, a function of the reaction rate of BuA, which is constant during interval II. Since an error was introduced in the initial monomer ratio (the initial value of MMA was lower than the desired one), the flow rate of MMA was more important at the beginning of the reaction, in order to bring back the monomer ratio to the desired value. The maximum admissible flow rate was voluntary fixed at 5e-4 mol/s, and therefore the monomer ratio was not corrected quickly. During this time, the obtained instantaneous composition was very close to the desired value, and converges quickly to the exact set-point. If the initial charge of MMA was higher than the desired one, the controller will set the value of Q_1 to zero until that the excess of monomer is consumed. A solution for this kind of perturbation, or drift in the polymer composition, is to control the cumulative polymer composition, in order to compensate for the error. In this work we will only investigate instantaneous polymer composition control.

During interval III, the reaction rate is a function of the concentration of monomer in the polymer particles, which decreases with time, and therefore Q_1 decreases linearly in interval III (since μ is constant).

The controller therefore performs well under simulation conditions. However, experimental validation of the controller is indispensable, and allows us to evaluate the model, the sensors (temperature resistances, balances), the actuators (pumps), the control strategy and the relationship between all of them. In several cases, the sensors and actuators possess a dead-time that is not taken into account in the model. An experimental study will allow us to evaluate the sensitivity of the controller to these parameters, and to perform the control experimentally.

6.2.2 Experimental

The pair of monomers MMA and BuA is chosen to evaluate the control strategy because of the strong composition drift that occurs if inadequate control is applied to the system. For example, as shown in Figure 6.3, we can see that the evolution of the copolymer composition during a copolymerisation of 60% MMA and 40% BuA is quite significant. At the beginning of the reaction, the copolymer is more rich in MMA, and copolymer produced at the end is much more rich in BuA. This clearly demonstrates the need to control the composition on-line.
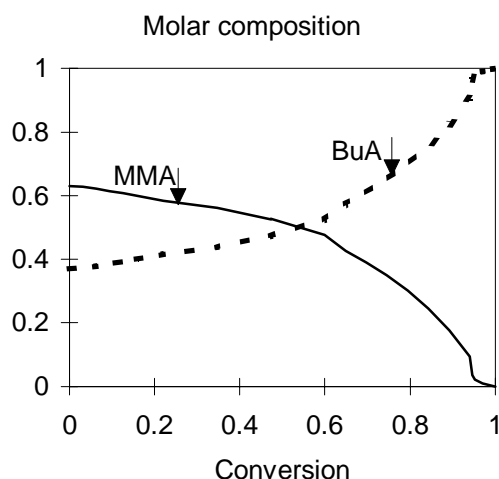
Figure 6.3: Experiment C5: Estimation of the instantaneous molar composition obtained by a batch copolymerization with the initial monomer composition of 43 % MMA-57%BuA.

In the semi-continuous control strategy we will initially charge all the desired amount of the less reactive monomer and the amount of the more reactive monomer required to correctly initialize the ratio N_1/N_2 that ensures the production of polymer with the desired composition. Thereafter, Q_1 is calculated by the control law given by equation 6.17. Q_2 can also be set to a positive known value if it was not possible to add all the desired amount of BuA in the initial charge, especially if this might provoke a large increase in the rate of heat produced (this specific problem will be investigated in the next chapter).

The polymerizations were carried out at 60°C in the 3 liter reactor, presented in Chapter 3. The heating, charging and deoxygenation of water and monomers is performed as

explained in Chapter 3. In order to avoid errors in composition of the initial monomer charge due to evaporation of the reactive species during degassing, the monomers are deoxygenated for only 5 to 10 minutes. The temperatures, the monomer mass fed to the reactor, and the pump voltage are measured every 10 seconds, and the data are saved in a file. The program containing the adaptive calorimetric procedure, the composition estimator and the control law are written in Matlab®, Simulink® and continuously communicate with the data file. Integration of the differential equations is realized using a variable step Adams-Moulton algorithm with maximum step size = 10s. This integration routine attempts to take the largest possible step consistent with the admissible error bounds. The continuous change in the integration step size allows us to perform the integration quickly.

In addition to the data acquired every 10 seconds, the program is based on infrequent experimental measurements of the gravimetric conversion. These values are obtained by analyzing the solids content of the infrequently withdrawn samples (every 10 to 60 minutes), using a thermobalance. Once available, these values are fed to the program. The control strategy starts calculating Q_1 at the beginning of the reaction based on the calibrated values of UA and Q_{loss} until samples are withdrawn to correct these estimates.

The desired flow rate (Q_1) is calculated in mol/s. However, in order to transmit this value to the pump, it must be expressed in volts. The relation between the voltage and the frequency of pumping is linear. A calibration was done a priori to determine the model governing the pump (frequency-flow rate). The obtained 'linear' model is implemented to the program and therefore the controller provides directly the voltage to be transmitted to the pump.

The objective of the first control experiments was to determine the optimal controller gains required to handle a convenient (rapid, nonoscillating) convergence of the composition. The recipes and the controller gains (κ_P and τ_I) used for these experiments are shown in Table 6.1. The composition set-point was 30% MMA-70% BuA for all of the experiments. The initial amounts of monomers were correctly chosen to minimize the composition drift at the beginning of the reaction. The flow rate of MMA was calculated from the controller 6.17 as a function of the chosen controller gains. The obtained polymer composition is validated by gas chromatography, GC.

Table 6.1: Experiments of copolymerization for the validation of the composition controller. Desired molar composition: 30% MMA-70% BuA.

\ Run Component \	C 11		C 12		C 13		C 14	
	Initial Charge(g)	Feed (g)	Initial Charge	Feed (g)	Initial Charge	Feed (g)	Initial Charge	Feed (g)
H_2O	1502	64	1501	67	1500	70.8	1504.7	70
MMA	53	150	53	150	53	150	53	150
BuA	400	-	400	-	400	-	400.8	-
Triton	4.09	5.14	5.55	5.1	7.9	5.4	8.0311	8.353
KPS	3.01	-	3.0455	-	3.0429	-	3.0506	-
κ_P	0.01		0.001		0.1		0.01	
τ_I	$1e^4$		$1e^8$		∞		∞	

The "best" controller gains will be those that allow us to find a smooth flow rate Q_1 that brings the composition to the desired trajectory quickly (if it is not well initialized, or if it deviates during the control experiment due to some perturbation), and maintain it on this trajectory with minimum oscillations. Simulations showed that Q_1 is primarily a function of the reaction rate of MMA (R_{P1}), which, in turn, must follow the rate of reaction of BuA (R_{P2}), especially if the initial amounts are correctly chosen. The PI part is indispensable if there is an error in the initial values of N_1 and N_2 or if a perturbation of the ratio N_1/N_2 occurs, which gives a positive error, ε. In this case, both the linear (PI) and nonlinear parts of the controller contribute to the action.

Figures 6.4a-6.4d show the values of Q_1 and the reaction rates of MMA and BuA, obtained during the different experiments.
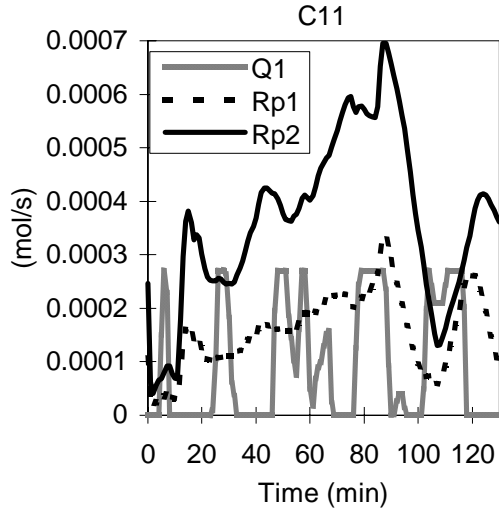
Figure 6.4a: Experiment C 11, κ_P=0.01 and τ_I=1×10^4.
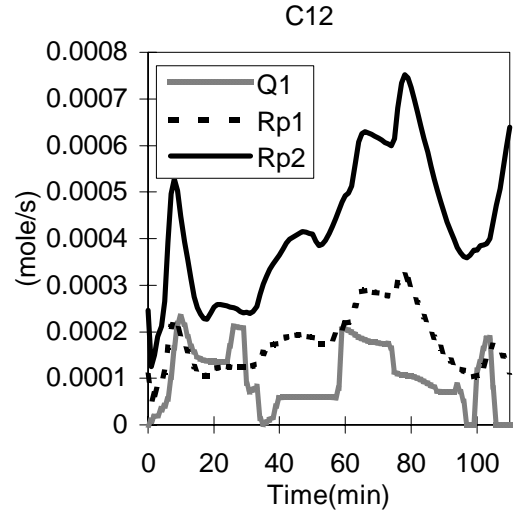
Figure 6.4b: Experiment C 12, κ_P=0.001 and τ_I=1×10^8.
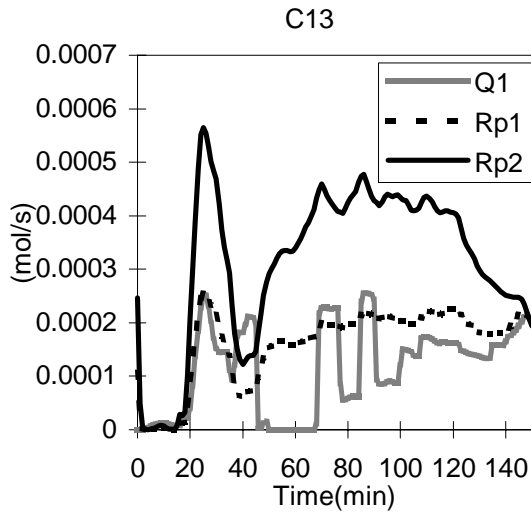
Figure 6.4c: Experiment C 13, κ_P=0.1 and τ_I=∞.
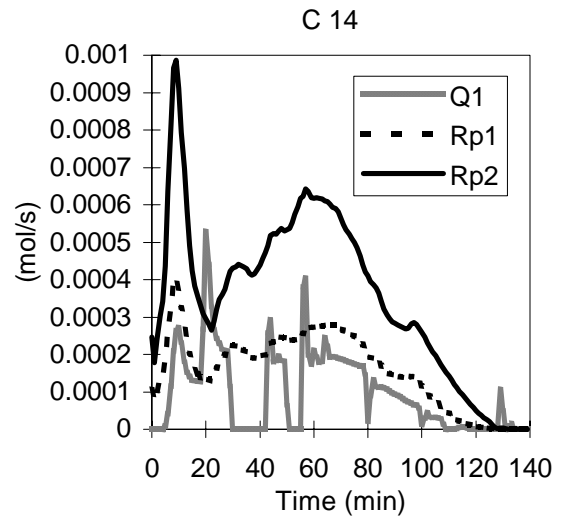
Figure 6.4d: Experiment C 14, κ_P=0.01 and τ_I=∞.

Instantaneous molar composition

Cumulative molar composition
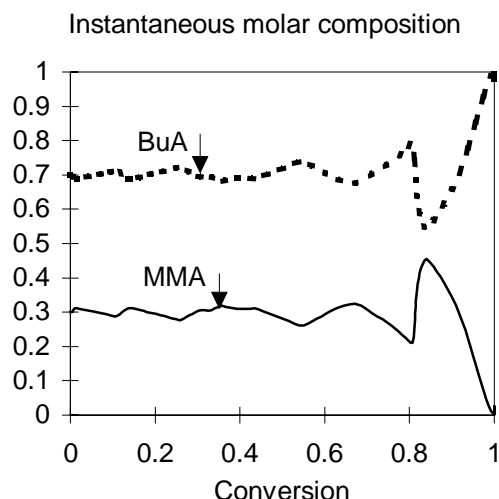
Figure 6.5a: Experiment C11. (κ_P=0.01 and τ_I=1×10^4). Set-point =30%MMA-70%BuA.
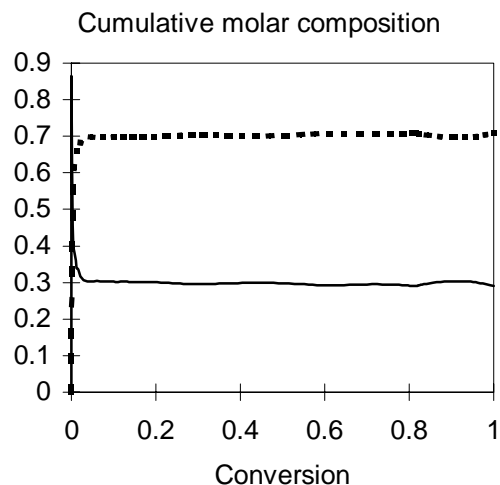
Figure 6.5b: Experiment C11. (κ_P=0.01 and τ_I=1×10^4). Results of the observer.

In experiment C11, a strong combined PI action was used (κ_P=0.01 and τ_I=1×10^4). Figure 6.4a shows that the value of Q_1 was therefore either zero or at the pump saturation value, which means that an almost bang bang controller is obtained. This kind of control is to be avoided since it exhausts the pumps and causes oscillations in the resulting instantaneous composition (Figure 6.5a and 6.5b). These oscillations become critical when there is a small amount of monomer in the reactor, since at this stage, the monomer ratios and thus the polymer composition become very sensitive to the monomer flow rate. In this experiment, the oscillations in the instantaneous composition increase at the end of the reaction, but the cumulative composition fortunately remained unaffected by these oscillations. In other cases, for example for the experiments that are almost always under starved conditions, the cumulative composition can be critically influenced.
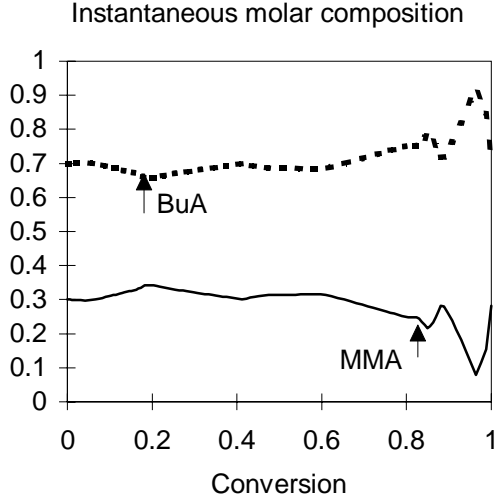
Figure 6.6a: Experiment C12: (κ_P=0.001, τ_I=1×10^8).
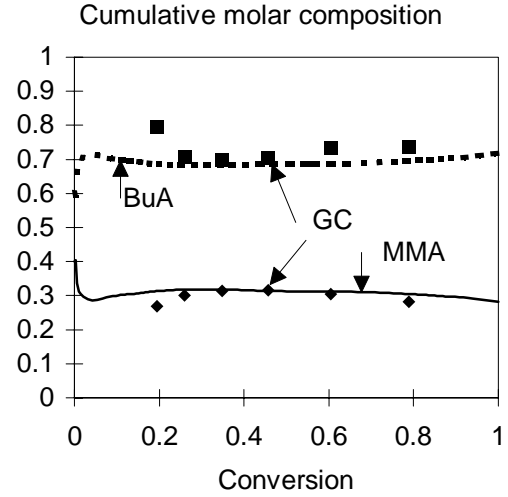
Figure 6.6b: Experiment C12: (κ_P=0.001, τ_I=1×10^8).

In experiment C12, smaller gains are used to adjust the controller (κ_P=0.001 and τ_I=1×10^8). Figure 6.4b shows that the obtained curve of Q_1 in this case follows the evolution of R_{P2}, but with a significant delay. The composition of the polymer produced in this case (Figure 6.6a and 6.6b)) also drifts from the set-point. In this case, the controller gains do not appear to be high enough.
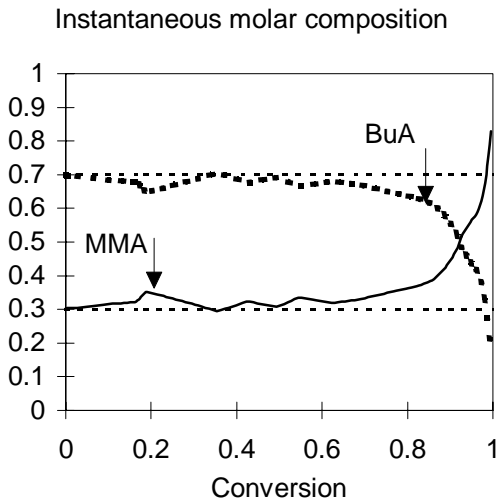
Figure 6.7a: Experiment C13 (κ_P=0.1 and τ_I=∞).
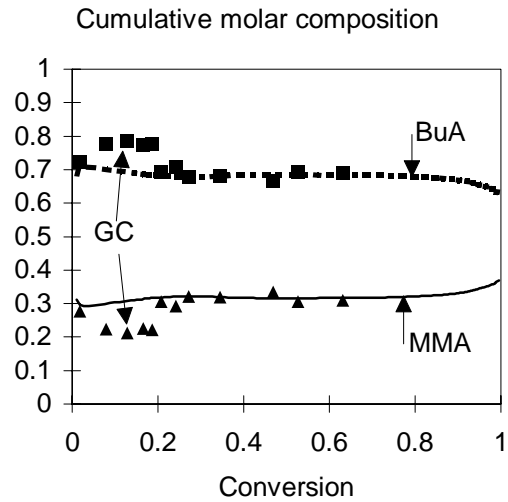
Figure 6.7b: Experiment C13 (κ_P=0.1 and τ_I=∞).

In experiment C13 the proportional gain is set to a higher value ($\kappa_P=0.1$) and $\tau_I=\infty$, since it was found that the integral action augments the calculation time of the controller and seems to be sensitive to the response time of the pump. Moreover, as we mentioned earlier, the I action is used to allow us to eliminate the static error that usually comes from a modeling error, and in our case, the observer accounts for modeling uncertainties. Therefore, the integral action is not necessary, and henceforth will not be used for the composition control.

Figure 6.4c shows that the resulting flow rate of MMA reasonably followed the evolution of the rate of reaction of BuA (R_{P2}) at the beginning of the reaction but at the end of reaction Q_1 followed the evolution of R_{P1} while R_{P2} was decreasing. This causes a drift in the ratio, R_{P1}/R_{P2}, and therefore in the polymer composition. This perturbation is due to an overbearing proportional action. The resulting polymer composition is represented by Figure 6.7a and 6.7b. The composition begins to drift from the set point at low conversion, resulting in a big drift at the end of the reaction that also influences the cumulative composition.
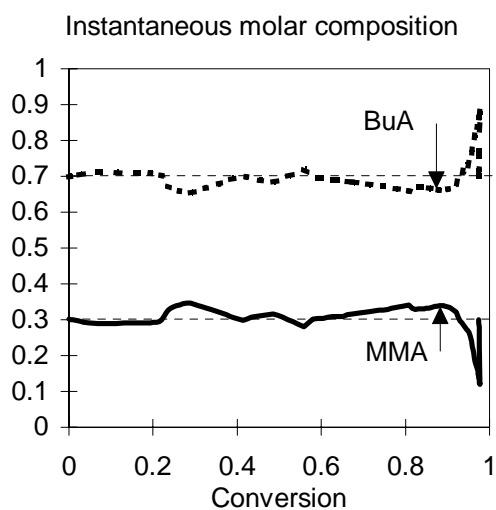
Figure 6.8a: Experiment C14: Estimations given by the continuous line, and experimental GC validation by the points.
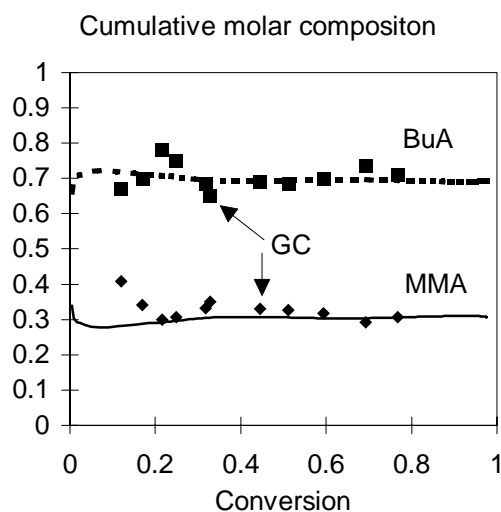
Figure 6.8b: Experiment C14: Cumulative polymer composition validated by experimental GC obtained off-line.

In experiment C14, the controller parameters were taken to be $\kappa_P=0.01$ and $\tau_I=\infty$. The curve of Q_1 is smooth and follows exactly the shape of R_{P1} and R_{P2}, except during the rapid

part of the reaction where small oscillations are observed in the curve of Q_1. In this experiment, the perturbations were not due to the controller, as was the case in experiment C11, but are due to the optimization procedure. Moreover, the controller was able to manipulate precisely Q_1 at high conversions.

It can be seen however that there is a little difference between the values of Q_1 and R_{P1}. This problem seems to be due to the actuator, which is the pump in our case. In fact, a steady-state offset was observed between the real mass (measured by the balance) and the mass calculated from the pump frequency, or model. This is due to the fact that the model (linear, first order, obtained by calibration) used to represent the pump is not exact, and the real flow rate depends on the preemulsion density, pressure in the reservoir, plus the fact that the pump has a dead-time that varies with the frequency that could not be accounted for. This error is integrated with time and a big difference between the predicted and real masse pumped accumulates at the end of the experiment.
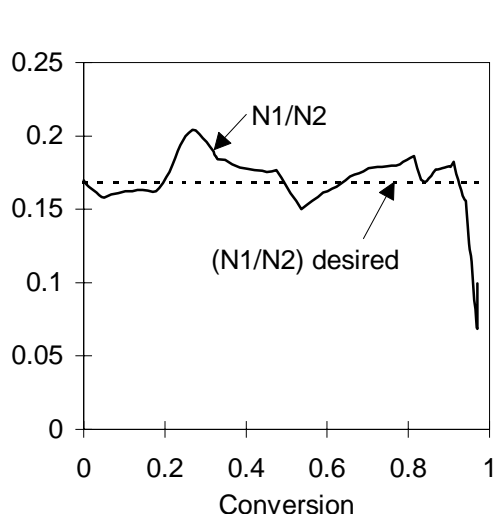
Figure 6.9a: Experiment C14: Real monomer ratio (N_1/N_2), and the desired one (N_1/N_2)^d.
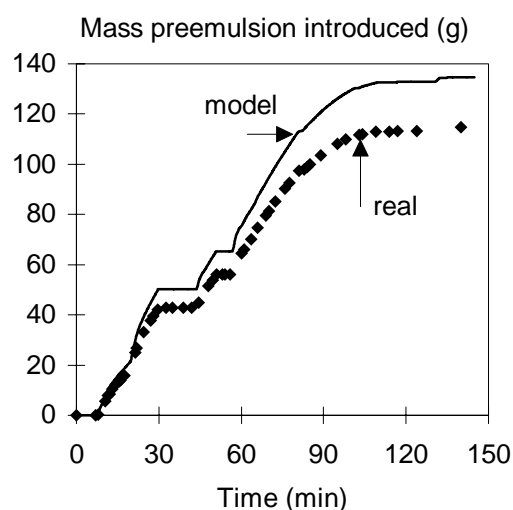
Figure 6.9b: C14: Difference between the mass obtained from the balance and from the open-loop model of the pump.

Figure 6.9b shows the difference between the real mass and the mass calculated from the model of the pump. It can be seen that we obtain a correct representation of the real mass at the beginning of the experiment, but there is a large difference between both values at the

end. A remedy to this problem would be to construct a local controller of the pump. This problem will be investigated in the next section.

The copolymer composition estimated during this experiment is presented in Figure 6.8a and b. It can be seen that the instantaneous composition is closer to the set-point and oscillates much less than the other experiments. The drift in the polymer composition in this experiment occurs at very high conversion due to the increase in the sensitivity of (monomer ratio, and therefore) the composition to the monomer flow rates, and perhaps to the difference in the pumped mass. The cumulative copolymer composition remains however constant throughout the reaction.

It is important to note that the controller objective is to minimize the difference between the desired monomer ratio, $(N_1/N_2)^d$, and the real one. The polymer ratio (F_1/F_2) is thereafter calculated by equation 6.10. In theory, controlling (N_1/N_2) must allow us to control (F_1/F_2). Figure 6.9a shows the obtained monomer ratio during the experiment C14. It can be seen that this ratio is maintained around the desire value up to high conversion.

In the next section, we will try to eliminate the steady-state offset between the real mass and the mass calculated from the model of the pump (relating voltage and flow rate).

6.2.3 Pump control

The objective of this section is to construct a local controller that verifies that a specific flow rate can actually be delivered to the reactor by the pump. This controller is important since the model of the pump was found to drift with time. The pump controller will be based on the measurements obtained by the balance, which are supposed to be exact.

The pump behavior can be represented by a first order model with a very small time constant, $\tau=10$ seconds. This constant is determined by performing a step change in the voltage of the pump, as shown in the following figure:
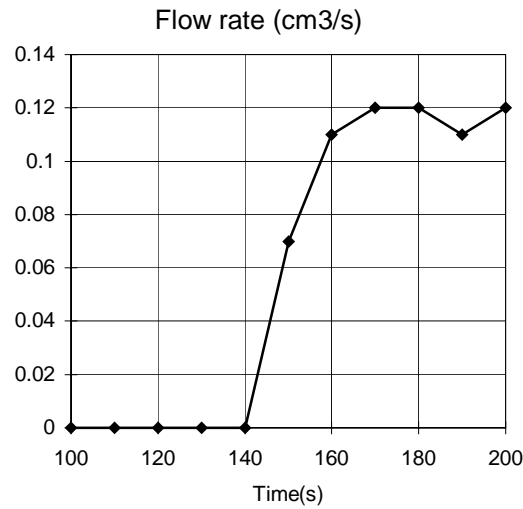
Figure 6.10: The response of flow rate to a step change in the pump voltage, at 140s from V=0 to V=4.

The pump behavior can therefore be represented by the following linear model:

$$\tau\dot{q} + q = k_1 V$$

where q is the flow rate in (cm^3/s) and V is the transmitted voltage, τ is the system time constant, and k_1 stands for the open-loop model gain, ($k_1=0.03=\alpha k_0$, α (cm^3/V)).

The first analyses consist of trying a PI controller, using either the flow rate or the mass as output of the controller. However, it was not evident to properly adjust the controller parameters, in both cases, by controlling the mass or the flow rate. It was noticed however that it would be better to control the pump flow rate than the total mass. Effectively, the controller of the total mass might give a lot of oscillations in the pump flow rate which might exhaust the pumps, see Figure 6.11. Moreover, it should be pointed out that the composition controller gives the desired flow rate. In this case, in order to apply the controller of the total mass, we will have to integrate the desired flow rate in order to calculate the desired mass. Therefore, it would be easier to control the pump flow rate. However, using a PI controller, we could not obtain good results.
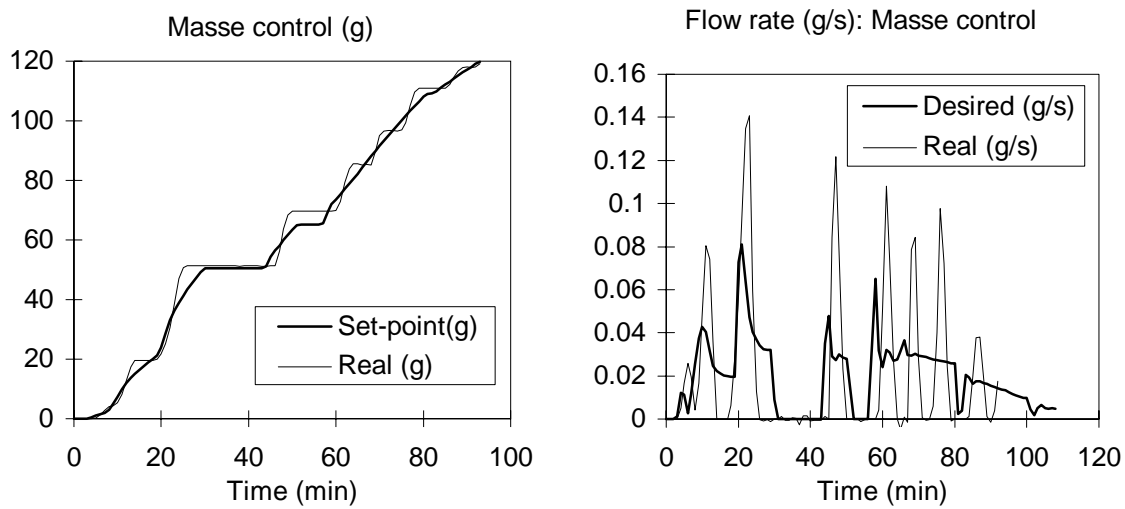
Figure 6.11: Controlling the pump using the total mass as output.

Therefore we propose to construct an internal model controller (IMC), of the type developed by Garcia and Morari (1982). The advantages of the IMC are that it guarantees the stability of the system, and handles the parameter uncertainties, the manipulated variable constraints and compensates the deadtime. The structure of the IMC is shown in Figure 6.12.
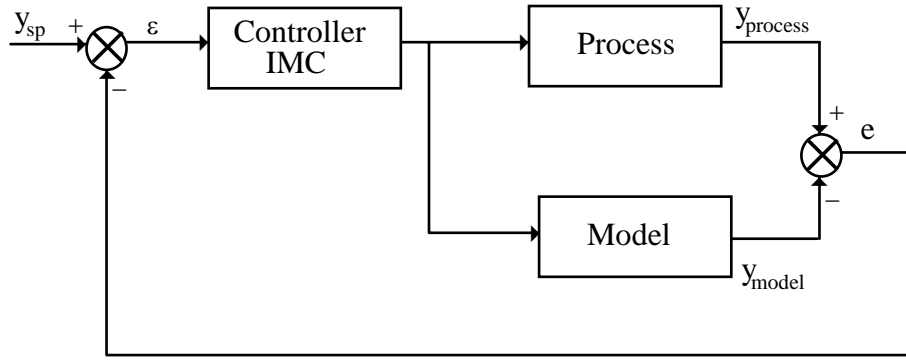
Figure 6.12: Internal model control (IMC) structure.

In theory, the transfer function of the model is divided into two parts:

$$M = G(s) = G^+(s).G^-(s) \qquad (6.18)$$

where s is the Laplace operator, $G^+(s)$ stands for the transfer function of the pure delay in the pump and the unstable part of the model (positive or imaginary zeros), and $G^-(s)$ represents the stable part of the model. In our case, $G^+(s)=1$, since

$$G(s) = \frac{k_1}{1 + \tau s} = G^-(s)$$

Therefore, the controller takes the following form:

$$C(s) = \frac{1}{G^-(s)} f(s) = \frac{u}{\varepsilon} \qquad (6.19)$$

where f(s) is a low pass filter that is varied for robustness and performance tuning,

$$f = \frac{1}{\left(1 + \tau_f s\right)^r}$$

τ_f is the desired closed loop time constant (τ_f=3s here), r is chosen such that the denominator order is greater than or equal to the numerator one, and is taken to be one here. The error ε is the difference between the desired output and modeling error (difference between the model output and the process real output):

$$\varepsilon = y_{sp} - \underbrace{e}_{y_{process} - y_{model}}$$

In order to test the controller we have chosen the highly variable flow rate trajectory shown in Figure 6.13. The real flow rate is obtained by deriving the mass obtained from the balance. The controller performance is shown in the Figure 6.13. The controller gives the desired mass without oscillations. However, a small offset can be noted in the obtained flow rate. This is due to the response time of the pump.
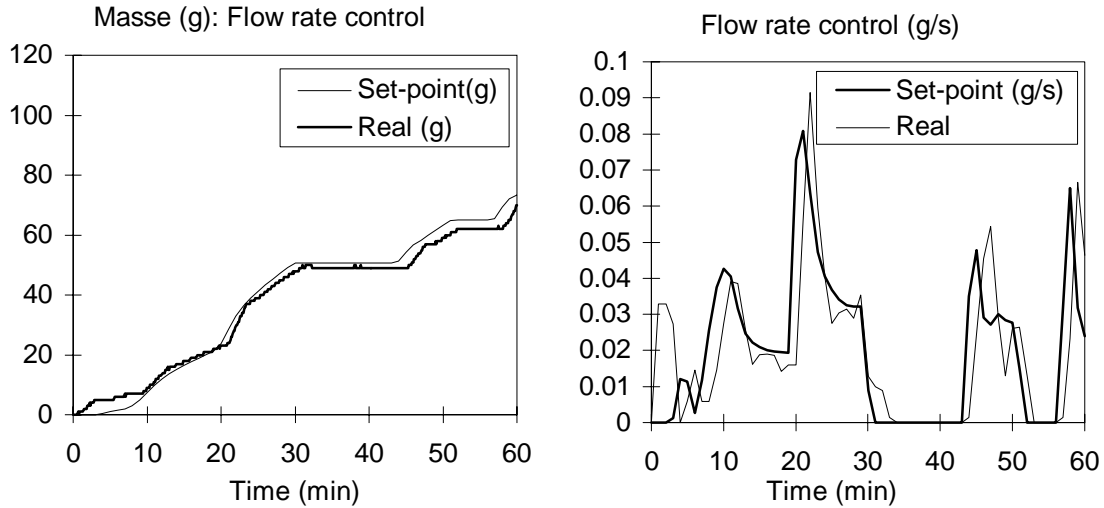
Figure 6.13: Pump control using the total mass as output and an IMC.

The use of a local controller of the pump allowed us to eliminate the error between the desired and real masses, whereas the open-loop model caused a steady-state difference between the desired flow rate and the obtained one, which results in an increasing difference between the real mass and desired one. In the following section the IMC of the pump will be used along with the nonlinear composition controller.

6.2.4 Decoupled composition/pump control

In this section both the nonlinear composition controller and the IMC of the pump are used simultaneously. Several experiments were carried out to validate the controllers. Several composition set-points were chosen. The recipes used throughout these experiments are given in Table 6.2. In all the experiments the parameters were chosen to be $\kappa_p = 0.01$ and $\tau_f = 3\,s$, as a result of experiments C11 to C14.

Table 6.2: Semi-continuous experiments for the validation of the control strategy.

\ Run	**C 15**		**C 16**		**C 17**	
COMPOSITION^{SP}	**30-70 %** MMA-BuA		**50-50 %** MMA-BuA		**70-30 %** MMA-BuA	
Component \	Initial Charge (g)	Feed (g)	Initial Charge(g)	Feed (g)	Initial Charge(g)	Feed (g)
H_2O	1498	71.5	1500	100.2	1500	100.2
MMA	53	150	132.3	217.5	257	320.8
BuA	400	-	400	-	300	-
Triton	8	8.7	8.35	8.54	8.04	8.61
SDS	-	0.35	-	0.58	-	0.602
KPS	3.01	-	3	-	3.01	-
Final Solids Content	26%		31%		33%	
Final particle diameter	266 nm		295 nm		315 nm	

In experiment C15 the composition set-point is 30% MMA-70% BuA by mole. Figures 6.13a-6.13c show the results obtained during this experiment.
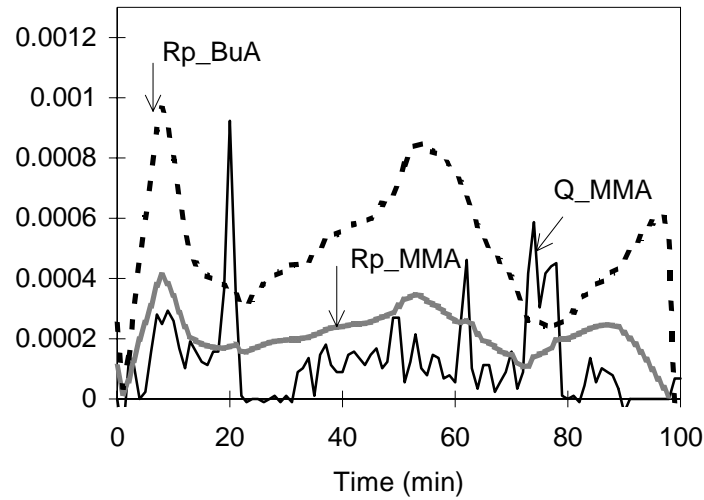
Figure 6.14a. Experiment C15. Reaction rate of MMA, BuA and flow rate of MMA (mol/s).

Figure 6.14a presents the reaction rates of MMA and BuA and the controlled flow rate of MMA. It can be seen that the curve of Q_1 has almost the same shape of R_{P1} and R_{P2}. The value of Q_1 is the result of both the composition controller and the local controller of the pump.
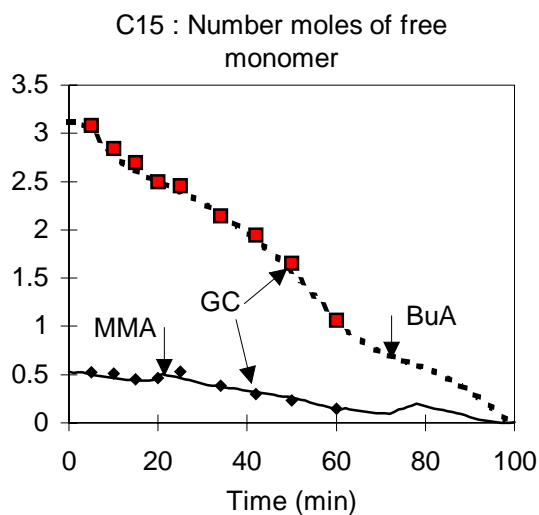
Figure 6.14b: Experiment C15. Desired composition = 30% MMA-70% BuA.
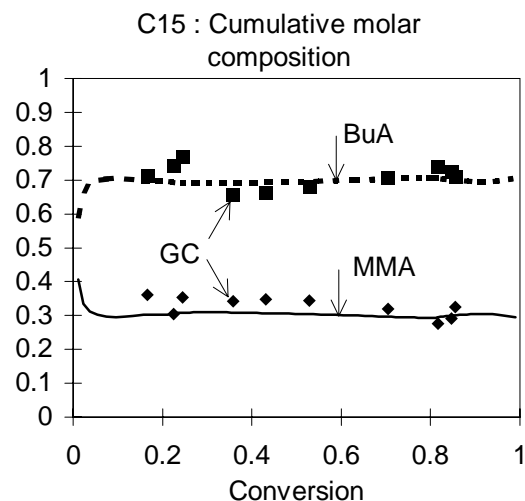
Figure 6.14c: Experiment C15. Desired composition = 30% MMA-70% BuA by mole.

Figure 6.14c shows that the cumulative composition was constant during the entire experiment. The composition was validated by off-line GC measurements. Figure 6.14b shows that the estimated number of moles of each monomer agrees with the off-line GC measurements.

In experiment C16, the composition set-point is 50% MMA-50% BuA by mole. Figures 6.14a-6.14e show the results of these experiments.
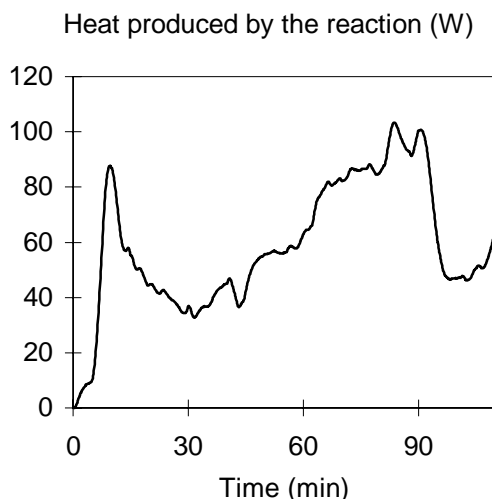
Figure 6.15a: ExperimentC16. Desired
composition = 50/50 MMA/BuA.
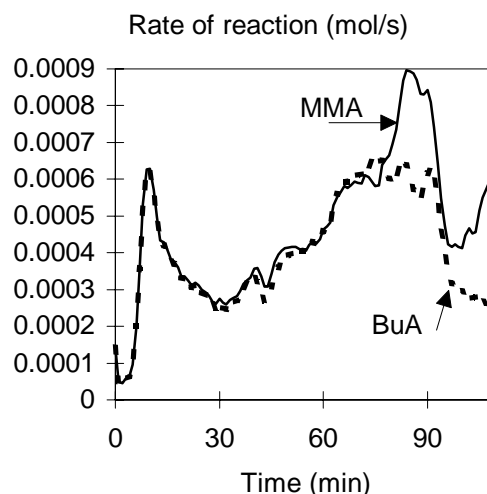
Figure 6.15b: Experiment C16. Desired
composition = 50/50 MMA/BuA.

The rate of heat produced by the reaction is shown in Figure 6.15a. A peak of heat is produced at the beginning of the reaction, during the particle nucleation. At the end of the reaction, the rate of heat produced by the reaction increases again, perhaps due to a gel effect. Since the desired composition is 50% MMA-50% BuA, the reaction rate of both monomers must be equal, as shown in Figure 6.15b. The figure shows that R_{P1} is maintained close to R_{P2} for most of the reaction. However, at the end of the experiment, the sensitivity of the reaction rate to the monomer flow rate yields a small difference between R_{P1} and R_{P2}. This difference influences the instantaneous composition that is shown in Figure 6.15c. The cumulative composition was found to be insensitive to these errors, since the rate of reaction at the end of the experiment is low and therefore the amount of monomer produced with this drift of composition is very small compared to the amount of polymer produced at the desired composition.
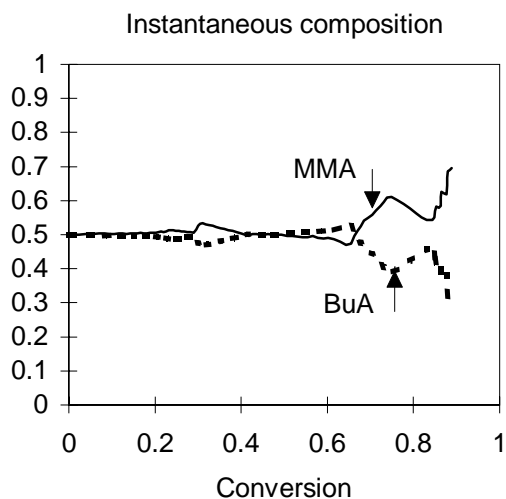
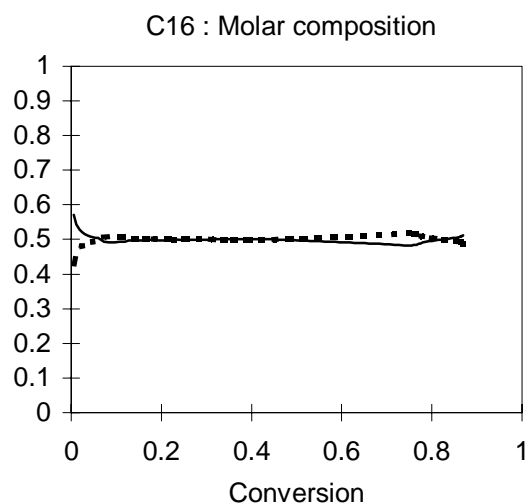Figure 6.15c. Experiment C16. Desired composition = 50/50 MMA/BuA

Figure 6.15d. Experiment C16. Desired composition = 50/50 MMA/BuA.

The polymer composition and individual conversions were validated by off-line GC measurements. Figure 6.15e shows the number of moles of free monomer versus time validated by the GC measurements.
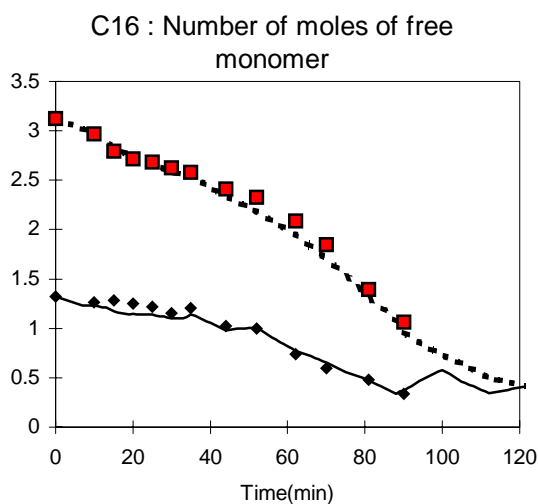

Figure 6.15e: Experiment C16. Composition = 50% MMA-50% BuA.

In experiment C17, the desired composition is 70% MMA-30% BuA. Figures 6.15a shows the overall and individual conversions obtained during this experiment. The monomer

conversion is validated by GC. Figure 6.16b shows that the cumulative composition was maintained constant throughout the reaction.
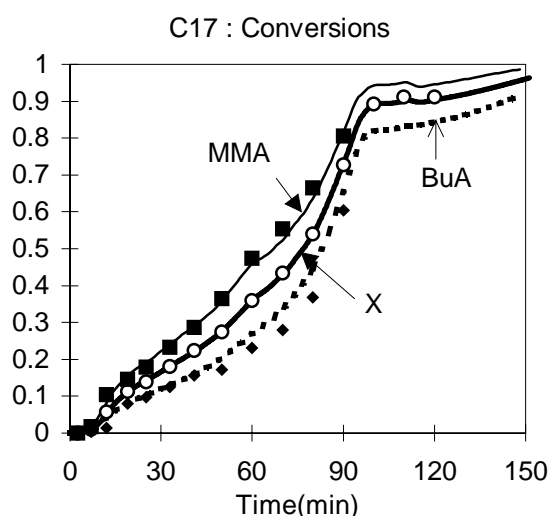
Figure 6.16a: Experiment C17. Overall conversion fitted to gravimetric measurements and individual conversions validated by GC.
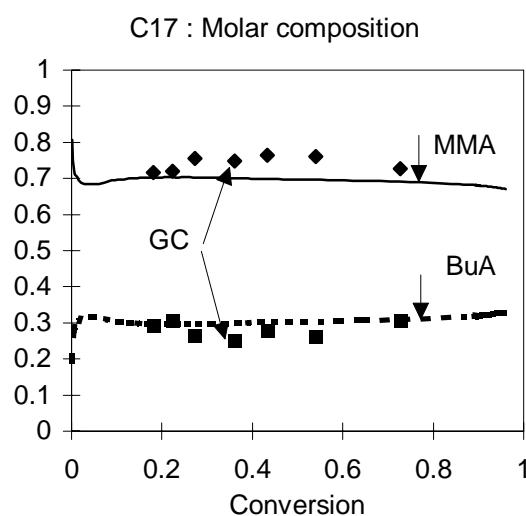
Figure 6.16b: Experiment C17. Desired cumulative composition 70% MMA-30% BuA. Validation by off-line GC.

Figure 6.17a shows the estimated evolution of $\bar{n}$ during these experiments. All the experiments present a similar evolution of the particles size and number (Figures 6.16c and 6.16d). However, it was observed that the increase in the value of $\bar{n}$ at high conversions was more important when the copolymer contains more MMA. In experiment C17, the polymer contains 70% MMA by mole. The increase in $\bar{n}$, in this experiment, seems to be due to a gel effect, produced because the glass transition temperature of the polymer is higher than the reaction temperature (Tg of MMA=100°C and Tg of BuA=-54), which decreases the radical mobility and therefore their termination. This increase in the value of $\bar{n}$ results in a higher reaction rate, that is clearly shown in Figure 6.17b, for experiment C17 (with 70% MMA).
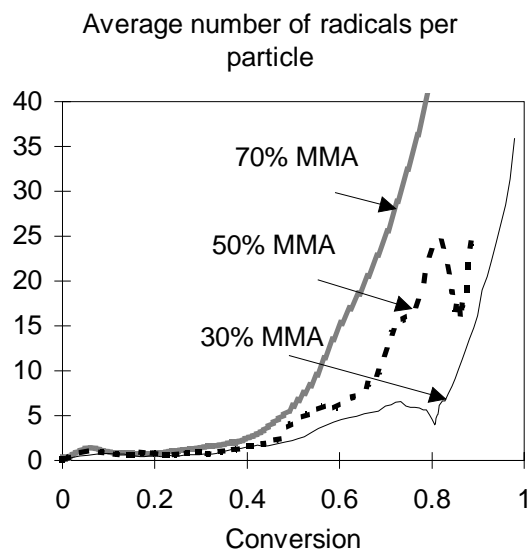
241

Figure 6.17a: $\bar{n}$ for the experiments C15 (30% MMA), C16 (50% MMA), and C17 (70% MMA).
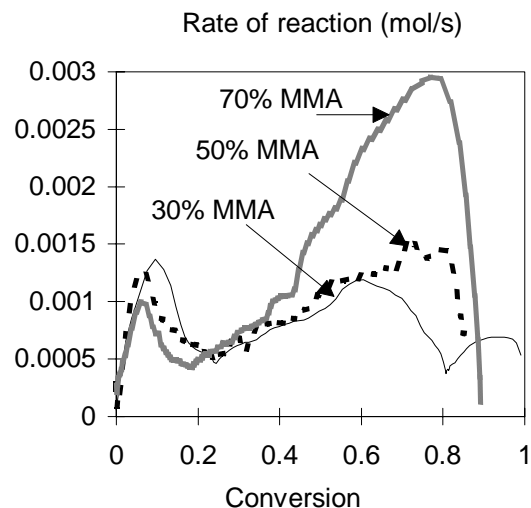

Figure 6.17b: R_P (mol/s) for the experiments C15, C16, and C17.
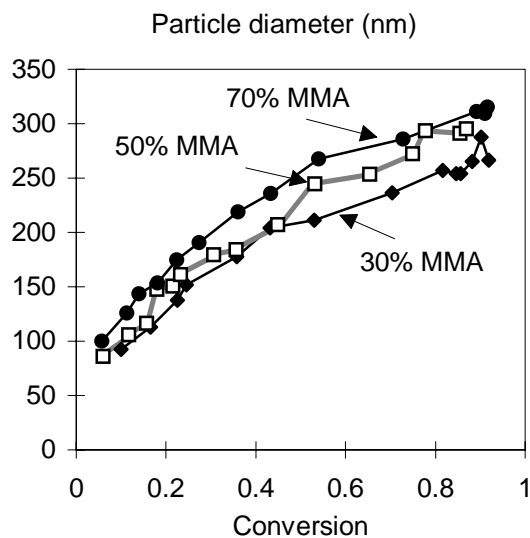

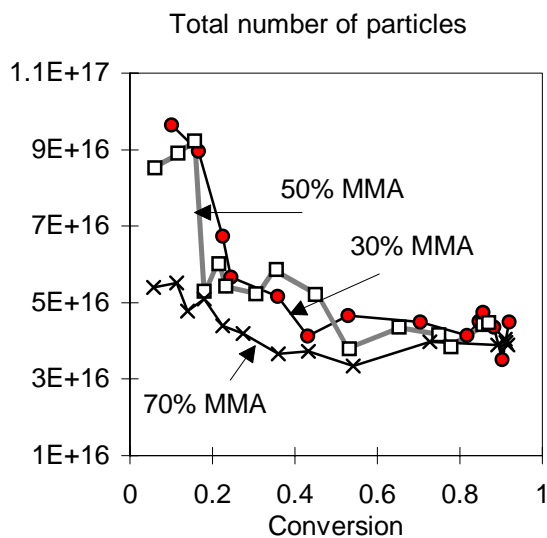Figure 6.17c: Particle size for experiments C15, C16, and C17.

Figure 6.17d: N_P^T for the experiments C15, C16, and C17.

6.3 Terpolymer composition control

6.3.1 Control law

The composition produced during a batch terpolymerization reaction involving monomers with different reactivities will undoubtedly vary if the composition is not azeotropic. Since three monomers are involved, a constant composition is obtained if the following two ratios are maintained at the desired values throughout the reaction:

$$\frac{F_1}{F_3} = \frac{R_{P1}}{R_{P3}} \quad \text{and} \quad \frac{F_2}{F_3} = \frac{R_{P2}}{R_{P3}} \tag{6.20}$$

Considering the model for hydrophobic monomers (i=1,2,3),

$$\dot{N}_i = Q_i - R_{Pi}$$
$$= Q_i - \mu[M_i^p]\left(K_{P1i}P_1^p + K_{P2i}P_2^p + K_{P3i}P_3^p\right) \tag{6.21}$$

that the monomers are not water soluble and that they have the same solubility in both parts of the organic phase (polymer and monomer) the composition ratio becomes:

$$\frac{F_1}{F_3} = \frac{N_1\left(a_1 K_{P11} + a_2 K_{P21} + a_3 K_{P31}\right)}{N_3\left(a_1 K_{P13} + a_2 K_{P23} + a_3 K_{P33}\right)} \tag{6.22}$$

$$\frac{F_2}{F_3} = \frac{N_2\left(a_1 K_{P12} + a_2 K_{P22} + a_3 K_{P32}\right)}{N_3\left(a_1 K_{P13} + a_2 K_{P23} + a_3 K_{P33}\right)}$$

where

$$a_1 = \frac{N_1}{N_3}\left(K_{P31}K_{P21}\frac{N_1}{N_3} + K_{P21}K_{P32}\frac{N_2}{N_3} + K_{P31}K_{P23}\right)$$

$$a_2 = \frac{N_2}{N_3}\left(K_{P12}K_{P31}\frac{N_1}{N_3} + K_{P12}K_{P32}\frac{N_2}{N_3} + K_{P32}K_{P13}\right) \tag{6.23}$$

$$a_3 = \left(K_{P13}K_{P21}\frac{N_1}{N_3} + K_{P23}K_{P12}\frac{N_2}{N_3} + K_{P13}K_{P23}\right)$$

Equation 6.22 shows that it is sufficient to manipulate the ratios N_1/N_3 and N_2/N_3 in order to keep the composition at some desired fractions, F_1/F_3 and F_2/F_3. If we assume that monomers 1 and 2 are more reactive than monomer 3, these ratios can be controlled by manipulating N_1 and N_2. The desired ratios $(N_1/N_3)^d$ and $(N_2/N_3)^d$ can be calculated from F_1/F_3 and F_2/F_3 from equations 6.22. Both ratios must be controlled simultaneously in order to guarantee the production of a polymer with the desired composition. This can be done by manipulating the flow rates of monomers 1 and 2 together. In order to do so, a controller of dimension two must be constructed using the terpolymerization model. The terpolymerization model of hydrophobic monomers is given by the following system:

$$\dot{x} = \begin{bmatrix} \dot{N}_1 \\ \dot{N}_2 \\ \dot{N}_3 \end{bmatrix} = \underbrace{\begin{bmatrix} -R_{P1} \\ -R_{P2} \\ Q_3 - R_{P3} \end{bmatrix}}_{f(x)} + \underbrace{\begin{bmatrix} 1 \\ 0 \\ 0 \end{bmatrix}}_{g_1(x)} \underbrace{Q_1}_{u_1} + \underbrace{\begin{bmatrix} 0 \\ 1 \\ 0 \end{bmatrix}}_{g_2(x)} \underbrace{Q_2}_{u_2} \tag{6.24}$$

$$y = \begin{bmatrix} h_1 \\ h_2 \end{bmatrix} = \underbrace{\begin{bmatrix} N_1 \\ N_2 \end{bmatrix}}_{h(x)}$$

where Q_1 and Q_2 are the two manipulated inputs of the system, N_1 and N_2 are taken to be the outputs of the model. All N_i values are obtained by the composition observer constructed in chapter 5.

In order to guarantee the controllability of the systems 6.24, the characteristic matrix must be nonsingular and the relative orders equal to one. The characteristic matrix corresponding to the system 6.24 is:

$$C(x) = \begin{bmatrix} L_{g_1}h_1 & L_{g_2}h_1 \\ L_{g_1}h_2 & L_{g_2}h_2 \end{bmatrix} = \begin{bmatrix} 1 & 0 \\ 0 & 1 \end{bmatrix} \tag{6.25}$$

and is therefore nonsingular.

For $r_1=1$, $r_2=1$, we calculate $< dh_i, ad_f^{r_i-1}(g) >$, i=1, 2 as defined in chapter 2:

$$\tag{6.26}$$

$$L_f h_1 = \frac{\partial h_1}{\partial x} f = \begin{bmatrix} 0 & 1 & 0 \end{bmatrix} \begin{bmatrix} -R_{P1} \\ -R_{P2} \\ Q_3 - R_{P3} \end{bmatrix} = -R_{P1} \neq 0$$

$$L_f h_2 = \frac{\partial h_2}{\partial x} f = -R_{P2} \neq 0$$

Therefore the relative orders $r_1=1$ and $r_2=1$.

We can therefore realize two input/output linearizing transformations, correlating Q_1 with N_1 and Q_2 with N_2:

$$\upsilon_1 = \Omega_1(x,u) = \sum_{k=0}^{1} \beta_{k0} L_f^k h_1 + (-1)^0 \beta_{10} < dh_1, ad_f^0(g_1) > u \qquad (6.27)$$

$$= \beta_{00} h_1 + \beta_{10} \frac{\partial h_1}{\partial x} f + \beta_{10} \frac{\partial h_1}{\partial x} g_1$$

$$= \beta_{00} N_1 + \beta_{10}(-R_{P1}) + \beta_{10} u_1$$

and the same transformation for input u_2:

$$\upsilon_2 = \Omega_2(x,u) = \sum_{k=0}^{1} \beta_{k1} L_f^k h_2 + (-1)^0 \beta_{11} < dh_2, ad_f^0(g_2) > u \qquad (6.28)$$

$$= \beta_{01} N_2 + \beta_{11}(-R_{P2}) + \beta_{11} u_2$$

We obtain the following inputs

$$u_1 = \frac{\upsilon_1 - \beta_{00} N_1}{\beta_{10}} + R_{P1} \qquad (6.29)$$

$$u_2 = \frac{\upsilon_2 - \beta_{01} N_2}{\beta_{11}} + R_{P2}$$

The external input υ_1 can be replaced directly by the set-point of N_1, or $\left(\upsilon_1 - \beta_{00} N_1\right)$ can be used to add a proportional loop as done in the case of copolymerization, and the same argument can be applied to υ_2:

$$u_1 = Q_1 = \frac{\kappa_{P1}}{\beta_{10}} \varepsilon_1 + R_{P1} \qquad (6.30)$$

$$u_2 = Q_2 = \frac{\kappa_{P2}}{\beta_{11}} \varepsilon_2 + R_{P2}$$

where u_i is in mol/s.

The controller parameters (κ_{Pi}, β_{1j}) must be chosen in a way that guarantees a stable composition profile. First of all, we can set $\beta_{10}=1$ and $\beta_{11}=1$ without any loss of generality. As we discussed in the last section, the proportional constant is indispensable in order to account for possible errors in the initial values and any perturbations, caused by the sensors or actuators. The integral action is important in order to account for model uncertainties.

However, since in our case the observer provides a closed-loop estimation of N_i and μ, and accounts therefore for possible model uncertainties, we will not add an integral part.

The values of κ_{P1}, and κ_{P2} are taken to be 0.01. Therefore, the controllers in equation 6.30 become:

$$Q_1 = 0.01 \times \left(N_3 \left(N_1 / N_3 \right)^d - N_1 \right) + R_{P1}$$

$$Q_2 = 0.01 \times \left(N_3 \left(N_2 / N_3 \right)^d - N_2 \right) + R_{P2}$$

$$(6.31)$$

6.3.2 *Experimental*

The system MMA, BuA, and VAc is chosen to validate the controller. In this system, the monomers MMA and BuA are more reactive than the VAc. The manipulated parameters are therefore the flow rates of MMA and BuA. The first investigation of the controller was done in simulation where the physical constants and reactivities of MMA, BuA, and VAc were implemented. The flow rate of VAc was set to zero during the simulation. The simulation results are shown in Figures 6.17a and 6.17b.
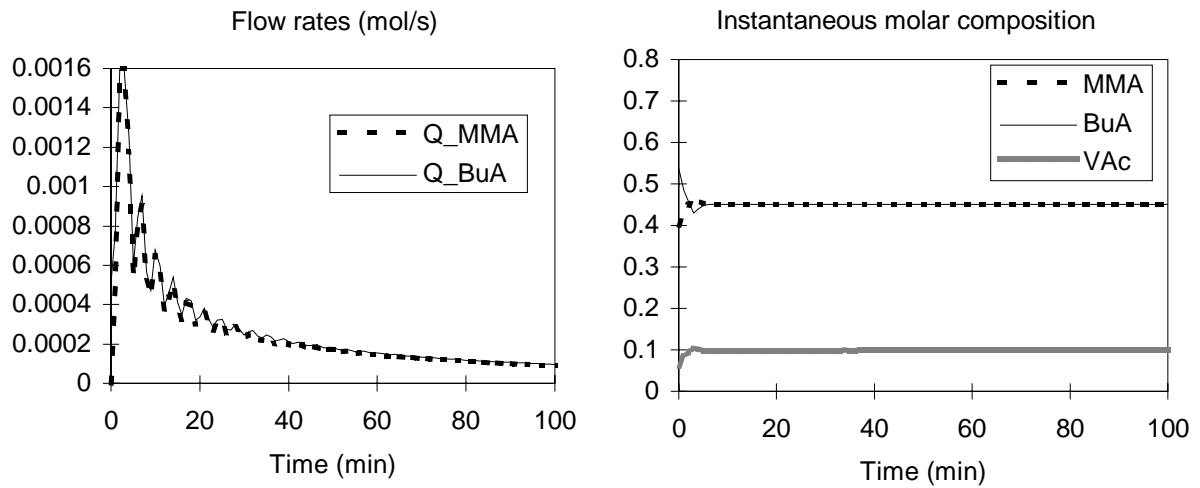

Figure 6.18a: Simulation of the controller.   Figure 6.18b: Simulation of the controller.

Figure 6.18b shows that the controller brings the composition to the desired value (45-45-10 MMA-BuA-VAc) even though the initial values contained an intended error in the monomer ratios. In Figure 6.18a, we can see that, even though Q_1 and Q_2 where calculated by two different controllers, the ratio Q_1/Q_2 was constant during the addition. Furthermore, it was found that:

$$Q_1 / Q_2 = \left(N_1 / N_2\right)_{initial}$$

In order to analyze this situation, let us rewrite the control objective, that is to maintain the monomer ratios at predefined values:

$$\frac{N_1}{N_3} = \left(\frac{N_1}{N_3}\right)^d \text{ and } \frac{N_2}{N_3} = \left(\frac{N_2}{N_3}\right)^d$$

However, if these ratios are constant, then the following ratio is also constant:

$$\frac{N_1}{N_2} = \frac{\left(N_1/N_3\right)^d}{\left(N_2/N_3\right)^d}$$

Therefore, it is sufficient to maintain this ratio N_1/N_2 at the desired value in the preemulsion, and to employ the single control law in equation 6.31 that maintains one of the monomer ratios at the desired value. The second ratio will be directly obtained if the monomer ratio (N_1/N_2) in the reactor is at the desired level. The possibility of introducing the monomers together has some advantages. First of all, this simplifies the experimental set-up, since a single pump is required in this case. Secondly, this guarantees that the monomer ratio N_1/N_2 in the feed remains at the desired value, even if a fault is produced in the pump. This will ensure that the monomer ratio N_1/N_2 in the reactor be at the desired value if and only if the ratio is correct in the reactor before the feed begins. This technique can be applied to any triplet of monomers. However, it should be clear that if a large perturbation causes the monomer ratio N_1/N_2 in the reactor to derive from the desired value, the controller will not be able in this case to rectify this error. Therefore, for monomers that have a wide difference in their reactivity ratios, it is recommended to employ two pumps.

In the case of MMA and BuA, it was found that these monomers react at the same ratio when involved in a terpolymerization with VAc, since it is impossible that MMA reacts without BuA being consumed. We have therefore used a single pump to introduce the monomers MMA and BuA. The flow rate of VAc is set to zero in these experiments since all the VAc was completely charged in the reactor at the beginning of the experiment. The recipes used to carry out these experiments are shown in table 6.3. Two different compositions were tested: 50:35:15 and 45:45:10 MMA:BuA:VAc by mole.

Table 6.3: Experiments of terpolymerization of MMA-BuA-VAc for the validation of the composition controller.

\ Run	C 23		C 26	
COMPOSITION^{SP}	45 - 45 - 10 % MMA-BuA-VAc		50 - 35 - 15 % MMA-BuA-VAc	
Component \	Initial charge (g)	Feed (g)	Initial charge (g)	Feed (g)
H_2O	1200	300	1200	300
MMa	23	450	33.6	640
BuA	60	544	54.3	550
VAc	86		172	-
Triton	6.87	7.8	7.42	8.91
DSS	-	3.06	-	3.01
KPS	3.097	-	3.096	-
Final particle diameter	242 nm		308 nm	
Final solids content	36%		44%	

In order to obtain a composition of 45-45-10 by mole, in experiment C23, the initial monomer ratios were found by equation 6.22 to be: $N_1/N_3=0.4648$ and $N_2/N_3=0.2269$, which gives: $N_1/N_2=2.0485$. This ratio is therefore set in the preemulsion. Figure 6.19a shows the evolution of the monomer ratios during this experiment. It can be seen that the monomer ratios oscillate around the desired values, especially at the end of the reaction. This is due to the fact that when the amount of monomer in the reactor is very small, the monomer ratio becomes very sensitive to the monomer feed rates. However, since the reaction rate decreases at the end of the reaction, even if the instantaneous composition oscillates slightly around the set-point (Figure 6.19b), the cumulative composition (Figure 6.19c) remained stable and close to the desired value. The instantaneous terpolymer composition is calculated from the monomer reaction rates, as given by the following equation:

$$F_i = \frac{R_{Pi}}{R_{P1} + R_{P2} + R_{P3}}$$

The cumulative composition is the integrated molar ratio of the amount of polymer i produced at every moment, with respect to the whole amount of monomer. The composition was validated by NMR off-line measurements. The NMR measurements show that a constant composition was maintained throughout the reaction. However, the NMR measurements present a difference with the estimated composition, at the beginning of the reaction.
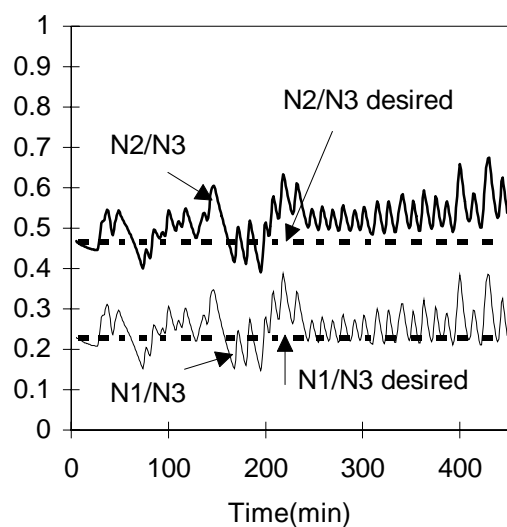

Figure 6.19a: Experiment C23. Monomer ratios N_1/N_3 and N_2/N_3, compared to the desired values. Desired composition = 45-45-10 by mole MMA-BuA-VAc.
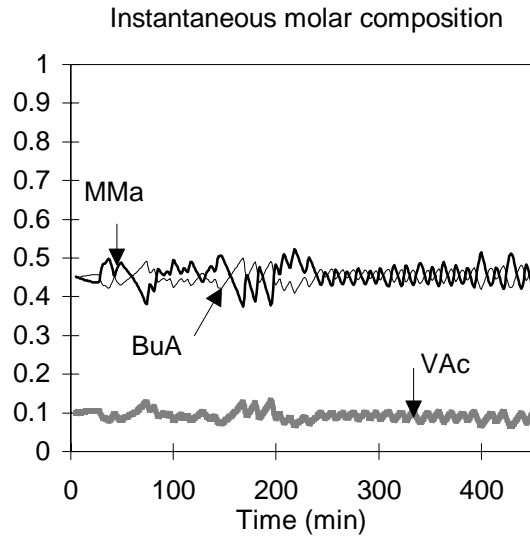
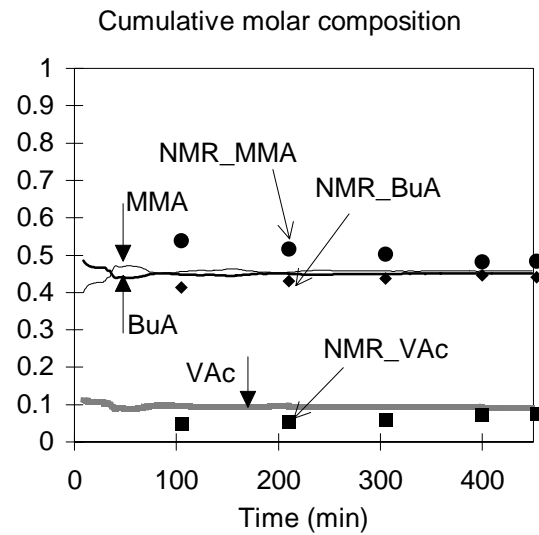Figure 6.19b: Experiment C23. SP=45-45-10 MMA-BuA-VAc.

Figure 6.19c: SP=45-45-10 MMA-BuA-VAc. Validation by NMR given by the points
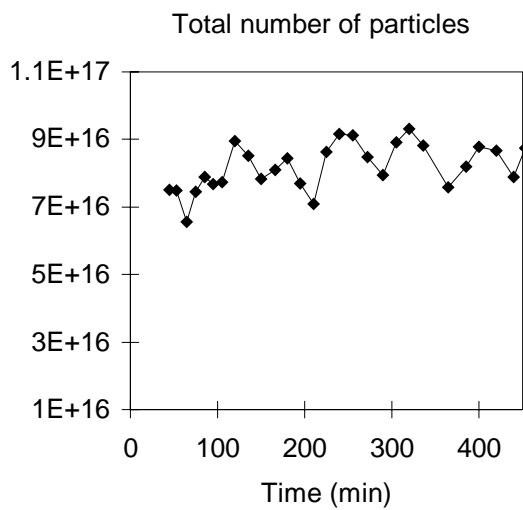

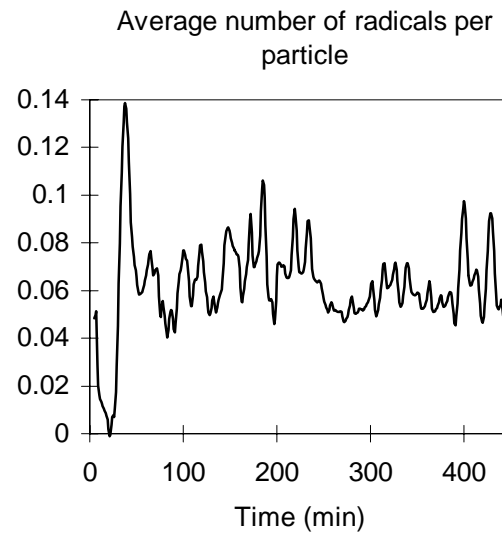Figure 6.19d: Experiment C23. Composition SP=45-45-10 MMA-BuA-VAc.

Figure 6.19e: Experiment C23. Composition SP=45-45-10 MMA-BuA-VAc.

The average number of radicals can be calculated off-line from the value of μ_2 estimated on-line by introducing the total number of particles determined from the off-line measurement of the particle diameter. The number of particles was found to be constant during the polymerization, as shown in Figure 6.19d. Figure 6.19e shows that the value of $\bar{n}$

was very low during this experiment. The oscillations in the curve of $\bar{n}$ are due to the sensitivity of the observer of $\bar{n}$ to variations in R_{pi}.

In experiment C26, the composition set-point was 50-35-15 MMA-BuA-VAc. The overall and individual conversions obtained for this experiment are shown in Figure 6.20a.
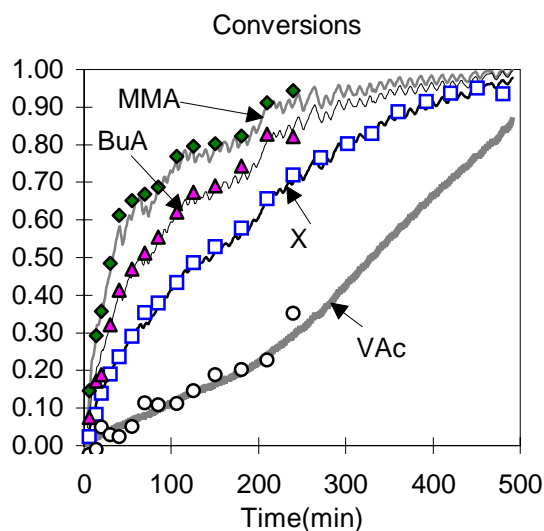

Figure 6.20a: Experiment C26. Experimental global conversion obtained by gravimetry, individual conversions validated by GC.
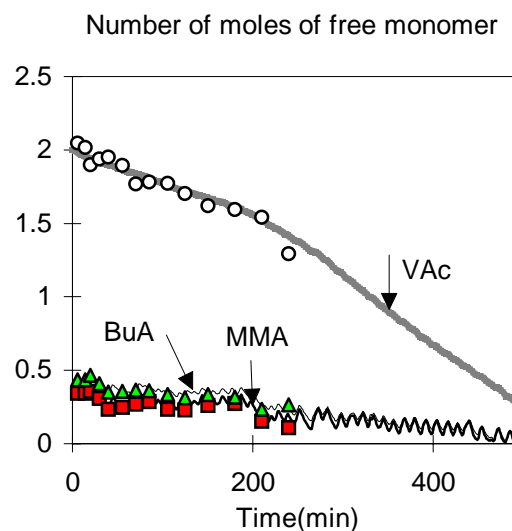
Figure 6.20b: Experiment C26. The number of moles of residual monomer is validated by GC.

The individual conversions were validated by measuring, off-line, the amount of residual monomer by means of GC. The obtained experimental measurements seem to agree with the estimated values. The estimated and experimental number of moles of residual monomer are shown in Figure 6.20b. The corresponding polymer composition produced at every moment is shown in Figure 6.20c.

Oscillations were observed in the instantaneous composition, especially at high conversions. The evolution of the cumulative composition however is stable and very close to the desired value, but does not exactly fit the experimental values obtained by NMR analysis of the terpolymer. However, if we look at Figures 6.19a and 6.19b, it can be seen that the GC measurements agree with the estimated values of the monomer individual conversions and the residual number of moles of monomer in the reactor. If we assume that the value of the polymer composition obtained by analyzing the polymer by NMR measurements is more precise than the value obtained by analyzing the residual monomer by GC, then the difference between the desired composition and the real one is due to a modeling error in the reaction

rates of monomers: K_{pij} and r_{ij}. The observer and controller are dependent on these kinetic data and therefore the estimation results are sensitive to the use of different reaction rate constants, as given by equations 6.22. At this level, the observer and controller work in an open-loop fashion, which means that the kinetic values are assumed to be well known. In fact, the reaction rate constants of the monomers used here, especially BuA, have widely been studied in the literature (e.g. Lyons et al. (1996), Gilbert (1995), van Herk (1997), Hutchinson et al. (1997), Beauchemin and Dubé (1999)), and several K_P values have been reported. The constants used in the control strategy are given in appendix II. They were chosen for use in the control strategy because they were found to give a realistic representation of the evolution of the process, in chapter 5.
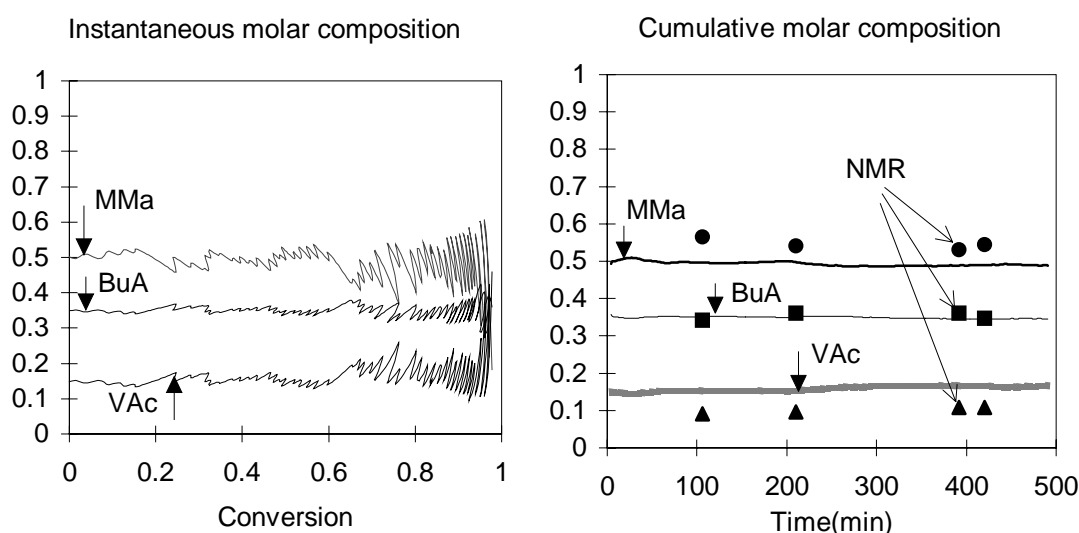

Figure 6.20c: Experiment C26. Desired composition=50-35-15 MMA-BuA-VAc. Validation by NMR measurements.

The estimated curve of $\bar{n}$ is given in Figure 6.20d. An increase in the value of $\bar{n}$ was observed at high conversion. This increase in $\bar{n}$ caused an increase in the reaction rate and therefore in the reaction temperature (Figure 6.20f). It can clearly be seen that the reaction temperature does not significantly exceed the reaction set-point, even though the experiment was done under isoperibolic conditions. For this reason, we did not use a controller of the thermostated bath during these experiments.

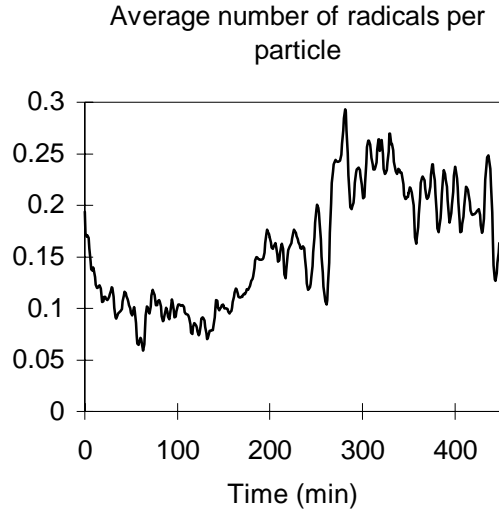Average number of radicals per particle

Total number of particles

Figure 6.20d: Experiment C26. $\bar{n}$ obtained off-line from the estimated value of μ_2.
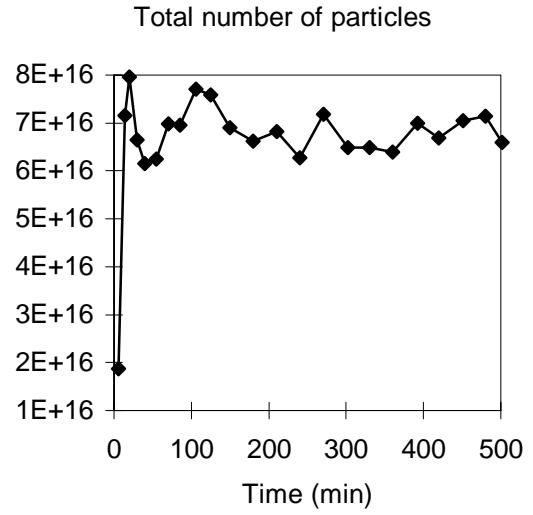
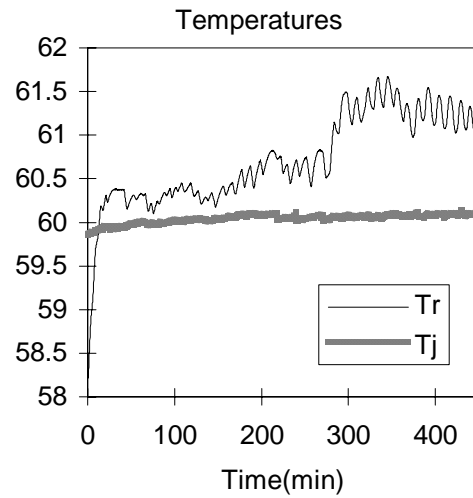Figure 6.20e: C26. N_P^T determined from the off-line particle diameter measurements.

Temperatures

Figure 6.20f: Experiment C26. Reactor (T_r) and jacket (T_j) temperatures.

6.4 Conclusion

The control strategy developed in this chapter is adapted for experimental practice. First of all, it is robust to uncertainties in the model of the pump. The technique does not therefore require excessive and frequent calibration, that would be necessary if the controller of the pump is not employed. Secondly, the composition control robustness is independent of the desired polymer composition. It was possible to maintain the composition of the polymer produced at a constant value for several compositions using the copolymerization system MMA/BuA and the terpolymerization system MMA/BuA/VAc. Finally, the technique does not require that we start the polymerization with a seed. A constant composition can be obtained even during the nucleation period.

The control strategy is dependent on the estimated calorimetric conversion. If an accurate estimation of the overall conversion is obtained by the calorimetric optimization procedure, the observer based on this estimate gives good estimates of the individual conversions, and the controller then tracks the desired composition trajectory.

It was observed that the estimation of the overall conversion is very sensitive to the flow rate variations at the end of the experiment and this leads to a composition drift, or oscillation. However, the amount of polymer produced at this time is not very important. We can therefore stop the control, and terminate the reaction in batch if the residual amount of monomer is not important, and does not effect the polymer final composition.

The control strategy developed in this chapter allowed us to realize the main objective of this work: maintaining the polymer composition at the desired value in copolymerization and terpolymerization processes. The technique is robust to modeling errors related to the evolution of the number of radicals in polymer particles, the monomer solubility in the aqueous phase, and to the pump model. However, the composition control necessitates good knowledge of the reaction kinetics, K_{pij} and r_{ij}. These parameters are usually well-known, or can be identified in laboratory scale experiments.

In the experiments tested in this chapter, all the desired amount of less reactive monomer was added at the beginning of the reaction. In our case, the reaction temperature was found to slightly exceed the reaction set-point temperature. However, in large reactors, the initial amount of monomer can produce a big increase in the reaction temperature which might be dangerous. For this reason, we give the possibility of adding the less reactive monomer in a fashion that guarantees operational security and the maximum productivity. This subject will be considered in the next chapter.

6.5 Nomenclature

Notation

A	a frequency factor (L/mol/s)
Ea	activation energy (kJ/mol)
K_{pij}	reaction rate constant between the active chain i and monomer j
$L_f h$	Lie derivative of the scalar field h with respect to the vector field f (hapter2)
$[M_i^p]$	concentration of monomer i in the polymer particles
$\bar{n}$	average number of radicals per particle
N_i	number of moles of free monomer i
N_P^T	total number of particles in the reactor
P_i^P	time averaged probability that the ultimate unit of an active chain is of type i
Q_i	molar flow rate of monomer i
R	universal gas constant (kJ/mol/K)
R_{pi}	rate of reaction of monomer i [mol/s]
u	input
V	voltage
x	state variables

Greek letters

ε	error
κ_p	proportional gain of the P controller
τ_I	integral gain of the PI controller
τ	system time constant (s)
μ	the number of moles of radicals in the polymer particles
υ	a linearizing input output transformation

6.6 Bibliography

1. Arzamendi, G. and J. M. Asua, Monomer addition policies for copolymer composition control in semi-continuous emulsion copolymerization, *J. Appl. Polym. Sci.* 38, 2019-2036, (1989).

2. Arzamendi, G., and J. M. Asua, Copolymer composition control during the seeded emulsion copolymerization of vinyl acetate and methyl acrylate, *Macromol. Chem., Macromol. Symp*, **35**, 36, 249-268, (1990).

3. Beauchemin, R.-C., and M. A. Dubé, bulk terpolymer composition prediction from copolymer reactivity ratios, *polym. react. Eng.*, **7**, 4, 485-499, (1999).

4. Buruaga, I. S., A. Echevarria, P. D. Armitage, J. C. de la Cal, J. R. Leiza, and J. M. Asua, On-line control of a semibatch emulsion polymerization reactor based on calorimetry, *AICHE*, **43**, 4, (1997)[a].

5. Buruaga, I. S., P. D. Armitage , J. R. Leiza, and J. M. Asua, On-line Control for maximum production rat of emulsion polymers of well defined polymer composition, *ECCE1*, **4-7**, 117-120, (1997)[b].

6. Buruaga, I. S., Ph. D. Armitage, J. R. Leiza, J. M. Asua, Nonlinear control for maximum production rate latexes of well-defined polymer composition, *Ind. Eng. Chem. Res.*, **36**, 4243-4254, (1997)[c].

7. Canu, P., S. Canegallo, M. Morbidelli, and G. Storti, Composition control in emulsion copolymerization. I. Optimal monomer feed policies, *J. Appl. Polym. Sci.* **54**, 1899-1917, (1994).

8. Choi, K. Y., Copolymer composition control policies for semibatch free radical copolymerization processes, *J. Appl. Polym. Sci.*, **37**, 1429-1433, (1989).

9. van Doremaele, G. H. J., H. A. S. Schoonbrood, J. Kurka, and A. L. German, Copolymer composition control by means of semicontinuous emulsion copolymerization, *J. Appl. Polym. Sci.*, **45**, 957-966, (1992).

10. Garcia, C. E., and M. Morari, Internal Model Control, 1. A unifying Review and some new results, *Ind. Eng. Chem. Process Des. Dev.*, **21**, 308-323, (1982).

11. Gilbert, R. G., a mechanistic approach, Colloid Science, R. H. Ottewill, and R. L. Rowell eds, (1995).

12. Gugliotta, L. M., G. Arzamendi, and J. Asua, Choice of monomer partition model in mathematical modeling of emulsion copolymerization systems, *J. Appl. Polym. Sci*, **55**, 1017-1039, (1995).

13. Guyot, A., J. Guillot, C. Graillat, and M. F. Llauro, Controlled composition in emulsion copolymerization application to butadiene-acrylonitrile copolymers, *J. Macromol. Sci. Chem.*, **A21(6&7)**, 683-699, (1984).

14. Hamielec, A. E., J. F. MacGregor, and A. Penlidis, Multicomponent free-radical polymerization in batch, semi-batch and continuous reactors, *Makromol. Chem. Macromol. Symp.*, **10**, 11, 521-570, (1987).

15. Hutchinson, R. A., J. H. McMinn, D. A. Paquet, Jr. S. Beuermann, and C. Jackson, A pulsed-laser study of penultimate copolymerization propagation kinetics for methylacrylate/n-butyl acrylate, *Ind. Eng. Res.*, **36**, 1103-1113, (1997).

16. Kravaris, C., R. A. Wright and J. F. Carrier, Nonlinear controllers for trajectory tracking in batch processes, *Computers Chem. Engng.*, **13**, ½, 73-82, (1989).

17. Leiza, J. R., J. C. de la Cal, G. R. Meira and J. M. Asua, On-line copolymer composition control in the semicontinuous emulsion copolymerization of ethyl acrylate and methyl methacrylate, *Polym. React. Eng.*, **1**, 4, 461-498, (1992-93).

18. Lyons, R. A., J. Hutovic, M. C. Piton, D. I. Christie, P. A. Clay, B. G. Manders, S. H. Kable, and R. G. Gilbert, Pulsed-laser polymerization measurements of the propagation rate coefficient for butyl acrylate, *Macromol.*, **29**, 1918-1927, (1996).

19. Saldivar, E., and W. H. Ray, Control of semicontinuous emulsion copolymerization reactors, *AIChE J.*, **43**, 8, (1997).

20. Schoonbrood, H. A.S., R. C; P. M. van Eijnatten, and A. L. German, Emulsion co- and terpolymerization of styrene, methyl methacrylate, and methyl acrylate. II. Control of emulsion terpolymer microstructure with optimal addition profiles, *J. of Polym. Sci.: Part A: Polymer Chem.*, **34**, 949-955,(1996)[b].

21. Tirrell, M., and K. Gromley, Composition control of batch copolymerization reactors, *Chem. Eng. Sci.*, 36, 367 (1981).

22. van Herk, A. M., Pulsed initiation polymerization as a means of obtaining propagation rate coefficients in free-radical polymerizations, *J.M.S.-Rec. Macromol. Chem. Phys.*, **C37**, 4, 633, 648, (1997).

CHAPTER VII ─────────────

MAXIMIZING PRODUCTIVITY

I-   Homopolymerization processes

II-   Copolymerization processes

III-   Terpolymerisation processes

7 MAXIMIZING PRODUCTIVITY

7.1 Introduction

Why maximize productivity? The objective of maximizing productivity in emulsion reactors is to manufacture lattices:

    ↻ with adequate final properties,

    ⧗ in the shortest possible time,

    ⛭ under safe conditions,

    💰 with reduced costs and added capacity.

How to maximize productivity in emulsion polymerization? In emulsion polymerization, the main locus of the reaction is the polymer particles. The overall productivity of the process depends therefore on the number and size of particles, on the concentration of monomer and radicals in the polymer particles, and on the reactor temperature. These variables are therefore the control inputs to maximize productivity.

Which control variables and why? The objective of this chapter is to maximize the productivity, while maintaining the polymer composition constant, if two or more monomers are used. The selected manipulated variable (among temperature, concentration of radicals and concentration of monomer) is the concentration of monomer in the polymer particles. On one hand, the use of the reaction temperature as a control variable of the reaction rate requires an improved study of the simultaneous temperature effect on the evolution of the final polymer properties (latex stability in particular) and will therefore not be considered here. On the other hand, the concentration of radicals in polymer particles is not going to be used to control the process. This concentration is usually not known and is difficult to model precisely, as it is very sensitive to inhibiting impurities and is governed by several factors, such as diffusion, adsorption and desorption phenomena that are not usually well understood and are difficult to manipulate explicitly.

However, while choosing the control variables, one must pay attention to the relation among them. If they are correlated, then the use of only one of them will not be an efficient method. In fact, the concentration of radicals in the polymer particles is affected by the concentration of monomer in the polymer particles, since the radical mobility, and therefore termination, in the polymer particles increases with increasing the concentration of monomer in the polymer particles. Therefore, maximizing the concentration of monomer in the polymer particles might not maximize the process productivity.

Our objective will be to maintain [M_P] at a set-point that is inferior to the saturation point, since exceeding this level will not help to increase the reaction rate, and it can provoke unwanted nucleation, thereby changing the particle size distribution.

Precautions in the control of the concentration of monomer in the polymer particles? As was shown in the last chapter, good composition control in emulsion co- and terpolymerizations can be achieved using calorimetry combined with some off-line measurements of the overall conversion. We outlined the possibility of composition control by other methods, described in the literature, where the most widely applied approach consists of introducing a mixture of monomers at the desired composition. However, in order to obtain good composition control with this technique it is necessary to use a very low flow rate of preemulsion, otherwise less reactive monomer(s) will accumulate in the reactor and the monomer composition will start to drift. For this reason, we presented a controlled feeding technique that can be adapted to increase productivity. The technique consisted of charging all the desired amount of the least reactive monomer at the beginning of the reaction, and to do a controlled feed of the other monomer(s).

Are there any other limitations? One of the simultaneous objectives of maximizing productivity is to ensure safe working conditions. In fact, provoking an increase in [M_P] might increase the reaction rate and therefore the heat produced by the reaction. However, physical limitations on the rate of heat removal exist, (such as the heat transfer coefficient, minimum jacket temperature and condenser heat load) and might sometimes prevent from evacuating all of the heat generated at high reaction rates. Attention must therefore be paid to the capacity of the cooling system (especially on large scale reactors) so that the reaction temperature remains lower than the critical temperature. A high increase in the reactor temperature

influences the polymer properties, such as, molecular weight, and might give rise to a runaway reaction (which might release environmentally dangerous substances, cause personal harm and material damage to the reactor).

The control strategy discussed in this chapter will thus have two objectives: simultaneously controlling the concentration of monomer in the polymer particles and the composition, while maintaining safe operating conditions. The concentration of monomer in the polymer particles must not exceed the saturation concentration and, if the heat produced exceeds the maximum admissible heat, then the concentration of monomer in the polymer particles is minimized. If this is not enough, other action must be taken, such as adding inhibitor. Here again, minimizing the concentration of monomer in the polymer particles might favor the gel effect which might increase the heat produced by the reaction. However, if the rate of heat produced by the reaction is exceeding the maximum admissible rate, or if we have a runaway reaction, we cannot imagine to add monomer to the reactor even if this might decrease the gel effect and decrease the reaction rate since sooner or later we will return to the same point.

How to quantify the jacket heat removal capability? The first thing to do is to estimate the maximum heat removal rate of the cooling system. In laboratory scale reactors, especially in emulsion polymerization at moderate solids content, the heat produced is generally immediately removed by the jacket under isoperibolic conditions. During the nucleation period, a high reaction rate can give rise to a rapid release of heat, and in this case a controlled cooling system should in fact be used to actively remove the produced amount of heat and to maintain isothermal conditions. However, in large scale reactors, even with an adapted cooling system, the large amount of monomer in the reactor and accompanied with the increase in viscosity (therefore a decrease in U), can make heat removal somewhat more difficult. In this case, the maximum cooling rate must be estimated on-line. This requires a good on-line estimation of U and a correlation between the heat removal rate and the heat released by the reaction (therefore the monomer flow rate). We discussed the on-line estimation of U in Chapter 3. Other studies have also treated these issues. For instance, Arzamendi and Asua (1991) proposed a method for the calculation of the monomer addition profiles for copolymer composition control with limited capacity for heat removal. They

simulated the thermal characteristics of an industrial reactor by isolating the jacket and placing a coil of heat transfer in the reactor.

Gloor and Warner (1996) quantified the heat removal capability by using a product that gives rise to more difficult heat removal than typical products, by means of increased viscosity. The heat transfer coefficient was then related to physical properties of the latex (viscosity, solids contents). During the reaction, the procedure starts by estimating the heat of polymerization (using a Mettler Toledo RC1 calorimeter), and then determining the best feed conditions (taking into consideration the constraints of safe operation, cost, and residual monomer level).

Buruaga et al. (1997c), also used calorimetry to maximize the production of vinyl acetate/butyl acrylate lattices under safe conditions and simultaneously maintain a production of a homogeneous copolymer composition. They proposed an empirical equation relating the rate of heat production by the reaction with the maximum heat removal rate (Q_{lim}). This latter depends on the heat transfer coefficient with the jacket, U, on the heat transfer area A, and on the difference between the reactor temperature and the jacket minimum temperature ($T_{j,min}$), as follows:

$$Q_{lim} = \alpha UA\left(T_R - T_{j,min}\right) \qquad (7.1)$$

where α is a corrective parameter. The authors tested two controllers: a proportional-integral (PI) (that tracks the flow rate of the less reactive monomer, the flow rate of the most reactive monomer being calculated by the composition controller) and a nonlinear model based controller (NLMBC), (that tracks the total amount of monomer to be added to the reactor). The objective of these controllers was to maintain the amount of heat produced at the maximum rate of heat removal. Both controllers gave satisfactory results. The controller of the total amount of monomers was also robust to sudden changes in the reaction rate, such as a shot of inhibitor. These experiments were carried out in an RC1 calorimeter. The control laws were implemented on an additional PC. In order to obtain continuous measurements of U, the authors developed a correlation based on the initial and final values of U, and on the solids contents.

In our work, no attempt was made to calculate the heat removal capacity of the 3 liter (the 7 liter reactor was not used for control studies) calorimeter. We will assume that the

maximum heat removal capacity is known and we simply impose a value to test the controller performance. We therefore fix an arbitrary value of Q_R that should not be exceeded. The concentration of monomer is thus limited either by the saturation concentration in the particles, or by this maximum value for Q_R (which ever is lower). Simultaneously, the co- and terpolymer composition must remain constant at all times.

In the first part of this chapter, we develop a controller of the concentration of monomer in the polymer particles and the rate of heat produced in emulsion homopolymerization, where obviously there is no problem of composition control. Therefore, the first step is the estimation of the concentration of monomers and radicals in the polymer particles. Next, we develop controllers of the heat released in co- and terpolymerization processes, while respecting the controllers developed earlier for the composition control. In the case of emulsion copolymerization, the flow rate of the less reactive monomer is used to maximize the concentration of monomer in the polymer particles, and the composition controller uses the flow rate of the most reactive monomer, as before. In the terpolymerization case, the composition controller contains 2 coupled controllers that manipulate the flow rates of the two more reactive monomers. This is coupled with a third controller that regulates the concentration of monomer in the polymer particles.

7.2 Homopolymerization processes

The major thrust of the work done in this thesis is the composition control, which is necessary when two or more monomers are involved in the reaction. For this reason we still did not address estimation or control in emulsion homopolymerization. However, several polymers are produced by means of batch, semi-continuous or continuous homopolymerization processes, e.g. poly styrene, poly vinyl acetate, poly methyl methacrylate and poly butyl acrylate. Several works treat the modeling of emulsion homopolymerization, e.g. Lin and Chiu (1982), Schork and Ray (1987) and Gilmore et al. (1993). Penlidis et al. (1985) studied the polymerization of vinyl acetate and reported theoretical and experimental results. The control of emulsion homopolymerization reactors was less studied than solution reactors. We can however mention, Semino and Ray (1995a and 1995b), concerning the population control and Jang and Lin (1991), treating the control of batch polymerization of VAc, by manipulating the temperature.

In order to maximize productivity under safe conditions, without influencing the latex quality, two objectives must be realized simultaneously:

- the amount of free monomer must not exceed the saturation concentration. An accumulation of monomer in the reaction might give rise to a thermal runaway, especially in large reactors, and might provoke secondary nucleation. This necessitates the measurement of $[M_1^P]$ at every moment.
- the amount of energy produced at each moment must be inferior to the maximum admissible rate, that is fixed by the cooling system. This necessitates the measurement of Q_R at every moment.

The material balance of a semi-continuous homopolymerization is:

$$\dot{N}_1 = Q_1 - R_{P1} \tag{7.2}$$

where, in emulsion homopolymerization, the rate of reaction of monomer is proportional to μ and $[M_1^p]$ and to the propagation constant of reaction of this monomer, K_{P1}, according to the following equation:

$$R_{P1} = K_{P1}\mu\left[M_1^p\right] \tag{7.3}$$

The concentration of radicals in polymer particles is given by:

$$\mu = \frac{\bar{n}N_P^T}{N_A} \tag{7.4}$$

where $\bar{n}$ is the average number of radicals per particle, N_P^T is the total number of particles in the reactor ($N_P^T = N_P \times V$), and N_A is Avogadro's number.

The material balance (7.2) shows that the reaction rate is determined by two main parameters: the number of moles of radicals, μ, and the concentration of monomer, $[M_1^p]$, in the polymer particles, assuming that K_{P1} is constant, since the reactor temperature is usually maintained constant during the reaction for quality control. Therefore, the maximum productivity is obtained when the product $\mu[M^p]$ is maximized. If these two parameters are independent, we can then maximize each of them separately, or only one of them, in order to maximize R_P. However, $[M^p]$ might influence μ by affecting the gel effect in the polymer particles. Therefore maximizing $[M^p]$ does not necessarily maximize R_P. Moreover, as mentioned throughout this work, the model of μ is not well known and is therefore not easily controlled. For these reasons, we will concentrate on maximizing the concentration of monomer in the polymer particles. We will however pay an attention to the rate of heat produced by the reaction, that must not exceed a specific point. If the rate of heat produced becomes important, our objective will be to minimize $[M^p]$.

In order to estimate the relation between Q_R and the reaction rate, then μ and $[M^p]$ must be known. In fact, the estimation of μ and $[M^p]$ is very important during the reaction. μ

infers a lot of information about the process, e.g. reaction rate (which allow us to control Q_R), molecular weight and number of particles. When the number of particles is constant, an increase in μ signifies an increase in $\bar{n}$, which might be due to a gel effect or some unforeseen event in the reactor.

To estimate $[M_1^p]$ and μ we will use the technique developed in Chapter 3 based on calorimetric measurements to estimate the monomer conversion on-line. In semi-continuous homopolymerization, the number of residual moles of monomer can directly be determined from the conversion, as follows:

$$X_g = \frac{\left(N_1^T - N_1\right)}{N_1^T} = 1 - \frac{N_1}{N_1^T} \qquad (7.5)$$

The total number of moles of free monomer at time t is the initial number of moles $N_{1,0}$ plus the sum of the molar flow rate (Q_1) added up to time (t):

$$N_1^T = N_{1,0} + \int_0^t Q_1 dt \qquad (7.6)$$

The concentration of monomer in the polymer particles depends on the maximum saturation of particles during interval II and in interval III, where monomer droplets vanishes, all the residual amount of monomer is in the polymer particles:

$$\left[M_1^p\right] = \begin{cases} \dfrac{\left(1-\phi_p^p\right)\rho_1}{MW_1}, & \text{Interval II} \\[4mm] \dfrac{N_1}{MW_1\left(\left(N_1^T - N_1\right)/\rho_{1,h} + N_1/\rho_1\right)}, & \text{else} \end{cases} \qquad (7.7)$$

where interval II is handled if and only if:

$$\frac{MW_1 N_1}{\rho_1} - \frac{\left(1-\phi_p^p\right)}{\phi_p^p}\left(\frac{MW_1}{\rho_{1,h}}\left(N_1^T - N_1\right)\right) \geq 0 \qquad (7.8)$$

and ρ_1 and $\rho_{1,homo}$ are the monomer and polymer densities, MW_1 the molecular weight of monomer and ϕ_p^p is the volumetric fraction of polymer in the polymer particles (polymer+monomer in the particles). The value of ϕ_p^p, under saturation conditions, can be

found in the literature for several polymers and monomers (e.g. Gilbert (1995)). Therefore, the concentration of monomer in the polymer particles can directly be measured.

If the monomer conversion is measured on-line, μ is the unique unknown variable in the material balance. Therefore, it can be directly obtained from the time variation of the number of moles of monomer. This requires the evaluation of the derivative of N_1, which might give rise to oscillations in the estimation of μ. We propose therefore to use an observer to estimate μ and N_1.

In the following section, we treat the estimation of μ and validate it experimentally. We then develop a control law that calculates the desired flow rate of monomer in order to maximize $[M^P]$, under safe conditions.

7.2.1 *Estimation of μ*

Consider the augmented system representing the unknown dynamic of μ by ε_μ:

$$\dot{N}_1 = Q_1 - \mu\left[M_1^p\right]K_{P1}$$
$$\dot{\mu} = \varepsilon_\mu$$
(7.9)

where $[M_1{}^P]$ is given by equation (7.7).

System (7.9) can be written in the following form:

$$\begin{bmatrix} \dot{N}_1 \\ \dot{\mu} \end{bmatrix} = \underbrace{\begin{bmatrix} 0 & -\left[M_1^P\right]K_{P1} \\ 0 & 0 \end{bmatrix}}_{A} \underbrace{\begin{bmatrix} N_1 \\ \mu \end{bmatrix}}_{x} + \underbrace{\begin{bmatrix} Q_1 \\ 0 \end{bmatrix}}_{q} + \begin{bmatrix} 0 \\ \varepsilon_\mu \end{bmatrix}$$
(7.10)
$$y = Cx = \begin{bmatrix} 1 & 0 \end{bmatrix} x = N_1$$

Under this form, we cannot directly apply the high gain observer, since one of its limitations is that the state matrix A be positive. In order to get around this problem, we can do a change of co-ordinates on μ by defining a new variable ς, such that:

$$\varsigma = -\mu$$
(7.11)

The system becomes:

$$\begin{bmatrix} \dot{N}_1 \\ \dot{\sigma} \end{bmatrix} = \underbrace{\begin{bmatrix} 0 & \left[M_1^P\right]K_{P1} \\ 0 & 0 \end{bmatrix}}_{A} \underbrace{\begin{bmatrix} N_1 \\ \varsigma \end{bmatrix}}_{x} + \underbrace{\begin{bmatrix} Q_1 \\ 0 \end{bmatrix}}_{u} + \begin{bmatrix} 0 \\ \varepsilon_\varsigma \end{bmatrix}$$
(7.12)
$$y = Cx = \begin{bmatrix} 1 & 0 \end{bmatrix} x = N_1$$

The new system (7.12) is already under a canonical form of observability. A high gain observer (Chapter 2) can be used without a change of co-ordinates. The observer is given by the following system:

$$\dot{\hat{N}}_1 = Q_1 + \left[M_1^P\right]K_P\hat{\varsigma} - 2\theta(\hat{N}_1 - N_1)$$

$$\dot{\hat{\varsigma}} = -\frac{\theta^2}{\left[M_1^P\right]K_P}(\hat{N}_1 - N_1) \tag{7.13}$$

This observer has been tested during the homopolymerization, of styrene (distilled), vinyl acetate, and butyl acrylate in the 7 liter calorimeter. The parameter θ was set to be equal to 0.01. The recipes of these experiments are given in Table 7.1 The number of radicals per particle was determined off-line, by introducing the number of particles, determined from the measurements of particle size.

Table 7.1: Homopolymerization recipes for the validation of the estimator of μ.

Component \ experiment	Styrene (15/3/99a)	Vinyl acetate	Methyl methacrylate
monomer	600	600	600
H_2O	2403	2400	2400
Dodecyl sulfate, sodium salt	4.56	-	-
Sodium dioctyl sulfosuccinate	-	3	3
Potassium persulfat	4.41	1.84	1.84
Final solid contents	20.5 %	19 %	14 %
Final particle size	107 nm	120 nm	111 nm

The temperature measurements are used to estimate the heat produced by the reaction on-line, and therefore the monomer conversion. As usual, these estimates are corrected by introducing some off-line measurements of the gravimetric conversion. This latter is used in the estimator based on the monomer material balance to estimate the number of moles of radicals in the polymer particles, μ. By definition, μ contains information on the number of particles and the average number of radicals per particles, $\bar{n}$. This latter parameter can help in the modeling and simulation of the evolution of radicals in the polymer particles (absorption, desorption and termination). $\bar{n}$ can be obtained from μ, if the number of particles is known.
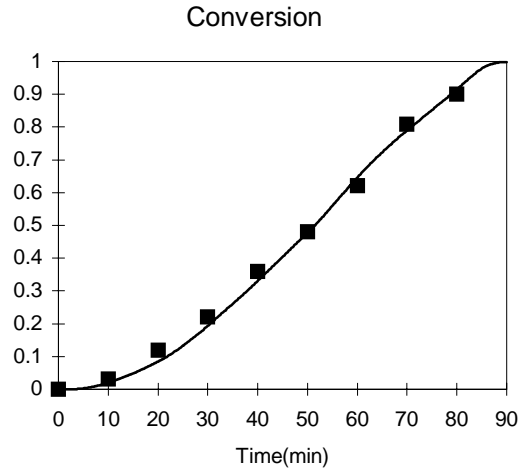
Figure 7.1: Overall estimated (—) and gravimetric conversions (▣) during the homopolymerization of styrene (15/3/99a).
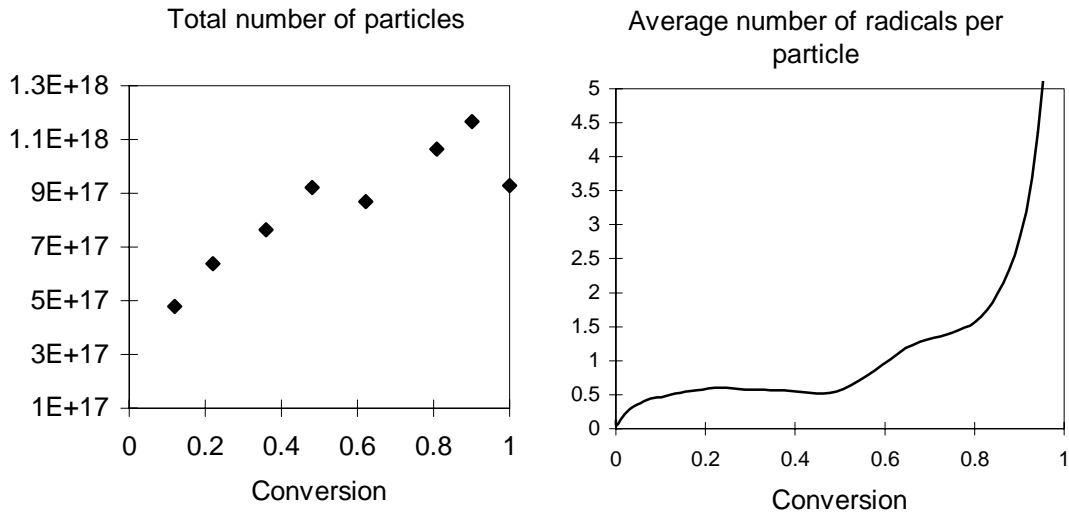

Figure 7.2: Total number of particles obtained, at left, and the estimated $\bar{n}$, at right, during the homopolymerization of styrene (15/3/99a).

Figure 7.2 shows the evolution of $\bar{n}$ during the homopolymerization of styrene. It can be seen that $\bar{n}$ is equal to 0.5 during interval II and increases at the end of the reaction, due to the gel effect, as expected. This demonstrates the feasibility of the approach and measurement techniques. It should be mentioned that the number of particles is estimated based on the measurement of the particle size by Dynamic Data Scattering. The precision of the technique must be taken into account when analyzing the variations in N_P^T and therefore in $\bar{n}$. The technique therefore gives us a good estimate of μ, but only tendencies in the variation of $\bar{n}$.
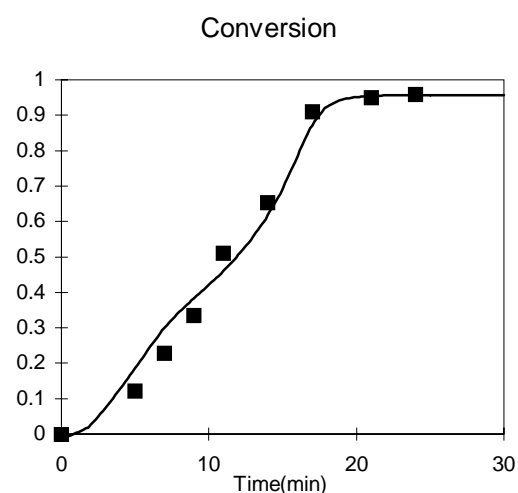
Conversion

Figure 7.3: Overall conversion estimated (—) and gravimetric conversion (▣).
Homopolymerization of Vinyl acetate.

Total number of polymer particles
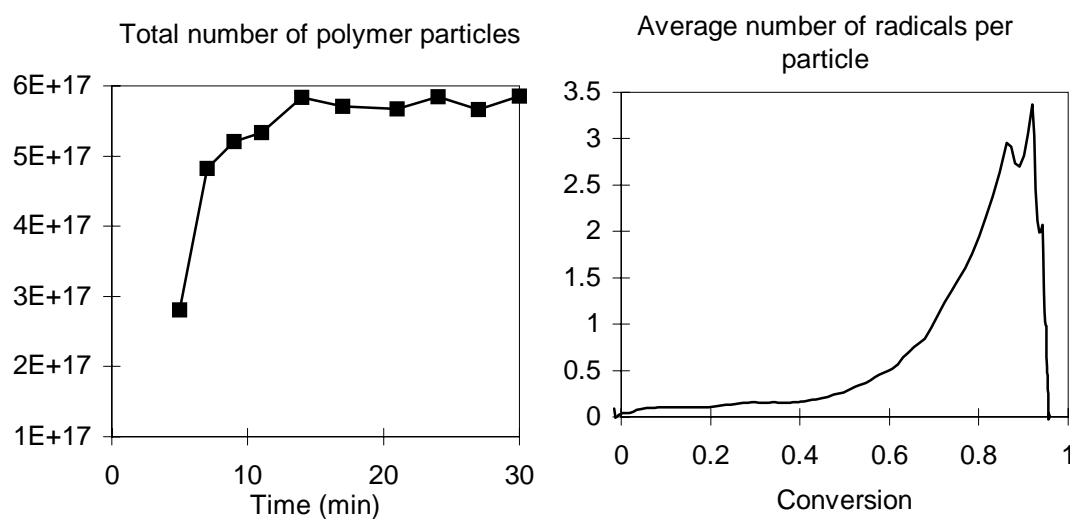
Average number of radicals per particle

Figure 7.4: Experiment homopolymerization of Vinyl acetate: Total number of particles in the reactor, at left, and the estimated $\bar{n}$, at right.

Figures 7.4 and 7.6 give the evolution of N_P^T and $\bar{n}$ during the homopolymerization of vinyl acetate and methyl methacrylate, respectively. In each case an increase of $\bar{n}$ noted at the end of the reaction.
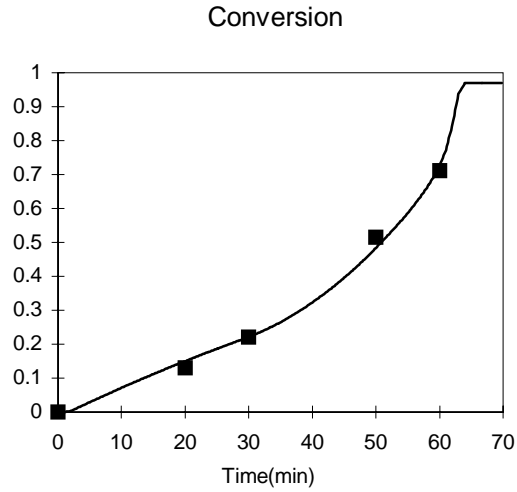
Conversion

Figure 7.5: Overall conversion estimated (——) and gravimetric conversion (▣).

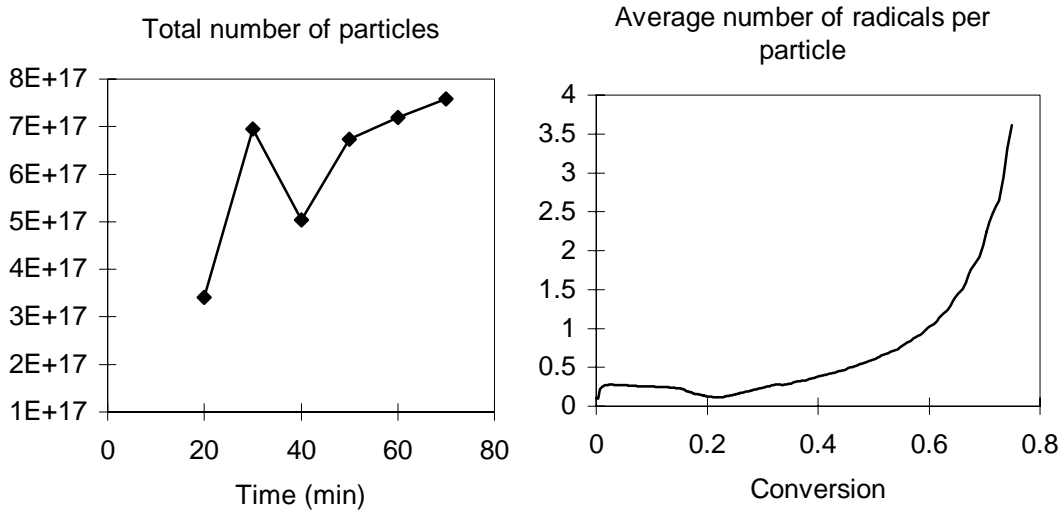Homopolymerization of methyl methacrylate, at right.

Figure 7.6: Experiment homopolymerization of methyl acrylate: Total number of particles in

the reactor, at left, and the estimated $\overline{n}$, at right.

In the next section, we will look at a control law of $[M^P]$ and Q_R based on the obtained estimate of μ.

7.2.2 Control of Q_R and $[M^p]$

The manipulated variable that allows us to control the concentration of monomer in the polymer particles is Q_1. Since the overall conversion can be obtained on-line by calorimetry, we can take N_1 as the model output. We can therefore directly write a control law that minimizes the error between the desired and real value of N_1. Since the reaction rate R_{P1} is nonlinear, here again we use a nonlinear control law with input/output linearization, as defined in Chapter 2.

Consider the material balance,

$$\dot{N}_1 = \underbrace{Q_1}_{u} - \underbrace{R_{P1}}_{f}$$

$$y = \underbrace{N_1}_{h=x}$$

(7.14)

Before calculating a transformation that renders the input/output comportment linear, we check if the relative order is equal to one, as defined in Chapter 2. For $r=1$, we calculate $< dh, ad_f^{r-1}(g) >$:

$$L_f h = \frac{\partial h}{\partial x} f$$
$$= -R_{P1} \neq 0$$

Therefore, the relative order of the system $r=1$. Therefore we calculate the following transformation :

$$\upsilon = \Omega(x,u) = \sum_{k=0}^{1} \beta_k L_f^k h + (-1)^0 \beta_1 < dh, ad_f^0(g) > u$$

$$= \beta_0 N_1 + \beta_1\left(- R_{P1}\right) + \beta_1 u$$

(7.15)

which implies:

$$u = \frac{\upsilon - \beta_0 N_1 + \beta_1 R_{P1}}{\beta_1}$$

(7.16)

We can use a linear P loop as an external input:

$$\upsilon - \beta_0 N_1 = \kappa_p \underbrace{(y^d - y)}_{\varepsilon} \tag{7.17}$$

Therefore,

$$u = Q_1 = \frac{\kappa_p}{\beta_1} \varepsilon + R_{P1} \tag{7.18}$$

where the value of the gain κ_p/β_1 was chosen to be equal to 0.01 as a compromise between rapidity of convergence and avoiding oscillations.

The desired output, $y^d = N_1^d$ is calculated by two equations. Fist of all N_1^d is calculated as a function of the maximum polymer saturation with monomer. The saturation condition is given by equation (7.8). The value of N_1^d that maintains the polymer particles at the saturation value, without an excess of monomer, is therefore:

$$N_1^d = \frac{N_1^T / \rho_{1,h}}{\left(\dfrac{1}{\rho_1} \dfrac{\phi_p^p}{\left(1 - \phi_p^p\right)} + \dfrac{1}{\rho_{1,h}} \right)} \tag{7.19}$$

On the other hand N_1^d that ensures the production of a heat that is lower than the maximum heat removal capability is calculated from the maximum heat permitted $Q_{R,max}$ that depends linearly on the rate of reaction:

$$\begin{aligned} Q_{R,max} &= \left(- \Delta H_{P1}\right) R_{P1} \\ &= \left(- \Delta H_{P1}\right) \mu \left[M_1^p\right] K_{p1} \end{aligned} \tag{7.20}$$

As we mentioned earlier, no attempt was made to calculate the heat removal capability of the cooling system in our small reactors, but we simply choose a $Q_{R, max}$ that should not be exceeded (and that we verified was attainable). Since we want to operate in phase III where there are no monomer droplets, $[M_1^p]$ is represented by the equation governing interval III. μ can be obtained from the observer defined in the last section. Therefore, we can calculate N_1^d from equation (7.20), and we obtain the following equation:

$$N_1^d = \frac{Q_{R,max} \, MW_1 / \rho_{1,h}}{\left(\left(-\Delta H_{P1} \right) \mu K_{P1} - Q_{R,max} \left(\dfrac{MW_1}{\rho_1} - \dfrac{MW_1}{\rho_{1,h}} \right) \right)} \qquad (7.21)$$

y^d is therefore the lowest value N_1^d obtained from the two equations (7.19) and (7.21). Tracking the minimum value of N_1^d allows us to maintain the polymer particles as close as possible from the saturation value and to minimize $[M^P]$ if the heat production rate exceeds the maximum permitted rate. In equation 7.21, μ is not manipulated to control Q_R, but is assumed to be known and independent of $[M^P]$.

The controller was tested in the simulation of homopolymerization of polystyrene. The amount of monomer and the number of radicals in the polymer particles were chosen in a way that both equations (7.19) and (7.21) are used to calculate N_1^d during the simulation.
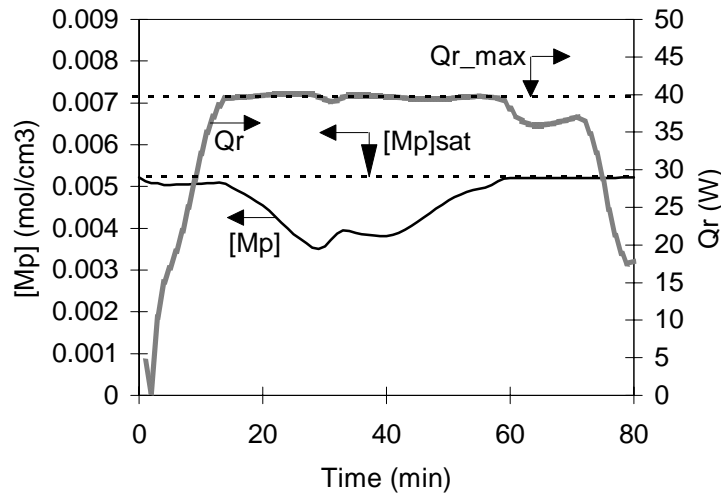

Figure 7.7: Simulation of styrene homopolymerization. The heat produced by the reaction and the concentration of monomer in the polymer particles.

Figure 7.7 shows clearly that the two objectives (maintaining the heat at the maximum allowed value and the concentration of monomer in the polymer particles at the saturation value as long as possible) are achieved. At the beginning of the reaction, the rate of heat release (Q_R) is inferior to $Q_{R,max} = 40$ W. In this case equation 7.19 is used to calculate N_1^d. When the heat released by the reaction attains $Q_{R,max}$, equation 7.21 is used to calculate N_1^d,

and the concentration of monomer in the polymer particles must now be inferior to the saturation value in order to prevent that the heat produced by the reaction term to exceed $Q_{R,max}$. If Q_R decreases, equation 7.19 is used again to bring the concentration of monomer in the polymer particles up to the saturation value. The flow rate of monomer, Q_1 obtained to satisfy the control strategy illustrated by Figure 7.7 is shown in Figure 7.8 below.
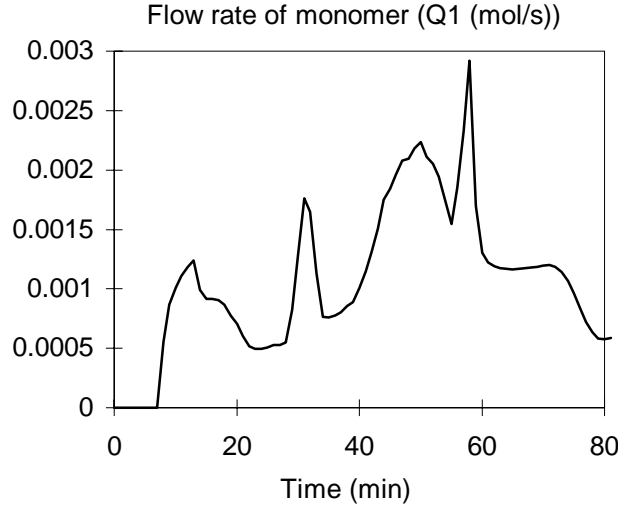

Figure 7.8 : Simulation of styrene homopolymerization. Flow rate of styrene (mol/s).

During the simulation we did not account for the dependence of μ on $[M^P]$, which allowed us to control Q_R by manipulating $[M_P]$. In fact, this is not usually true. Therefore, as stated earlier, we will emphasize on controlling $[M^P]$.

The control strategy was experimentally tested during the styrene homopolymerization, where no attempt was made to control the heat produced by the reaction. The mean objective was to maintain $[M_P]$ at $0.5 \times [M_P]^{sat}$. The recipe used during this experiment is shown in Table 7.2.

Table 7.2: Homopolymerization of poly styrene. Control of [M_P].

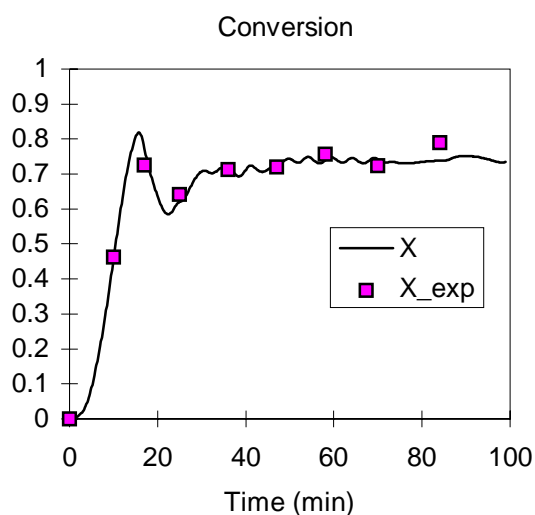| \ experiment Component \	C32	
	Initial charge	Preemulsion
Styrene	104	600
H_2O	1329	300
Dodecyl sulfate, sodium salt	3	-
Triton	-	9.47
Potassium persulfat	3.03	-
Temperature	70 °C	
Final solid contents	23 %	
Final particle size	88 nm	

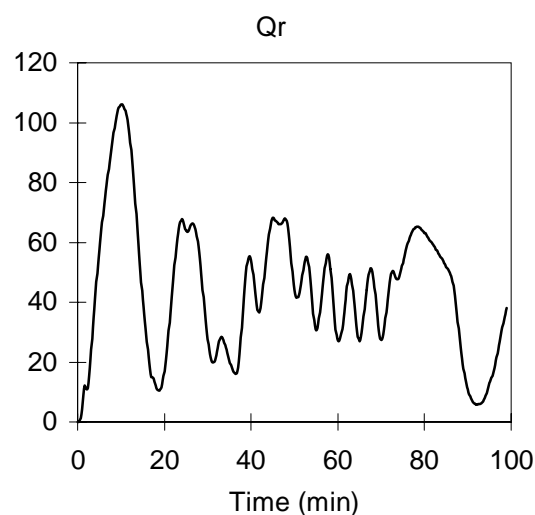Figure 7.9a: Experiment C32. Estimated conversion by calorimetry.

Figure 7.9b: C32. Heat produced by the reaction (W), obtained by calorimetry.

Figures 7.9a and b show the monomer conversion and the heat produced by the homopolymerization of styrene. The monomer addition starts at 15 minutes of the reaction, since the initial monomer charge allowed the concentration of monomer in the polymer particles to be superior than the desired value until this moment. Thereafter, it can be seen that the conversion was maintained almost constant during the semi-continuous part.
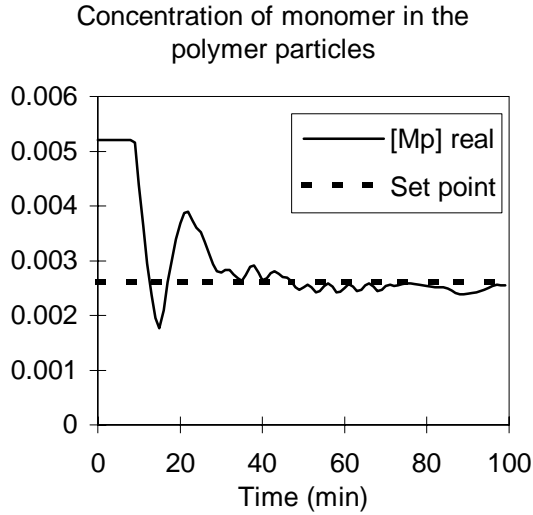
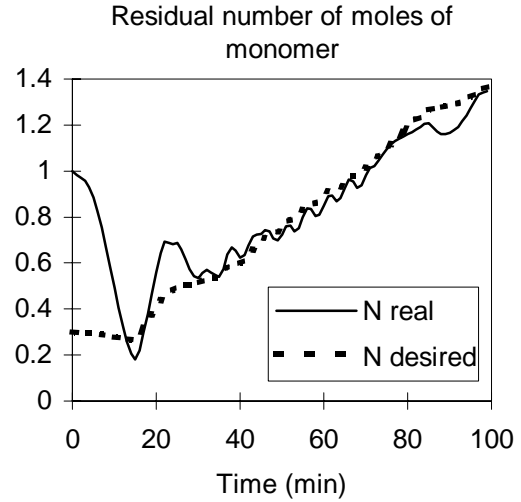Figure 7.9c: Experiment C32. [M$_P$] (mol/cm^3).

Figure 7.9d: Experiment C32. Real and desired number of moles of monomers.

However, it can be seen that Q$_R$ oscillates during the semi-continuous part of the reaction. This is due to the oscillations in the concentration of monomer in the polymer particles, Figure 7.9c. The figure shows that at the beginning of the reaction [M$_P$] was maintained at the saturation value for 10 minutes. When the value of [M$_P$] becomes to be inferior to the set-point, the controller is activated. However, since at the beginning of the reaction the estimations are based on the initial estimate of UA, the estimated conversion was not very precise. This caused a drift in the controller until the convergence of the optimization loop is achieved. Thereafter, it can be seen that the concentration of monomer in the polymer particles is maintained at the set-point, with some oscillations that are usually due to the optimization technique.

7.3 Copolymerization processes

In Chapter 6 we developed a control strategy that allowed us to maintain the copolymer composition at a predefined value, where the control variable was the flow rate of the more reactive monomer. The less reactive monomer could be entirely charged at the beginning of the reaction, or can be introduced separately at a known flow rate. introducing all the desired amount of the less reactive monomer might in some cases liberate more heat than the cooling system is able to evacuate. Therefore, the less reactive monomer must be introduced in semi-continuous fashion. It is preferable added to maintain the amount of free monomer in the reactor around the saturation value of polymer particles, unless the rate of heat produced by the reaction in this case exceeds the maximum admissible value, where we have to minimize $[M^P]$.

The control strategy will include the control law used to track the polymer composition, and that calculates the flow rate of the more reactive monomer in order to maintain N_1/N_2 at the required value (i.e. that yields the desired composition). In addition, the flow rate of the less reactive monomer is used to maintain the polymer particles saturated with monomer, under the condition that the heat released by the reaction does not exceed a predefined value, $Q_{R,max}$. The two controls must be coupled in a way that permits to realize all these objectives together. Q_2 is however calculated first in a way that maintains $[M^P]$ at $[M^P]^{sat}$, and then Q_1 is calculated in a way that maintains (N_1/N_2) at $(N_1/N_2)^d$. The sum of both Q_1 and Q_2 must not allow $[M^P]$ to exceed $[M^P]^{sat}$.

We consider again the copolymerization material balance, with the control output N_2:

$$\dot{x} = \begin{bmatrix} \dot{N}_1 \\ \dot{N}_2 \end{bmatrix} = \underbrace{\begin{bmatrix} Q_1 - R_{P1} \\ -R_{P2} \end{bmatrix}}_{f(x)} + \underbrace{\begin{bmatrix} 0 \\ 1 \end{bmatrix}}_{g(x)} \underbrace{Q_2}_{u} \tag{7.22}$$

$$y = \underbrace{N_2}_{h(x)}$$

283

Assuming that N_1 is the more reactive monomer, then its flow rate is calculated by the nonlinear control law that tracks the ratio (N_1/N_2), developed in Chapter 6, as given by the following equation:

$$Q_1 = .01 \times \left(N_2 \left(N_1 / N_2 \right)^d - N_1 \right) + R_{P1} \tag{7.23}$$

In order to maximize $[M^P]$ under safe conditions, we calculate the desired N_2 (since N_1 is calculated by the first control law) that allows us to maintain the concentration of monomer in the polymer particles at the saturation value, and the desired N_2 that ensures the production of a quantity of heat inferior to the set-point. The lowest value between the two calculations ensures maximizing $[M^P]$ and operating under safe conditions.

First of all, we calculate the desired N_2 needed to maintain $[M^p]$ at $[M^p]^{sat}$. The polymer particles are saturated with monomer if the volume of free monomer is superior or equal to the desired volume of monomer required to saturate the polymer particles, represented by the following equation:

$$\alpha N_1 + \beta N_2 \geq \gamma \tag{7.24}$$

with:

$$\alpha = \frac{MW_1}{\rho_1} + \frac{MW_1}{\rho_{1,h}} \frac{\left(1 - \phi_p^p \right)}{\phi_p^p}$$

$$\beta = \frac{MW_2}{\rho_2} + \frac{MW_2}{\rho_{2,h}} \frac{\left(1 - \phi_p^p \right)}{\phi_p^p}$$

$$\gamma = \frac{\left(1 - \phi_p^p \right)}{\phi_p^p} \left(\frac{MW_1 N_1^T}{\rho_{1,h}} + \frac{MW_2 N_2^T}{\rho_{2,h}} \right)$$

The desired number of moles of the less reactive monomer (N_2^d) is therefore given by the following equation:

$$N_2^d = \frac{\gamma}{\alpha \left(\dfrac{N_1}{N_2} \right)^d + \beta} \tag{7.25}$$

By introducing $(N_1/N_2)^d$, this relation ensures that the polymer particle be saturated, and that no excess of monomer be introduced. This means that if a certain amount of monomer is desired to saturate the polymer particles, then a specific quantity of the less reactive monomer is added, and the composition control permits to add the desired amount of N_1 that maintains N_1/N_2 at the desired value, and this amount is precisely the amount of monomer needed to complete the polymer saturation with monomer. Controlling $[M^p]$ is therefore not decoupled from the composition control law.

Secondly, we calculate a set-point $N_2{}^d$ that is used to maintain Q_R inferior to $Q_{R,max}$. The total heat produced by the reaction is the linear sum of the heat produced by each monomer, as follows:

$$Q_R = \left(-\Delta H_{P1}\right)R_{P1} + \left(-\Delta H_{P2}\right)R_{P2} \tag{7.26}$$

Since μ and R_{pi} are estimated, we can calculate N_2 that is needed to take the heat production up to $Q_{R,max}$.

$$N_2^d = \cfrac{MW_2 N_2^T / \rho_{2,h}}{\left(\cfrac{\Delta H_{P2}\mu}{\left(Q_{R,max} - \Delta H_{P1}R_{P1}\right)}\left(\cfrac{K_{P11}\left(\cfrac{N_1}{N_2}\right)^d}{\left(\cfrac{N_1}{N_2}\right)^d + \cfrac{K_{P12}}{K_{P211}}} + \cfrac{K_{P22}}{1 + \cfrac{K_{P21}}{K_{P12}}\left(\cfrac{N_1}{N_2}\right)^d}\right) - MW_2\left(\cfrac{1}{\rho_2} - \cfrac{1}{\rho_{2,h}}\right)\right)} \tag{7.27}$$

y^d is the minimum $N_2{}^d$ obtained from the equations (7.25) and (7.27).

Now we construct a control law that permits to minimize the error between N_2 and $y^d = N_2{}^d$. First of all, we calculate the relative order, as defined in Chapter 2. For $r=1$, $<dh, ad_f^{r-1}(g)>$ gives:

$$\begin{aligned} L_f h &= \frac{\partial h}{\partial x} f \\ &= -R_{P2} \neq 0 \end{aligned}$$

The relative order of the system is therefore equal to 1 and we can directly calculate an input/output linearizing transformation, as follows,:

$$\upsilon = \Omega(x,u) = \sum_{k=0}^{1} \beta_k L_f^k h + (-1)^0 \beta_1 <dh, ad_f^0(g)> u \tag{7.28}$$

$$= \beta_0 N_2 + \beta_1\left(-R_{P2}\right) + \beta_1 u$$

which implies:

$$u = \frac{\upsilon - \beta_0 N_2 + \beta_1 R_{P2}}{\beta_1} \tag{7.29}$$

We can use a linear P loop as an external input υ:

$$\upsilon - \beta_0 N_2 = \kappa_p \underbrace{(y^d - y)}_{\varepsilon} \tag{7.30}$$

Therefore,

$$u = Q_2 = \frac{\kappa_p}{\beta_1} \varepsilon + R_{P2} \tag{7.31}$$

where the parameters were chosen to be $\kappa_p = .01$, $\beta_0 = 0$ and $\beta_1 = 1$.

We will consider the pair MMA-BuA to validate the controllers. A small amount of each monomer is charged at the beginning of the reaction. Table 7.3 gives the recipe used to test the controllers. Since MMA is the more reactive of both monomers, its flow rate is used to control the copolymer composition, and the flow rate of BuA is used to maximize $[M^P]$. Two flow streams are necessary. In one of them, the required amount of surfactant needed to maintain stable emulsions is added creating thereby a "preemulsion". In the second flow stream, we simply introduce the required amount of pure monomer.

Table 7.3: Experiment for the validation of the controller. Copolymerization Recipe.

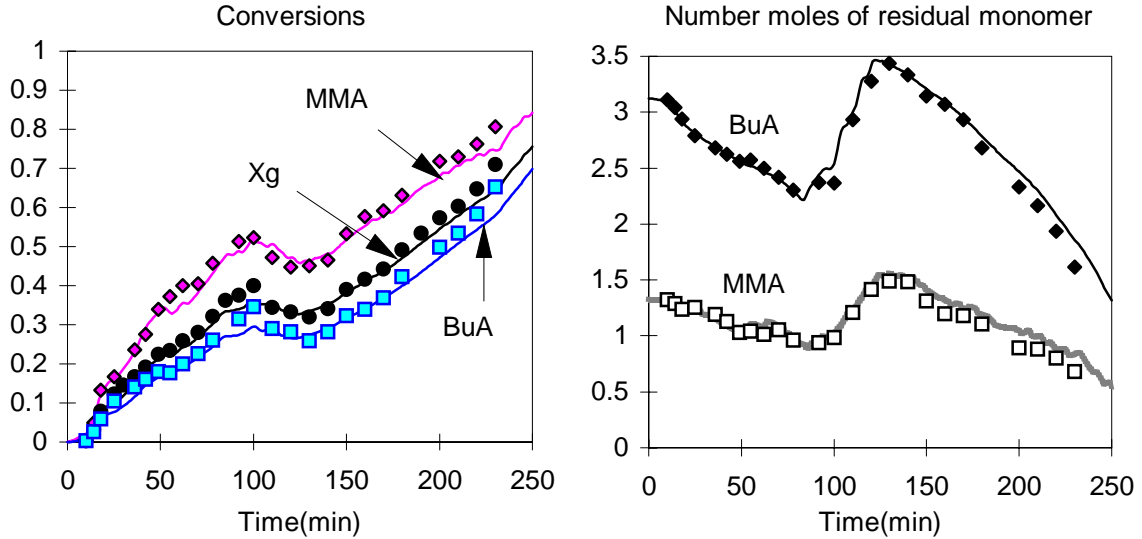| \ Run	C 19		
COMPOSITION^{SP}	**50-50 %** by mol (MMa-BuA)		
Temperature	60%		
Component \	Initial charge	Feed 1 (g)	Feed 2 (g)
H_2O	1500	100	-
MMa	133	354.6	-
BuA	400	-	200
Triton	7.79	8.011	-
DSS	-	0.636	-
KPS	3	-	-
Final particle size	398 nm		
Final Solids Contents	40.26 %		

Figure 7.10: Experiment C19: Overall and individual conversions, at left, and the number of moles of free monomers, MMA and BuA. Experimental measurements, represented by the discontinuous points, are obtained by GC.

Figure 7.10 shows the instantaneous overall conversion obtained by calorimetry. Samples were withdrawn each 15-20 minutes in order to correct the unknown variables related to UA and Q_{loss}. The measured conversion is then used in the nonlinear high gain observer (Chapter 4) to estimate the evolution of the number of moles of each monomer, Figure 7.10 at right, and therefore the individual conversions, Figure 7.10 at left. These estimations present a good agreement with the independent experimental GC measurements done off-line.

The decrease in the overall conversion is due to the addition of BuA at a high flow rate in order to maintain the concentration of monomer in the polymer particles under saturation conditions.
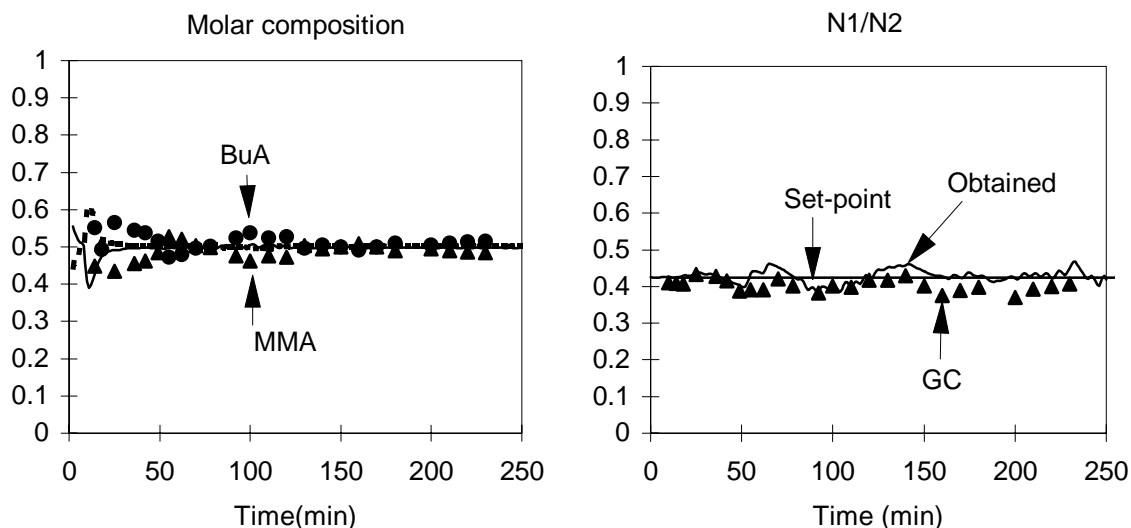
Figure 7.11: Experiment C19: Cumulative molar fractions of each homopolymer in the copolymer, at left and the molar monomers ratio, at right. Experimental measurements, represented by the discontinuous points, are obtained by GC.

Figure 7.11, at left, shows the obtained copolymer composition, and, at right, the obtained (N_1/N_2). As discussed in Chapter 6, the composition controller minimizes the error between (N_1/N_2) and (N_1/N_2)^d, that is calculated as a function of the reactivities of the involved monomers. It can be seen that both the monomer ratio and the copolymer composition are in good agreement with the set-point. The experimental values on the figures are obtained by GC as well.
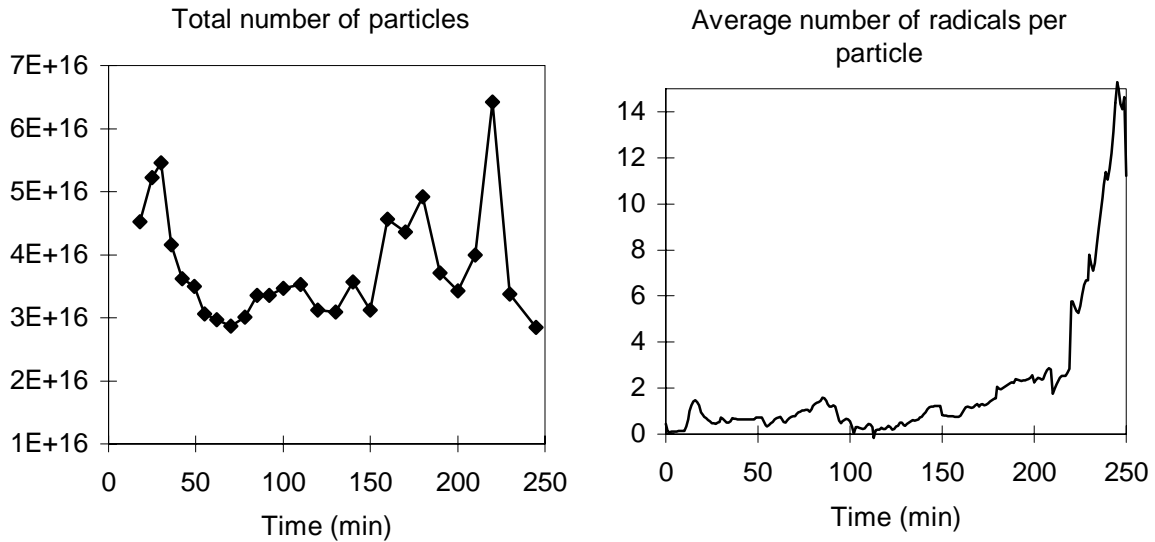
Figure 7.12: Experiment C19: $N_P{}^T$, at left. Average number of radicals per particle, at right.

From the on-line estimation of the total number of moles of radicals in the polymer particles, and once the particle size is determined off-line, the average number of radicals per particle can be determined. Figure 7.12 shows that the number of particles was almost constant during the reaction. The figure also shows the estimated number of particles and the estimated value of $\bar{n}$. An increase in $\bar{n}$ can be observed at the end of the reaction, which is probably due to a gel effect.
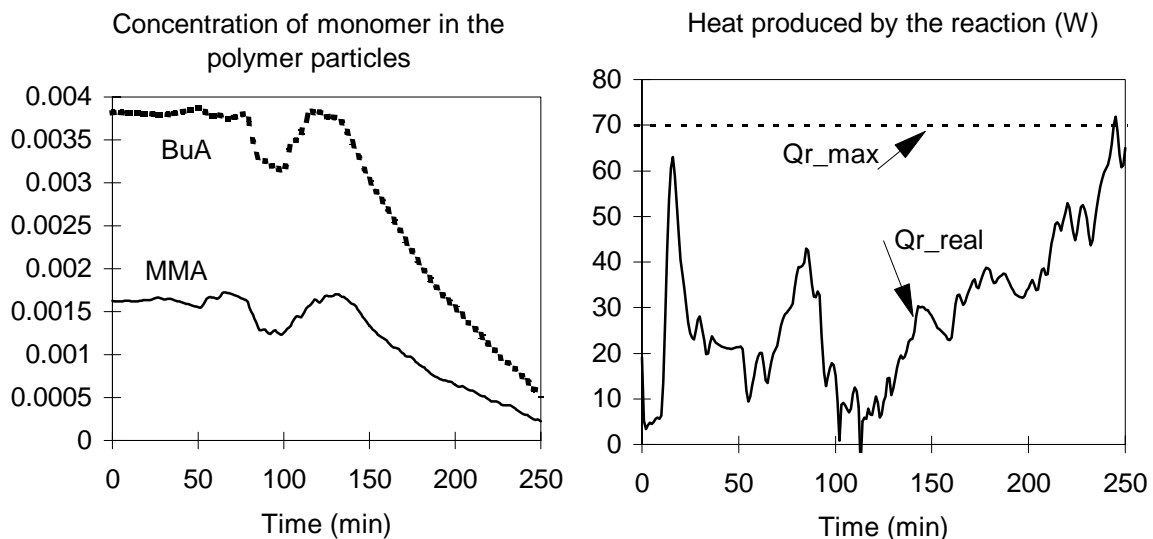

Figure 7.13: Experiment C19: Instantaneous concentration of each monomer in the polymer particles, at left, and instantaneous heat generation rate due to polymerization, at right.

The concentrations of monomer in the polymer particles (Figure 7.13, at left) can be determined from the estimated number of moles of free monomer in the reactor. The heat released by the reaction can also be calculated precisely from the reaction rates (even though it was approximately estimated by calorimetry), and is shown in Figure 7.13, at right. The maximum permitted heat rate was arbitrarily fixed at 70W. Q_R was always inferior to the maximum admissible rate. However, it can be seen that saturating the polymer particles does not allow us to maximize Q_R. The value of Q_R seems to be more sensitive to changes in μ than in $[M^P]$.
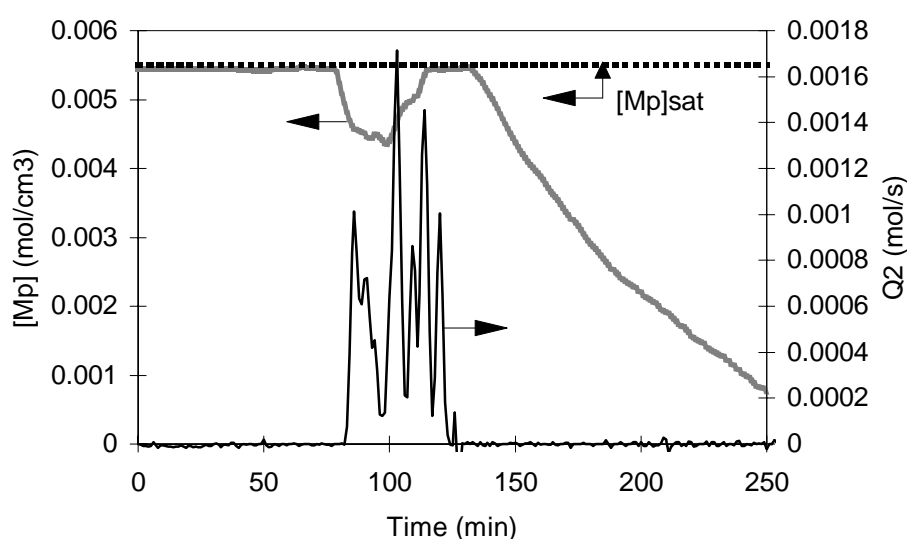

Figure 7.14: Experiment C19: The concentration of monomer in the polymer particles, the maximum saturation concentration, and the flow rate of BuA, Q_2, versus time.

Figure 7.14 shows that the total monomer concentration in polymer particles and the flow rate of BuA versus time. It can be seen that during interval II, where the polymer particles are saturated with monomer (due to an important initial charge), Q_2 was equal to zero. When the monomer concentration in polymer particles starts to decrease, Q_2 becomes non zero (for one hour) and brings the monomer concentration back to the saturation value, without exceeding it. At 130 minutes, we voluntarily stop the addition of BuA in order to consume the added monomer. As Q_2 goes back to zero, the concentration of monomer in polymer particles decreases with conversion, in interval III.

It is important to note that the heat produced by the reaction (Figure 7.14,) was inferior to the maximum permitted heat flow while BuA is fed to the reactor, and therefore,

the control objective, y^d, was calculated from equation (7.25), in order to maintain $[M^p]$ at $[M^p]^{sat}$. The time delay observed in the saturation of polymer particles is due to the fact that Q_2 calculates the total amount (Q_1+Q_2) to be added to saturate the polymer particles but adds only Q_2, and waits for the first control law to add enough monomer 1, in the next step, in order to complete the saturation of the particles and to take (N_1/N_2) back to the desired value, both at the time in question.

In a conclusion, we have seen that both control laws (composition and reaction rate) are coupled, and that this approach allows us to satisfy all control objectives at the same time. An important physical constraint to take into consideration is the maximum possible flow rate (limited by the pumps). Q_2 and Q_1 must be of the same order, otherwise, the composition controller might take a lot of time to compensate the addition of Q_2 and to bring the monomer ratio back to the set-point, which might affect the polymer composition.

7.4 Terpolymerisation processes

Consider the terpolymerization material balance,

$$\dot{x} = \begin{bmatrix} \dot{N}_1 \\ \dot{N}_2 \\ \dot{N}_3 \end{bmatrix} = \underbrace{\begin{bmatrix} Q_1 - R_{P1} \\ Q_2 - R_{P2} \\ -R_{P3} \end{bmatrix}}_{f(x)} + \underbrace{\begin{bmatrix} 0 \\ 0 \\ 1 \end{bmatrix}}_{g(x)} \underbrace{Q_3}_{u} \tag{7.32}$$

$$y = \underbrace{N_3}_{h(x)}$$

The flow rates of the two more reactive monomers Q_1 and Q_2 are given by the composition control laws, developed in Chapter 6, as follows:

$$Q_1 = 0.01 \times \left(N_3 (N_1 / N_3)^d - N_1 \right) + R_{P1}$$

$$Q_2 = 0.01 \times \left(N_3 (N_2 / N_3)^d - N_2 \right) + R_{P2} \tag{7.33}$$

They can therefore be considered as known inputs in the model. As was the case in the last section, our objective is to control Q_3 such that $[M^p]$ is as close as possible to $[M^p]^{sat}$ and Q_R is inferior to $Q_{R,max}$, while simultaneously maintaining the terpolymer composition at the desired value. We first calculate N_3^d that satisfies these conditions and then we develop the control law.

The polymer particles are exactly saturated, with no excess monomer found in the form of monomer droplets, if the following condition is valid:

$$N_1 \delta_1 + N_2 \delta_2 + N_3 \delta_3 = \frac{\left(1 - \phi_p^p\right)}{\phi_p^p} \sigma \tag{7.34}$$

where :

$$\delta_i = MW_i \left(\frac{1}{\rho_i} + \frac{\left(1 - \phi_p^p\right)}{\rho_{i,h} \, \phi_p^p} \right) , i=1, 2, 3$$

and

$$\sigma = \sum_{j=1}^{3} \frac{MW_j N_j^T}{\rho_{2,h}}$$

Therefore, the N_3^d is directly calculated, and is given by:

$$N_3^d = \frac{\left(\dfrac{1-\phi_p^p}{\phi_p^p}\right)\sigma}{\left(\delta_1\left(\dfrac{N_1}{N_3}\right)^d + \delta_2\left(\dfrac{N_2}{N_3}\right)^d + \delta_3\right)} \tag{7.35}$$

On the other hand, the maximum heat production rate is:

$$Q_{R,max} = \sum_{i=1}^{3}\left(-\Delta H_{Pi}\right)R_{Pi} \tag{7.36}$$

The number of moles of monomer 3 to obtain the maximum production rate is given by:

$$N_3^d = \frac{Q_{R,max} - \left(-\Delta H_{P1}\right)R_{P1} - \left(-\Delta H_{P2}\right)R_{P2}}{\mu_2 N_a\left(-\Delta H_{P3}\right)\left(K_{P13}\left(\dfrac{N_1}{N_3}\right)^d a_1 + K_{P23}\left(\dfrac{N_2}{N_3}\right)^d a_2 + K_{P33}a_3\right)} \tag{7.37}$$

where

$$a_1 = K_{P31}K_{P21}\left(\frac{N_1}{N_3}\right)^d + K_{P21}K_{P31}\left(\frac{N_2}{N_3}\right)^d + K_{P31}K_{P23}$$

$$a_2 = K_{P12}K_{P31}\left(\frac{N_1}{N_3}\right)^d + K_{P12}K_{P32}\left(\frac{N_2}{N_3}\right)^d + K_{P32}K_{P13}$$

$$a_3 = K_{P13}K_{P21}\left(\frac{N_1}{N_3}\right)^d + K_{P23}K_{P12}\left(\frac{N_2}{N_3}\right)^d + K_{P13}K_{P23}$$

Now, we denote by y^d the minimum value between N_3^d calculated by equation (7.35) and (7.37). We can then develop an input/output linearizing control law that calculates Q_3 that tracks y^d. First of all, the relative order of the system equals one since:

$$L_f h = \frac{\partial h}{\partial x} f = \begin{bmatrix} 0 & 0 & 1 \end{bmatrix} \begin{bmatrix} Q_1 - R_{P1} \\ Q_2 - R_{P2} \\ -R_{P3} \end{bmatrix} = -R_{P3} \neq 0$$

An input/output linearizing transformation is therefore:

$$\upsilon = \Omega(x,u) = \sum_{k=0}^{1} \beta_k L_f^k h + (-1)^0 \beta_1 < dh, ad_f^0(g) > u \tag{7.38}$$

$$= \beta_0 N_3 + \beta_1 \left(-R_{P3} \right) + \beta_1 u$$

Then,

$$u = \frac{\upsilon - \beta_0 N_3}{\beta_1} + R_{P3} \tag{7.39}$$

As usually, the external input $\left(\upsilon - \beta_0 N_3 \right)$ is replaced by a linear P loop

$$u = \frac{\kappa_P}{\beta_1} \left(y^d - y \right) + R_{P3} \tag{7.40}$$

where $\kappa_p = 0.01$, and $\beta_1 = 1$.

In order to validate the control law, a terpolymerization experiment (MMA-BuA-VAc) has been carried out, with some amounts of each monomer charged at the beginning of the reaction. Thereafter, the two more reactive monomers (MMA, BuA) are added at a controlled flow rate that ensures the production of a constant terpolymer composition. As we discussed in Chapter 6, it is possible to introduce both MMA and BuA at the same flow rate in order to maintain the ratios (N_1/N_3) and (N_1/N_3) at the desired ones. The desired amount of VAc (the less reactive) is added at a flow rate that maintains $[M^p]$ at $[M^p]^{sat}$ under the condition $Q_R \leq Q_{R,max}$. The recipe used for this terpolymerization experiment is shown in Table 7.4.

Table 7.4: Experiment for the validation of the controller. Terpolymerization Recipe.

\ Run	C 29		
COMPOSITION^{SP}	**50-35-15 %** by mol (MMa-BuA-VAc)		
Temperature	60%		
Component \	Initial charge	Feed 1 (g)	Feed 2 (g)
H_2O	1200	400	-
MMa	28.6	705	-
BuA	46.1	611	-
VAc	146.2	-	300
Triton	6.63	9.43	-
DSS	-	3.057	-
KPS	3.0959	-	-
Final particle size	320 nm		
Final Solids Contents	46.5 %		

Figure 7.15 shows the evolution of the overall and individual conversions (of MMA, BuA and VAc) obtained from the calorimetric adaptive observer and the composition observer for terpolymerization processes (described in Chapter 5).
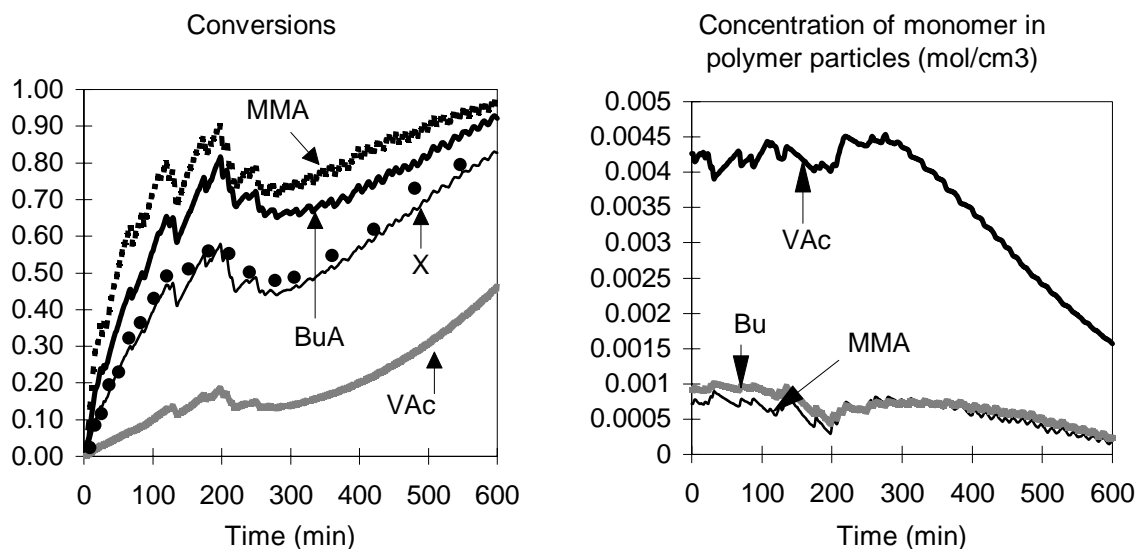

Figure 7.15 : C29, Overall and individual conversions, at left, and the concentration of each monomer in the polymer particles, at right.
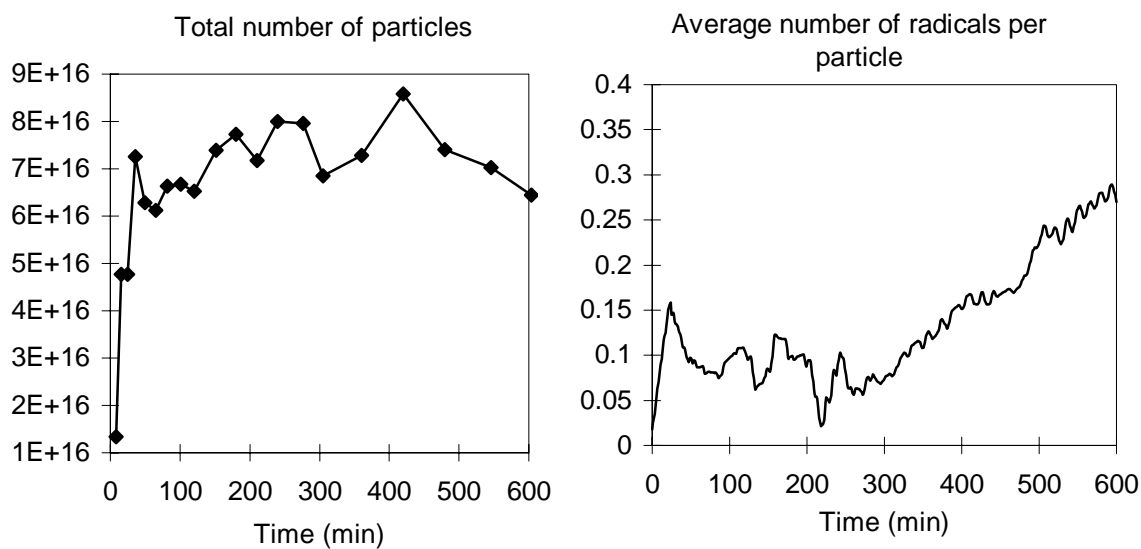

Figure 7.16 : Experiment C29. The total number of particles in the reactor, at left, and the average number of radicals per particle, at right.

The estimated $\bar{n}$ is shown in Figure 7.16. An increase in the value of $\bar{n}$ was observed at the end of the reaction. The increase starts at 55% of conversion, where the solids content was 17%. This increase is must likely be due to a gel effect.

297

In Figure 7.17, it can be seen that the flow rate of VAc, Q_3, was mainly determined by equation (7.35), and therefore the control objective was to maintain the concentration of monomer in the polymer particles at the saturation value. The initial amount of monomers was sufficient to maintain saturation conditions for about 120 minutes. During this time, the flow rate of VAc, Q_3, was equal to zero. When $[M^p]$ starts to be lower than the saturation value, Q_3 increases to take $[M^p]$ back to the saturation value. Simultaneously, a check of the heat produced by the reaction is done. Q_3 is set equal to zero if the heat production rate is superior than 25 Watts (chosen arbitrarily).
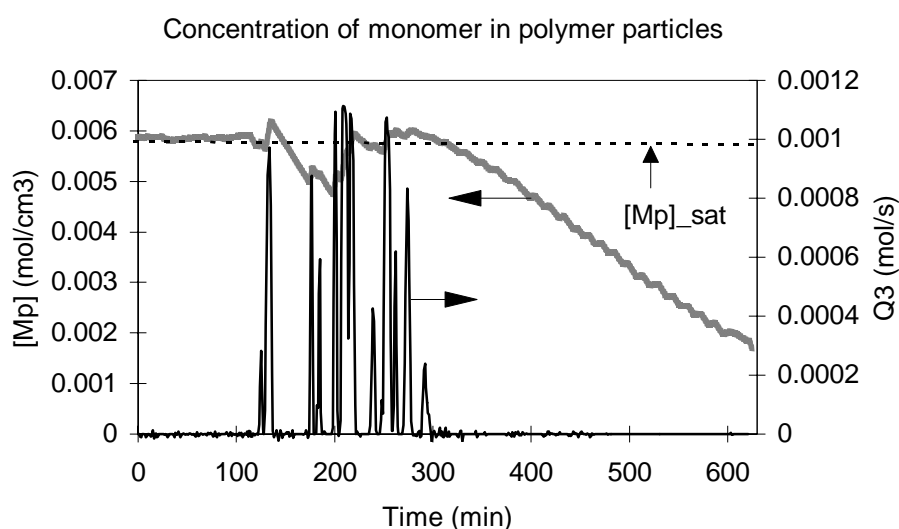

Figure 7.17: C29, Flow rate of the monomer the less reactive, Q_3 and the concentration of monomers in the polymer particles, $[M^p]$.

When the heat produced by the reaction begins to exceed the maximum permitted value, due to a gel effect, the flow rate of VAc goes back to zero. And since the heat production rate continues to increase, Q_3 stays at zero. Since the controller manipulated variable is the monomer flow rates, the controller cannot reduce Q_R especially that the increase in the value of Q_R is due to increasing the number of radicals in the polymer particles.

In the case of this experiment, the composition controller was maintained active until the end of the reaction, and therefore the flow rate of the most reactive monomers was positive. This was not found to be particularly dangerous since the chosen value for $Q_{R,max}$ was not really a critical value for the reaction safety. On the other hand, if Q_R exceeds the

maximum value permitted to maintain safe operations, then all flow rates must probably be stopped. Moreover, the rate of heat production by the reaction must be decreased by adding inhibitor, or cold water to the reactor.
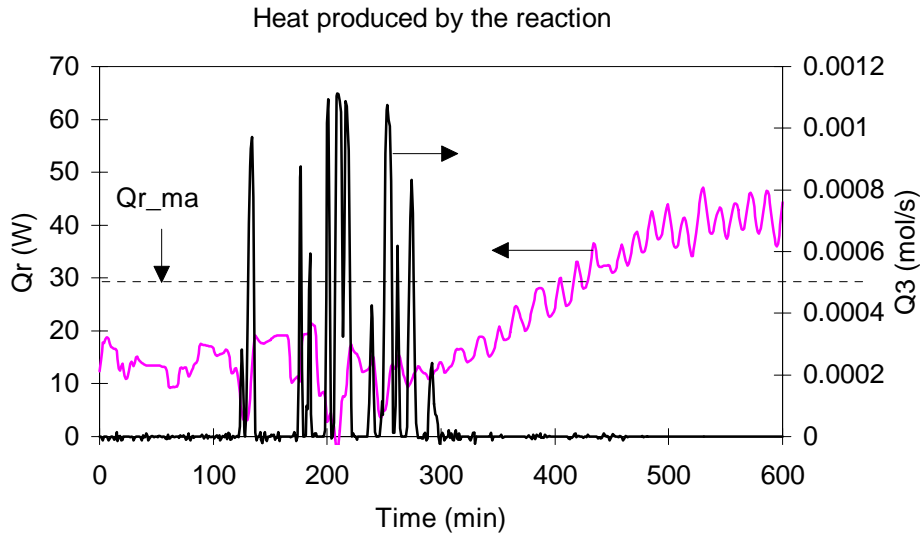

Figure 7.18: C29. Flow rate of monomer 3 and the rate of heat production by the reaction.

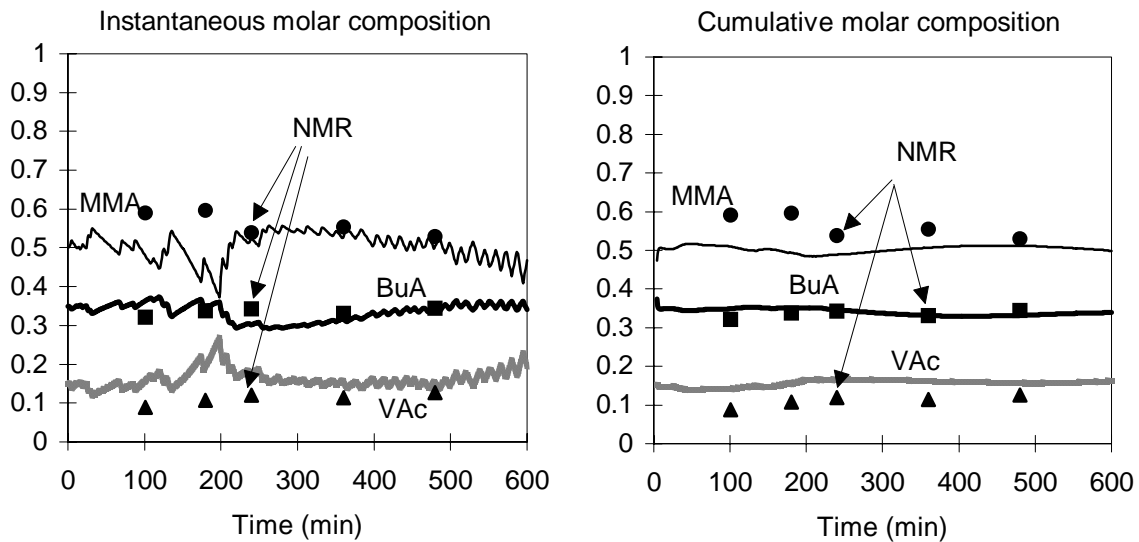Figure 7.19: C29. Instantaneous molar composition, at left, and the cumulative molar composition, at right. The estimations are represented by the continuous lines and the experimental NMR results are represented by the points.

The composition was controlled simultaneously by Q_1 and Q_2, the flow rates of MMA and BuA. The obtained composition is shown in Figure 7.19. The figure shows the molar

fraction of each monomer in the polymer. The estimated values (from the high gain observer), are given by the continuous lines. The estimations were validated off-line by NMR. In Figure 7.19 at left, the instantaneous molar composition shows that the composition control is sensitive to Q_3, and during the time that the composition control law takes to bring (N_1/N_3) and (N_2/N_3) back to the desired values, a little composition drift arises. Figure 7.19, at right, shows that the cumulative terpolymer composition is less sensitive to this strong variation in the value of Q_3, but is not in good agreement with the experimental NMR measurements. This problem can be solved by reducing the maximum flow rate allowed by the pump controlling Q_3. However, this will increase the time required to saturate the polymer particles. Therefore, the choice of the saturation value of Q_3 must be a compromise between rapidity of convergence of the controller, and reducing its negative impact on the evolution of the polymer composition.

7.5 Conclusion

In this chapter we presented several control laws that were successfully applied to homo-, co-, and terpolymerization processes. These control laws allows us to manipulate the process productivity, and to simultaneously maintain the polymer composition at the desired value (in co- and terpolymerization). The objectives by maximizing productivity are maintaining the particles saturated with monomer (without exceeding the saturation value) as long as the heat produced by the reaction does not exceed the maximum heat removal capacity, limited by the jacket.

The main information about the process is obtained by calorimetry (procedure developed in Chapter 3), and for the different observers developed in Chapters 4 and 5. The composition control laws developed in Chapter 6 were simultaneously used with the control laws developed in this chapter.

7.6 Nomenclature

Notation

A	surface area between the jacket and the reactor [m²]
K_{pi}	reaction rate constant of the active chain i with monomer i
K_{pij}	reaction rate constant between the active chain i and monomer j
$L_f h$	Lie derivative of the scalar field h with respect to the vector field f (hapter2)
$[M_i^p]$	concentration of monomer i in the polymer particles
MW_i	molecular weight of monomer i
$\bar{n}$	average number of radicals per particle
N_a	Avogadro's number
N_i	number of moles of free monomer i
N_i^T	total number of moles of monomer i introduced to the reactor
N_P^T	total number of particles in the reactor
Q_i	molar flow rate of monomer i
Q_{lim}	maximum heat removed by the jacket [W]
R_{pi}	rate of reaction of monomer i [mol/s]
$T_{j,min}$	minimum jacket temperature [°C]
T_R	reactor temperature [°C]
u	input
U	heat transfer coefficient between the jacket and the reactor, [W/m²/°C]
x	state variables
X	conversion
y	output
y^d	set-point

Greek letters

ε_i	a function representing the dynamic of i
ϕ_p^p	volumetric fraction of polymer in the polymer particles
κ_p	proportional gain of the P controller
μ	the number of moles of radicals in the polymer particles
ρ_i	monomer density (g/cm^3)
$\rho_{i,h}$	homopolymer density (g/cm^3)
υ	a linearizing input output transformation

Acronyms

BuA	Butyl acrylate
DSS	Dioctyl sulfosuccinate de sodium, (surfactant)
KPS	Potassium persulfate, (initiator)
MMA	Methyl methacrylate
P	proportional controller
SDS	Dodecyl sulfate, sodium salt, (surfactant)
STY	Styrene
VAc	Vinyl acetate

7.7 Bibliography

1.   Arzamendi, G., and J. Asua, Copolymer composition of emulsion copolymers in reactors with limited capacity for heat removal, *Ind. Eng. Chem. Res.*, **30**, 1342-1350, (1991).

2.   Buruaga, I. S., Ph. D. Armitage, J. R. Leiza, J. M. Asua, Nonlinear control for maximum production rate latexes of well-defined polymer composition, *Ind. Eng. Chem. Res.*, **36**, 4243-4254, (1997c).

3.   Gilbert, R. G., a mechanistic approach, Colloid Science, R. H. Ottewill, and R. L. Rowell eds, (1995).

4.   Gilmore, C.M., G. W. Poehlein, and J. Schork, Modeling poly(vinyl alcohol)-stabilized vinyl acetate emulsion polymerization. I. Theory, *J. Appl. Polym. Sci.*, **48**, 1449-1460, (1993).

5.   Gloor, P. E., and R. J. Warner, Developing feed policies to maximize productivity in emulsion polymerization processes, *Thermochimica Acta*, **289**, 243-265, (1996).

6.   Jang, S. S., P. H., discontinuous minimum end-time temperature/initiator policies for batch emulsion polymerization of vinyl acetate, *chem. Eng. Sci.*, **46**, 12, 3153-3163, (1991).

7.   Lin, C.-C., W.-Y. Chiu, Simulation and optimal design of seeded continuous emulsion polymerization process, *J. Appl. Polym. Sci.*, **27**, 1977-1993, (1982).

8.   Penlidis, A., J. F. MacGregor and A. E. Hamielec, A theoretical and experimental and experimental investigation of the batch emulsion polymerization of vinyl acetate, **3**, 3, 185-218, (1985).

9.   Shork, F. J., and W. H. Ray, The development of the continuous emulsion polymerization of methyl methacrylate, *J. Appl. Polym. Sci.*, **34**, 1259-1276, (1987).

10. Seminot, D., W. H. Ray, Control of systems described by population balance equations-I. Controllability analysis, *Chem. Eng. Sci.*, **50**, 11, 1805-1824, (1995a).

11. Seminot, D., W. H. Ray, Control of systems described by population balance equations-II. Emulsion polymerization with constrained control action, *Chem. Eng. Sci.*, **50**, 11, 1825-1839, (1995b).

CONCLUSIONS AND PERSPECTIVES

CONCLUSIONS AND PERSPECTIVES

A very useful step before controlling a process would be to identify the controlled variables (e.g. composition, particle size distribution), that have the largest influence on the final product properties. Secondly, one must determine the manipulated variables (e.g. temperature, flow rates) that allow us to exert a significant influence on these controlled variables. Finally, on-line information about the controlled variables is required in order to apply a control strategy. Since most of the important properties are not measurable directly, in several processes, state estimation techniques are usually combined with the control design to accomplish these objectives.

The main objective of the research reported here was to control the polymer composition in emulsion polymerization processes, which is the single most important parameter in terms of determining the final polymer properties. Since the composition is not usually measured on-line, we have developed a software sensor to estimate its evolution, based on the available measurements of the process: the temperatures in the reactor and in the cooling jacket. The control strategy was realized in three steps:

- Calorimetry was used to obtain an estimate of the overall monomer conversion and the rate of heat produced by the polymerization. The procedure involves nonlinear estimation and optimization techniques that are solely based on the temperature measurements in the reactor, the inlet and outlet, and on infrequent gravimetric measurements. This procedure is applicable to large scale reactors, and, in principal, can also be applied to other polymerization reactors, such as solution or suspension reactors.

- Secondly, a high gain nonlinear observer was employed to estimate the evolution of the polymer composition in both co- and terpolymerization processes. The observer is based on the material balance of monomers and on the measurement of the total conversion (obtained by any on-line technique). It is therefore clear that the more accurate our estimate of conversion is, the more precise the estimation of the polymer composition will

be. The advantages of this method are that it is not sensitive to errors in the initial conditions and to modeling errors (such as the reaction rate constants), and does not require a model for the number of radicals in polymer particles. A study of the sensitivity of the estimates of polymer composition to the reaction in the aqueous phase has shown that (for the monomers tested in this work) the reaction can be assumed to take place only in the polymer particles for the composition control. The estimators give also an estimate of the concentration of radicals in the polymer particles that is very interesting in studying the kinetics of the process.

- Based on the estimated polymer composition, a nonlinear control strategy was developed to maintain a specific composition, using the monomer feed flow rates of the most reactive monomer(s) as manipulated variables. Composition control requires a single input/ single output control strategy (flow rate of the most reactive monomer) in copolymerization, and a multi input/ multi output control (flow rates of the two most reactive monomers) for terpolymerization processes. The final part of the research concerned simultaneous control of the polymer composition and the concentration of monomer in the polymer particles.

Concerning the control of the heat produced by the reaction in realistic situations, it would be essential first to estimate the 'real' heat removal capacity of the jacket. Secondly, a study of controlling $\mu[M_P]$ must be done in order to fulfil this purpose. The use of the initiator flow rate would be an efficient means of controlling μ and therefore maximizing the process productivity. Finally, if we want to control the concentration of monomer in the polymer particles under safe conditions, other manipulated variables such as a supplementary cooling loop, or the addition of small amounts of inhibitor, must be studied.

This work has demonstrated the feasibility of our approach in the control of the polymer composition. However, it is clear that we have only begun to address some of the issues related to the more global theme of polymerization reactor control. We can identify several factors that influence the final polymer properties, such as molecular weight and particle size distribution. The same estimation and control strategies can be used in these applications. Additional on-line sensors are probably required in order to fulfil the control of

these parameters. For instance, we can envisage using infrared spectroscopy for the monitoring of the particle size distribution. The combination of the estimated number of moles of radicals in polymer particles with the number of particles can be used to estimate and control the molecular weight distribution.